



UNIVERSITÀ
DEGLI STUDI
DI MILANO



UNIVERSITÀ DEGLI STUDI DI MILANO

PhD School in Molecular and Cellular Biology

Department of Bioscience

XXXIII Cycle

PhD Thesis

Characterisation of *AUXIN RESPONSE FACTOR 5/MONOPTEROS* post-transcriptional and post-translational regulations during *Arabidopsis thaliana* development

Cavalleri Alex

Scientific Tutor: prof. Lucia Colombo

PhD director: prof. Martin M. Kater

Academic year: 2019/2020

“L’imparare non è lo stesso che sapere: vi sono gli eruditi e gli scienziati, la memoria forma i primi, la filosofia i secondi.”

“Ma la filosofia non si può imparare?”

“La filosofia non s’impara, la filosofia è la riunione delle scienze imparate nel genio che le applica.”

“Vediamo” disse Dantès. “Che cosa m’insegnerete per primo? Ho smania di cominciare, ho sete di scienza.”

“Tutto!” disse Faria.

Alexandre Dumàs

Index

Riassunto	6
Abstracts	8
1. <i>MP</i> translation initiation is modulated by an auxin dependent alternative splicing event	9
2. Alternative splicing generates a MONOPTEROS isoform required for ovules development.....	10
3. Auxin modulates MP post-translational regulation in root development	11
Aim of the thesis	12
Introduction	15
1. <i>Arabidopsis thaliana</i> as a model species.....	16
2. Auxin biosynthesis and polar transport.....	17
3. Auxin signalling.....	18
3.1 AUXIN RESPONSE FACTOR family	21
3.2 The AUXIN RESPONSE FACTOR 5/MONOPTEROS (ARF5/MP)	23
3.3 Auxin independent <i>ARFs</i> regulation.....	24
4. Auxin and flower development.....	25
4.1 Floral meristem determinacy.....	28
4.2 Gynoecium development	29
5. Auxin and ovules development.....	31
6. Auxin and root development	33
References	36

Results and discussion	47
1. <i>MP</i> translation initiation is modulated by an auxin dependent alternative splicing event	49
1.1 Detection of predicted <i>MP</i> mRNAs splicing isoforms.....	49
1.2 Evaluation of <i>MP</i> isoforms translational efficiency.....	51
1.3 Auxin regulates <i>MP</i> leader intron alternative splicing.....	53
1.4 Identification of <i>MP</i> alternative translation start site.....	55
1.5 Discussion.....	57
2. Alternative splicing generates a MONOPTEROS isoform required for ovules development.....	60
2.1 <i>MP</i> is expressed and functional in auxin minima regions during ovules development.....	60
2.2 Identification of a <i>novel MP</i> alternative splicing event linked to the translation of a truncated <i>MP</i> protein isoform.....	63
2.3 <i>MPint11</i> is sufficient to restore ovules development in <i>mp</i> mutants.....	66
2.4 Absence of the <i>MPint11</i> isoform leads to alteration in the ovule development process.....	68
2.5 Discussion.....	71
3. Auxin modulate <i>MP</i> post-translational regulation in root development.....	74
3.1 <i>MPint11</i> isoform is functional in rescue <i>mp</i> related phenotype during root development.....	74
3.2 Combined analyses of <i>MP</i> reporter lines reveal differential post-translational regulations of <i>MP</i> isoforms in the RAM.....	76
3.3 Canonical <i>MP</i> protein stability is related to auxin concentration.....	80
3.4 Proteasome activity leads to <i>MP</i> protein degradation in auxin minima.....	82
3.5 <i>MP</i> canonical protein accumulation is dynamically modulated during lateral root development.....	84
3.6 Discussion.....	87
References.....	90

Conclusions and future perspectives	94
Material and methods	98
1. Plant material and growth conditions	99
2. RNA extraction and cDNA synthesis	99
3. Droplet digital PCR assay	100
4. Polysome fraction extraction and RNA extraction	100
5. Co-IP followed by ms/ms on <i>MP:MP-GFP (mr)</i> reporter line	101
6. Auxin and Bertezomib treatments	102
7. Real time and data analysis	102
8. Generation, genotyping and phenotyping of CRISPR mutant alleles	102
9. Optical and confocal microscopy	103
10. RNA deep-sequencing analysis	103
11. Sequence conservation analysis	104
12. Primers table	105
References	108
Appendices	110
Auxin and Flower Development: A Blossoming Field	
Alternative splicing generates a MONOPTEROS isoform required for ovule development	
Auxin regulated <i>MONOPTEROS</i> leader intron splicing modulates translation initiation in <i>Arabidopsis thaliana</i>	

Riassunto

Durante il mio dottorato mi sono focalizzato sullo studio dei meccanismi regolativi dell'*AUXIN RESPONSE FACTOR 5 / MONOPTEROS* in *Arabidopsis thaliana*, analizzando come le sue regolazioni post-trascrizionali e post-traduzionali siano coinvolte nella modulazione della sua attività in diversi contesti di sviluppo. MONOPTEROS è un fattore trascrizionale coinvolto in molti processi che vanno dallo sviluppo embrionale fino alla formazione degli ovuli. A livello molecolare, MONOPTEROS promuove l'attivazione di geni target in risposta alla percezione cellulare dell'auxina. La mia ricerca ha permesso di identificare tre nuovi eventi regolativi di questo gene, i quali prevedono due diversi eventi di splicing alternativo del trascritto con la formazione di isoforme proteiche diverse e la regolazione post-traduzionale della loro stabilità. Questi dati mostrando che MONOPTEROS, durante lo sviluppo riproduttivo e in particolare degli ovuli, è funzionale per l'attivazione della trascrizione dei suoi target in modo indipendente dalla classica regolazione mediata dall'auxina, la quale prevede la sua inattivazione in domini di bassa concentrazione ormonale. Inoltre, questi risultati mostrano l'esistenza di nuove funzionalità dell'auxina stessa sulla modulazione della sua attività. Infatti, abbiamo osservato che gli eventi di splicing alternativo descritti per *MONOPTEROS* possono essere modulati dalle variazioni di concentrazione di questo ormone, suggerendo una sua azione non solo a livello di regolazione dell'attività trascrizionale degli ARF, ma anche a livello post-trascrizionale. In modo analogo, i nostri risultati indicano che l'auxina può anche giocare un ruolo nella regolazione dell'accumulo delle diverse isoforme proteiche di MONOPTEROS generate a partire dagli eventi di splicing alternativo. Abbiamo infatti descritto che, durante lo sviluppo della radice, diverse isoforme di MONOPTEROS vengono accumulate o degradate in modo differenziale in relazione ai livelli ormonali. L'insieme dei risultati che ho ottenuto durante il mio dottorato permettono di delineare un nuovo scenario di funzionamento e regolazione di MONOPTEROS, implementando l'attuale conoscenza del meccanismo di attività dell'auxina e degli ARF.

Abstracts

1. *MP* translation initiation is modulated by an auxin dependent alternative splicing event

The AUXIN RESPONSE FACTOR 5/MONOPTEROS (ARF5/MP) is a transcriptional factor involved in the activation of downstream targets upon auxin signalling. MP has been shown to be involved in the regulation of several biological processes in *Arabidopsis thaliana*. Despite MP functions have been deeply studied, little is known about its intrinsic regulative mechanisms, and how auxin regulate them. In this work we characterised the existence of a predicted alternative splicing event of a leader intron sequence located in *MP* 5'UTR. We show that *MP* alternative spliced mRNA is preferentially accumulated in inflorescences tissues. Interestingly, this alternative splicing event seems to be positively regulated by exogenous auxin application, a modulation which involves the action of the previously described alternative splicing regulative module NSRs-ASCO. Moreover, the absence of the leader intron sequence in the alternative spliced mRNA results in the usage of a downstream start codon for translational start. Thanks to the characterisation of two novel CRISPR/Cas9-generated *mp* mutant alleles, and by ribosomes profiling datasets analysis we propose that the fourth in-frame AUG on *MP* open reading frame can be used as alternative translational start site, without impairing protein structure and function. Our results show that auxin can modulate *MP* transcript maturation, generating alternative spliced mRNA variants and flexibility in the translational start codon usage, revealing a new level of auxin functions on *ARFs* modulation.

2. Alternative splicing generates a MONOPTEROS isoform required for ovules development

Auxin is one of the main designers of plant development and organs differentiation and its function relies on its differential accumulation with the generation of points of high and low hormone content. At cellular level, auxin signaling impacts on the transcriptomic landscape through the modulation of the interplay between AUX/IAA repressor proteins and AUXIN RESPONSE FACTOR transcriptional factors. AUX/IAAs and ARFs compose a combinatorial system in which AUX/IAAs binding to ARFs negatively regulates their ability to activate the transcription of downstream targets. Upon auxin sensing, AUX/IAAs stability is compromised through their direct ubiquitination and degradation, allowing transcriptional activator ARFs to promote gene expression. Among transcriptional activator ARFs, ARF5/MONOPTEROS (MP) has been shown to be a key integrator of auxin signaling for many developmental events, through the activation of the transcription of target genes above auxin threshold concentration. We show that in ovules, MP is expressed and functional in domains of low auxin content. We described that *MP* post-transcriptional regulations are involved in this process through the generation of a biologically functional mRNA splicing variant, whose translation generates a protein isoform lacking the AUX/IAA interaction domain. Indeed, the alternative *MPint11* isoform was able to partially complement *mp* mutants defects and ovule developmental process. Interestingly, also the canonical MP protein results partially functional for complementation of ovules formation, with a similar behavior to the one observed for *MPint11*. Our results suggest that MP functions relies on the combined activity of both its isoforms with the evidence that, during ovules development, MP domains involved in AUX/IAAs binding are not strictly required. These findings describe a novel scenario in which, not only MP is able to work uncoupled from the classical auxin signaling model, but also in which post-transcriptional regulation controls the formation of a functional isoform required for correct ovules development.

3. Auxin modulates MP post-translational regulation in root development

Polar auxin transport and accumulation has been shown to be fundamental for correct root patterning and differentiation and AUXIN RESPONSE FACTOR transcriptional factors are directly involved in these processes. ARF5/MP has been shown to be a crucial integrator of auxin signalling for primary root formation, root meristem maintenance and lateral roots development. MP was previously described to positively regulate the transcription of its downstream targets upon auxin concentration increase. Nevertheless, recent studies reveal that MP activity during reproductive development relies on different protein isoforms, acting uncoupled from the classical auxin signalling model. These observations suggest that, also in root development, MP function might be integrated by these regulations, leading to the establishment of a novel *scenario* of auxin mediated MP modulation. In this work we show that MP and alternative MPint11 isoforms undergo differential post-translational regulations both in the root apical meristem and in lateral roots primordia, which impact on their stability and accumulation. We observed that high auxin levels allow canonical MP protein accumulation, whereas sub-threshold auxin concentration determines its degradation by the proteasome. On the other side, alternative MPint11 isoform escapes from this regulation, allowing its broader accumulation. These regulative mechanisms might impact on a differential functionality of MP and MPint11 isoforms during root development, as suggested by their differential ability to restore *mp* mutant phenotype at the seedling level. Our results reveal a completely new level of ARFs modulation mediated by auxin, showing that its level not only determines ARFs transcriptional behaviour but also might impact differentially on their stability, acting as a bridge from post-transcriptional to post-translational regulations.

Aim of the thesis

MP has been shown to integrate auxin signalling into functional responses in a plethora of different developmental processes. From root development to ovule formation *MP* has to work in a vast number of different contexts, suggesting that a great plasticity of its functionality and response is needed. In light of this, we decided to characterise the different regulative mechanisms to which *MP* undergoes, considering post-transcriptional, translational and post-translational regulation. As already observed for other *ARFs*, such regulations can completely change how auxin perception is converted into cellular responses. The classical auxin signalling paradigm is constantly challenged by the progress of the scientific community, indicating the existence of much more levels of complexity. Indeed, unveil genes specific regulations might integrate this model helping in the intimate understanding of plant development and auxin functions. Besides *MP* has been deeply studied across the years, the knowledge about its intrinsic regulative mechanisms is still poorly understood. Our main aim has been the characterisation of *MP* functions and regulations in reproductive development with a specific focus on ovules formation. We initially characterised the existence of predicted or completely new *MP* post-transcriptional regulations, which involve modulations of alternative splicing or of the translational initiation. Furthermore, we observed that these regulations are mediated by alternative auxin signalling events, suggesting a further level of complexity in the auxin mediated *ARFs* regulation. Moreover, we considered how these *MP* post-transcriptional regulations integrated the classical auxin response in the biological processes studied, combining these novelties with expression analysis and reporter lines studies. Thanks to these findings, we observed that *MP* function during ovule development relies on the generation of different protein isoforms which can work partially uncoupled from auxin signalling. Nevertheless, at the same time we enquired our self on how post-transcriptional regulations impact on *MP* function in a more systemic way, by concentrating our attention on other developmental contexts as root development. In this case our aim has been to clarify how *MP* post-transcriptional and post-translational regulations interplay and how auxin is involved in these processes. We observed that different *MP* protein isoforms, generated by our previously described post-transcriptional events, shown different degrees of sensibility to auxin-mediated post-translational regulation, which impact on their stability and accumulation. These findings bring to the establishment of completely new scenario in which auxin not only regulated the transcriptional activity of *ARFs* but also works as a bridge from their post-transcriptional to post-translational regulations, for a fine control of their functions in the

different developmental events. Our results suggest that such regulative mechanisms operate in tissue and stage specific manner. Nevertheless, these studies contribute to shed light on a completely new field of auxin functions.

Introduction

1. *Arabidopsis thaliana* as a model species

Arabidopsis thaliana is a dicotyledon belonging to the *Brassicaceae* family, originated around 6 MYA. Despite its low importance under an agronomic point of view *Arabidopsis* studies have permitted enormous discoveries in plants development, helping the foundation of modern plant biology [1]. *Arabidopsis thaliana* is a small plant with a fast life cycle, which takes 6 weeks to go from seeds to fully developed plants with mature fruits (siliques) under long day growing conditions (16h of light), at a constant temperature of 22°C. Beyond the size and growing rate, *Arabidopsis* has the advantage to possess a relatively small genome of around 125 million nucleotide pairs on five chromosomes, making it ideal for a complete characterization under a genetic point of view. Indeed, *Arabidopsis thaliana* genome has been fully sequenced and annotated in the 2000 (Arabidopsis Sequencing Consortium, 2000). *Arabidopsis* offers a diversity of molecular tools for the characterization of its developmental processes, as example is easily transformed by *Agrobacterium tumefaciens* and site specifically mutagenized with the CRISPR/CAS9 tool [2]. Nowadays, community collections are available for the individual research groups, as the Nottingham *Arabidopsis* Stock Centre (NASC, <http://arabidopsis.info/>), which preserves more than 30.000 homozygous T-DNA mutant lines, extremely useful for reverse-genetics approaches. In addition to this, information about genes expression profiles, functions, and many other aspects are available in databases as the Arabidopsis information resource (TAIR, www.arabidopsis.org) and Araport (www.araport.org). These databases are constantly updated with data generated by the scientific community, providing extremely useful resources for plant research. *Arabidopsis* research has contributed to clarify many aspects of plant biology, as the flower development process with the formation of the ABC model or the signalling pathways and the molecular function of many Phyto-hormones as auxin [3].

2. Auxin biosynthesis and polar transport

Developmental processes of plants, as for other living beings, are finely regulated at multiple levels and the hormonal control is one the most important. During plants growth multiple hormones interplay and auxin has been shown to be one of the main regulators controlling differentiation and organogenesis. Auxin biosynthesis occurs through tryptophan dependent or independent pathways. In the tryptophan dependent biosynthesis routes tryptophan is converted into IAA thanks to 4 main pathways: the indole-3-pyruvic acid (IPA) pathway, the indole-3-acetaldoxime (IAOx) pathway, the indole-3-acetamide (IAM) pathway and the tryptamine (TAM) one [4]. Only the IPA and TAM pathways have been characterized in more detail, highlighting their relevance during plant development. In the IPA route, the IAA precursor is the indol-3-pyruvic acid (IPyA), which is produced by TRYPTOPHAN AMINOTRANSFERASE OF ARABIDOPSIS (TAA) enzymes family from the tryptophan. IPyA is then converted to IAA by YUCCA enzymes [5,6]. YUCCA enzymes are also involved in the TAM pathway; indeed they catalyse the conversion of the tryptamine to N-hydroxyl-tryptamine, which is converted into IAA thanks to following steps [7].

Essential for auxin function is its transport from the points of biosynthesis to specific plant tissues, a process which include both long and short distance movements. While long distance transport may occur thanks to the vascular tissues, short distance trafficking relies on specific cellular transporters [8]. In the apoplastic environment, IAA has a neutral form thanks to the low pH (around 5.5), resulting in its passive diffusion through the plasma-membrane into the cytosol. Once in the cytosol, the higher pH (around 7) drives IAA ionization due to the de-protonation of the carboxyl residues, avoiding passive diffusion towards the apoplast. For this reason, auxin movement among cells depends on the activity of two main carrier families: the PIN-FORMED (PIN) family and the ABCB family [9,10]. In *Arabidopsis thaliana*, PIN family is formed by 8 trans-membrane proteins which can be divided into 2 groups in relation to the structure of the hydrophilic loop between the two transmembrane domains. The “long” PINs include PIN 1, 2, 3, 4, 6, 7 which are asymmetrically localized on cells plasma-membranes and are responsible for auxin efflux. PIN 5, 8 belong to the “Short” PINs group, are localized into the endoplasmic reticulum and act as intracellular regulators of auxin compartmentalization and homeostasis [11,12]. Concerning the ABCB transporters, they are a group of 21 proteins, belonging to the ABC transporters super-family. In particular, ABCB 1, 4 and 19 have been shown to be directly

involved in auxin polar efflux. PIN proteins and ABCB transporters can work independently or synergistically to regulate auxin efflux, indeed it has been proved the interaction between PIN1 and ABCB19, and between PIN2 and ABCB1 [13]. Despite auxin influx into the cell may happen *via* passive diffusion, this process can be enhanced by specific influx carriers as AUX1 and LIKE-AUX1 (LAX) proteins, especially in relation to rapid changes in auxin intracellular concentration [9,13].

Polar transport might generate auxin gradients and the formation of points of auxin maxima and minima which act as the main designers of plant development [7]. Indeed, the disruption of polar auxin transport (PAT) results in damaging numerous plant developmental processes as reported for *pin* mutants, or for treatments with PAT inhibitors drugs [14–16]. As example, in *pin1* mutants point of auxin maxima and minima can't be formed, leading to a lack of lateral organs formation [14]. Similarly, mutation in *PINOID (PID)*, which acts as a kinase regulating PIN activity, leads to alteration in PAT showing similar alteration to the one observed for *pin* mutants [17,18]. Auxin flows correlate with PIN proteins cellular polar localization, predicting the points of auxin accumulation and the sites of organs primordia formation, cell-types specification, division and expansion [19]. Indeed, the functionality of local auxin maxima in controlling organs development is suggested by the fact that external application of auxin on *pin1* inflorescences is sufficient to restore flowers bud formation [20]. PIN sub-cellular localization may be highly dynamic, driving rapid switch in auxin flux in association to external or endogenous signals.

3. Auxin signalling

Auxin polar accumulation, resulting from a concerted interplay among its biosynthesis, transport and degradation, is pivotal for the developmental processes related to its activity [21]. The core change caused by auxin levels increase is related to modulation of the transcriptome, with a response which comprises up and down regulation of a set of auxin responsive genes [22]. Among factors involved in the auxin-mediated transcriptional regulation a fundamental role is played by the *AUX/IAA* gene family and by the *AUXIN RESPONSE FACTORS (ARF)* transcriptional factor family [23]. *AUX/IAA* is a family of 29 genes in *Arabidopsis thaliana*, which works as negatively regulators of gene expression [22,24]. *AUX/IAAs* are nuclear localized proteins characterized by three domains, with the

ability to interact with ARFs transcriptional factor thanks to their c-terminal domain. Essential for AUX/IAAs function is a domain called degron which works as target sequence for the SCR^{tir1} E3 ubiquitin ligase complex [25]. The SCR^{TIR1/AFB} E3 ubiquitin ligase complex is able to regulate AUX/IAAs accumulation and stability, promoting their degradation by the 26s proteasome through poly-ubiquitination of the degron. AUX/IAAs are recognised and bound to the SCR^{TIR1/AFB} E3 ubiquitin ligase complex by the F-box TIR1/AFB, conferring specificity to the binding [26].

ARF is a family of transcriptional factors shown to directly regulate the expression of auxin responsive genes. *ARF* genes are expressed in all plant tissues, with specific expression patterns, working synergistically or in antagonistic way to generate a complex *scenario* which governs plant developmental processes [27]. ARFs are B3 type transcriptional factors which bind to specific sequences in the promoter of the auxin responsive genes named auxin-response elements (AuxREs) [28]. The main regulators of ARFs activity are reported to be the AUX/IAAs that interact with them through their c-terminal domain, which is conserved between the two family [29]. AUX/IAAs can interact, on the other side, with co-repressor such as TOPLESS (TPL) by their domain I (EAR domain), which can consequentially recruit chromatin modifiers, inhibiting ARF mediated gene regulation [30].

The mechanism of auxin perception has been clarified thanks to the identification of the F-box TIR1/AFB of the SCR^{TIR1/AFB} E3 complex as the intracellular auxin receptor. Indeed, auxin bind TIR1 in correspondence to a hydrophobic pocket, making available an interactive surface for AUX/IAAs. In this *scenario*, auxin is required to stabilize the TIR1-AUX/IAA interaction, promoting AUX/IAAs degradation by the SCR^{TIR1/AFB} E3 complex activity [23,26]. In cells with auxin low concentration, while ARFs are bind to the AuxREs, the absence of auxin in the TIR1 binding pocket makes AUX/IAAs stable and free to bind ARFs PB1 domain. In cells with high auxin concentration, the AUX/IAAs degradation by the proteasome is enhanced thanks to their increased affinity to the TIR1 receptor, a change that makes an higher ratio of ARFs protein active to promote auxin mediated gene regulation [8]. Auxin response is excellently integrated by the presence of 6 TIR1 /AFB co-receptors in *Arabidopsis thaliana*, with the evidence that different pairs of TIR1/AFB-AUX/IAAs shown a great diversity in auxin affinity, making its perception potentially dissimilar among different cells [31]. In addition to this, different ARFs and AUX/IAAs interact with specific affinity and, at the same time, ARFs can interact with each other creating homo or hetero complexes that show higher or lower affinity to specific AuxREs. ARFs transcriptional activators and

repressors might also compete for the same AuxREs, adding a further level of complexity to the auxin induced gene regulation (fig.1)[23,30,32].

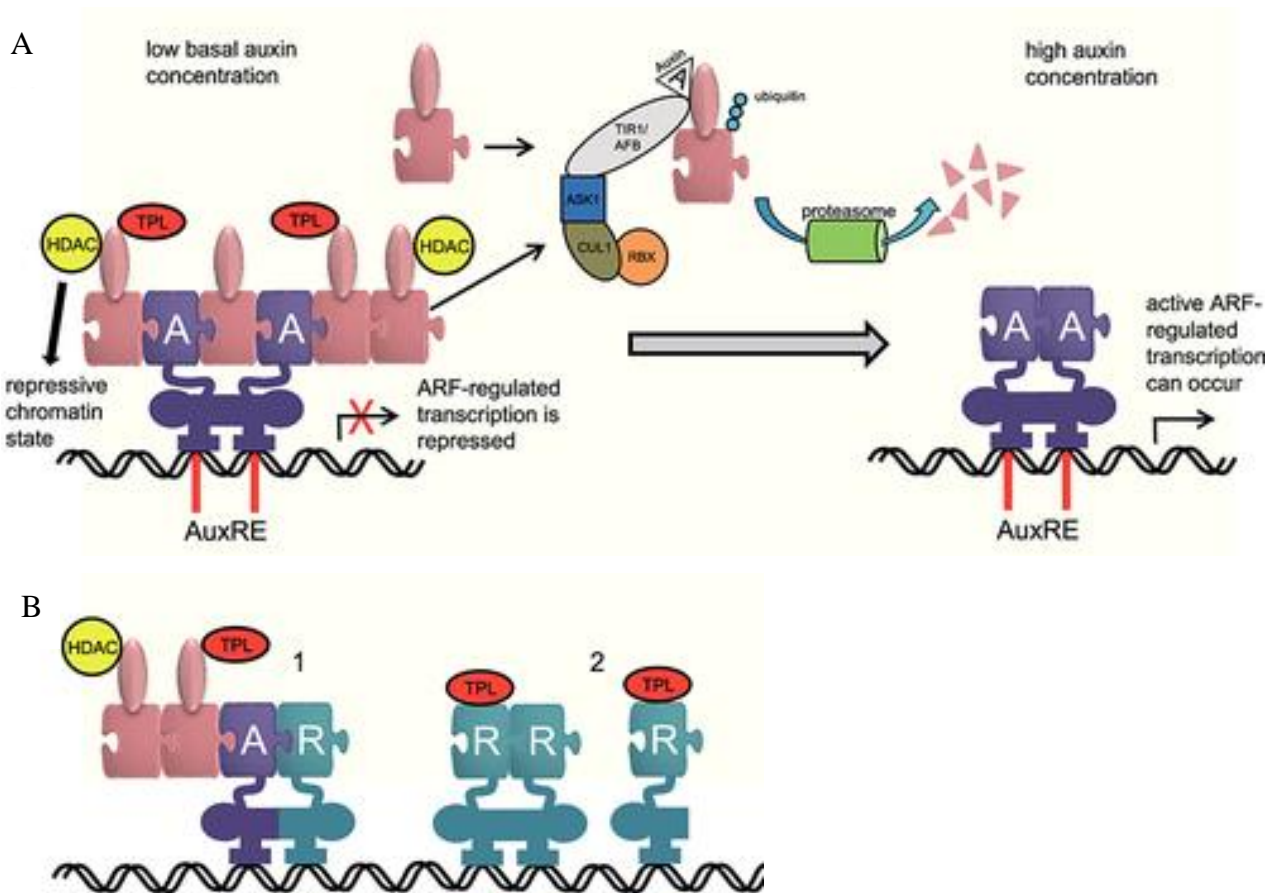


Fig.1: Auxin signalling and ARFs-AUX/IAAs function: (A) scheme of ARFs activity regulation mediated by AUX/IAAs interaction. (B) Mechanism of activator (purple) and repressor (blue) ARFs interplay for target genes regulation. 1, repressors ARFs might interact with activator one to inhibit targets genes expression. 2, repressors ARFs work in competition with activator ARFs for AuxREs requisition. (adapted from Chandler, 2016)

3.1 AUXIN RESPONSE FACTOR family

ARFs family is composed by 22 gene and one pseudo-gene in *Arabidopsis thaliana*, which share a conserved through the evolution modular structure [33]. *ARFs* can be transcriptional activator or repressor and are divided into 3 classes (A, B, C)[34]. All *ARFs* protein have at the N-terminal the B3-type DNA binding domain that binds to auxin-response elements (AuxREs) [28]. AuxREs are formed by a TGTCTC consensus core which can be direct or repeated in a palindromic way [24,35]. Even if the TGTCTC core has been considered the main component of the AuxRE sequences, structural analysis of *ARFs* DBD have revealed an higher affinity to the core sequence TGTCGG [36,37]. In some cases, to the DBD is also associated to a dimerization domain (DD), involved in *ARFs* interaction [37]. Indeed, *ARFs* can homo and heterodimerize to enhance the stability of the binding to the palindromic AuxREs and modulate target genes expression [38]. While the DBD is well conserved among all *ARFs*, the MIDDLE REGION (MR) central domain, is more variable and confer the transcriptional activator or repressor features. The sub-class A comprises activator *ARFs* which are *ARFs* 5, 6, 7, 8, 19, characterized by a MR rich in glutamine, serine and leucine. The other *ARFs* are divided in classes B and C and are transcriptional repressors, activity associated with enrichment in serine, proline and leucine in the MR [39,40]. With the exception of *ARFs* 3,13, 17 and the pseudo-gene *ARF23* all other *ARFs* have at the c-terminal a domain called PB1 domain. The PB1 domain is essential for protein-protein interactions and displays its functionality mediating *ARF*-AUX/IAA complexes formation [32]. The PB1 domain is also involved in *ARF*-*ARF* dimerization even if with an affinity shown to be from 10 to 100 times lower respect to *ARF*-AUX/IAA interaction [41]. The class B and C *ARFs* display a low affinity to AUX/IAAs, suggesting that their contribution to auxin signalling might involve work in an antagonistic way respect to *ARFs* belonging to class A through their interaction or/and by the competition for the AuxREs sequences (fig 1, 2) [42,43]. At sub-threshold auxin concentration, even if A *ARFs* are bound to the AuxREs sequences, the recruitment of co-repressors and histone deacetylases (HDA) by the AUX/IAA linked to the PB1 domain determines a repressive configuration of the chromatin [44]. The model of target genes activation by class A *ARFs* upon auxin sensing has been proposed to involve chromatin accessibility rearrangement mediated by a switch in their interacting partners involved in chromatin modification. For example, it has been reported that *ARF5/MONOPTEROS* interacts with the BODENLOS(IAA12)-TOPLESS-HDA19 complex

in auxin minima, while the auxin induced degradation of BODENLOS results in the recruitment by its MR domain of two SWI/SNF ATPase, BRAHMA (BRM) and SPLAYED (SYD). BRM and SYD are ATPase involved in the disruption of the histone-DNA connections, supporting chromatin accessibility and genes transcription [45]. The increased accessibility of the target loci then can facilitate further association of regulative factors, exponentially enhancing auxin effect on transcriptome regulation [46].

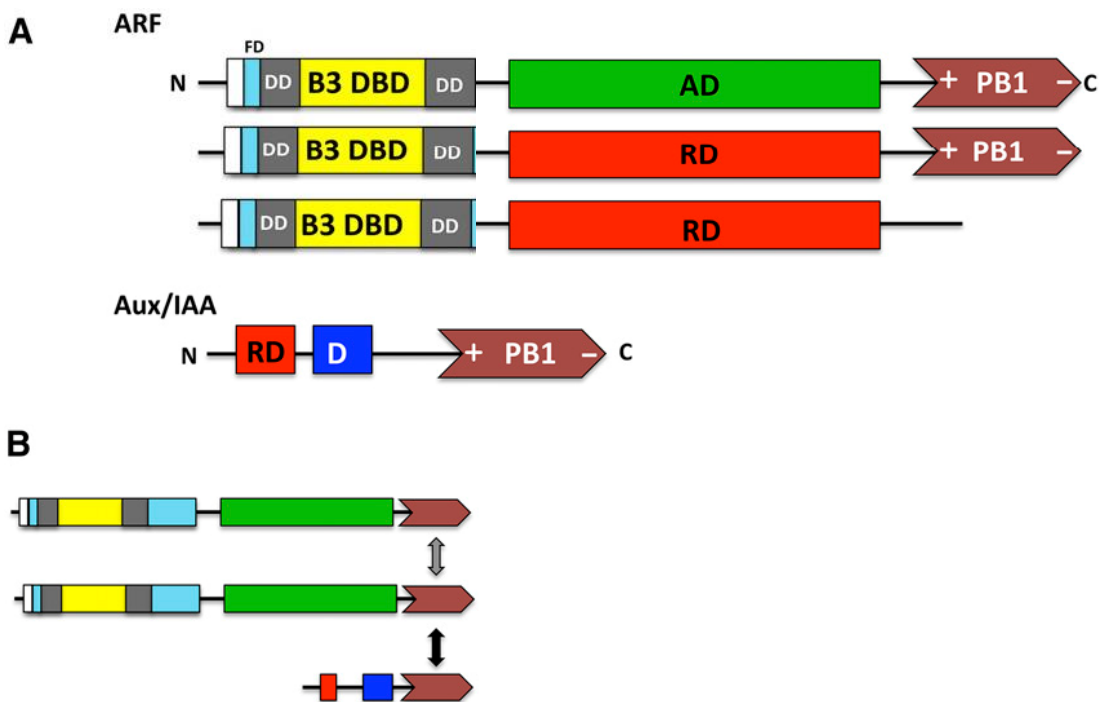


Fig.2: (A) Schematic representation ARFs and AUX/IAAs structure. In yellow the N-terminal B3 DBD while in grey the dimerization domain (DD). AD in green represent the activation domain of class A ARFs, while RD in red the repressor domain of classes B and C ARFs and the EAR domain of AUX/IAAs proteins. In brown the C-terminal PB1 domain. The blue box in AUX/IAAs scheme represent the degron domain. (B) ARFs can dimerize through the PB1 domain, even if with a low affinity respect to the ARF-AUX/IAAs interaction mediated by the same domain. (Adapted from Guilfoyle, 2015).

3.2 The AUXIN RESPONSE FACTOR 5/MONOPTEROS (ARF5/MP)

Among class A ARFs the *AUXIN RESPONSE FACTOR 5/MONOPTEROS (ARF/MP)* is one of the most studied since it has been shown to be involved in many plant developmental processes. *MP* was initially described as a TF required for embryo development. Indeed, *mp* mutants show alterations at the seedling level which include impaired cotyledons, reduced hypocotyl and absence of the root [47]. Particularly, *MP* was described as an activator of its targets in cells with auxin maxima and involved in the definition of the embryo apical-basal axis besides the formation of the primary root [48]. *MP* function and regulation in embryo development has been cleared thanks to the identification of the *AUX/IAA12/BODENLOS (BDL)* as the main *MP* interactor in the auxin minima, inhibiting its function of transcriptional activator [49]. Sequentially, *MP* has been shown to be involved in many more developmental contexts, such as in vascular tissues development thanks to the activation of the transcriptional factor *ATHB8*. *MP/BDL* module function is also associated to post embryonic root development and in lateral root formation [50,51]. Many *mp* mutant alleles were obtained, showing different degrees of penetrance and severity of the impaired phenotypes. The most severe alleles (as the *arf5.1* or *mp-13*) are associated with severe embryo defects and, consequently, those *mp* alleles almost do not show a post embryonic development [52]. Nevertheless, weak *mp* mutants, as the *mpS319*, homozygous plants might reach the reproductive stage, allowing the characterization of *MP* functions in later developmental stages [53]. Weak *mp* mutant plants, at the reproductive level, show dramatic alteration in inflorescences and flowers structure, resulting completely sterile. *MP* has been shown to be a master regulator of flower development process, directly activating the expression of a set of targets which govern flowers formation [54]. Moreover, *MP* plays a central role in ovules differentiation, integrating auxin signalling for ovules primordia formation and enhancing the expression of the genes essentials for ovules development [55].

3.3 Auxin independent *ARFs* regulation

Despite auxin action in plant development has been well characterized, many aspects of *ARFs* regulation are still largely unknown. It has been described that 13 out of 23 *Arabidopsis thaliana* *ARFs* have in their 5' UTR 1 to 6 uORFs [56,57]. The upstream open reading frames (uORFs) are small sequences generally located in the 5' UTR of many eukaryotes mRNAs. uORFs lead to ribosomal arrest and negatively regulate the translation of the downstream ORF, increasing the dissociation of the ribosomes from the mRNA [58]. Indeed, it has been described that uORFs in *ARF3* mRNA regulate its translation, modifying its activity during flower and gynoecium development. Likely, also *ARF5* uORFs has been shown to negatively affect its translation in in-vitro assays [58].

It has been proposed that also alternative splicing (AS) may be a key component of *ARFs* regulation. Alternative splicing is a useful tool which allows the formation of alternative protein isoforms, increasing genes versatility in the various developmental processes. It has been demonstrated *ARF8 pre-mRNA* undergoes alternative splicing events, generating 3 alternative protein isoforms: *ARF8.1*; *ARF8.2* and *ARF8.4* which have tissue-specific accumulations and different functions during stamens and anthers development [59]. Also *ARF4 pre-mRNA* thanks to an AS event generates two protein isoforms: *ARF4* and Δ *ARF4* showing different activities during carpels development [33]. Additionally, in the last *Arabidopsis* genome annotation (Araport11), it has been predicted an alternative splicing event for *MP*, in which the last part of the *pre-mRNA* 5'UTR is recognised as a leader intron. The presence of uORFs in *ARFs* transcripts and the generation of alternative protein isoforms thanks to *pre-mRNA* AS suggest the existence of further level of complexity in *ARFs* regulation. These mechanisms can be partially or completely uncoupled from the classical auxin pathway, modulating its effects on plant development.

ARFs abundance and accumulation patterns can be post-transcriptionally regulated by *miRNAs*, as already reported for *ARF6* and *8*, which are targets of the *miR167* and for *ARF10,16* and *17*, targets of the *miR160*[60,61]. *miRNAs* are small non-coding RNAs generally associated to the RNA-induced silencing complex (RISC) in the cytoplasm. *miRNAs* share high sequence similarity with their *mRNA* targets which, once recognised, are cleaved and degraded by the RISC. Another important non-coding small RNAs-based regulative mechanism, acting on *ARFs*, involves the action of short interfering RNAs

(siRNAs). While miRNAs arise from the processing of local secondary structures of RNAs, siRNAs are generated from long RNA duplexes or extended RNA hairpins, and can operate epigenetic regulations or work as factors involved in gene post-transcriptional silencing [62]. In particular, it has been identified a siRNA called trans-acting small interfering RNA (*ta-siRNA*), which is encoded from the *TAS3* locus and share a high sequence similarity with some *ARFs*. *Ta-siRNA* has been shown to directly regulate *ARF2*, 3 and 4 abundance, restricting their accumulation pattern [63].

4. Auxin and flower development

Flowers arise as primordia from the flower meristem (FM) which differentiate from the peripheral zone (pz) of the inflorescence meristem (IM) and, as lateral organs, their specification is strictly related to auxin accumulation and signalling [64]. The crucial activity of auxin in flower formation results clear in view of the dramatic alteration in inflorescence structure in mutants for PAT. For example, in *Arabidopsis thaliana pin1-1* mutant auxin can't be differentially accumulated along the inflorescence, losing the distinction in points of high and low auxin content. Consequentially, inflorescence structure and flower development result completely impair, leading to the formation of a pin-like shoot [14]. On the other side, local application of auxin in ianolin past on *pin1-1* mutant inflorescences is able to restore flower formation in the point of the application, proving the flower development to be a process strictly related to described elevated auxin levels[20]. In addition to PAT also precise spatio-temporal auxin biosynthesis has been proved to be crucial for the specification of auxin maxima in the inflorescences meristem and, consequentially, for correct flower development and fertility [65]. The centrality of local auxin activity for flowers bud formation is also suggested by the pin-like phenotype of the *mpS319* weak *mp* mutant inflorescences. During flower specification auxin signalling and ARFs activity are involved in the activation of multiple pathways. One of the first events is the limitation of the pluripotency of the cells pool that will give raise to the new primordium, allowing the acquisition of flower meristem identity. In this process a crucial role is played by the downregulation of the meristematic identity gene *SHOOTMERISTEMLESS (STM)*. By in-situ hybridization, *STM* is over accumulated in inflorescence meristems of *mpS319*, and its accumulation is even higher in the triple mutant *mp / arf3 (ettin) / arf4*, resulting in a complete loss of the ability to produce

flower primordia. ARF3/ETTIN has been proved to directly bind *STM* locus, suggesting a direct silencing of *STM* expression for flower fate acquisition. On the other side, MP activate the expression of the I KNOX repressor *FIL*, responsible for *STM* silencing. Furthermore, ETTIN and *FIL* has been found to directly bind and repress the expression of the I KNOX gene *BREVIPEDICELLUS (BP)*, involved in the maintenance of the meristematic identity. Even if MP, ARF3/ETTIN and ARF4 work on parallel pathways to repress *STM* and *BP* expression, it has been proved that *FIL* can create a complex with ETTIN and ARF4, able to recruit chromatin modifiers as the histone deacetylase HDA19, that might lead to *STM* gene silencing [66].

The auxin-induce chromatin remodelling plays a crucial role in the re-programming of the meristematic cells meant to develop into flowers primordia and two components of this process are the SWI/SNF ATPase *BRAHMA (BRM)* and *SPLAYED (SYD)*, responsible for increase chromatin accessibility. *BRM* and *SYD* are expressed in the early flower primordia and their involvement in flower initiation pathway has been pointed out by the reduction of flower primordia in both *mpS319/syd* double mutant and in *mpS319* plants expressing an artificial microRNA responsible for *BRAHMA (miR-BRM)* downregulation. Furthermore, *brm syd* double mutants and *syd/(miR-BRM)* plants develop pin-like inflorescences, previously described for mutants in auxin polar transport and response. It has been proved that MP not only is able to bind *BRM* and *SYD* proteins, but also that the binding results enhanced by auxin application. In addition to this, *BRM* and *SYD* bind MP direct targets *FIL*, *LFY*, *ANT* and *TMO3* [46]. Increasing auxin concentration leads to degradation of AUX/IAAs, making MP suitable for the recruitment of SWI/SNF containing complexes. This switch promotes the re-arrangement of the chromatin state of MP targets, allowing their transcriptional activation and flower primordia initiation.

Even if auxin polar accumulation is essential for the specification of flower meristem founder cells in IM peripheral zone (pz), it has been demonstrated that auxin is also accumulated with a gradient from the pz to the central zone (cz) of the meristem, similarly to MP accumulation pattern, suggesting a function of auxin response in meristem identity maintenance. The meristematic identity of cells in the cz is controlled by the regulatory loop between *WUSCHEL (WUS)* and *CLAVATA3 (CLV3)*, through the function of the *CLAVATA 1 / 2* receptors. *CLV3* expression is regulated by MP direct target *DORNROSCHEN (DRN)*, indeed *CLV3* expression results drastically reduced in *drn* mutant. In addition to this, the double mutant of *drn* and its closest homologue *dornroschen-like (drnl)*, *drn/drnl*, develop

an enlarged meristem in association with a higher accumulation of *WUS* transcript, supporting the importance of MP – DRN pathway in meristem regulation [53,67].

During floral meristem identity acquisition one of the most important auxin function is the activation of the expression of *LEAFY (LFY)*. LFY, together with APETALA 1 (AP1), controls the switch from IM to FM identity, acting as a master regulator of flower development. *lfy* mutants shown dramatic alteration in flower development which include differentiation of IM in place of FM, and formation of flowers with inflorescence-like characteristics [68]. *LFY* is expressed in incipient flower primordia and it is directly regulated by MP [69]. Indeed, MP has been shown to bind *LFY* locus, activating its transcription under high auxin levels. LFY is essential for FM identity acquisition and plays also a role in FM initiation, as suggested by the reduction in flowers primordia in the *mpS319/lfy-2* double mutant. Likewise, LFY accumulation has been proved to partially rescue the *mpS319* defect in flowers initiation, suggesting the existence of multiple auxin-related pathways involved in FM initiation. In addition to this, MP directly activate the transcription of two AINTEGUMENTA-LIKE / PLETHORA transcription factors: *AINTEGUMENTA (ANT)* and *AINTEGUMENTA-LIKE6*. ANT and AIL6 are developmental regulators involved in multiple plant growth aspects. They not only work synergistically with LFY to control FM initiation under the control of MP and auxin signalling, but also directly activate *LFY* expression and finely regulate the proper timing of FM identity acquisition. Indeed, *LFY* expression results delayed in *ant / ail6* double mutant resulting in a delay in FM specification. According to this scenario, ANT and AIL6 work both downstream and in parallel to MP for *LFY* regulation. [70]. Interestingly, LFY is also involved in a positive feedback loop on auxin pathway, leading to the maintenance of the auxin maxima essential for the complete flower differentiation. [54,69].

4.1 Floral meristem determinacy

An essential process for flower development and for the specification of the different flower organs, is the control of the floral meristem determinacy. One of the master regulators of floral meristem determinacy is the MADS-box transcriptional factor AGAMOUS (AG), whose final function is to promote FM termination, indeed *ag* mutants develop indeterminate floral meristems. This function is mediated by repressing the meristematic identity marker *WUSHEL* thanks to the recruitment of the Polycomb Group (PcG) on *WUS* locus and thanks to the activation of *WUS* repressor *KNUCKLES (KNU)* [71,72]. On the other side, AG is antagonized by the action of APETALA2 (AP2) which works as an activator of *WUSHEL* expression [73]. AG-AP2 interplay regulates multiple pathways involved in meristem determinacy, and it has been shown that the regulation of auxin homeostasis is one of them. In particular, AG directly activate the expression of *CRABS CLAW (CRC)* encoding for a transcriptional factor belonging of the YABBY family. CRC represses the expression of the transcriptional factor *TORNADO (TRN2)*, a regulator of auxin homeostasis, required for organs differentiation [74]. The role of AG and CRC in the regulation of auxin homeostasis in the floral meristem is also pointed out by their involvement in the activation of the transcription of the auxin biosynthesis factor *YUCCA 4 (YU4)*. Even if AG and CRC don't directly interact, it has been proved that AG is able to bind *YUC4* promotor, increasing chromatin accessibility thanks to the recruitment of the chromatin remodelling factors CHROMATIN REMODELING FACTOR 11 and 17 (CHR11 / 17). On the other side, CRC is able to directly bind and activate *YUC4* expression [75]. These observations show that auxin homeostasis is an important component of floral meristem determinacy and it is superbly regulated by multiple parallel pathways. AG activate CRC expression, resulting in the modulation of auxin homeostasis though *TRN2* downregulation, while AG and CRC together promote auxin biosynthesis thanks to *YUC4* activation.

The AG-AP2 FM determinacy pathway is also integrated by the function of the *AUXIN RESPONSE FACTOR 3 / ETTIN (ARF3/ETT)*. ETT has been shown to work together with AG in the repression of *WUS* expression in the FM. Indeed, the combination of *ett* mutants with the weak *ag* mutant allele *ag-10* strongly enhance the floral meristem indeterminacy defects. Moreover, *ETT* expression is positively regulated by AG, even if in an indirect way since AG doesn't directly bind *ETT* locus. Finally, *ETT* function in FM determinacy is negatively regulated by AP2 which directly repress it [76].

In addition to its relationship with AG and AP2, ETT plays also an important role in FM determinacy by repressing cytokinin activity. Cytokinin are a negative regulators of FM determinacy as suggested by the aggravation of the indeterminacy phenotype of *ag-10* FMs treated with cytokinin. ETT has been found to directly repress the expression of the *ISOPENTENYLTRANSFERASE 3/5/7 (IPT 3/5/7)*, encoding for enzymes involved in cytokinin biosynthesis. Furthermore, ETT represses the expression of the cytokinin receptor *ARABIDOPSIS HISTIDINE KINASE 4* and indirectly the expression of *LONELY GUY (LOG)*, required for cytokinin biosynthesis [77].

4.2 Gynoecium development

The FM determinacy is intimately related to the differentiation of the female reproductive organ, named the gynoecium, since its differentiation occurs from the centre of the meristem in response to the depletion of the meristematic cells pool. This fact is also supported by the complete loss of the gynoecium in *ag* mutants, suggesting that FM determinacy is essential for female organ differentiation [74,78]. In *Arabidopsis thaliana* flower, the gynoecium has a cylindrical structure and it is formed by two carpels which, during flower development, get fused together leading to the formation of a new meristematic tissue along the join edges called carpel margin meristem (CMM). The CMM originates the placenta, that gives rise to ovules, the septum and the transmitting tract. On the other side, carpels will form the valves of the ovary [79,80]. The mature pistil is formed by the stigma, the style, the ovary which encloses ovules and the gynophore that connects the gynoecium to the flower. The stigma is a specialized structure that facilitates pollination and pollen germination, allowing pollen tubes growing into the style and the transmitting tract to reach ovules. Internally, the septum divides the ovary in two halves along the medial axis, leading to the acquisition of a bilateral symmetry by the ovary. Externally, on the same plane, the replum divides the two valves which represent the ovary lateral domains. Between the replum and the valves a narrow domain of cells form the valve margin, which will allow seeds dispersal at fruit maturity. The gynoecium is also defined by an adaxial-abaxial developmental pattern. In the adaxial side, the CMM activity leads to the formation of placenta, ovules and septum whereas the abaxial side, lacks of meristematic properties (fig.3) [81,82].

One of the best characterize ARF involved in pistil development is ETTIN whose activity has been shown to be required to establish the apical/basal and adaxial/abaxial developmental patterns, as supported by the characterization of *arf3/ett* mutants. In *ett*, these alterations include reduction in valves and the expansion of the stigmatic tissue, with the ectopic development in the abaxial domain of transmitting tract and stigma [80,83]. The alteration in the adaxial/abaxial axis specification it has also been described in plants carrying mutation in *KANADI (KAN)* genes [84]. *KAN* genes encode for GARP transcriptional factors and are involved in adaxial / abaxial identity acquisition in many plant organs. At least *KAN1* and *KAN4* have been proved to directly interact with *ETT*, forming a complex required for axis development [85]. An interesting process during the gynoecium development is the switch from bilateral to radial symmetry required to form the style. Two main factors involved in this process are the transcriptional factor *SPATULA (SPT)* and *INDEHISCENT (IND)*. *Spt* mutants do not develop the radial symmetry required to form the style and the stigma and, in *spt/ind* double mutants, the style and stigma defects resulted enhanced. The bilateral to radial symmetry transition requires dynamic changes in auxin concentration. Auxin maxima are initially two foci in the lateral domain in the gynoecium apex, and became four in the next developmental stage with two extra foci in the medial domain. Lateral on, just before the style development, one ring of high auxin concentration is required. It seem that a *SPT/IND*-dependent rearrangement of PIN proteins is responsible for this temporal changes of auxin concentration [86]. *IND* action on PINs organization pass through the direct repression of *PINOID (PID)*, that encode for the serine-threonine kinase required for a proper PIN proteins localization [18]. In addition to *IND-SPT* roles in the regulation of auxin transport during gynoecium development, it has been shown that *SPT* can interact with the bHLH transcriptional factors *HECATE* to regulate *PIN1* and *PIN3* expression and, at the same time, block cytokinin signalling [87].

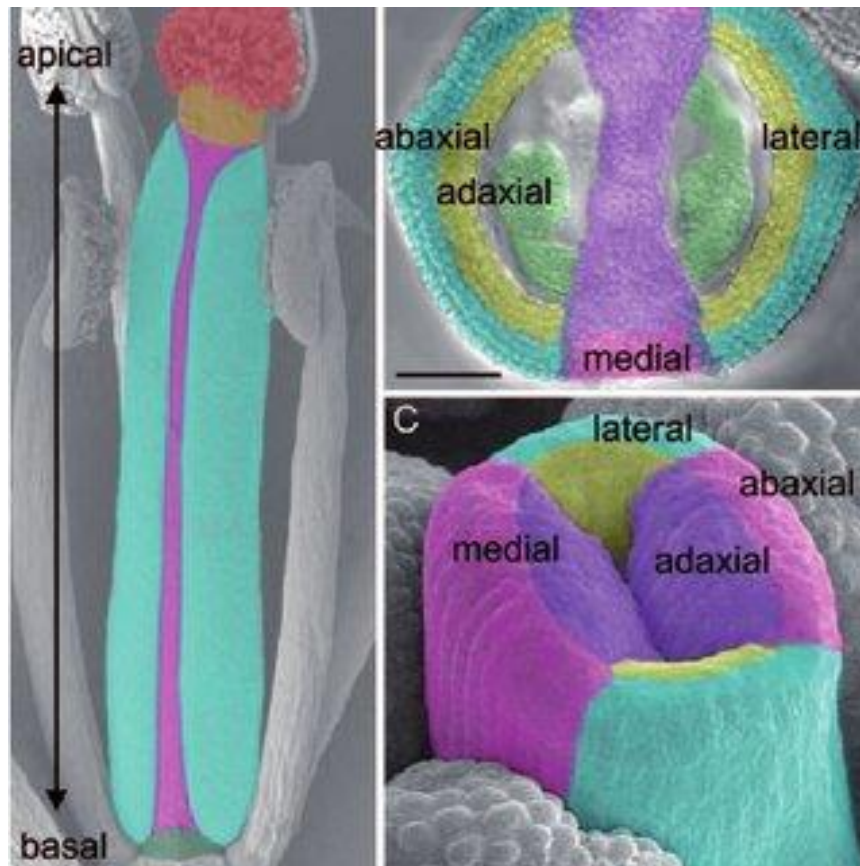


Fig.3: Mature *Arabidopsis thaliana* gynoecium with axis differentiation and different tissues. (adapted from Larsson and Sundberg, 2013)

5. Auxin and ovules development

The main function of the gynoecium in flowering plants is to give rise and protect ovules which, after the double fertilization, develop into the seeds. Ovules originate as lateral primordia from periclinal division of the placenta, and they can be distinguished into three main structures along the proximal-distal axis: funiculus, chalaza and nucellus. The funiculus works as a link between the ovule and the pistil while from the chalaza will develop the outer and inner integuments, that after the double fertilization originate the seed coat. The nucellus will differentiate the female germ line progenitor named Megaspore Mother Cell (MMC) that upon mega-sporogenesis and mega-gametogenesis will give rise to female gametophyte [88]. The MMC undergoes meiosis producing 4 haploids megaspores. Three megaspores degenerate while the remaining one, the functional megaspore, after 4 rounds of mitosis gives rise to the mature embryo sac. The embryo sac, or female gametophyte, is formed by

three antipodal cells at the chalazal pole, the bi-nucleated central cell and, at the micropylar pole, the egg cell and the two synergid cells [89]. As lateral primordia, ovules formation is associated with polar auxin transport and to the formation of auxin maxima points. PIN1 and PIN3 act during ovules development process generating auxin fluxes toward ovules primordia tip and supporting primordia initiation. Indeed, ovule number is greatly reduced in *pin1-5* weak mutant [90]. Ovules primordia specification and growth is a concerted interplay between meristematic activity and the establish of points of separation around the new developing organs known as organ boundaries. Ovule primordia growth and their later development are associated with the function of many transcriptional factors such as AINTEGUMENTA (ANT) and HUELLENLOS (HLL) whose mutants show reduction in ovules number and severe developmental defects [91,92]. On the other side, the two main players involved in ovule boundaries specification are the NAC transcription factors *CUC1* and 2. Indeed, *cuc1/cuc2* double mutant fails to develop a full ovules set and never gives viable seeds [93]. Auxin signalling is integrated into ovules primordia initiation and development by the function of MP. In the *mpS319*, the few pistils that are formed lack of the placental tissue and consequentially of ovules [53]. MP has been demonstrated to directly bind *ANT*, *CUC1* and *CUC2* regulatory regions, activating their transcription[55]. Therefore, MP function not only is required for primordia growth but also for the correct specification of the boundary regions. *CUC 1* and 2 are also involved in *PIN1* expression and cellular polar localization, reinforcing auxin flux toward the primordium tip for the following ovule developmental stages (fig.4) [55]. It has been reported that auxin signalling is also essential for the positional specification of the different embryo sac cells. Indeed, mutation in *ARFs* and in *TIR* genes, as well as ectopic expression of *YUCCA* genes, result in switches in female gametophyte cells identity, losing synergids cells or shifting micropylar cells identity toward the chalazal end [94–96]. Also *ARF3/ETT* contributes to ovule development process, positively regulating the megaspore mother cell (MMC) identity acquisition. *ARF3/ETT* mis-expression in ovules epidermal cells cause supernumerary MMCs formation. It has been proposed that the *TAS3 ta-siRNA* limits *ARF3/ETT* expression patten in ovules primordia, avoiding excessive MMCs [97].

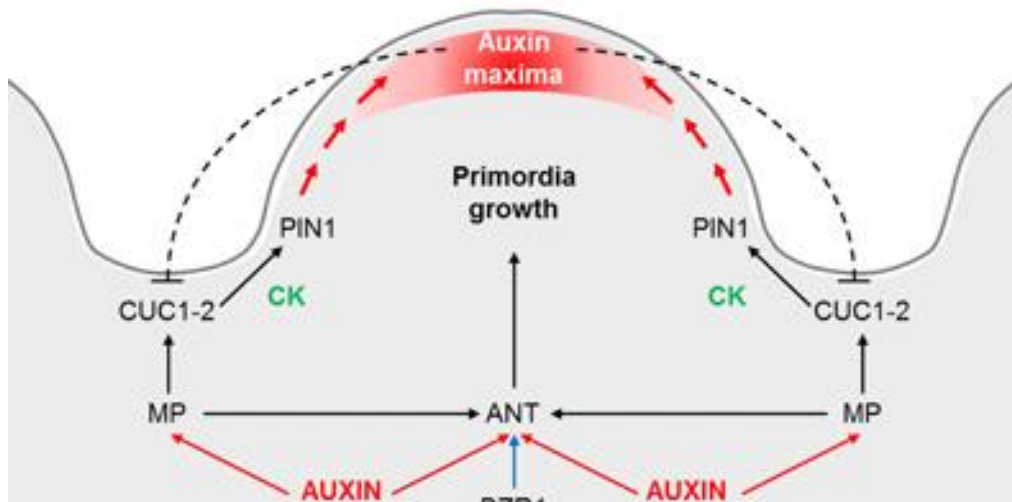


Fig.4: Model of ovules primordia formation. *MP* activity is triggered by auxin levels and results in *ANT* and *CUC1,2* expression, controlling primordia expansion and boundaries set. *CUC1* and *CUC2* are then involved in *PIN1* activation, leading to auxin accumulation in the primordia tip. (adapted from Cucinotta *et al.*, 2014).

6. Auxin and root development

Even if the main focus of our research has been auxin effects on *Arabidopsis* reproductive development, ARFs function and auxin signalling are also intimately related to root development process. Root system not only offers support to the aerial part of the plant, but also represent the interconnection point with the soil, working for nutrient and water uptake and monitoring the environmental conditions. Roots are formed by different tissue types, organised along the proximal-distal and radial axis. Along the proximal-distal axis, at the root tip, root apical meristem (RAM) host the quiescent center (QC) that contains the stem cells. [98]. The RAM is the point of root elongation and, the continue cells division, brings cells from the RAM to the elongation zone where cells acquire their identity. Along the radial axis in the elongation zone, from the external toward the centre of the root, it is possible to distinguish: the epidermis, the cortex, the endodermis, the pericycle and the central stele where vascular tissues originate [99]. Auxin has been shown to promote root initiation and inhibit root elongation, suggesting its involvement in multiple root developmental pathways [100]. The stem cell niche and the root tip are points of auxin biosynthesis, contributing to auxin pool for PAT [101]. However, the major part of auxin accumulated in the root is shoot derived, and moved by the action of PINs creating a robust pattern of maxima and minima

points. Auxin is transported in the vasculature from the shoot to the root tip by PIN 1,3 and 7 and it is distributed in the root cap. Then, PIN proteins in the outer cell layers redistribute auxin back toward the shoot until the transition between the RAM and the elongation zone, creating a flux loop. Once there, auxin is re-directed in the central stele to the vascular auxin stream (fig.5) [102]. Auxin fluxes generate a point of maxima in the QC, and it has been shown that PAT disruption leads to alternation in root patterning and differentiation. In addition, ectopic auxin accumulation is sufficient to induce root re-organization[103]. The specification and maintenance of the root stem cells niche is associated with the function of two AP2 class transcriptional factors: PLETHORA 1,2. *PLT 1,2* are transcribed in relation to auxin maxima and have a peak of expression in the QC. Particularly, mutation in these genes are associated to loss of root stem cells while, ectopic expression of *PLT2*, leads to formation of ectopic root meristems [104]. Additionally, it has been reported that the combination of *mp* and *arf7* mutations disrupt the function and organization of the root apical meristem. On the other side, the single *arf7* mutant does not show alternation in RAM organisation, suggesting that MP plays a crucial role in root meristem maintenance. It has been shown that MP, through the direct binding and activation of PINs, promotes auxin polar transport in root, supporting its development [105,106].

Auxin plays also a role in lateral roots (LR) formation. LRs originate from few cells of the pericycle, in association to auxin maxima in the nearby vascular tissue. LR initials start to proliferate and form a primordium which growth on the radial axis toward the epidermis [107]. Auxin biosynthesis, transport and signalling are key points in LRs set and development. Indeed, PAT disruption and mutation in several *AUX/IAAs* are associated to alteration in LRs differentiation [64]. In addition, *arf7/arf19* double mutant is associated to a dramatic reduction in LRs, but multiple ARFs are involved in this developmental process as suggested by the reduction and in the positional alteration of LRs in *mp* mutants [108,109]. ARF7 and ARF19 directly activate the expression of *LATERAL ORGAN BOUNDARIES-DOMAIN 16* and *29 (LBD16,29)* genes, which act as positive regulators of LRs formation [110].

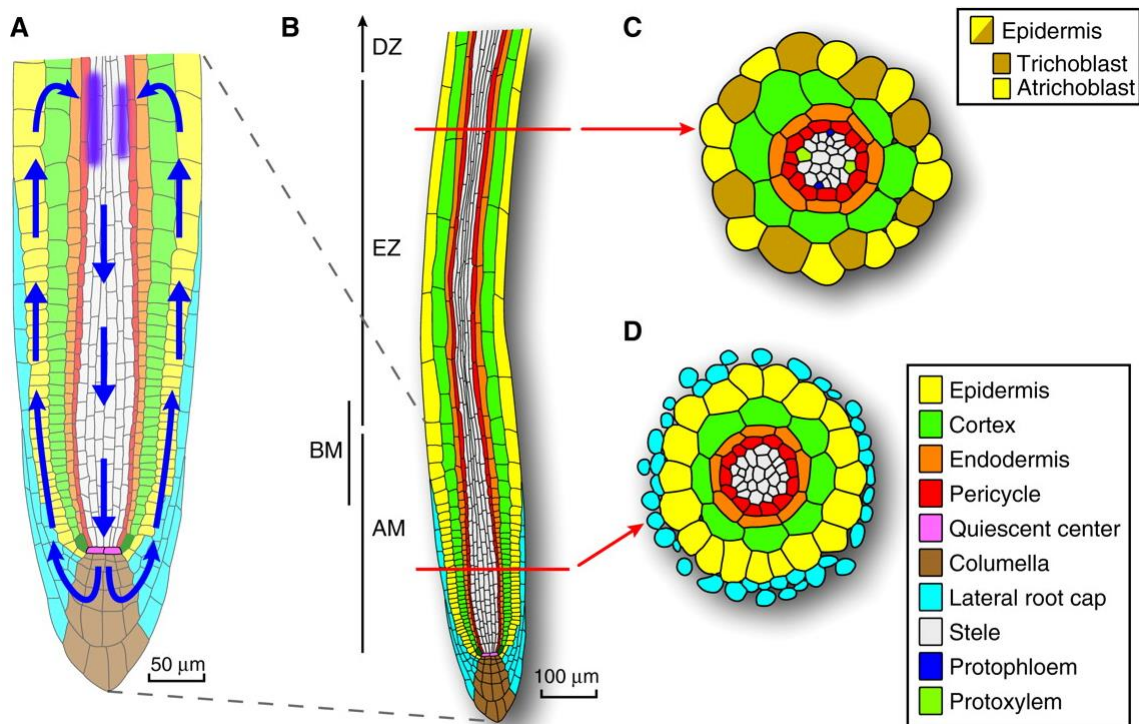


Fig.5: *Arabidopsis thaliana* primary root organization. (A) Auxin fluxes in the root tip: Auxin flows from the shoot to the root tip and is subsequently re-distributed through the epidermis generating a loop. (B) Longitudinal division of root tip zones along the proximal-distal axis: AM, root apical meristem; EZ, elongation zone; DZ, differentiation zone. (C, D) Different tissues that compose the root in cross-section in the root apical meristem and in the elongation zone. (adapted from Benfey, 2012)

Auxin and ARFs transcriptional factors are one of the bases of the whole plant life cycle, driving almost the totality of the different developmental processes that have to be activated and regulated, from root organization to ovule development. Auxin offers the basal signals for new organs growth, tissues organisation and maintenance. This makes auxin and ARFs study of great importance to understand and unveil the molecular mechanisms behind plant life and growth. In particular, we have focused our attention of the study of MP, which has been shown to be a fundamental connector from auxin perception to cellular response in both vegetative and reproductive growth.

References

1. Woodward, A.W., and Bartel, B. (2018). Biology in bloom: A primer on the arabidopsis thaliana model system. *Genetics* 208, 1337–1349.
2. Fauser, F., Schiml, S., and Puchta, H. (2014). Both CRISPR/Cas-based nucleases and nickases can be used efficiently for genome engineering in *Arabidopsis thaliana*. *Plant J.* 79, 348–359.
3. Provart, N.J., Alonso, J., Assmann, S.M., Bergmann, D., Brady, S.M., Brkljacic, J., Browse, J., Chapple, C., Colot, V., Cutler, S., *et al.* (2016). 50 years of Arabidopsis research: Highlights and future directions. *New Phytol.* 209, 921–944.
4. Woodward, A.W., and Bartel, B. (2005). Auxin: Regulation, action, and interaction. *Ann. Bot.* 95, 707–735.
5. Mashiguchi, K., Tanaka, K., Sakai, T., Sugawara, S., Kawaide, H., Natsume, M., Hanada, A., Yaeno, T., Shirasu, K., Yao, H., *et al.* (2011). The main auxin biosynthesis pathway in Arabidopsis. *Proc. Natl. Acad. Sci. U. S. A.* 108, 18512–18517.
6. Enders, T.A., and Strader, L.C. (2015). Auxin activity: Past, present, and future. *Am. J. Bot.* 102, 180–196.
7. Vanneste, S., and Friml, J. (2009). Auxin: A Trigger for Change in Plant Development. *Cell* 136, 1005–1016.
8. Teale, W.D., Paponov, I.A., and Palme, K. (2006). Auxin in action: signalling, transport and the control of plant growth and development. *Nat. Rev. Mol. Cell Biol.* 7, 847–859. Available at: <http://www.nature.com/doi/10.1038/nrm2020>.
9. Zazimalova, E. (2015). Why So Many? -- Auxin Transporters .pdf. 1–15.
10. van Berkel, K., de Boer, R.J., Scheres, B., and ten Tusscher, K. (2012). Polar auxin transport: Models and mechanisms. *Dev.* 140, 2253–2268.
11. Křeček, P., Skůpa, P., Libus, J., Naramoto, S., Tejos, R., Friml, J., and Zažímalová, E. (2009). The PIN-FORMED (PIN) protein family of auxin transporters. *Genome Biol.* 10, 249. Available at: <http://genomebiology.biomedcentral.com/articles/10.1186/gb-2009-10-12-249>.

12. Wisniewska, J., Xu, J., Seifartová, D., Brewer, P.B., Růžička, K., Blilou, L., Rouquié, D., Benková, E., Scheres, B., and Friml, J. (2006). Polar PIN localization directs auxin flow in plants. *Science* (80-.). 312, 883.
13. Titapiwatanakun, B., and Murphy, A.S. (2009). Post-transcriptional regulation of auxin transport proteins: Cellular trafficking, protein phosphorylation, protein maturation, ubiquitination, and membrane composition. *J. Exp. Bot.* 60, 1093–1107.
14. Okada, K., Ueda, J., Komaki, M.K., Bell, C.J., and Shimura, Y. (1991). Requirement of the auxin polar transport system in early stages of Arabidopsis floral bud formation. *Plant Cell* 3, 677–684.
15. Fujita, H., and Syono, K. (1996). Genetic analysis of the effects of polar auxin transport inhibitors on root growth in Arabidopsis thaliana. *Plant Cell Physiol.* 37, 1094–1101.
16. Muday, G.K., and DeLong, A. (2001). Polar auxin transport: Controlling where and how much. *Trends Plant Sci.* 6, 535–542.
17. Bennett, S.R.M., Alvarez, J., Bossinger, G., and Smyth, D.R. (1995). Morphogenesis in pinoid mutants of Arabidopsis thaliana. *Plant J.* 8, 505–520.
18. Benjamins, R., Quint, A., Weijers, D., Hooykaas, P., and Offringa, R. (2001). The PINOID protein kinase regulates organ development in Arabidopsis by enhancing polar auxin transport. *Development* 128, 4057–4067.
19. Grieneisen, V.A., Xu, J., Marée, A.F.M., Hogeweg, P., and Scheres, B. (2007). Auxin transport is sufficient to generate a maximum and gradient guiding root growth. *Nature* 449, 1008–1013.
20. Reinhardt, D., Mandel, T., and Kuhlemeier, C. (2000). Reinhardt. 12, 1–12. Available at: papers3://publication/uuid/3FD5FE71-D17A-4D77-A9BA-20DFC000B01E.
21. Paciorek, T., and Friml, J. (2006). Auxin signaling. *J. Cell Sci.* 119, 1199–1202.
22. Paponov, I.A., Paponov, M., Teale, W., Menges, M., Chakrabortee, S., Murray, J.A.H., and Palme, K. (2008). Comprehensive transcriptome analysis of auxin responses in Arabidopsis. *Mol. Plant* 1, 321–337. Available at: <http://dx.doi.org/10.1093/mp/ssm021>.
23. Lavy, M., and Estelle, M. (2016). Mechanisms of auxin signaling. *Dev.* 143, 3226–

3229.

24. Ulmasov, T., Murfett, J., Hagen, G., and Guilfoyle, T.J. (1997). Creation of a Highly Active Synthetic AuxRE. *Society* 9, 1963–1971. Available at: <http://www.pubmedcentral.nih.gov/articlerender.fcgi?artid=157050&tool=pmcentrez&rendertype=abstract>.
25. Ramos, J.A., Zenser, N., Leyser, O., and Callis, J. (2001). Rapid degradation of auxin/indoleacetic acid proteins requires conserved amino acids of domain II and is proteasome dependent. *Plant Cell* 13, 2349–2360.
26. Tan, X., Calderon-Villalobos, L.I.A., Sharon, M., Zheng, C., Robinson, C. V., Estelle, M., and Zheng, N. (2007). Mechanism of auxin perception by the TIR1 ubiquitin ligase. *Nature* 446, 640–645.
27. Rademacher, E.H., Möller, B., Lokerse, A.S., Llavata-Peris, C.I., Van Den Berg, W., and Weijers, D. (2011). A cellular expression map of the Arabidopsis AUXIN RESPONSE FACTOR gene family. *Plant J.* 68, 597–606.
28. Li, S.-B., Xie, Z.-Z., Hu, C.-G., and Zhang, J.-Z. (2016). A Review of Auxin Response Factors (ARFs) in Plants. *Front. Plant Sci.* 7, 1–7. Available at: <http://journal.frontiersin.org/Article/10.3389/fpls.2016.00047/abstract>.
29. Guilfoyle, T.J. (2015). The PB1 domain in auxin response factor and aux/IAA proteins: A versatile protein interaction module in the auxin response. *Plant Cell* 27, 33–43.
30. Leyser, O. (2018). Auxin signaling. *Plant Physiol.* 176, 465–479.
31. Irina, L., Villalobos, a C., Lee, S., Oliveira, C. De, Ivetac, A., Brandt, W., Armitage, L., Sheard, L.B., Tan, X., Parry, G., *et al.* (2012). A combinatorial TIR1/AFB-Aux/IAA co-receptor system for differential sensing of auxin. *Nat. Chem. Biol.* 8, 477–485.
32. Vernoux, T., Brunoud, G., Farcot, E., Morin, V., Van Den Daele, H., Legrand, J., Oliva, M., Das, P., Larrieu, A., Wells, D., *et al.* (2011). The auxin signalling network translates dynamic input into robust patterning at the shoot apex. *Mol. Syst. Biol.* 7.
33. Finet, C., Berne-Dedieu, A., Scutt, C.P., and Marlétaz, F. (2013). Evolution of the ARF gene family in land plants: Old domains, new tricks. *Mol. Biol. Evol.* 30, 45–56.
34. Okushima, Y., Overvoorde, P.J., Arima, K., Alonso, J.M., Chan, A., Chang, C., Ecker,

- J.R., Hughes, B., Lui, A., Nguyen, D., *et al.* (2005). Functional Genomic Analysis of the AUXIN RESPONSE FACTOR Gene Family Members in *Arabidopsis thaliana*. *Plant Cell* 17, 444–463. Available at: <http://www.plantcell.org/content/17/2/444.short>.
35. Guilfoyle, T., Hagen, G., Ulmasov, T., and Murfett, J. (1998). How does auxin turn on genes? *Plant Physiol.* 118, 341–347.
 36. Liao, C.Y., Smet, W., Brunoud, G., Yoshida, S., Vernoux, T., and Weijers, D. (2015). Reporters for sensitive and quantitative measurement of auxin response. *Nat. Methods* 12, 207–210.
 37. Boer, D.R., Freire-Rios, A., Van Den Berg, W.A.M., Saaki, T., Manfield, I.W., Kepinski, S., López-Vidriero, I., Franco-Zorrilla, J.M., De Vries, S.C., Solano, R., *et al.* (2014). Structural basis for DNA binding specificity by the auxin-dependent ARF transcription factors. *Cell* 156, 577–589.
 38. Ulmasov, T., Hagen, G., and Guilfoyle, T.J. (1999). Dimerization and DNA binding of auxin response factors. *Plant J.* 19, 309–319.
 39. Guilfoyle, T.J., and Hagen, G. (2007). Auxin response factors. *Curr. Opin. Plant Biol.* 10, 453–460.
 40. Weijers, D., and Wagner, D. (2016). Transcriptional Responses to the Auxin Hormone. *Annu. Rev. Plant Biol.* 67, 539–574.
 41. Han, M., Park, Y., Kim, I., Kim, E.H., Yu, T.K., Rhee, S., and Suh, J.Y. (2014). Structural basis for the auxin-induced transcriptional regulation by Aux/IAA17. *Proc. Natl. Acad. Sci. U. S. A.* 111, 18613–18618.
 42. Richter, R., Behringer, C., Zourelidou, M., and Schwechheimer, C. (2013). Convergence of auxin and gibberellin signaling on the regulation of the GATA transcription factors GNC and GNL in *Arabidopsis thaliana*. *Proc. Natl. Acad. Sci. U. S. A.* 110, 13192–13197.
 43. Roosjen, M., Paque, S., and Weijers, D. (2018). Auxin Response Factors: Output control in auxin biology. *J. Exp. Bot.* 69, 179–188.
 44. Chandler, J.W. (2016). Auxin response factors. *Plant Cell Environ.* 39, 1014–1028.
 45. Bezhani, S., Winter, C., Hershman, S., Wagner, J.D., Kennedy, J.F., Chang, S.K.,

- Pfluger, J., Su, Y., and Wagner, D. (2007). Unique, shared, and redundant roles for the Arabidopsis SWI/SNF chromatin remodeling ATPases Brahma and Splayed. *Plant Cell* 19, 403–416.
46. Wu, M.F., Yamaguchi, N., Xiao, J., Bargmann, B., Estelle, M., Sang, Y., and Wagner, D. (2015). Auxin-regulated chromatin switch directs acquisition of flower primordium founder fate. *Elife* 4, 1–20.
47. Berleth, T., and Jürgens, G. (1993). The role of the *monopteros* gene in organising the basal body region of the Arabidopsis embryos. *Trends Genet.* 9, 299. Available at: <http://linkinghub.elsevier.com/retrieve/pii/016895259390246E>.
48. Hardtke, C.S., and Berleth, T. (1998). The Arabidopsis gene *MONOPTEROS* encodes a transcription factor mediating embryo axis formation and vascular development. *EMBO J.* 17, 1405–1411. Available at: <http://www.ncbi.nlm.nih.gov/pubmed/9482737> <http://www.pubmedcentral.nih.gov/articlerender.fcgi?artid=PMC1170488>.
49. Weijers, D., Schlereth, A., Ehrismann, J.S., Schwank, G., Kientz, M., and Jürgens, G. (2006). Auxin triggers transient local signaling for cell specification in Arabidopsis embryogenesis. *Dev. Cell* 10, 265–270.
50. De Smet, I., Lau, S., Voß, U., Vanneste, S., Benjamins, R., Rademacher, E.H., Schlereth, A., De Rybel, B., Vassileva, V., Grunewald, W., *et al.* (2010). Bimodular auxin response controls organogenesis in Arabidopsis. *Proc. Natl. Acad. Sci. U. S. A.* 107, 2705–2710.
51. Donner, T.J., Sherr, I., and Scarpella, E. (2009). Regulation of preprocambial cell state acquisition by auxin signaling in Arabidopsis leaves. *Development* 136, 3235–3246.
52. Odat, O., Gardiner, J., Sawchuk, M.G., Verna, C., Donner, T.J., and Scarpella, E. (2014). Characterization of an allelic series in the *MONOPTEROS* gene of Arabidopsis. *Genesis* 52, 127–133.
53. Cole, M., Chandler, J., Weijers, D., Jacobs, B., Comelli, P., and Werr, W. (2009). *DORNROSCHEN* is a direct target of the auxin response factor *MONOPTEROS* in the Arabidopsis embryo. *Development* 136, 1643–1651.
54. Yamaguchi, N., Wu, M.F., Winter, C.M., Berns, M.C., Nole-Wilson, S., Yamaguchi, A.,

- Coupland, G., Krizek, B.A., and Wagner, D. (2013). A Molecular Framework for Auxin-Mediated Initiation of Flower Primordia. *Dev. Cell* 24, 271–282.
55. Galbiati, F., Sinha Roy, D., Simonini, S., Cucinotta, M., Ceccato, L., Cuesta, C., Simaskova, M., Benkova, E., Kamiuchi, Y., Aida, M., *et al.* (2013). An integrative model of the control of ovule primordia formation. *Plant J.* 76, 446–455.
 56. Nishimura, T., Wada, T., Yamamoto, K.T., and Okada, K. (2005). The Arabidopsis STV1 protein, responsible for translation reinitiation, is required for auxin-mediated gynoecium patterning. *Plant Cell* 17, 2940–2953.
 57. Hayashi, N., Sasaki, S., Takahashi, H., Yamashita, Y., Naito, S., and Onouchi, H. (2017). Identification of Arabidopsis thaliana upstream open reading frames encoding peptide sequences that cause ribosomal arrest. *Nucleic Acids Res.* 45, 8844–8858.
 58. Calvo, S.E., Pagliarini, D.J., and Mootha, V.K. (2009). Upstream open reading frames cause widespread reduction of protein expression and are polymorphic among humans. *Proc. Natl. Acad. Sci. U. S. A.* 106, 7507–7512.
 59. Ghelli, R., Brunetti, P., Napoli, N., De Paolis, A., Cecchetti, V., Tsuge, T., Serino, G., Matsui, M., Mele, G., Rinaldi, G., *et al.* (2018). A newly identified flower-specific splice variant of AUXIN RESPONSE FACTOR8 regulates stamen elongation and endothecium lignification in arabidopsis. *Plant Cell* 30, 620–637.
 60. Mallory, A.C., Bartel, D.P., and Bartel, B. (2005). MicroRNA-directed regulation of Arabidopsis AUXIN RESPONSE FACTOR17 is essential for proper development and modulates expression of early auxin response genes. *Plant Cell* 17, 1360–75.
 61. Wu, M.F., Tian, Q., and Reed, J.W. (2006). Arabidopsis microRNA 167 controls patterns of ARF6 and ARF8 expression, and regulates both female and male reproduction. *Development* 133, 4211–4218.
 62. Vazquez, F., Vaucheret, H., Rajagopalan, R., Lepers, C., Gascioli, V., Mallory, A.C., Hilbert, J.L., Bartel, D.P., and Cr  t  , P. (2004). Endogenous trans-acting siRNAs regulate the accumulation of arabidopsis mRNAs. *Mol. Cell* 16, 69–79.
 63. Williams, L., Carles, C.C., Osmont, K.S., and Fletcher, J.C. (2005). A database analysis method identifies an endogenous trans-acting short-interfering RNA that targets the Arabidopsis ARF2, ARF3, and ARF4 genes. *Proc. Natl. Acad. Sci. U. S.*

A. 102, 9703–9708.

64. Alvarez-Buylla, E.R., Benítez, M., Corvera-Poiré, A., Chaos Cador, Á., de Folter, S., Gamboa de Buen, A., Garay-Arroyo, A., García-Ponce, B., Jaimes-Miranda, F., Pérez-Ruiz, R. V., *et al.* (2010). Flower Development A. S. of P. Biologists
65. Brumos, J., Robles, L.M., Yun, J., Vu, T.C., Jackson, S., Alonso, J.M., and Stepanova, A.N. (2018). Local Auxin Biosynthesis Is a Key Regulator of Plant Development. *Dev. Cell* 47, 306-318.e5.
66. Chung, Y., Zhu, Y., Wu, M.F., Simonini, S., Kuhn, A., Armenta-Medina, A., Jin, R., Østergaard, L., Gillmor, C.S., and Wagner, D. (2019). Auxin Response Factors promote organogenesis by chromatin-mediated repression of the pluripotency gene SHOOTMERISTEMLESS. *Nat. Commun.* 10.
67. Luo, L., Zeng, J., Wu, H., Tian, Z., and Zhao, Z. (2018). A Molecular Framework for Auxin-Controlled Homeostasis of Shoot Stem Cells in Arabidopsis. *Mol. Plant* 11, 899–913. Available at: <https://doi.org/10.1016/j.molp.2018.04.006>.
68. Weigel, D., Alvarez, J., Smyth, D.R., Yanofsky, M.F., and Meyerowitz, E.M. (1992). LEAFY controls floral meristem identity in Arabidopsis. *Cell* 69, 843–859.
69. Li, W., Zhou, Y., Liu, X., Yu, P., Cohen, J.D., and Meyerowitz, E.M. (2013). LEAFY controls auxin response pathways in floral primordium formation. *Sci. Signal.* 6.
70. Yamaguchi, N., Jeong, C.W., Nole-Wilson, S., Krizek, B.A., and Wagner, D. (2016). AINTEGUMENTA and AINTEGUMENTA-LIKE6/ PLETHORA3 Induce LEAFY expression in response to auxin to promote the onset of flower formation in arabidopsis. *Plant Physiol.* 170, 283–293.
71. Liu, X., Kim, Y.J., Müller, R., Yumul, R.E., Liu, C., Pan, Y., Cao, X., Goodrich, J., and Chen, X. (2011). AGAMOUS terminates floral stem cell maintenance in arabidopsis by directly repressing WUSCHEL through recruitment of Polycomb Group proteins. *Plant Cell* 23, 3654–3670.
72. Sun, B., Xu, Y., Ng, K.H., and Ito, T. (2009). A timing mechanism for stem cell maintenance and differentiation in the Arabidopsis floral meristem. *Genes Dev.* 23, 1791–1804.
73. Huang, Z., Shi, T., Zheng, B., Yumul, R.E., Liu, X., You, C., Gao, Z., Xiao, L., and

- Chen, X. (2017). *APETALA2* antagonizes the transcriptional activity of *AGAMOUS* in regulating floral stem cells in *Arabidopsis thaliana*. *New Phytol.* *215*, 1197–1209.
74. Yamaguchi, N., Huang, J., Xu, Y., Tanoi, K., and Ito, T. (2017). Fine-tuning of auxin homeostasis governs the transition from floral stem cell maintenance to gynoecium formation. *Nat. Commun.* *8*.
75. Yamaguchi, N., Huang, J., Tatsumi, Y., Abe, M., Sugano, S.S., Kojima, M., Takebayashi, Y., Kiba, T., Yokoyama, R., Nishitani, K., *et al.* (2018). Chromatin-mediated feed-forward auxin biosynthesis in floral meristem determinacy. *Nat. Commun.* *9*, 1–7.
76. Liu, X., Dinh, T.T., Li, D., Shi, B., Li, Y., Cao, X., Guo, L., Pan, Y., Jiao, Y. and Chen, W. (2014). *AUXIN RESPONSE FACTOR 3* integrates the functions of *AGAMOUS* and *APETALA2* in floral meristem determinacy. *Plant J.* *80*, 629-641
77. Zhang, K., Wang, R., Zi, H., Li, Y., Cao, X., Li, D., Guo, L., Tong, J., Pan, Y., Jiao, Y., *et al.* (2018). *AUXIN RESPONSE FACTOR3* regulates floral meristem determinacy by repressing cytokinin biosynthesis and signaling. *Plant Cell* *30*, 324–346.
78. Marsch-Martínez, N., and de Folter, S. (2016). Hormonal control of the development of the gynoecium. *Curr. Opin. Plant Biol.* *29*, 104–114.
79. Cucinotta, M., Di Marzo, M., Guazzotti, A., de Folter, S., Kater, M.M., and Colombo, L. (2020). Gynoecium size and ovule number are interconnected traits that impact seed yield. *J. Exp. Bot.* *71*, 2479–2489.
80. Sessions, R.A., and Zambryski, P.C. (1995). *Arabidopsis* gynoecium structure in the wild type and in *ettin* mutants. *Development* *121*, 1519–1532.
81. Moubayidin, L., and Østergaard, L. (2017). Gynoecium formation: an intimate and complicated relationship. *Curr. Opin. Genet. Dev.* *45*, 15–21.
82. Larsson, E., Franks, R.G., and Sundberg, E. (2013). Auxin and the *Arabidopsis thaliana* gynoecium. *J. Exp. Bot.* *64*, 2619–2627.
83. Alvarez, J., and Smyth, D.R. (1998). Genetic pathways controlling carpel development in *Arabidopsis thaliana*. *J. Plant Res.* *111*, 295–298.
84. Bowman, J.L., Eshed, Y., and Baum, S.F. (2002). Establishment of polarity in

angiosperm lateral organs. *Trends Genet.* 18, 134–141.

85. Pekker, I., Alvarez, J.P., and Eshed, Y. (2005). Auxin Response Factors Mediate Arabidopsis Organ Asymmetry via Modulation of KANADI Activity. *Plant Cell* 17, 2899–2910.
86. Moubayidin, L., and Østergaard, L. (2014). Dynamic control of auxin distribution imposes a bilateral-to-radial symmetry switch during gynoecium development. *Curr. Biol.* 24, 2743–2748.
87. Gremski, K., Ditta, G., and Yanofsky, M.F. (2007). The HECATE genes regulate female reproductive tract development in *Arabidopsis thaliana*. *Development* 134, 3593–3601.
88. Cucinotta, M., Colombo, L., and Roig-Villanova, I. (2014). Ovule development, a new model for lateral organ formation. *Front. Plant Sci.* 5, 1–12.
89. Yadegari, R., Drews, N.G. (2004). Female Gametophyte Development. *The Plant Cell* 16, S133-S141.
90. Ceccato, L., Masiero, S., Sinha Roy, D., Bencivenga, S., Roig-Villanova, I., Ditengou, F.A., Palme, K., Simon, R., and Colombo, L. (2013). Maternal Control of PIN1 Is Required for Female Gametophyte Development in *Arabidopsis*. *PLoS One* 8, 2–8.
91. Elliott, R.C., Betzner, A.S., Huttner, E., Oakes, M.P., Tucker, W.Q.J., Gerentes, D., Perez, P., and Smyth, D.R. (1996). AINTEGUMENTA, an APETALA2-like gene of *Arabidopsis* with pleiotropic roles in ovule development and floral organ growth. *Plant Cell* 8, 155–168.
92. Schneitz, K., Baker, S.C., Gasser, C.S., and Redweik, A. (1998). Pattern formation and growth during floral organogenesis: HUELLENLOS and AINTEGUMENTA are required for the formation of the proximal region of the ovule primordium in *Arabidopsis thaliana*. *Development* 125, 2555–2563.
93. Ishida, T., Aida, M., Takada, S., and Tasaka, M. (2000). Involvement of CUP-SHAPED COTYLEDON genes in gynoecium and ovule development in *Arabidopsis thaliana*. *Plant Cell Physiol.* 41, 60–67.
94. Liu, Z., Miao, L., Huo, R., Song, X., Johnson, C., Kong, L., Sundaresan, V., and Yu, X. (2018). ARF2-ARF4 and ARF5 are Essential for Female and Male Gametophyte

Development in Arabidopsis. *Plant Cell Physiol.* 59, 179–189.

95. Panoli, A., Martin, M.V., Alandete-Saez, M., Simon, M., Neff, C., Swarup, R., Bellido, A., Yuan, L., Pagnussat, G.C., and Sundaresan, V. (2015). Auxin import and local auxin biosynthesis are required for mitotic divisions, cell expansion and cell specification during female gametophyte development in *Arabidopsis thaliana*. *PLoS One* 10.
96. Sundaresan, V., and Skinner, D.J. (2018). Recent advances in understanding female gametophyte development. *F1000Research* 7, 1–9.
97. Su, Z., Zhao, L., Zhao, Y., Li, S., Won, S.Y., Cai, H., Wang, L., Li, Z., Chen, P., Qin, Y. and Chen, X. (2017). The THO complex non-cell autonomously represses female germline specification through the *TAS3-ARF3* module. *Curr Biol.* 11, 1597-1609.
98. Ishikawa, H., and Evans, M.L. (1995). Specialized zones of development in roots. *Plant Physiol.* 109, 725–727.
99. Overvoorde, P., Fukaki, H., and Beeckman, T. (2010). Auxin control of root development. *Cold Spring Harb. Perspect. Biol.* 2, 1–17.
100. Bonner, J., and Koepfli, J.B. (1939). The Inhibition of Root Growth by Auxins. *Am. J. Bot.* 26, 557.
101. Petersson, S. V., Johansson, A.I., Kowalczyk, M., Makoveychuk, A., Wang, J.Y., Moritz, T., Grebe, M., Benfey, P.N., Sandberg, G., and Ljung, K. (2009). An auxin gradient and maximum in the arabidopsis root apex shown by high-resolution cell-specific analysis of IAA distribution and synthesis. *Plant Cell* 21, 1659–1668.
102. Petricka, J.J., Winter, C.M., and Benfey, P.N. (2012). Control of Plant Root Development. *Annu. Rev. Plant Biol.* 63, 563–590.
103. Sabatini, S., Beis, D., Wolkenfelt, H., Murfett, J., Guilfoyle, T., Malamy, J., Benfey, P., Leyser, O., Bechtold, N., Weisbeek, P., *et al.* (1999). An auxin-dependent distal organizer of pattern and polarity in the *Arabidopsis* root. *Cell* 99, 463–472.
104. Aida, M., Beis, D., Heidstra, R., Willemsen, V., Blilou, I., Galinha, C., Nussaume, L., Noh, Y.S., Amasino, R., and Scheres, B. (2004). The *PLETHORA* genes mediate patterning of the *Arabidopsis* root stem cell niche. *Cell* 119, 109–120.

105. Hardtke, C.S., Ckurshumova, W., Vidaurre, D.P., Singh, S.A., Stamatiou, G., Tiwari, S.B., Hagen, G., Guilfoyle, T.J., and Berleth, T. (2004). Overlapping and non-redundant functions of the Arabidopsis auxin response factors MONOPTEROS and NONPHOTOTROPIC HYPOCOTYL 4. *Development* 131, 1089–1100.
106. Krogan, N.T., Marcos, D., Weiner, A.I., and Berleth, T. (2016). The auxin response factor MONOPTEROS controls meristem function and organogenesis in both the shoot and root through the direct regulation of PIN genes. *New Phytol.* 212, 42–50.
107. De Smet, I., Vanneste, S., Inzé, D., and Beeckman, T. (2006). Lateral root initiation or the birth of a new meristem. *Plant Mol. Biol.* 60, 871–887.
108. Okushima, Y., Overvoorde, P.J., Arima, K., Alonso, J.M., Chan, A., Chang, C., Ecker, J.R., Hughes, B., Lui, A., Nguyen, D., *et al.* (2005). Functional genomic analysis of the AUXIN RESPONSE FACTOR gene family members in Arabidopsis thaliana: Unique and overlapping functions of ARF7 and ARF19. *Plant Cell* 17, 444–463.
109. de Smet, I. (2010). Multimodular auxin response controls lateral root development in Arabidopsis. *Plant Signal. Behav.* 5, 580–582.
110. Okushima, Y., Fukaki, H., Onoda, M., Theologis, A., and Tasaka, M. (2007). ARF7 and ARF19 regulate lateral root formation via direct activation of LBD/ASL genes in Arabidopsis. *Plant Cell* 19, 118–130.

Results and discussion

I will divide the main results of my PhD in three parts, in according to the different research lines that I have followed during these years and these parts will be entitled:

1. *MP* translation initiation is modulated by an auxin dependent alternative splicing event
2. Alternative splicing generates a MONOPTEROS isoform required for ovules development
3. Auxin modulate *MP* post-translational regulation in root development

The first two parts regard the study of the post-transcriptional regulation of *MP* with a specific focus on the reproductive development, while in the last one we investigate *MP* post-translational regulation during root development.

1. *MP* translation initiation is modulated by an auxin dependent alternative splicing event

1.1 Detection of predicted *MP* mRNAs splicing isoforms

MP activity has been the focus of many studies across the years, helping to shed light on auxin signalling. Despite this, little is known about mechanisms involved in *MP* post-transcriptional and post-translational regulation. In Arabidopsis genome re-annotation Araport11 web site [1] was predicted the existence of two *MP* mRNA isoforms (AT1G19850.1 and AT1G19850.2), due to the alternative splicing of a intron sequence located mainly in the 5' UTR of the transcript. Indeed, 308bp of the intron are at the end of the 5' UTR and 28 bp belong to the annotated first exon (fig. 1.1 A). In order to confirm the presence of the predicted *MP* mRNAs, and to quantify their abundance, we performed PCR-based analysis on cDNA retro-transcribed from total RNA of two biological replicates of different plant tissues: 6 days old seedlings, rosette leaves and inflorescences. We designed two primer couples to detect either canonical or alternative isoforms. *ACTIN 10* has been used to verify the absence of genomic DNA in the samples and cDNA quality. The primer couple for the canonical isoform has the primer reverse complementary to a sequence within the leader intron. On the other side, the alternative isoform amplification relies on a forward primer matching on the junction generated by the removing of the alternative spliced sequence. We detected both isoforms in all plant tissues analysed, observing a higher expression of the canonical isoform respect to the alternative one's. (fig1.1 A,B). Additionally, to quantify the abundance of the alternative transcript respect to the canonical one we designed specific primer pairs for Real-time qPCR. The normalized expression level of the alternative transcript was around the 8% respect to the canonical isoform in seedlings and leaves, whereas in the inflorescences the amount was of the 18% (fig.1.1 C).

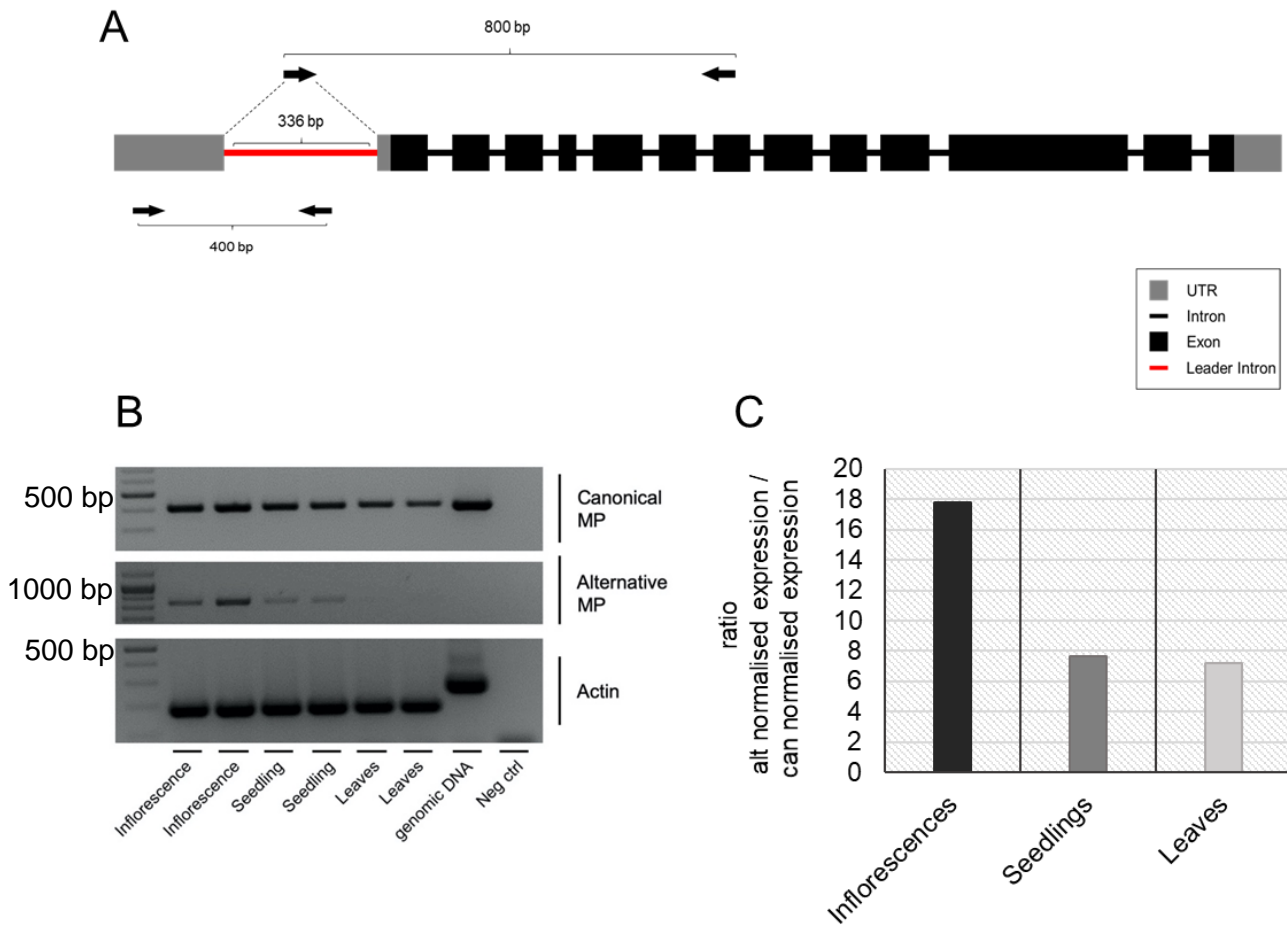


Fig.1.1: Detection of two predicted *MP* isoforms which differ for the alternative splicing of a leader intron sequence in the 5'UTR. (A) Scheme of the leader intron position and primer couples designed for the selective amplification of *MP* isoforms. (B) PCRs for canonical and alternative transcript detection, performed on cDNAs from two biological replicates of different plant tissues. *Actin10* has been used to confirm cDNA quality and to verify the absence of gDNA contamination. (C) Real-time qPCR-based analysis for alternative transcript expression evaluation in relation to the canonical transcript one. The data are the combination of two biological replicates for each tissue. The graph represents the ratio between alternative transcript normalised expression and canonical transcript normalised expression ($[\text{alt normalised expression} : \text{can normalised expression}] * 100$). While in inflorescences samples the alternative transcript has a normalised expression which is the 18% of the canonical transcript one, in seedlings and leaves it is of the 7 to 8 %.

1.2 Evaluation of *MP* isoforms translational efficiency

For many *ARFs* it was predicted the presence of uORF sequences in their 5'UTR. Indeed, *ARF* 2,3,4,5,6,7,8,9,10,11,17,18 have from 1 to 6 uORFs in the 5'UTR, potentially involved in translation regulation through ribosomes arrest and dissociation [2]. *MP* has 4 uORFs that negatively affect its translation in-vitro assays [3] and we found that, 3 out of the 4 uORFs in *MP*, were located in the alternative spliced leader intron. The absence of the 3 uORFs in the alternative spliced *MP* mRNA, suggests a possible enhanced translation of this isoform respect to the canonical one (fig.1.2 A). In order to evaluate the translational efficiency of the two isoforms, we tested their association with the polysome fraction by performing a polysome profiling experiment. Efficiently translated mRNAs are usually associated with the polysomes. On the other side, mRNAs with a low translational rate are associated to one or few ribosomes. Polysomes profiling allows to divide polysomes and monosomes complexes, thanks to their molecular weight on a sucrose gradient. This leads to the generation of different fractions, among which is evaluated the association of mRNAs of interest with polysome or monosome [4,5]. We performed polysome extraction on two biological replicates of Col-0 wild type inflorescences, since we observed an enrichment of the alternative *MP* isoform in this tissue. We analysed four different fractions from the polysome profiling: free mRNAs (RNA not associated to ribosomes and therefore not translated), monosomes (RNA poorly translated), light polysomes (RNA actively translated) and heavy polysomes (RNA highly translated). From each fraction we extracted the RNA and retrotranscribed it into cDNA that was used to evaluate *MP* isoforms distribution among the different translational complexes. Unexpectedly, canonical and alternative *MP* mRNA splicing variants shown a similar translational efficiency, with around the 64% of their total RNA in the four fractions associated with heavy polysomes. As control, we also tested the distribution of known highly and poorly translated transcripts among fractions. In particular, as highly translated control we checked *ACTIN 10* mRNAs while we used *SQUAMOSA PROMOTER BINDING PROTEIN-LIKE 3 (SPL3)* as poorly translated mRNA (fig.1.2 B).

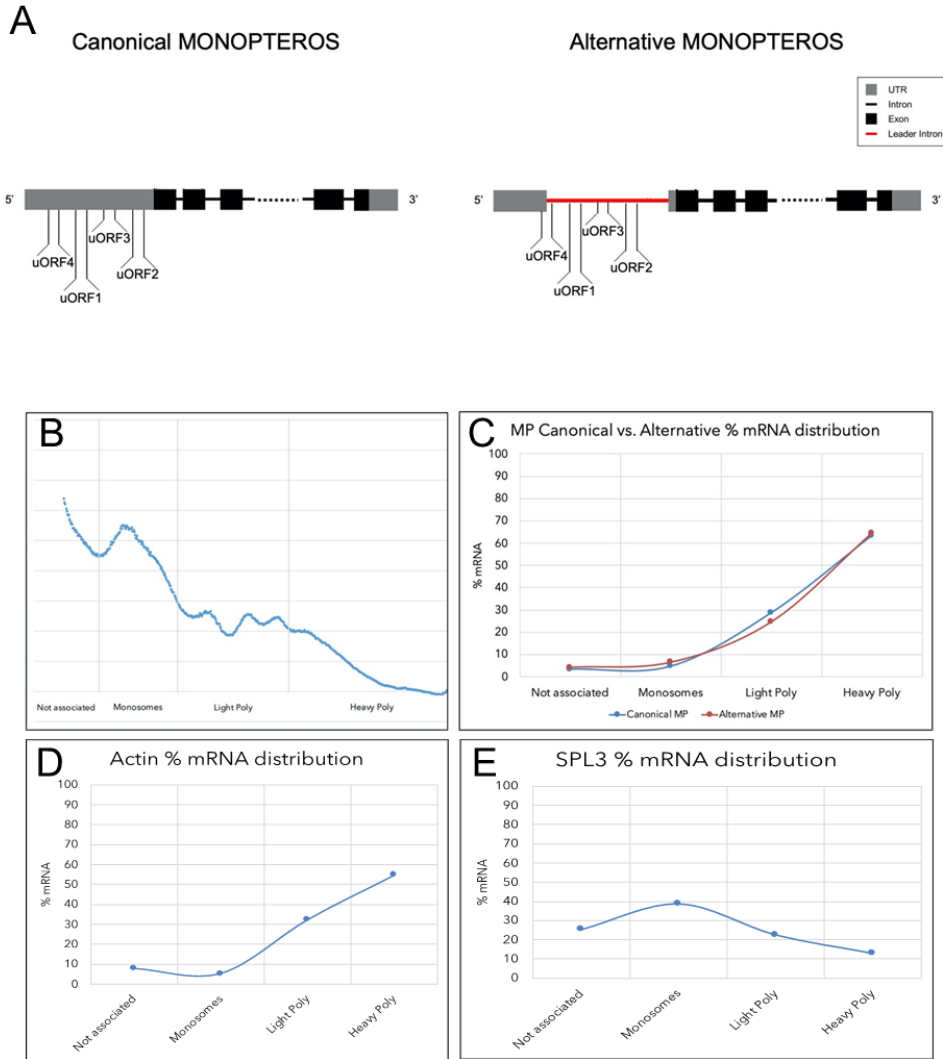
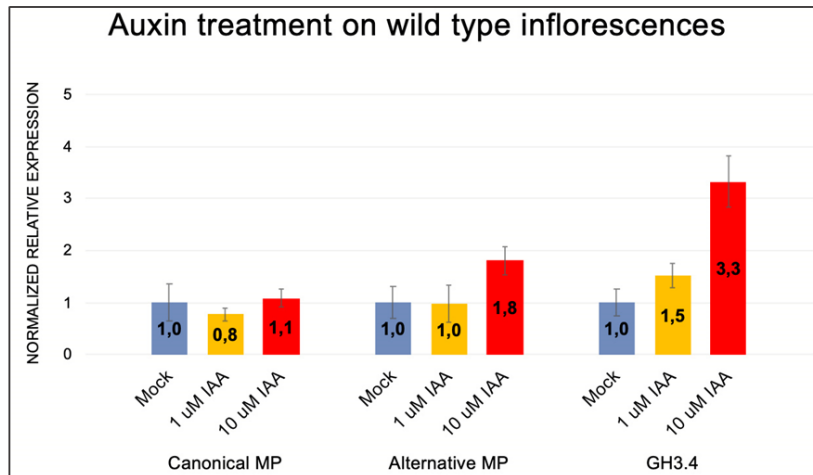


Fig. 1.2: Evaluation of canonical and alternative *MP* isoforms translational efficiency by polysome profiling. (A) Scheme of *MP* uORF sequences position. The splicing of the leader intron leads to the removal of 3 out of 4 uORFs. (B) Polysome profiling graph, based on the absorbance (λ :260nm) of the sucrose gradient across the time of the fractionation. The shape of the graph allows the identification of the fractions containing the different translational complexes: free mRNAs, monosomes, light polysomes and heavy polysomes. (C) Distribution of canonical and alternative mRNAs among the fractions. The quantity of target mRNA in each fraction is expressed as percentage of the total amount of the mRNA in the four fractions, considered as 100. *MP* isoforms are translated with a similar efficiency. (D,E) Distribution of highly translated mRNAs (*ACTIN*) and poorly translated ones (*SPL3*) among the fractions.

1.3 Auxin regulates *MP* leader intron alternative splicing

In literature, it has been described that auxin can modulate alternative splicing events, dependently on the action of a family of RNA-binding proteins called NUCLEAR SPECKLE RNA-BINDING PROTEINS (NSRs) [6]. NSRs are nuclear localized proteins, working as alternative splicing regulators of target mRNAs. Additionally, it has been shown that NSRs interact with the long non-coding RNA *ASCO*, which acts as a competitor for targets binding. NSRs-*ASCO* generate a module of alternative splicing regulation, involved in the major changes in alternative splicing patterns in relation to auxin [6]. For this reason, we decided to investigate a possible involvement of auxin and NSRs-*ASCO* module in the regulation of the alternative splicing event associated to the two *MP* isoforms generation. Consequently, six biological replicates of Col-0 wild type inflorescences were treated with exogenous IAA at different concentrations (1 and 10 μ M). After RNA extraction and cDNA synthesis we compared by Real-time qPCR canonical and alternative *MP* mRNAs expression levels between mock and treated samples. In all the replicates, at the highest concentration (10 μ M), the canonical isoform expression didn't change between mock and treated samples. Whereas, we observed a statistically significant increase of the alternative isoform level in IAA treated samples (fig.1.3 A). As positive control for IAA treatment we tested the expression level of the auxin responsive gene *GRETCHEN HAGEN 3.4 (GH3.4)* previously described to be induced by high auxin levels [7]. *MP* promotor activity is not modulated by auxin, as suggested by the expression level of the canonical mRNA between mock and treated samples. Whereas, the first intron alternative splicing seems to be enhanced by IAA, leading to the increase of the amount of this isoform in IAA treated samples. To verify the involvement of the NSRs-*ASCO* module in the auxin-dependent *MP* alternative splicing, we performed IAA treatments on inflorescences belong to *ASCO* RNA interference plants (*ASCO-RNAi*) and on *nsr a/b* double mutant plants (provided from Prof. Martin Crespi). We performed treatments on three biological replicates with 10 μ M IAA, using Col-0 wild type inflorescences as control. No changes in quantity were observed for the canonical *MP* isoform in all genotypes tested. On the other side, we observed loss of the alternative *MP* isoform induction, in relation to auxin application in both *ASCO RNAi* and *nsr a/b* (fig.1.3 B). Our results suggest that the *MP* first intron splicing is regulated by auxin through the action of the NSRs-*ASCO* module.

A



B

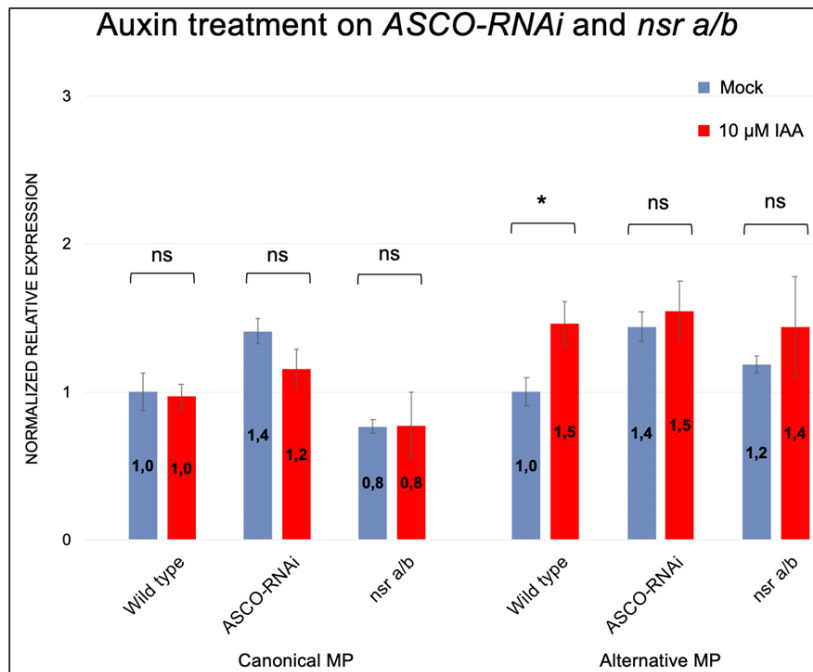


Fig.1.3: Canonical and alternative *MP* transcripts response to auxin changes. (A) Representative result of IAA treatment on Col-0 wild type inflorescences. Auxin increase induce alternative *MP* transcript expression while we didn't observe changes in canonical *MP* one. For each target the expression level in the mock sample has been set at 1. (B) Graph obtained by the combination of three biological replicates of auxin treatment on Wild-type, *ASCO-RNAi* and *nsr a/b* inflorescences. Induction of alternative *MP* transcript expression upon auxin increase is lost when the NSR-*ASCO* module is impaired. *GH3.4* has been tested as positive control for IAA treatment on each sample, showing an enrichment of around 5-fold (not shown). For each target the expression level in the mock sample has been set at 1. T-test Student performed between mock and IAA treatment pairs. ns: not significant, **: $p < 0.01$

1.4 Identification of *MP* alternative translation start site

As mentioned before, *MP* first intron includes 28 bp encoding for the first 9 aa of MP protein, including the annotated translational start codon. Upstream *MP* DBD encoding sequence there are 4 ATGs. The first and the second ATGs are at position +1 and +3, while the third and fourth are respectively at position +33 bp and +108 bp, respect to the annotated start site. In the alternative *MP* isoform, the first two AUGs are lost, making the third and fourth ones possible alternative translational start sites, which can be used without impair the DBD sequence. In order to unveil the putative translational start site of *MP* alternative mRNA, we analysed available datasets of ribosomes profiling with the GWIPS-vis software [8–10] which reveals the position and number of ribosomes on the mRNA, allowing to identify ORF translational starting point. The analyses of these data sets reveal enrichments in sequencing reads at the 4th *MP* AUG, indicating this AUG as a putative translation start site (fig.1.4 A). Interestingly, to the fourth AUG results associated a higher number of reads respect to the annotated one, suggesting a possible flexibility in translational start site usage even in presence of the first AUG. In order to confirm the functionality of the fourth *MP* AUG as translation start codon, we introduced a point mutation downstream the third ATG but before the fourth one, causing the generation of a premature stop codon exactly before the putative alternative start one. We took advantage of the CRISPR/CAS9 genome editing tool, designing a guide RNA complementary to *MP* sequence from +40 to +60 bp after the annotated start site. We obtained two independent F3 mutant lines, homozygous for the CRISPR/CAS9 editing without the CRISPR T-DNA, and we named them *mpT56* and *mpA54*. *mpT56* was characterized by the insertion of a thymidine at position +56 bp, causing a frameshift and the insertion of a premature stop codon at position +103 bp. *mpA54* has the deletion of an adenine at position +54 bp, with a premature stop codon at +71 bp (fig. 1.4 B). In both cases, mutants did not show any difference from wild type plants. The fourth AUG, being positioned downstream the CRISPR-generated stops, can be used as start codon to lead the translation of a fully functional MP protein. Additionally, to confirm the WT-like properties of our alleles, we decided to cross *mpT56* plants with plants heterozygous for the weak T-DNA recessive *mp* mutant allele *mpS319* [11]. We obtained biallelic *mpT56/mpS319* plants, which shown no alteration in all the developmental processes. Indeed, no defects were observed in relation to plant germination, vegetative growth or fertility (fig.1.4 C).

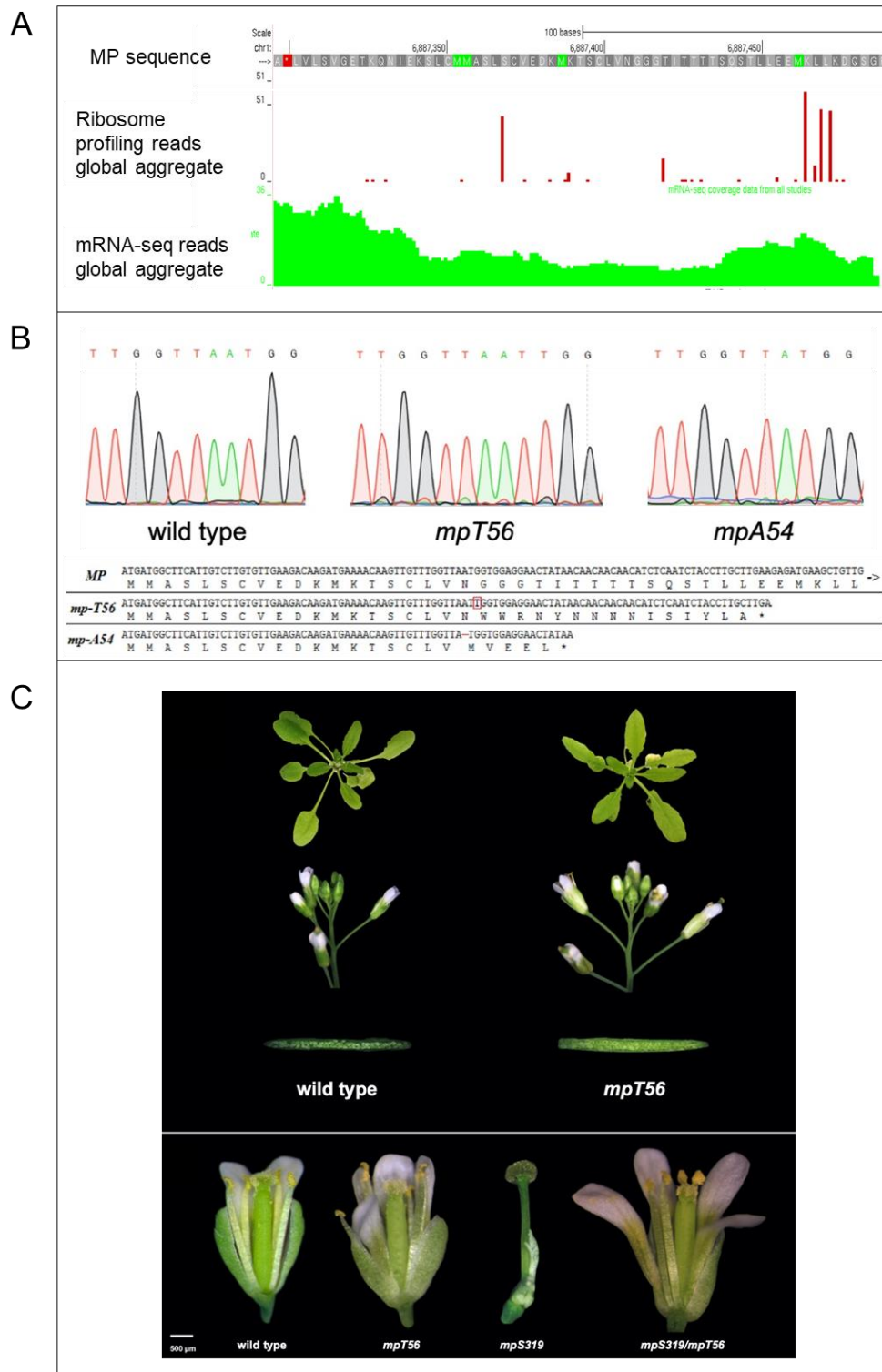


Fig.1.4: *MP* translation initiation relies on multiple start codons. (A) GWIPS-viz analysis results performed on ribosome profiling available datasets [8–10]. The region considered in the analysis comprehends a portion of the 5'UTR the first exon and part of the first intron of *MP* genomic locus. The first row corresponds to *MP* protein sequence, the second one to the global aggregate of mapped reads from the ribosome profiling datasets. The last row is the global aggregate of mRNA-Seq reads of all the studies. (B) Sequencing results of CRISPR-generated editing in *mpT56* and *mpA54* homozygous lines. For both the alleles is reported the protein translated from the putative start codon until the premature stop codon caused by the frameshift. (C)

Phenotypic analyses of *mpT56* homozygous plant, reported as indicative of the Wild-type like phenotype of our CRISPR-generated alleles. In the last portion of the image the comparison of mature flowers of Wild type, *mpT56*, *mpS319* and biallelic *mpS319/mpT56*. No differences were observed among wild type, *mpT56* and *mpS319/mpT56* flowers.

1.5 Discussion

Alternative splicing is a powerful tool which modulates proteins functions and plasticity and represents a common regulatory mechanism for the major part of *Arabidopsis* genes (Zhang *et al.*, 2017). Our findings suggest that alternative splicing is also involved in *MP* regulation, leading to the generation of different isoforms, with specific accumulations in the different plant tissues. By sequence analyses, we found that *MP* leader intron is characterised by the presence of a conserved motif (CGATT), putative involved in the intron-mediated enhancement (IME). IME is a mechanism in which intron retention leads to an increase of mRNA accumulation respect to the intron-less mRNA variant. IME signals are generally located at the 5' end of genes or in their 5'UTR, and lead to transcripts accumulation prior transcription. It has been shown that IME introns generally increase mRNA accumulation from 2 to 10-fold, [12,13]. *MP* canonical mRNA results highly accumulated respect to the alternative one, and we speculate that this may be related to the presence of the IME sequence in the first intron. On the other side, we observed that *MP* alternative isoform is preferentially accumulated in inflorescences respect to other plant tissues, suggesting that this alternative splicing event, may be differentially regulated during plant development.

Although in-vitro studies previously reported that *MP* uORF sequences negatively affect its translation, in inflorescences seems to not take place. Indeed, from polysomes profiling experiments, canonical and alternative transcripts are equally associated to the heavy polysomes fraction, indicting a similar translational efficiency despite the presence of the 5'UTR uORFs.

Auxin, in addition to regulate *MP* protein function, plays also a role in the regulation of its transcript maturation. *MP* leader intron alternative splicing is enhanced by auxin increase, and the NSRs-ASCO module seems to be a core component of this modulation. Recently, it has been described that *ASCO* is also involved in the binding of the core component of the spliceosome PRP8a, regulating its activity and the transcriptome population [14]. In

collaboration with Prof. Ueli Grossniklaus, we obtained preliminary results of MP putative protein partners in inflorescences, thanks to CO-IP followed by MS/MS experiments on MP-GFP reporter line. Among MP putative interactors we found, in three biological replicates, that MP was able to bind *in-vivo* with PRP8. In particular, we identified PRP8 respectively with 3,2 and 5 unique peptides in the three replicates (Fig.1.5)

MP

Transcriptional factor B3 family protein / auxin-responsive factor AUX/IAA-like prot...		All Biological Samples						
Protein	Accession	Category	Bio Sample	MS/MS Sample	Prob	%Spec	#Pep	#Uni...
Transcriptional factor B3 family protein / auxin-responsiv...	AT1G19850.1	MP1	BioSample 4		100%	0,82%	21	39
Transcriptional factor B3 family protein / auxin-responsiv...	AT1G19850.1	MP2	BioSample 5		100%	1,0%	22	46
Transcriptional factor B3 family protein / auxin-responsiv...	AT1G19850.1	MP3	BioSample 6		100%	0,58%	19	32

B

PRP8

Pre-mRNA-processing-splicing factor Chr1:30118052-30127574 FORWARD LENG...		All Biological Samples						
Protein	Accession	Category	Bio Sample	MS/MS Sample	Prob	%Spec	#Pep	#Uni...
Pre-mRNA-processing-splicing factor Chr1:30118052-3...	AT1G80070.1	MP1	BioSample 4		100%	0,069%	3	
Pre-mRNA-processing-splicing factor Chr1:30118052-3...	AT1G80070.1	MP2	BioSample 5		100%	0,054%	2	
Pre-mRNA-processing-splicing factor Chr1:30118052-3...	AT1G80070.1	MP3	BioSample 6		100%	0,069%	5	

Fig.1.5: Result of Co-IP followed by MS/MS on three biological replicates of *MP:MP:GFP* reporter line inflorescences, performed according to [16]. The experiment has been performed on three biological replicates of Wild type inflorescences as control. (A) MP peptides found in the three *MP:MP:GFP* biological replicates. No MP peptides were detected in the wild type negative control. (B) PRP8 peptides recognised specifically in *MP:MP:GFP* biological replicates. No PRP8 peptides were observed in Wild type controls, indicating it as a putative MP protein interactor.

We speculate that *MP* might be involved in alternative splicing regulation upon auxin perception by interacting with the spliceosome core. That might impact on *ASCO* and consequentially *NSRs* activity, leading to the modulation of its own splicing or the splicing of target genes. Much has to be done to verify this hypothesis, nevertheless this can help to characterize a completely new mechanism of *ARFs* activity.

Finally, we show that alternative splicing might impact on translation initiation leading to flexibility in the start codon usage. *The* fourth *MP* AUG can be used as alternative start codon, without impair its protein function. Indeed, while it has been deeply described that mutation in *MP* downstream regions are associated with dramatic effects on plant development, the CRISPR-generated alleles were not associated to alterations in plant development.

2. Alternative splicing generates a MONOPTEROS isoform required for ovules development

2.1 MP is expressed and functional in auxin minima regions during ovule development

Ovules differentiate from the pistil and are structures formed both by sporophytic and gametophytic tissues. Particularly, at the beginning of their development ovules are formed by three main domains: the proximal precursor of the funiculus connected with the placenta, the central chalaza from which the integuments differentiate and the apical-distal nucella, where occurs the mega-sporogenesis and mega-gametogenesis. It has been described that MP is one of the master regulators of ovules formation, directly activating a set of genes involved in ovules primordia differentiation and growth [15]. Previous studies in our lab have focused on the characterisation of *MP* expression pattern in ovules primordia, in relation to auxin concentration. In ovules primordia, auxin maxima were described to be associated to few cells at the tip of the nucella [16]. To better investigate auxin pattern in this context the reporter lines *DR5v2::ntdTomato* and DII-VENUS were used. The *DR5v2::ntdTomato* is a reporter line for the detection of peaks of auxin signalling. It is based on the presence of the synthetic promotor *DR5v2*, made by repetitions of the AuxRE core sequence bound by class A ARFs. In this way, in points of auxin maxima, *DR5v2* promoter derives the expression of the *ntdTOMATO*. *DII-VENUS*, on the other side, is a reporter for auxin minima. It is composed by the constitutive promotor *RPSA*, which drives the expression *AUX/IAAs* degron domain fused in-frame with the *VENUS*. Once translated, the DII domain confers stability to the fusion protein only in absence of auxin, allowing the visualisation of points of auxin minima [17]. As expected, the *DR5v2::ntdTOMATO* reporter was visible only in the apical part of ovules primordia, in three following developmental stages. Whereas, the proximal part of primordia, including the chalaza and the boundaries with the nucella, were associated to a low auxin level, as indicated by the DII-VENUS signal (fig. 2.1 G-L). Surprisingly, by *in-situ hybridization* *MP* was found to be expressed in domains of auxin minima. Likely, *MP* protein accumulation pattern from the *MP::MP::GFP* reporter line [19], was coincident to its expression profile and contextual to auxin minima (Fig. 2.1 A-F).

In such *scenario*, *MP* should be bound by *AUX/IAAs*, working as a repressor of the transcription. In order to verify *MP* transcriptional behaviour this context, we studied *TMO3*,

TMO5, *CUC1* and *CUC2* expressions, targets which were previously described to be directly regulated by MP [15,18,19]. All these genes were expressed in MP protein accumulation domain, suggesting a positive function of MP on their transcription, despite the sub-threshold auxin concentration (fig. 2.1 J-O).

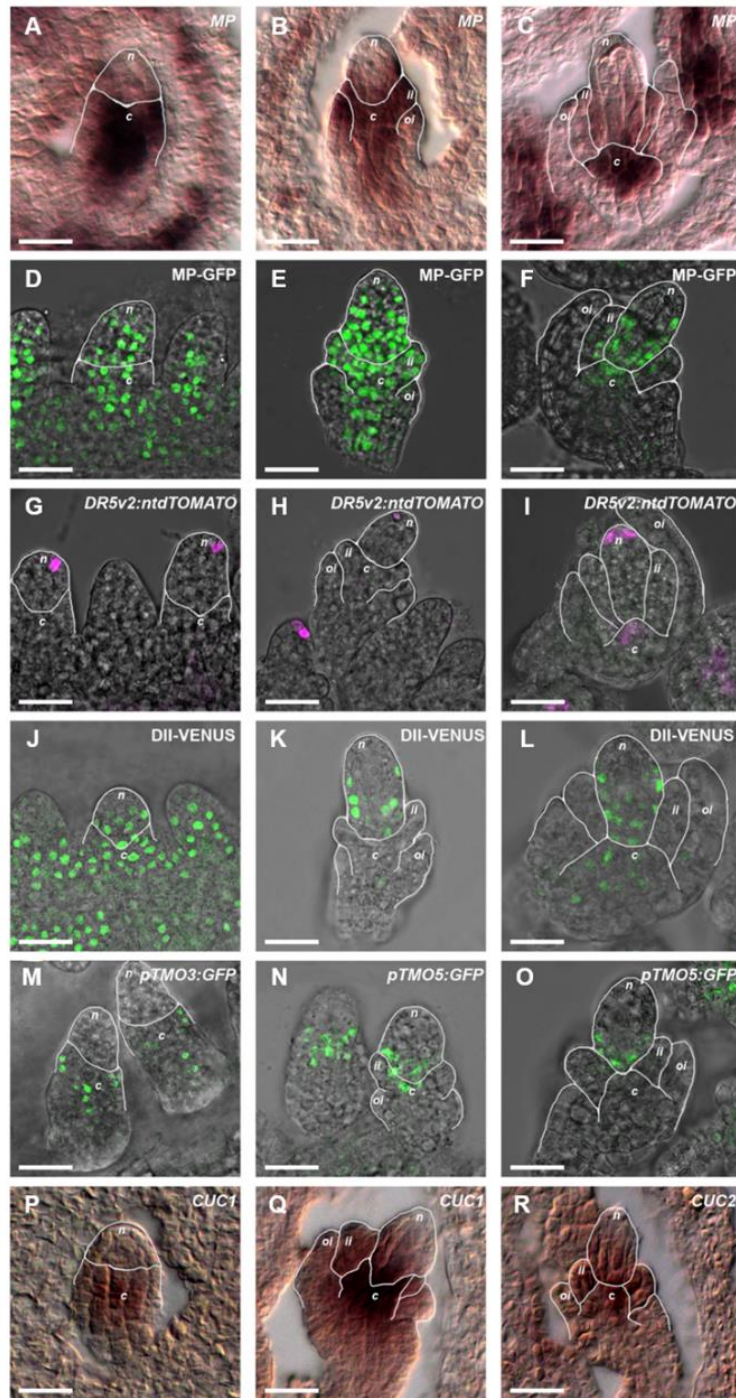


Fig. 2.1: Expression analysis of *MP* and its direct targets in relation to auxin levels during ovules primordia development. (A–C) *in situ* hybridisation of *MP* transcript during ovules formation. *MP* is expressed in the basal part of ovules primordia in three following developmental stages. (D–F) *pMP:MP-GFP* translational reporter line shown the same accumulation pattern of *MP* in-situ hybridisations. (G–I, J–L) *DR5v2::ntdTomato* and *DII::VENUS* auxin reporter lines in the same primordia stages considered for *MP* expression analysis. *MP* is transcribed and translate in domains of auxin minima. (M, N, O) Respectively, *pTMO3::3xnGFP* (M) and *pTMO5::3xnGFP* (N, O) expression pattern in ovules primordia. (P–R) *CUC1* and *CUC2* expression pattern in ovules primordia detected by *in-situ* hybridisation. All *MP* direct targets are expressed contextually to *MP* protein accumulation domain, in auxin minima regions. Different ovule structures (n: nucellus; c: chalaza; ii: inner-integument; oi: outer-integument) are outlined in white. Scale bar: 20 μ m.

2.2 Identification of a *novel MP* alternative splicing event, linked to the translation of a truncated MP protein isoform

Class A ARFs transcriptional behaviour, as discussed above, is strictly related to auxin levels and AUX/IAAs interaction through the C-terminal PB1 domain. Nevertheless, in literature it has been described that ARFs functions may be modulated by post-transcriptional regulations as the alternative splicing. We decided to investigate the existence of novel alternative splicing events for *MP*, which might be associated to the translation of an alternative protein able to work as activator in auxin minima. In collaboration with Prof. Aureliano Bombarely, we performed a deep RNA-seq (100 million reads) on wild type inflorescences material. We have been able to detect few reads matching partially, or completely, *MP* eleventh intron sequence. Although we detected a low number of reads on the eleventh intron, this result suggests the existence of an alternative splicing event associated to its retention (fig. 2.2 A). To confirm the presence of the alternative spliced *MP* mRNA, we performed PCRs on cDNA from three biological replicates of diverse tissues including: inflorescences, leaves and 6 days old seedlings. To avoid artefacts from possible gDNA contaminations, we designed specific couple of primers. In particular, the detection of the alternative spliced mRNA, relies on a forward primer matching on eleventh intron sequence while, the reverse one, is complementary to the exon-exon junction between the last two *MP* exons. We designed this PCR in order to amplify only cDNA molecules retrotranscribed from processed *MP* mRNA, in which the last intron is absent but the eleventh one is retained. In seedlings, we detected a low amount of the alternative transcript and no amplification was observed in leaves. Nevertheless, we have been able to successfully detect the intron-11-retaining isoform, called *MPint11*, in all inflorescence samples (fig.2.2 B). To evaluate the abundance of *MPint11* isoform, droplet digital PCR (ddPCR) was performed. The ddPCR is a powerful technique which allows the identification of the absolute number of target cDNA molecules in a sample [20]. Thanks to this approach we found, in two biological replicates of inflorescences cDNA, that *MPint11* isoform was around the 6% of the total *MP* transcript (fig.2.2 C). Interestingly, within the eleventh intron a premature stop codon (UGA) is present on MP ORF, 55 bp downstream the intron starting point. Canonical MP protein is composed by 902 aa, and aa 793 to aa 876 correspond to the C-terminal PB1 domain. *MPint11* translation generates a MP protein isoform of 815 aa, due to the presence of the premature stop codon, resulting in the absence of the PB1

domain. Indeed, the last 18 aa of MPint11 protein are intron encoded, making the aa from 793 to aa 797 the only ones related to the PB1 domain (fig. 2.2 D).

It has been deeply characterized that MP, lacking the PB1 domain, can't interact with AUX/IAAs, escaping from the classical auxin regulation [21, 22]. For this reason, we speculated that the existence of the natural occurring MPint11 isoform, could be related to the auxin sub-threshold induction of MP targets in ovules primordia. To verify that this alternative splicing event was associated to the translation of the MPint11 alternative protein we checked *MPint11* behaviour in polysomes profiling. We performed polysomes extraction from Col-0 wild type inflorescences and we obtained three fractions along the sucrose gradient: monosomes, light polysomes and heavy polysomes. We successfully detected *MPint11* transcript association with polysomes fractions, even if with a lower percentage respect to the canonical one. Indeed, while the 70% of the canonical *MP* mRNA was associated to heavy polysomes, this percentage was 40% for the alternative *MPint11*. Nevertheless, this result indicates active translation of the alternative spliced mRNA, associated to the production of the MPint11 protein variant (fig.2.2 E).

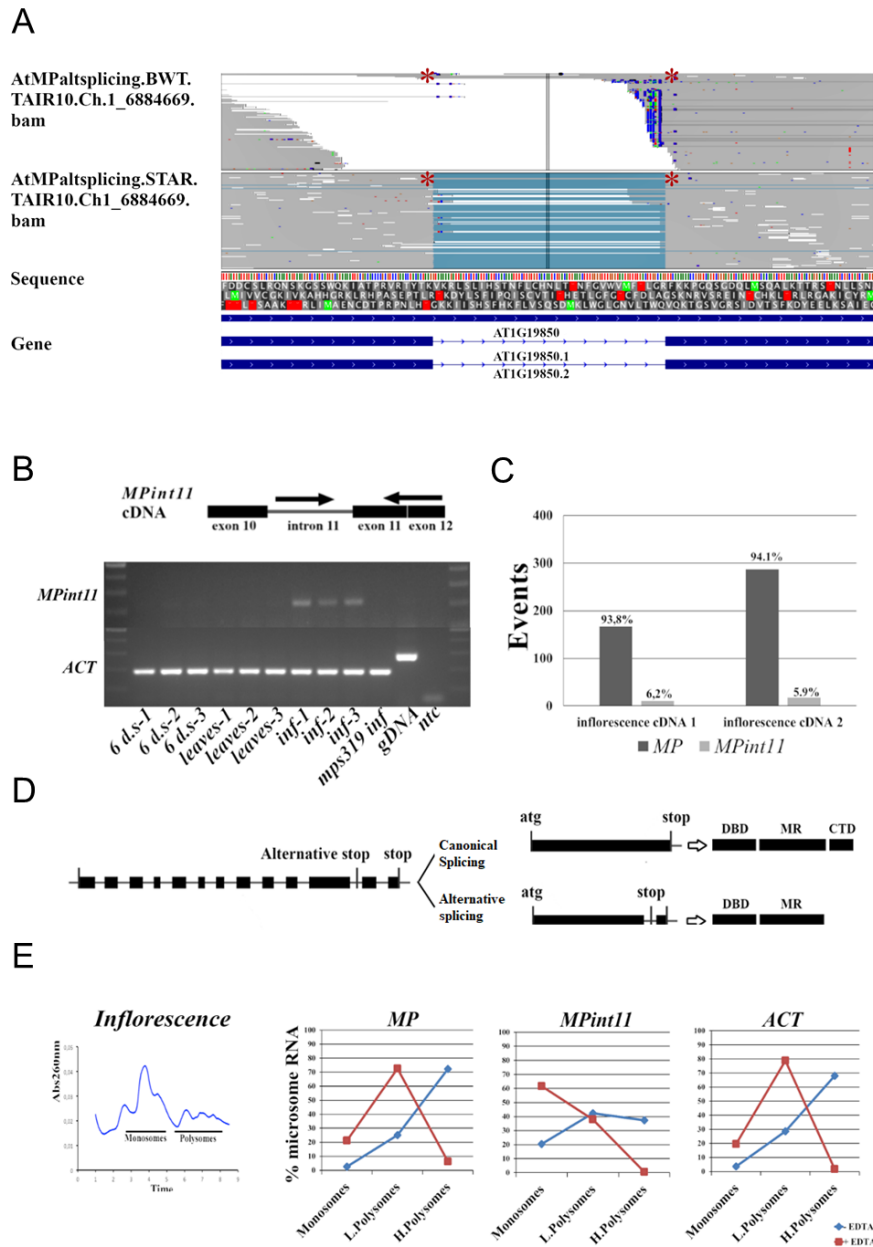


Fig.2.2: Identification of *MP* eleventh intron alternative splicing event, associated to the generation of the *MPint11* isoform. (A) RNA-seq results. Zoom-in the region of *MP* intron eleven where are visible reads mapping to the intron. (B) PCR for the specific amplification of *MPint11* with the scheme of primers matching. The PCR has been performed on three biological replicates of cDNA retro-transcribed from RNA of 6 days old seedlings, leaves and inflorescences. (C) *MP* and *MPint11* isoforms abundance by ddPCR. In both the biological replicates, the alternative mRNA results to be around 6% of total transcript. (D) Scheme of protein isoforms translated from *MP* and *MPint11* transcripts. The stop codon in the eleventh intron sequences leads to the translation of a natural truncated *MP* protein lacking the c-terminal PB1 domain. (E) Polysomes profiling results for *MP* and *MPint11*. Three fractions have been obtained from the sucrose gradient (monosomes, light polysomes and heavy polysomes). The line in blue represent the abundance of a transcript in each fraction which is expressed as percentage of the total transcript quantity among the fractions. The red line is referred to EDTA-treated samples. EDTA disrupts polysome complexes, leading to a shift of the transcripts toward the lighter fractions. This control allows to ensure that the presence of a mRNA in a fraction is indeed due to its association to ribosomes instead to its molecular weight.

2.3 *MPint11* is sufficient to restore ovule development process in *mp* mutants

Even though, *MPint11* isoform expression results to be significantly lower respect the expression of the canonical one, its association to polysomes brought us to hypothesise its possible relevance for reproductive development. For this reason, we generated the *pMP:MPint11-GFP* construct and we used it to rescue the weak *mp* mutant *mpS319*. *mpS319* homozygous plants that reach the reproductive phase, as discussed above, have great alterations in inflorescence structure, with a reduced ability to produce lateral organs and sterile flowers due to the presence of radialized pistils without ovules. We obtained three independent lines, homozygous for the *mpS319* allele with the *pMP:MPint11-GFP* construct. In all cases, we observed a partial complementation of several developmental defects associated to the *mpS319* mutant. Indeed, we observed a partial rescue in plant morphology, lateral organs development and flowers formation. Importantly, whereas almost the totality of *mpS319* pistils don't develop ovules, we observed that the 67% of the total pistils analysed for *mpS319 pMP:MPint11-GFP* rescue lines, developed an average of 36 ovules each one (fig. 2.3 B, fig. 2.4 A).

In addition to this, 60% of *mpS319 pMP:MPint11-GFP* ovules normally complete their development, presenting a fully develop embryo sac encased by the sporophytic integuments. On the other side, the 40% of *mpS319 pMP:MPint11-GFP* ovules, displayed alterations in integuments structure, closing only partially ovules micropylar end. Rarely, *mpS319* pistils develop few ovules characterized by a completely impaired megagametogenesis and aberrant integuments and, especially considering this, the ability of *MPint11* to drive ovule development process is pointed out (fig. 2.4 B, D, E, F).

We also verified *MPint11* functionality to rescue strong *mp* mutants, as the *arf5-1*. *pMP:MPint11-GFP* restored fertility and inflorescence morphology in *arf5-1* background, with results similar to the one observed for the *mpS319* allele.

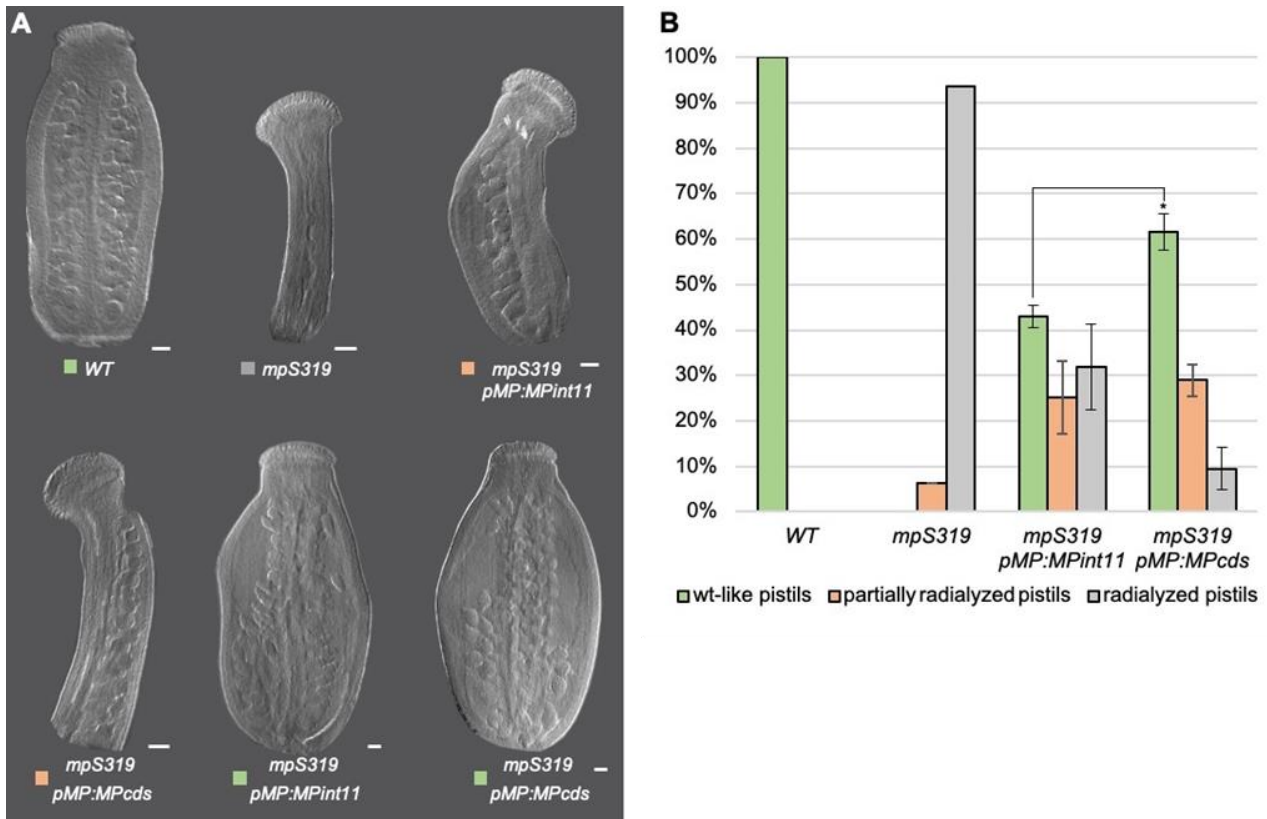


Fig 2.3: *MPint11* and *MPcds* differential rescue of pistil development process in the *mpS319* mutant. (A) Wild type pistil, *mpS319* pin-like pistil, mono-carpel pistils in *mpS319 pMP:MPint11-GFP* and *mpS319 pMP:MPcds* rescue lines and wild type-like pistils in the same backgrounds. (B) While the totality of *mpS319* pistils are dramatically impaired, respectively the 40% and the 63% of them have a wild-type like phenotype in *mpS319 pMP:MPint11-GFP* and *mpS319 pMP:MPcds* lines. *MPint11* and *MPcds* show a differential ability to drive pistil development process, indeed the percentage of Wild type-like pistils was statistically higher in *MPcds* rescue lines. Values are means \pm SE for three independent lines. * $p < 0.05$ (one-way ANOVA and Tukey's HSD test; $n = 60$ pistils from 10 plants of three independent lines)

2.4 Absence of the *MPint11* isoform leads to alteration in the ovule development process

In parallel to *MPint11* complementation, we investigated how the specifically absence of the alternative isoform could impact on plant development. For this reason, we decided to complement the *mpS319* mutant with just the canonical *MP* using the *pMP:MPcds* construct (provided from our collaborator Prof. Dolf Weijers). We obtained three independent rescue lines, with an expression level of the transgene similar to the one observed in *MPint11* ones. In *mpS319* background, *MPcds* expression restored lateral organs formation and inflorescence structure, similarly to *MPint11*. Whereas, *MPcds* showed a higher functionality to drive pistils development and patterning. Indeed, the 90% of *mpS319 pMP:MPcds* pistils (67% in *mpS319 pMP:MPint11-GFP*) successfully develop ovules, even if a ratio of these pistils still present defects as partial radialisation (fig.2.3 A,B).

Unexpectedly, *mpS319 pMP:MPcds* and *mpS319 pMP:MPint11-GFP* plants showed a similar degree of complementation of ovules primordia development, forming an average of around 40 ovules per pistil (fig. 2.4 A). Nevertheless, analysing fully developed ovules, we noticed a reduced ability of canonical *MPcds* respect to alternative *MPint11*, to restore integuments growth. The 60% of *mpS319 pMP:MPcds* mature ovules analysed present protruding embryo sacs, due to miss-closure of the integuments at the micropylar (fig. 2.4 B, G). As mentioned above, this percentage was of the 40% in *MPint11* rescue lines, resulting in a higher ratio of Wt-like ovules and indicating an enhanced ability of *MPint11*, respect to *MPcds*, to drive integuments development (fig.2.4).

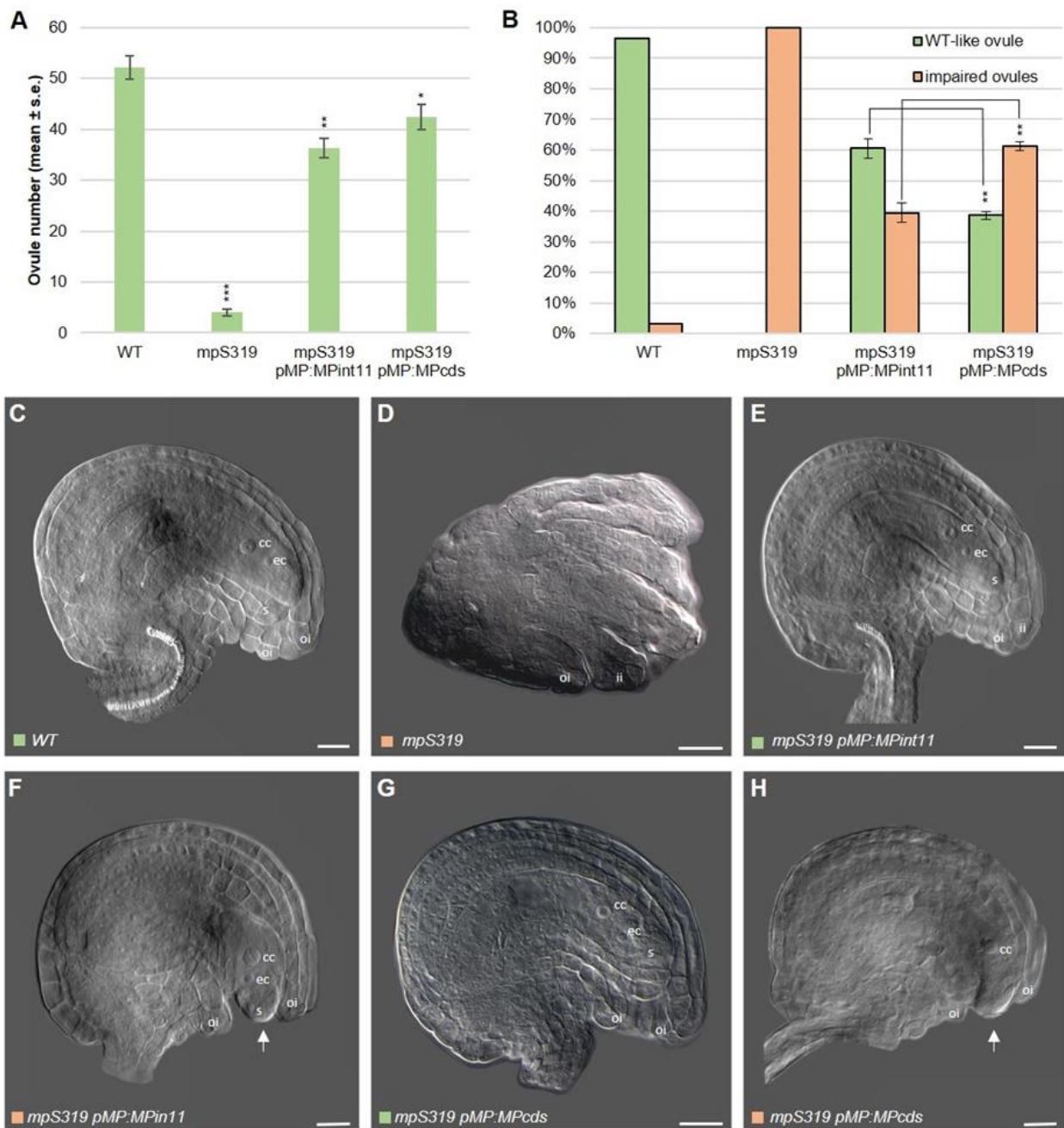


Figure 2.4. *MPint11* is required for ovules integuments development. (A) mean of ovules per pistil in wild type, *mpS319*, *mpS319 pMP:MPint11-GFP* and *mpS319 pMP:MPcdfs* lines. $p^* < 0.05$; $p^{**} < 0.01$ and $p^{***} < 0.001$ (one-way ANOVA and Tukey's HSD test; $n = 3$ pistils from five plants of three independent lines). (B) wild type-like and impaired ovules percentage on the total number of ovules analysed in wild type, *mpS319*, *MPint11* and *MPcdfs* rescue lines. *MPint11* show a higher functionality during ovules development respect to the canonical *MPcdfs* as suggested by the statistically significant increase in the number of wild type-like ovules in *mpS319 pMP:MPint11-GFP*. $p^{**} < 0.01$ (one-way ANOVA and Tukey's HSD test; $n = 200$ ovules from plants of three independent lines). (C) Wild type ovule. (D) *mpS319* aberrant ovule. (E) *mpS319 pMP:MPint11-GFP* wild type-like ovule. (F) *mpS319 pMP:MPint11-GFP* partially aberrant ovule with unclosed integuments and protruding embryo-sac. (G) *mpS319 pMP:MPcdfs* wild type-like ovule. (H) *mpS319 pMP:MPcdfs* partially aberrant ovule with unclosed integuments and protruding embryo-sac. (White arrows indicate the embryo sac protruding. cc, central cell; ec, egg cell; ii, inner integument; oi, outer integument; s, synergid).

As for the *MPint11* isoform we used the *MPcds* to rescue the strong *arf5.1* allele, obtaining a similar complementation level to the one previously observed.

We also evaluated the restoration of the expression of MP targets, analysed during ovule development process. We used cDNAs, retrotranscribed from inflorescences RNAs, of all the independent rescue lines obtained with the two constructs. We found that the expression of *ANT*, *CUC1*, *CUC2*, *TMO3* and *TMO5* was similar to the one observed in Wild type control, in both *MPint11* and *MPcds* rescue lines. These results were in line with the phenotypic observation about pistils and ovules formation. However, we observed a reduction in *CUC2* expression in *mpS319 pMP:MPint11-GFP* respect to Wild type control and to *mpS319 pMP:MPcds*, even if it was enhanced respect to the one observed in the homozygous *mpS319*. Additionally, we also evaluated the expression level of *LFY*, involved in floral meristem identity acquisition and flower development. As expected, in both *mpS319 pMP:MPint11-GFP* and *mpS319 pMP:MPcds* we observed a partial complementation of *LFY* expression, as suggested by the partial rescue of the flower development process (fig.2.5).

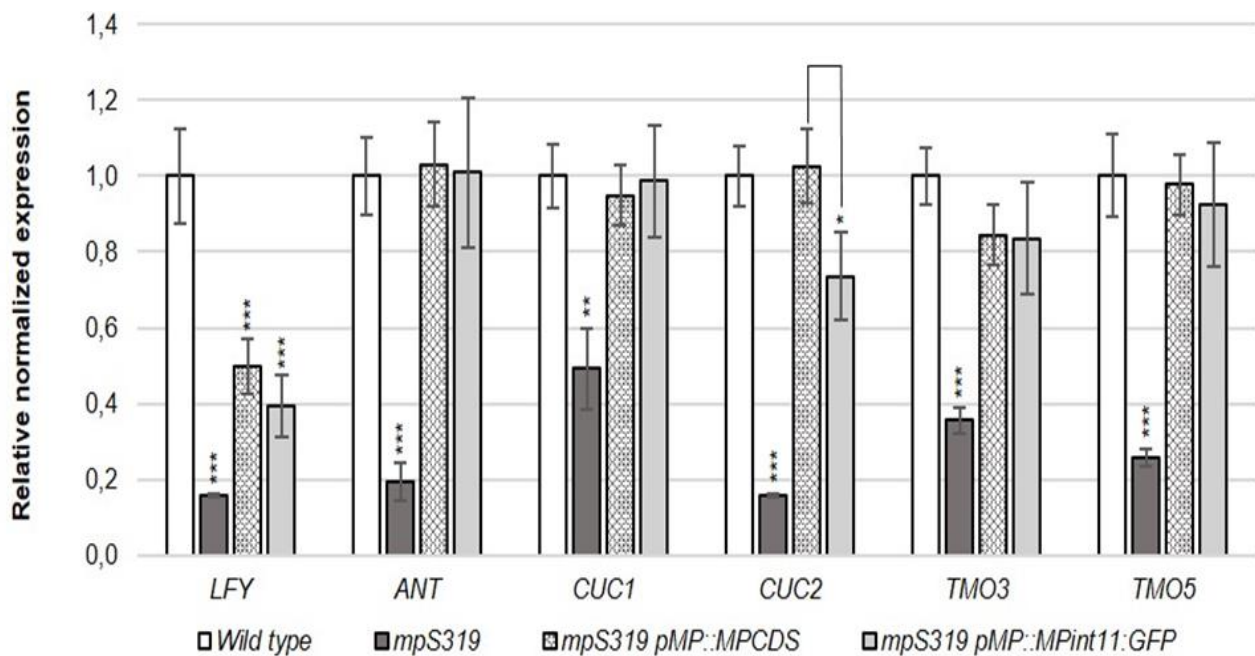


Fig. 2.5. MP direct targets complementation in *MPint11* and *MPcds* rescue lines. Normalisation based on *ACT8-2* and *UBI10* mRNA levels. Error bars indicate the S.E. calculated on three biological replicates. $p^* < 0.05$; $p^{**} < 0.01$ and $p^{***} < 0.001$ (one-way ANOVA and Tukey's HSD test)

2.5 Discussion

Our results indicate that, in the developmental contexts that we have analysed, MP C-terminal domain is not strictly required for its activity, suggesting its ability to work uncoupled from the classical auxin-AUX/IAAs regulation and be an activator of its direct targets despite auxin levels. We characterised a new *MP* alternative splicing event associated to the translation of a natural truncated protein variant, lacking the PB1 domain, required during ovule development. Interestingly, from conservation analyses, we found that *MP* eleventh intron sequence was highly conserved among *Arabidopsis* genus and in other members of the Brassicaceae family, with a level comparable to the one of the coding regions and higher respect to the one of other *MP* introns (fig. 2.6)

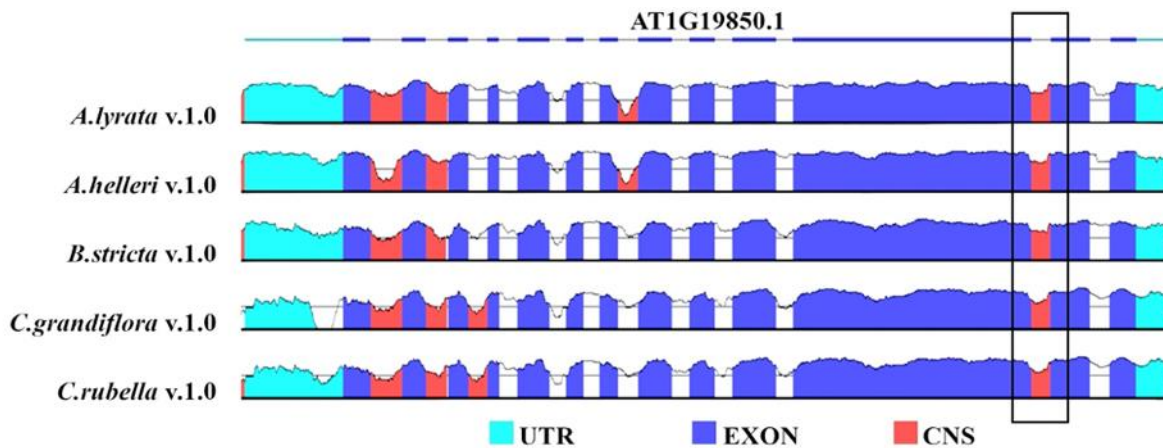


Fig.2.6. Evolutionary conservation of *MP* genomic sequence in: *Arabidopsis thaliana*, *A. lyrata*, *A. halleri*, *Boechera stricta*, *Capsella grandiflora* and *C. rubella*. The plot represents fragments with more than 70% nucleotide sequence conservation. Introns 1, 2 and 11 are depicted in pink and indicated as conserved non-coding sequences (CNS).

We found that, the presence of MP C-terminal domain was not required to regulate the transcription of its targets, indeed we observed a similar degree of complementation of direct targets expression in both *MPint11* and *MPcds* rescue lines. In literature, it has been reported that DBD is sufficient to allow MP to recognise AuxREs sequences, since it is also the domain involved in MP homodimerization [22,23]. Moreover, it has been shown that MP protein, without the PB1 domain, maintain the ability to recruit the chromatin modifier BRM and SYD through the MR, leading to chromatin remodelling [19]. *MPint11* and *MPcds*

complementation results, suggest that both isoforms are sufficient to restore many plant developmental processes, but alone they are not enough to completely fulfil all functions required in the diverse plant developmental contexts. Even if the number of ovules primordia was similarly restored in the diverse rescue lines, the canonical MP showed a higher functionality during flower and pistil development. On the other side, *MPint11* is required for further ovule developmental stages and integuments growth. Preliminary data show that, intron eleventh retention might be partially regulated by auxin levels. We evaluated the expression level of *MPint11* isoform by Real-time qPCR on cDNA, retro-transcribed from two biological replicates of Col-0 wild type inflorescences treated with IAA. Interestingly, we observed a reduction of the 30% in *MPint11* expression in IAA treated samples respect to mock controls. These results suggest that, auxin might act as a negative regulator of the alternative transcript generation (fig. 2.7). We speculate that, *MPint11* might be especially needed to support MP function in auxin minima, while its role in auxin maxima might be less relevant. In this *scenario*, alternative splicing can be used to modulate MP activity in the different hormonal environments. Furthermore, the fact that MP is involved in PIN1 expression and polar localisation [24], suggests that it has to be functional even at a sub-threshold auxin concentration, in order to drive auxin polar distribution and accumulation.

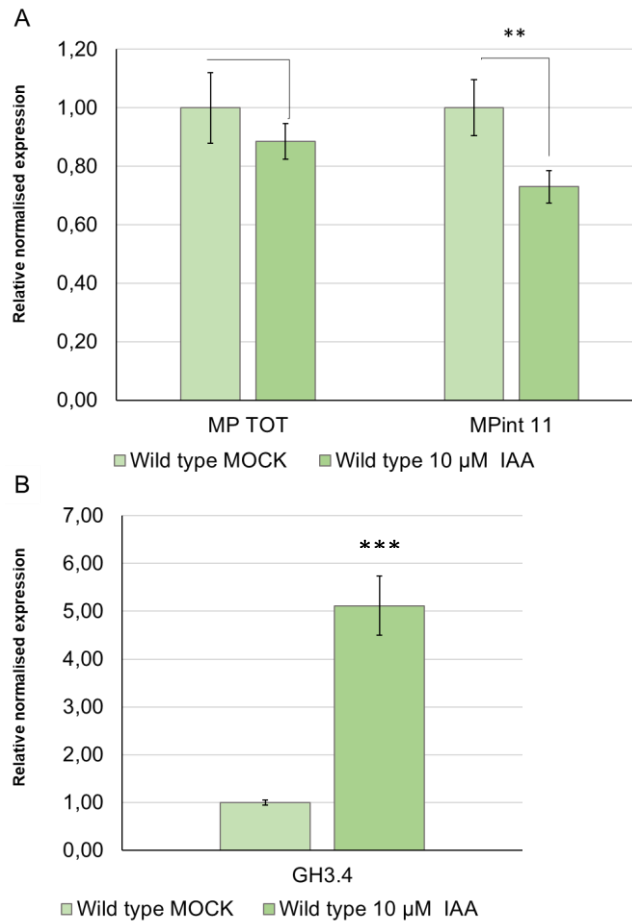


Fig. 2.7. Auxin treatment negatively impacts on *MPint11* expression. Graphs are generated by the combination of two biological replicates of IAA and mock treatment on Col-0 wild type inflorescences. Each biological replicate is composed by 3 to 5 inflorescences for each treatment. (A) *MP* and *MPint11* expression between mock controls and treated samples with 10 μM IAA. (B) *GH3.4* has been used as positive control for auxin signalling induction in relation to IAA application. ** p<0.01, *** p<0.001 (t-test students performed on mock vs treatment pairs)

3. Auxin modulates MP post-translational regulation in root development

3.1 MPint11 isoform is functional in rescue *mp* related phenotype during root development

MP characterisation has pointed out its importance in embryo and root development, suggesting its role in embryo axis formation and root initiation [25–28]. Auxin has been shown to directly regulate root organization and meristematic activity maintenance, and MP is involved in these processes regulating auxin polar transport through PINs activation [24]. For these reasons, we decided to investigate about *MP* canonical versus *MPint11* alternative isoforms relevance and regulation during root development process. *mp* mutants have different degrees of aberrant phenotypes penetrance at the seedling level, which include absence of the root or the presence of impaired cotyledons [29]. In *mpS319* mutant, around 40% to 50% of the expected homozygous, obtained by self-fertilization of the heterozygous, lack the primary root (fig.3.1 B). In order to test the functionality of *MP* isoforms in this developmental context, we compared the ratio of seedlings with *mp*-related phenotype in *mpS319 pMP:MPint11-GFP* and *mpS319 pMP:MPcds* rescue lines. Interestingly, we observed a differential efficiently rescue of *MP* isoforms. Indeed, while the 33% of expected *mpS319* homozygous seedlings from *mpS319/+ pMP:MPcds* plants present severe defects, this percentage was of the 15% in the *mpS319/+ pMP:MPint11-GFP* offspring (fig. 3.1 A).

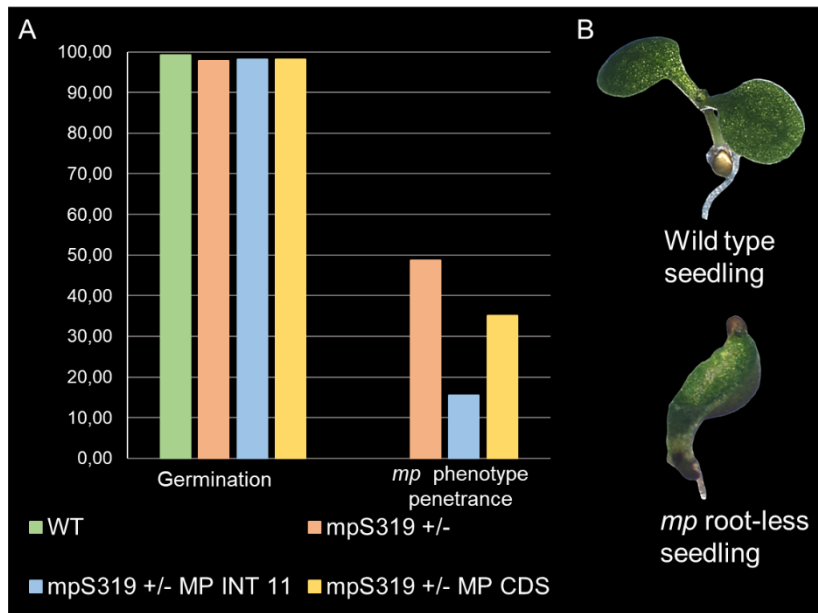


Fig. 3.1. Complementation of *mp* phenotype at seedling level by *MPint11* and *MPcdfs* in the *mpS319* mutant. (A) Germination rate and *mp* phenotype penetrance in wild type, *mps319 +/-*, *mpS319 +/- pMP:MPint11-GFP* (single copy) and *mpS319 +/- pMP:MPcdfs* (single copy) offspring. *mp* phenotypes penetrance is calculated considering that the expected homozygous are 1/4 of the total seeds for *mps319 +/-*, *mpS319 +/- pMP:MPint11-GFP* (single copy) and *mpS319 +/- pMP:MPcdfs* (single copy). Moreover, the calculation consider that only 3/4 of the expected homozygous in *mpS319 +/- pMP:MPint11-GFP* (single copy) and *mpS319 +/- pMP:MPcdfs* (single copy) will inherit the construct. N=300 seeds from independent lines for each genotype. (B) example of wild type like 5 days old seedling and severe *mpS319* root-less seedling

3.2 Combined analyses of MP reporter lines reveal differential post-translational regulations of MP isoforms in the RAM

*MPc*ds and *MPint11* differential ability to restore embryo and root development, brought us to speculate about the existence of their specific functions and regulations. To address to this hypothesis, in collaboration with Prof. Anthony Bishopp, we analysed different MP reporter lines in the root tip with the purpose to study, at the same time, *MP* transcriptional pattern and canonical and alternative proteins accumulation domains. In particular, we took advantage of two reporter lines. The first one carries a construct formed by the genomic sequence of *MP*, fused in-frame with the *eGFP* sequence in its eleventh exon, under the control of *MP* native promotor. Once translated, the eGFP results inside the MR domain, a region common to both MP and MPint11 proteins. As consequence, from this construct, two different fusion proteins are produced: the full-length MP-eGFP (mr) and the alternative MPint11-eGFP(mr). This makes the eGFP signal visible, a combination of MP isoforms accumulation patterns (fig. 3.2 E). Despite the position of the eGFP, *MP::MP:eGFP(mr)* construct results completely functional for the complementation of *mp* mutant *mpB4149* [28]. The second reporter line considered (*MP::MP:VENUS-2aP-mTORQUOISE* provided from Prof. Anthony Bishopp) was designed as a dual-purpose reporter line. This reporter line carries a construct made by *MP* native promotor, driving the expression of *MP* genomic sequence, fused in-frame at the 3' end with the *VENUS*. Downstream to the *VENUS* is present the sequence of the 2a peptide and the *mTORQUOISE*, associated to a nuclear localization signal. The 2a is a peptide of 18 aminoacids which induce the so-called event of "Stop-Carry On" at its translation. Once the ribosome reaches the 2a peptide c-terminal, the translation is arrested, leading to the release of the newly produced protein. Contextually, translation re-starts immediately on the same mRNA, allowing the production of multiple proteins from the same transcript [30]. The *MP::MP:VENUS-2aP-mTORQUOISE* reporter gives information, at the same time, about *MP* transcriptional and translational domains, thanks to the mTQ signal, and about canonical MP accumulation pattern thanks to the MP-*VENUS*(ct) fusion protein one (fig. 3.2 B). From reporter lines analyses result that *MP* is transcribed and translate in almost all RAM cells (mTQ signal in magenta). Similarly, MP-eGFP(mr) reporter line, which allows the visualisation of both MP protein isoforms accumulation, shows a similar behaviour. Interestingly, we observed that canonical MP protein (MP-*VENUS* ct) was accumulated in precise tissues which comprise: the middle of

the central stele, the qc, the columella and the epidermis. These results suggest that, MP and MPint11 isoforms, undergo specific post-translational modification in the RAM having a different stability. While the canonical MP is accumulated only in few domains, the alternative MPint11 has a broader pattern, leading to an expansion of *MP:MP-eGFP(mr)* signal (fig. 3.2 A, C). To confirm the differential accumulation of canonical MP protein, we considered in the analysis an additional reporter line (provided from Prof. Dolf Weijers). This reporter line was similar to the *MP::MP:eGFP(mr)* one, with the exception that the eGFP was cloned at *MP* 3' end. As observed before, canonical MP-eGFP(ct) fusion protein was distributed as the MP-VENUS(ct) one, confirming the results described above (fig. 3.2 D).

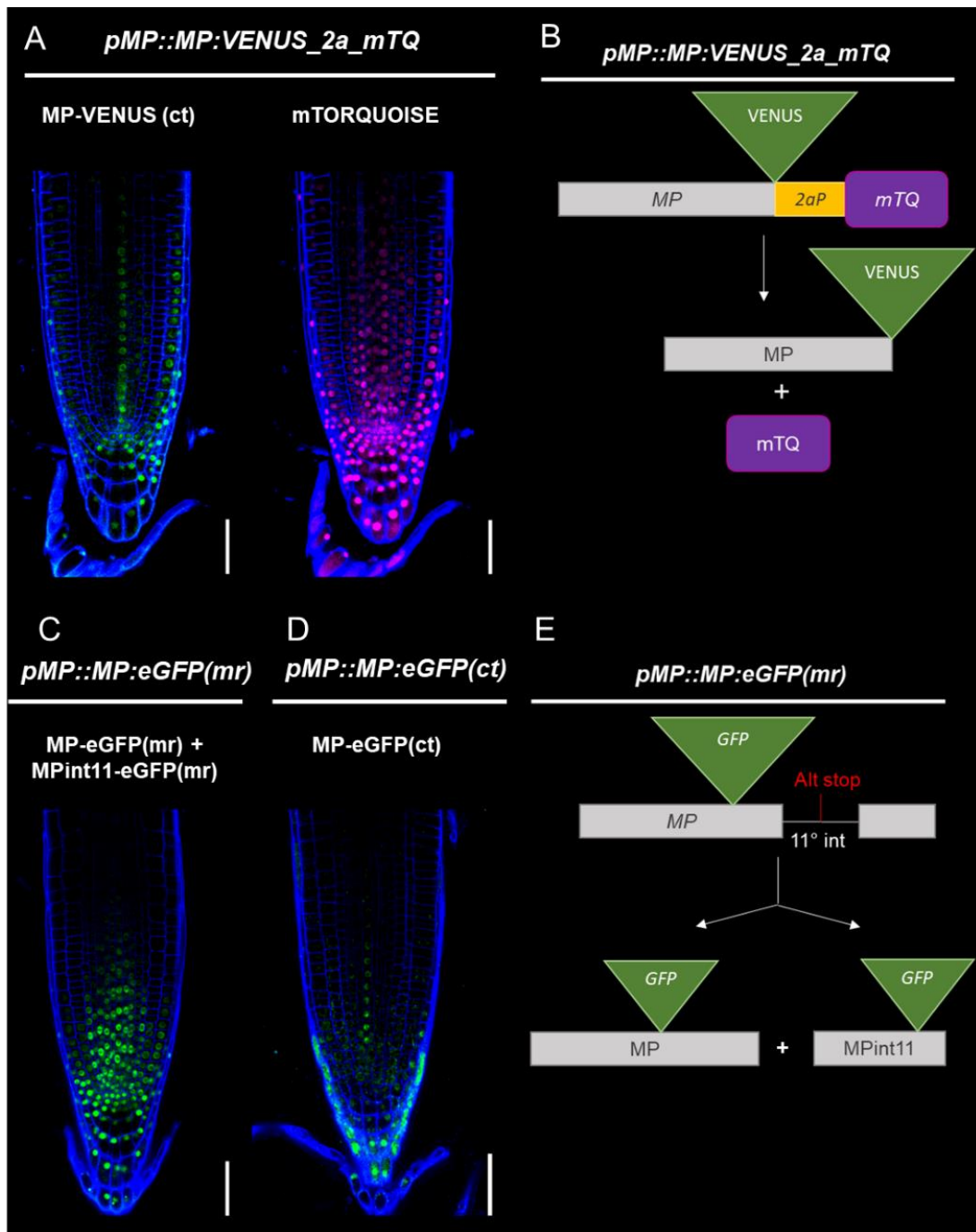


Fig. 3.2. *MP* reporter lines analysis in the RAM. (A) *MP::MP:VENUS:2aP-mTORQUOISE* signals in the RAM. *MP* is expressed and translated in the whole main-root tip (mTQ in magenta), whereas canonical *MP* is accumulated just in precise tissues (VENUS in green). (B) Scheme of *MP::MP:VENUS:2aP-mTORQUOISE* reporter line structure. The presence of the 2A peptide allows the translation of different proteins from the same transcript. (C) *MP::MP:eGFP(mr)* reporter line signal in the RAM. The eGFP signal is a combination of the accumulation patterns of *MP-eGFP(mr)* and *MPint11-eGFP(mr)* fusion proteins. (D) *MP::MP:eGFP(ct)* signal in the RAM. This construct leads to the translation of the *MP-eGFP(ct)* fusion protein, which show the same accumulation pattern of the *MP-VENUS(ct)* one. (E) Scheme of *MP::MP:eGFP(mr)* reporter line structure. The eGFP sequence, being located in a common region to *MP* and *MPint11*, leads to the translation of two fusion proteins from the same construct: *MP-eGFP(mr)* and *MPint11-eGFP(mr)*. Scale bars: 50µM

In order to verify that these observations were due to MP post-translational peculiar regulatory mechanisms, we performed similar experiments for *ARF6* and *ARF8* (fig. 3.3 A, B). *ARF6* and *ARF8* were expressed and translated in the whole RAM and we didn't see any differences between transcriptional and translational patterns, indicating that the phenomenon observed with *MP::MP:VENUS-2aP-mTORQUOISE* reporter line was due to a specific regulative mechanism associated to MP protein, instead to construct-related artefacts.

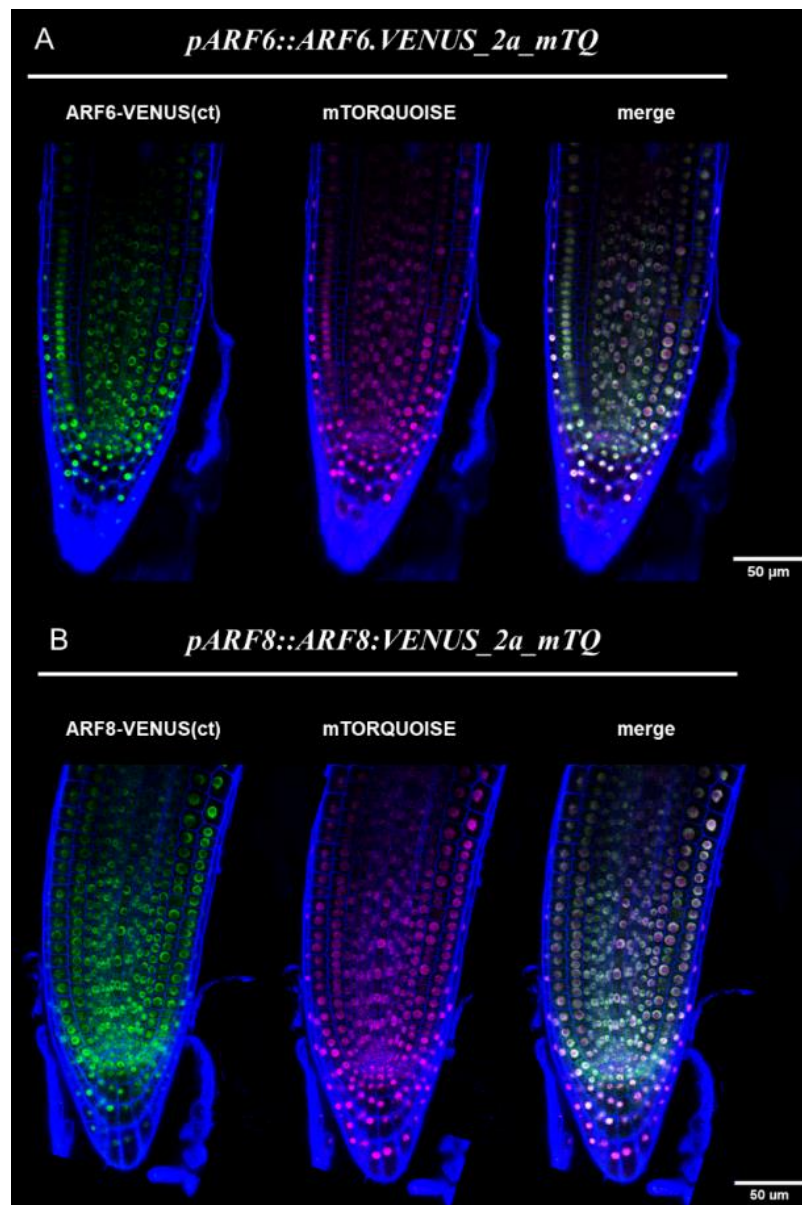


Fig. 3.3. Double purpose reporter lines for *ARF6* and *ARF8*. (A) *ARF6::ARF6:VENUS-2aP-mTORQUOISE* reporter line in the RAM. (B) *ARF8::ARF8:VENUS-2aP-mTORQUOISE* reporter line in the RAM. In both cases no differences have been observed between promoter activity regions and protein accumulation patterns.

3.3 Canonical MP protein stability is related to auxin concentration

The specific accumulation pattern of MP canonical protein brought us to hypothesise that additional factors might be involved in the regulation of its stability at a post-translational level. In the root apex, auxin maxima points have been deeply characterised, leading to the formulation of the auxin inverted cascade model: auxin is mobilised through the central stele in the root tip and then re-directed in the epidermis toward the shoot [31]. Since MP-VENUS(ct) and MP-eGFP(ct) fusion proteins were specifically present in tissues described to be points of auxin maxima, we speculated that high auxin level might be directly correlated to MP protein accumulation. To test this hypothesis, we treated *MP::MP:VENUS-2aP-mTORQUOISE* 5 days old seedlings with exogenous IAA, and we compared mTQ and VENUS signals between mock and treated samples. While mTQ signal didn't change between control and IAA treatment, confirming that *MP* promoter activity is not influenced by IAA, we observed an expansion of MP-VENUS(ct) fusion protein accumulation domain, confirming a positive function of auxin on MP stability (fig. 3.4 A). Since the major changes observed were associated to MP-VENUS (ct) accumulation pattern in the central stele, we measured the fluorescent signal intensity in this region. As expected, we didn't observe differences in mTQ fluorescent signal between mock and treated samples whereas, we found a statistical significance increase in MP-VENUS (ct) intensity (fig. 3.4 C). As control for auxin levels change in association to IAA treatment, we performed the experiment in parallel on *DR5::GFP* reporter line 5 days old seedlings. Indeed, we observed a statistically significant increase in GFP signal (fig. 3.4 B, D).

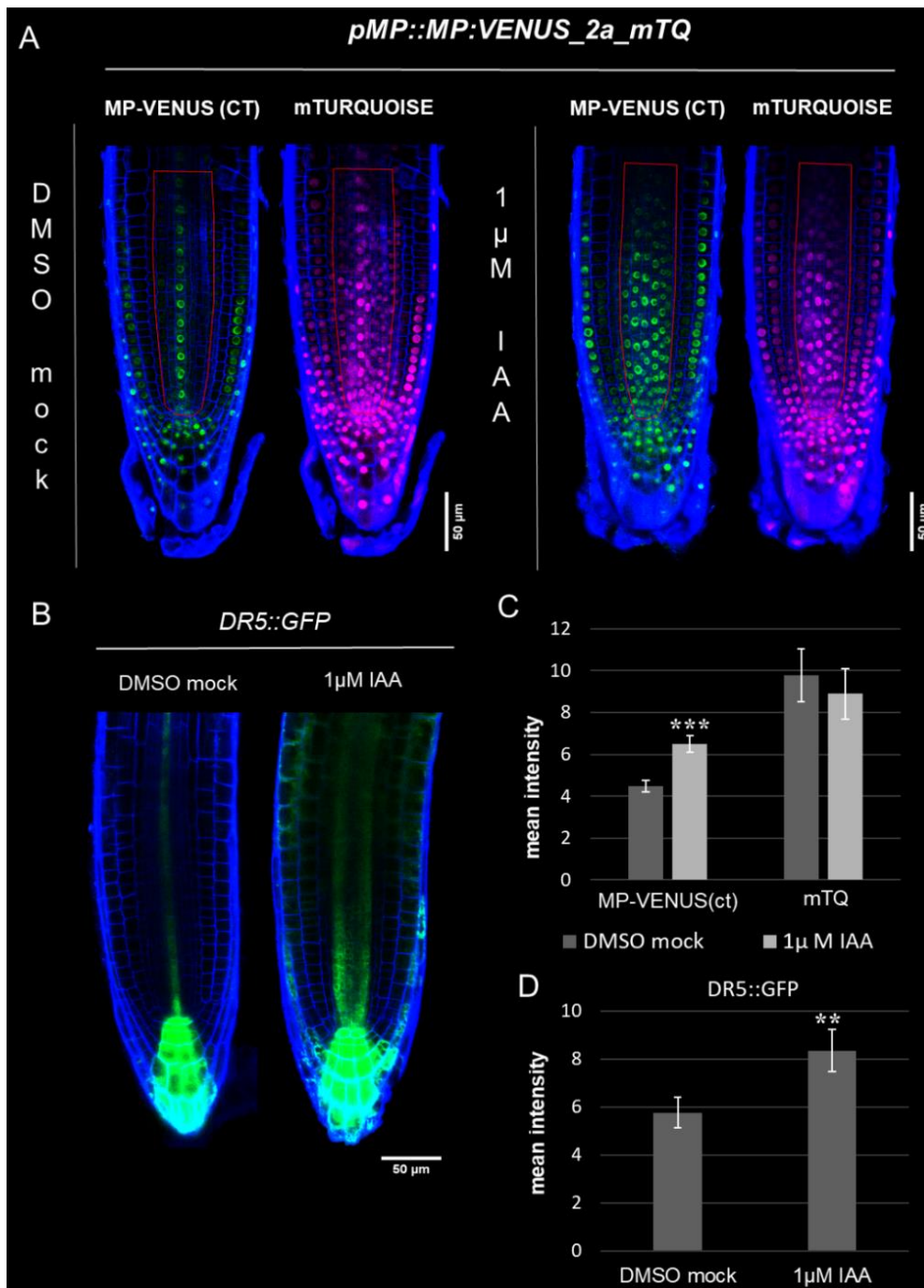


FIG. 3.4. Auxin treatment on *MP::MP:VENUS:2aP-mTORQUOISE* and *DR5::GFP* 5 days old seedlings. (A) *MP::MP:VENUS:2aP-mTORQUOISE* expression patterns in DMSO mock control and 1 μM IAA treatment. Auxin increase leads to MP-VENUS(ct) fusion protein accumulation in the whole MP promotor activity domain. The red polygons indicated the regions considered for signal intensity measurement. (B) *DR5::GFP* signal in DMSO mock control and 1 μM IAA treatment. (C) VENUS and mTQ signals intensity in *MP::MP:VENUS:2aP-mTORQUOISE* 5 days old seedlings in association to DMSO mock control or IAA treatment. VENUS intensity is statistically enhanced in association to auxin application. (D) GFP signal intensity in *DR5::GFP* 5 days old seedlings in association to DMSO mock control or IAA treatment. (C,D) Data are presented as mean ± S.E. of signal intensity of 15 plants for each reporter line in both the treatment conditions. Measurements were performed with ImageJ software. *** p<0.001, ** p<0.01, (t-test students performed on mock vs treatment pairs).

3.4 Proteasome activity leads to MP protein degradation in auxin minima

The presence of the mTQ signal not only is an indication of *MP* transcription but it is also associated to *its* translation. The *mTORQUOISE* sequence, been located downstream to *MP-VENUS* and the *2aP*, is translated only after the event of “Stop-Carry On”, implicating *MP-VENUS* previous translation. This observation suggests that, canonical *MP* protein is translated in the whole RAM but is subsequentially degraded in points of auxin minima and accumulated in auxin maxima. We speculated that proteasome activity could be involved in this process and, to confirm this hypothesis we treated *MP::MP:VENUS-2aP-mTORQUOISE* 5 days old seedlings with a proteasome inhibitor drug (bertezomib). Proteasome inhibition directly impacted on *MP-VENUS* (ct) stability, leading to an expansion of its accumulation domain even in auxin minima regions (fig. 3.5 A). As before, we measured mTQ and VENUS fluorescent signals in the central stele. As expected, we observed a statistically significant increase in *MP-VENUS* intensity in association to bertezomib treatment (fig. 3.4 B). Likely, while the VENUS:mTQ signal intensity ratio was around 0.6 in DMSO control, it raised to around 1.2 in association to proteasome inhibition (fig. 3.5 C).

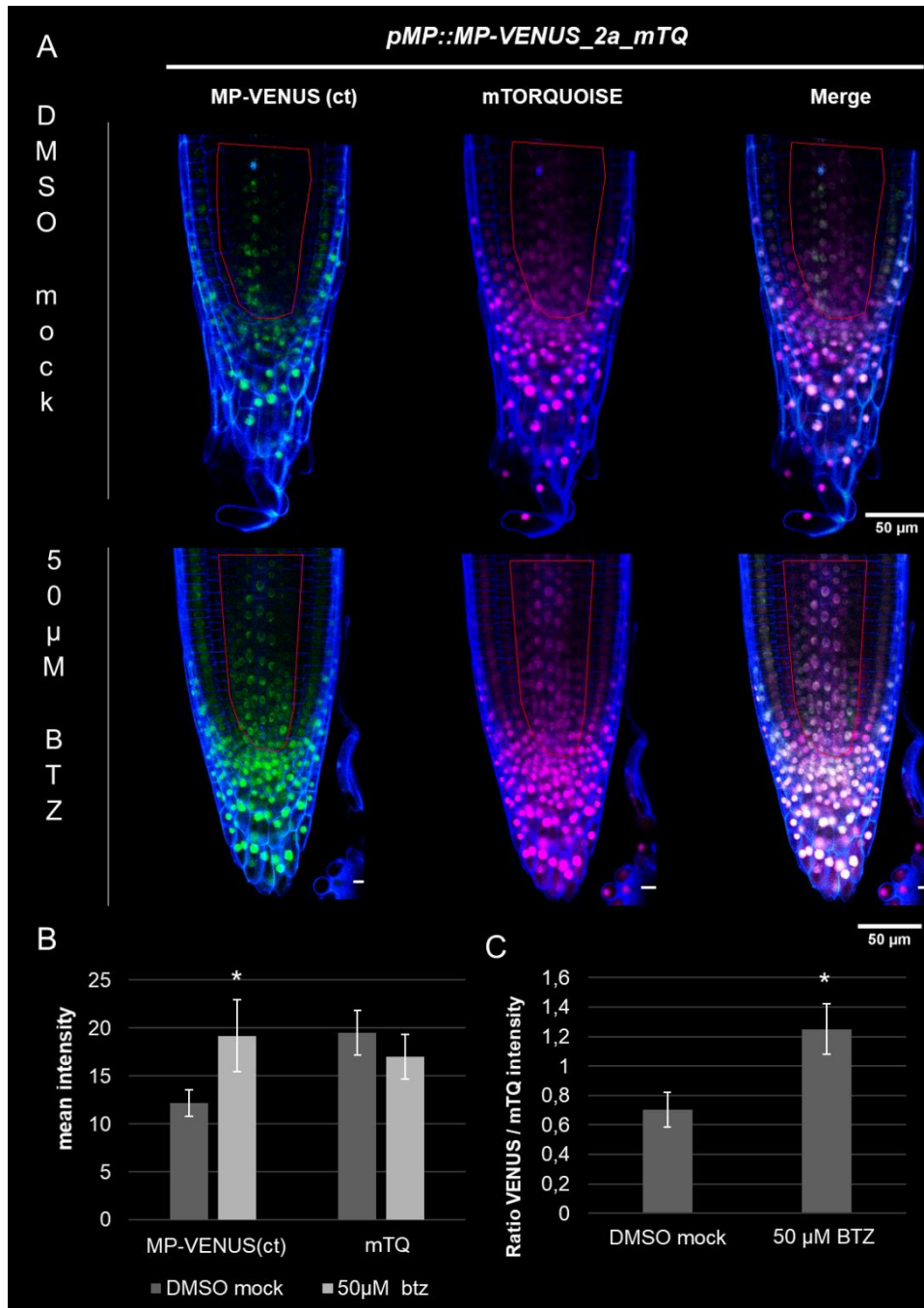


Fig. 3.5. Bertezomib treatment on *MP::MP:VENUS:2aP-mTORQUOISE* 5 days old seedlings. (A) *MP::MP:VENUS:2aP-mTORQUOISE* expression patterns in DMSO mock control and 50 μ M BTZ treatment. MP-VENUS(ct) fusion protein is stabilised by proteasome inhibition. The red polygons indicated the regions considered for signal intensity calculation (B) VENUS and mTQ signals intensity in *MP::MP:VENUS:2aP-mTORQUOISE* 5 days old seedlings in association to DMSO mock control or BTZ treatment. VENUS intensity is statistically enhanced in association to proteasome inhibition. (C) ratio between VENUS and mTQ signals intensity in DMSO mock control and 50 μ M BTZ treatment. Data are presented as mean \pm S.E. of signal intensity of 10 plants in both the treatment conditions. Measurements were performed with ImageJ software. * $p < 0.05$ (t-test students performed on mock vs treatment pairs).

3.5 MP canonical protein accumulation is dynamically modulated during lateral root development

MP has been proposed to be also important for lateral root development process, acting synergistically with ARF7 and ARF19 to promote primordia organisation and growth [32]. For this reason, we decided to analyse *MP::MP:VENUS-2aP-mTORQUOISE* and *MP::MP:eGFP(mr)* reporter lines in lateral root primordia, with the aim to understand if MP and MPint11 undergo the same post-translational regulations observed in the RAM. LRs (lateral root) originate from few cells in the pericycle and their development can be divided into 8 stages, in relation the number of cells by which are composed and in relation to their internal organisation. In particular, we focused our attention on stages II, IV, VII and VIII. While stages II and IV can be considered early phases of later root development, at stage VII and VIII LR cells start to acquire their identity, with the specification of: epidermis, cortex, endodermis and pericycle [33]. At stages II and IV, we observed that *MP* was transcribed and translated in the whole LR primordium (mTQ signal). Interestingly, we didn't observe differences between MP-VENUS (ct) and MP-eGFP (mr) / MPint11-eGFP(mr) accumulation patterns in these stages (fig. 3.6 A, B). At stages VII and VIII, while *MP* expression domain remained associated to all LR tissues, similarly to MP-eGFP (mr) / MPint11-eGFP(mr) pattern, MP-VENUS (ct) fusion protein was confined in few cells at the apex of the primordium (fig. 3.6 A, B). This event suggested that, during LRs formation, MP canonical protein undergoes post-translational regulation, as in the primary root.

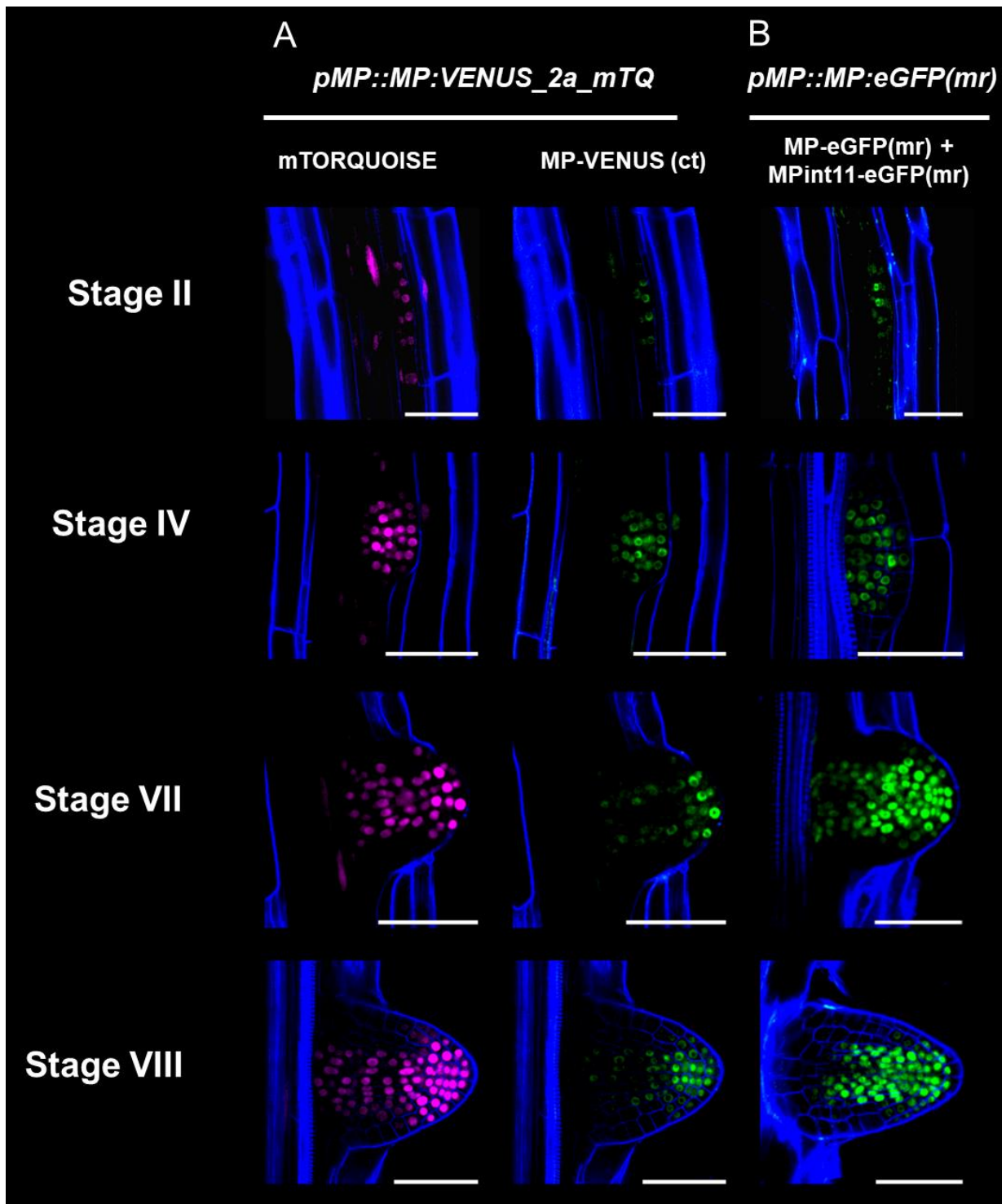


Fig. 3.6. *MP* reporter lines analysis in lateral root primordia. (A) *MP::MP:VENUS:2aP-mTORQUOISE* reporter line in LR primordia at stages: II, IV, VII, VIII. No differences were observed between mTQ and MP-VENUS(ct) domains at stages II and IV. MP-VENUS(ct) fusion protein is accumulated in the distal part of primordia at stages VII and VIII while *MP* transcription and translation (mTQ) remain broader. (B) *MP::MP:eGFP(mr)* reporter line in LR primordia at stages: II, IV, VII, VIII. In all the developmental stages considered *MP::MP:eGFP(mr)* reporter show the same pattern of the *MP* transcription and translation domain. Scale bar: 20 μ m

We have also analysed *ARF6::ARF6:VENUS-2aP-mTORQUOISE* and *ARF8::ARF8:VENUS-2aP-mTORQUOISE* reporter lines in the same LR primordia developmental stages. As already observed in the RAM, *ARF6* and *ARF8* were expressed, translated and accumulated in the same tissues in all different stages considered (shown in fig. 3.7 only stage 8 as indicative one).

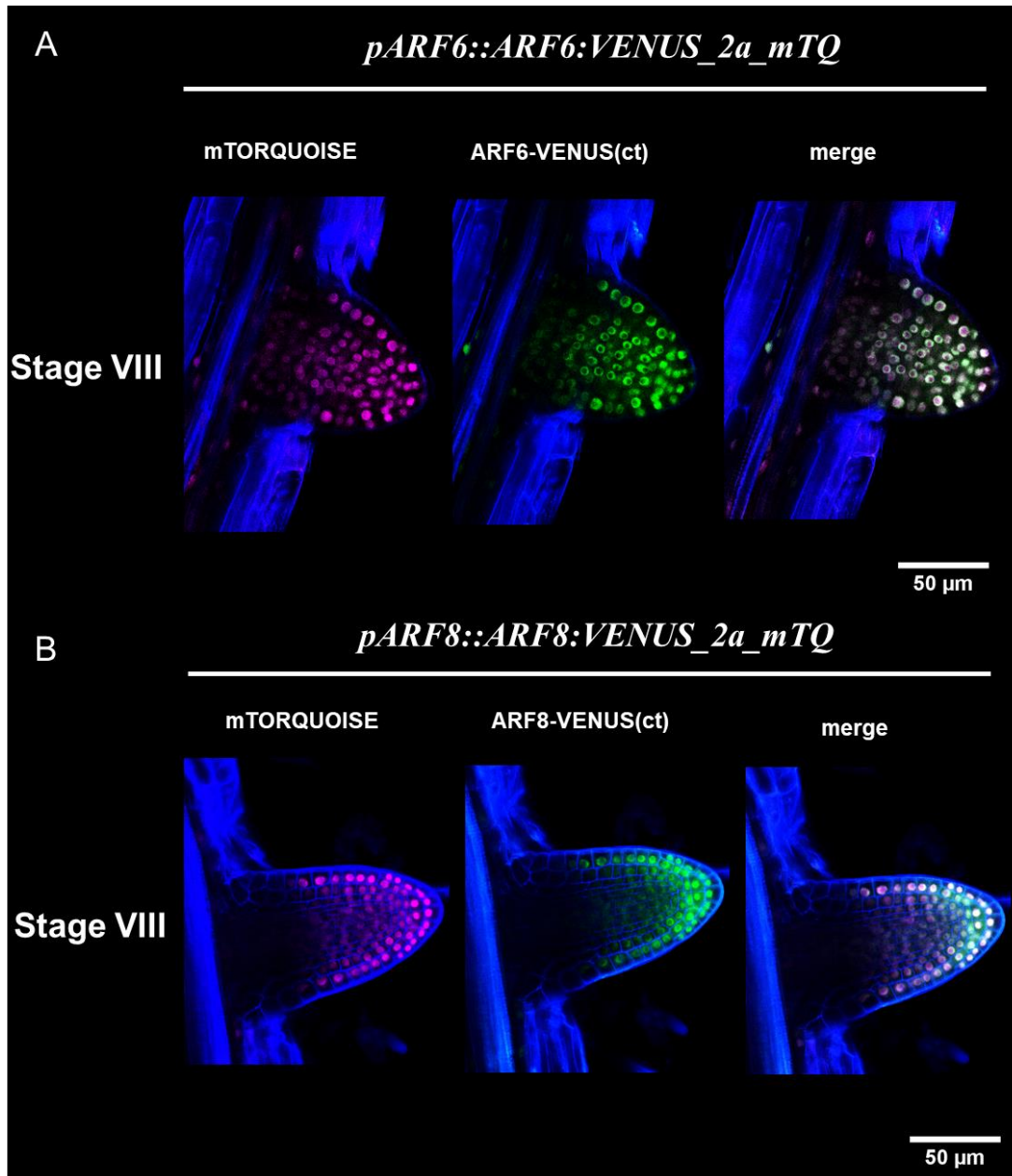


Fig. 3.7. Double purpose reporter lines for *ARF6* and *ARF8* during lateral root development. (A) *ARF6::ARF6:VENUS-2aP-mTORQUOISE* reporter line in LR primordia at stage VIII. (B) *ARF8::ARF8:VENUS-2aP-mTORQUOISE* reporter line in LR primordia at stage VIII. No differences have been observed between mTQ and VENUS signals. Stage VIII reported as indicative one for all the stages analysed.

3.6 Discussion

Our results show that, alternative MPint11 isoform activity is required not only during reproductive development, but also in embryo and root organization. MPint11 is functional in rescue *mp* alteration at the seedling level, with a rate higher respect to the one observed for canonical MP. MP and MPint11 undergo specific post-translation regulation, which impact on their stability and accumulation. We speculate that MPint11, been stable in a broader context, might be involved in a higher number of developmental processes, showing and enhanced ability respect to canonical MP in restoring primary root formation. In relation to this, it has been shown that MP directly induce the expression of the miR390 in the RAM, through the direct binding of an AuxRE element in miR390 encoding gene promotor [34]. *MiR390* is involved in auxin response regulation in the root tip and positively regulates the production of the *ta-siRNA* which modulates ARF2, 3 and 4 abundance. In the RAM, miR390 promotor is active in domains of auxin maxima and minima. Despite this, from our observations result that canonical MP protein is present only in domains of auxin maxima. We speculate that, the presence of the broadly accumulated MPint11 isoform might support miR390 transcription, explaining its expression pattern in the RAM.

Our results suggest a completely new level of auxin-mediated regulation on ARFs. Indeed, we found that auxin directly impact not only of their transcriptional functionality but also on their protein stability. We observed that high auxin levels promote MP protein accumulation whereas, sub-threshold auxin concentrations lead to its degradation by the proteasome. This mechanism is also integrated by the presence of multiple MP protein isoforms with differential sensibility to this process, leading to the establishment of a *scenario* in which auxin signalling appears to be much more complex respect to what is already known. We speculate that, the specific degradation of MP protein might be linked to the presence of the PB1 domain, since it is the only domain absent in the alternative MPint11. The PB1 domain is involved in protein-protein interaction events and it mediates the binding with AUX/IAAs. Our hypothesis is that the association of AUX/IAAs to the PB1, in auxin minima, may recruit additional factors which could bring MP to the proteasome. Whereas, the absence of AUX/IAAs in auxin maxima might result in MP stabilisation. We are going to test this hypothesis studying MP-VENUS(ct) pattern in presence of a stabilised version of IAA12/BODENLOS, which can't be degraded in auxin maxima. In this scenario, the constitutive presence of BDL bound to MP PB1 should bring to lose of MP-VENUS(ct)

recombinant protein signal. Interestingly, reporter lines analysis during ovule development reveals that, in this context, MP-VENUS(ct) and MP-eGFP(mr)/MPint11-eGFP(mr) share similar accumulation patterns. Indeed, these fusion proteins were accumulated in auxin minima regions in the proximal part of primordia (fig. 3.8). This result suggests that canonical MP degradation in auxin minima is a process specifically related to root tissues. In relation to this, our previous studies pointed out the functionality of MP and MPint11 for ovules formation, showing that these isoforms were able to work uncoupled from auxin regulation to promote ovules primordia formation and growth. Moreover, from these studies emerged that the PB1 was not strictly necessary to regulate MP function during reproductive development. In light of this, the differential behaviour of canonical MP protein post-translational regulation, from root to ovule, is in line with its differential ability to rescue the diverse *mp* phenotypic alterations. Indeed, while canonical MP results largely functional for ovules development complementation, supporting its functionality as transcriptional activator in auxin minima in this context, it shows a lower ability in restore root development in *mpS319* mutant.

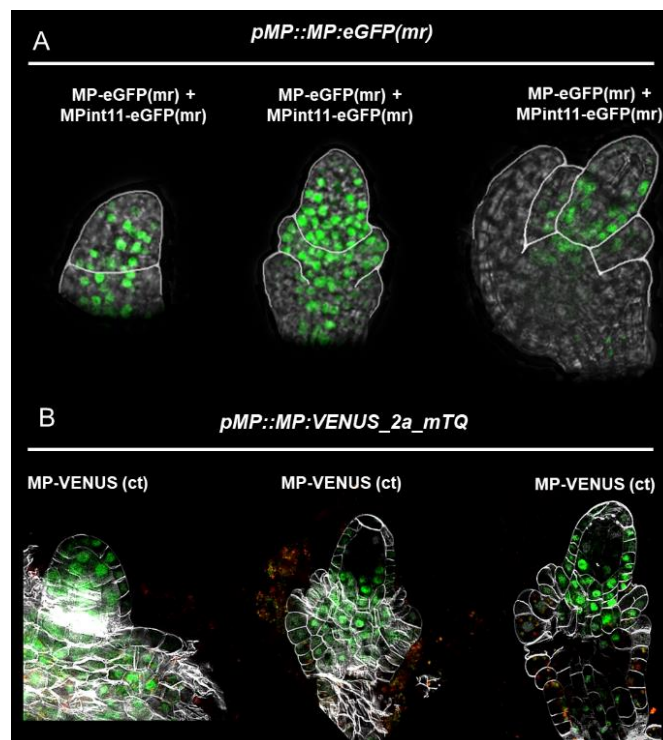


Fig. 3.8. *MP::MP:eGFP(mr)* and *MP::MP:VENUS:2aP-mTORQUOISE* reporters in free following developmental stages of ovules primordia. (A) MP-eGFP(mr) + MPint11-eGFP cumulative accumulation pattern from *MP::MP:eGFP(mr)* reporter line. (B) MP-VENUS(ct) accumulation pattern from *MP::MP:VENUS:2aP-mTORQUOISE* reporter line. In this developmental context MP-eGFP(mr) + MPint11-eGFP and MP-VENUS(ct) share the same domains, suggesting that the canonical MP degradation in auxin minima is a regulative mechanism related to root development.

Concerning lateral root development, even in this context canonical MP shows different behaviours in relation to the developmental stage considered. While MP and MPint11 have the same accumulation pattern in early developmental stages (II-IV), they show differences once reached the later ones (VII-VIII). Indeed, canonical MP is stabilised only in the distal part of the primordia at stages VII and VIII (fig. 3.9 A). As previously described, LR primordia are characterised by general high levels of auxin from stage I to IV, however auxin is mobilised in few cells in the primordium apex from stage V to VIII [33,35] (fig. 3.9 B). This behaviour is coincident with MP-VENUS(ct) one suggesting that, also in lateral roots, canonical MP protein stability is related to auxin levels.

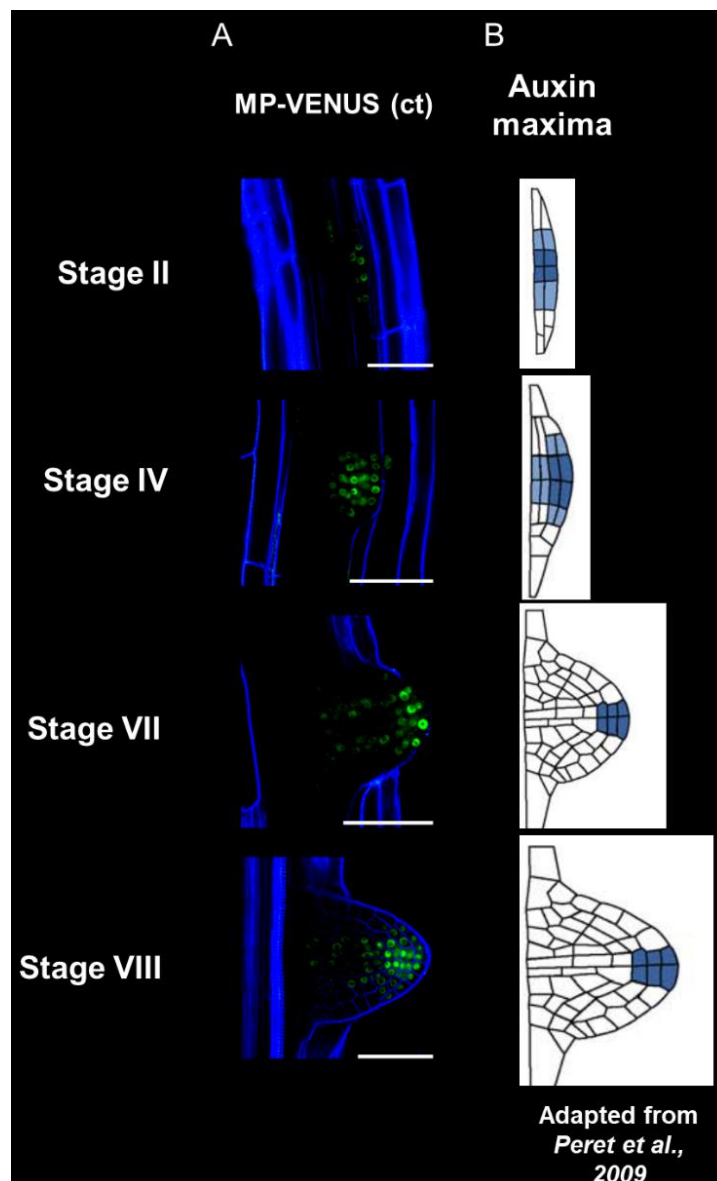


Fig. 3.9. MP-VENUS(ct) fusion protein accumulation in lateral root primordia follow the points of auxin maxima as described in [34]. Scale bar: 20 μ m.

References

1. Cheng, C.Y., Krishnakumar, V., Chan, A.P., Thibaud-Nissen, F., Schobel, S., and Town, C.D. (2017). Araport11: a complete reannotation of the *Arabidopsis thaliana* reference genome. *Plant J.* *89*, 789–804.
2. Hayashi, N., Sasaki, S., Takahashi, H., Yamashita, Y., Naito, S., and Onouchi, H. (2017). Identification of *Arabidopsis thaliana* upstream open reading frames encoding peptide sequences that cause ribosomal arrest. *Nucleic Acids Res.* *45*, 8844–8858.
3. Nishimura, T., Wada, T., Yamamoto, K.T., and Okada, K. (2005). The *Arabidopsis* STV1 protein, responsible for translation reinitiation, is required for auxin-mediated gynoecium patterning. *Plant Cell* *17*, 2940–2953.
4. Zanetti, M.E., Chang, I.F., Gong, F., Galbraith, D.W., and Bailey-Serres, J. (2005). Immunopurification of polyribosomal complexes of *Arabidopsis* for global analysis of gene expression. *Plant Physiol.* *138*, 624–635.
5. Lecampion, C., Floris, M., Fantino, J.R., Robaglia, C., and Laloi, C. (2016). An easy method for plant polysome profiling. *J. Vis. Exp.* *2016*, 1–7.
6. Bardou, F., Ariel, F., Simpson, C.G., Romero-Barrios, N., Laporte, P., Balzergue, S., Brown, J.W.S., and Crespi, M. (2014). Long Noncoding RNA Modulates Alternative Splicing Regulators in *Arabidopsis*. *Dev. Cell* *30*, 166–176. Available at: <http://dx.doi.org/10.1016/j.devcel.2014.06.017>.
7. Sugawara, S., Mashiguchi, K., Tanaka, K., Hishiyama, S., Sakai, T., Hanada, K., Kinoshita-Tsujimura, K., Yu, H., Dai, X., Takebayashi, Y., *et al.* (2015). Distinct Characteristics of Indole-3-Acetic Acid and Phenylacetic Acid, Two Common Auxins in Plants. *Plant Cell Physiol.* *56*, 1641–1654.
8. Hsu, P.Y., Calviello, L., Wu, H.Y.L., Li, F.W., Rothfels, C.J., Ohler, U., and Benfey, P.N. (2016). Super-resolution ribosome profiling reveals unannotated translation events in *Arabidopsis*. *Proc. Natl. Acad. Sci. U. S. A.* *113*, E7126–E7135.
9. Liu, M.J., Wu, S.H., Wu, J.F., Lin, W.D., Wu, Y.C., Tsai, T.Y., Tsai, H.L., and Wu, S.H. (2013). Translational landscape of photomorphogenic *Arabidopsis*. *Plant Cell* *25*, 3699–3710.
10. Lukoszek, R., Feist, P., and Ignatova, Z. (2016). Insights into the adaptive response of *Arabidopsis thaliana* to prolonged thermal stress by ribosomal profiling and RNA-Seq. *BMC Plant Biol.* *16*, 1–13. Available at: <http://dx.doi.org/10.1186/s12870-016-0915-0>.

11. Cole, M., Chandler, J., Weijers, D., Jacobs, B., Comelli, P., and Werr, W. (2009). DORNROSCHEN is a direct target of the auxin response factor MONOPTEROS in the Arabidopsis embryo. *Development* 136, 1643–1651.
12. Parra, G., Bradnam, K., Rose, A.B., and Korf, I. (2011). Comparative and functional analysis of intron-mediated enhancement signals reveals conserved features among plants. *Nucleic Acids Res.* 39, 5328–5337.
13. Rose, A.B., Carter, A., Korf, I., and Kojima, N. (2016). Intron sequences that stimulate gene expression in Arabidopsis. *Plant Mol. Biol.* 92, 337–346. Available at: <http://dx.doi.org/10.1007/s11103-016-0516-1>.
14. Rigo, R., Bazin, J., Romero-Barrios, N., Moison, M., Lucero, L., Christ, A., Benhamed, M., Blein, T., Huguet, S., Charon, C., *et al.* (2020). The Arabidopsis Inc RNA ASCO modulates the transcriptome through interaction with splicing factors. *EMBO Rep.* 21, 1–19.
15. Galbiati, F., Sinha Roy, D., Simonini, S., Cucinotta, M., Ceccato, L., Cuesta, C., Simaskova, M., Benkova, E., Kamiuchi, Y., Aida, M., *et al.* (2013). An integrative model of the control of ovule primordia formation. *Plant J.* 76, 446–455.
16. Ceccato, L., Masiero, S., Sinha Roy, D., Bencivenga, S., Roig-Villanova, I., Ditengou, F.A., Palme, K., Simon, R., and Colombo, L. (2013). Maternal Control of PIN1 Is Required for Female Gametophyte Development in Arabidopsis. *PLoS One* 8, 2–8.
17. Liao, C.Y., Smet, W., Brunoud, G., Yoshida, S., Vernoux, T., and Weijers, D. (2015). Reporters for sensitive and quantitative measurement of auxin response. *Nat. Methods* 12, 207–210.
18. Schlereth, A., Möller, B., Liu, W., Kientz, M., Flipse, J., Rademacher, E.H., Schmid, M., Jürgens, G., and Weijers, D. (2010). MONOPTEROS controls embryonic root initiation by regulating a mobile transcription factor. *Nature* 464, 913–916. Available at: <http://www.nature.com/doi/10.1038/nature08836>.
19. Wu, M.F., Yamaguchi, N., Xiao, J., Bargmann, B., Estelle, M., Sang, Y., and Wagner, D. (2015). Auxin-regulated chromatin switch directs acquisition of flower primordium founder fate. *Elife* 4, 1–20.
20. Singh, C., and Roy-Chowdhuri, S. (2016). Quantitative real-time PCR: Recent advances.
21. Nanao, M.H., Vinos-Poyo, T., Brunoud, G., Thévenon, E., Mazzoleni, M., Mast, D., Lainé, S., Wang, S., Hagen, G., Li, H., *et al.* (2014). Structural basis for oligomerization of auxin transcriptional regulators. *Nat. Commun.* 5, 3617.

22. Tiwari, B.S., Hagen, G., Guilfoyle, T. (2003). The Roles of Auxin Response Factor Domains in Auxin-Responsive Transcription. *The plant cell* 15, 533-543.
23. Boer, D.R., Freire-Rios, A., Van Den Berg, W.A.M., Saaki, T., Manfield, I.W., Kepinski, S., López-Vidriero, I., Franco-Zorrilla, J.M., De Vries, S.C., Solano, R., *et al.* (2014). Structural basis for DNA binding specificity by the auxin-dependent ARF transcription factors. *Cell* 156, 577–589.
24. Krogan, N.T., Marcos, D., Weiner, A.I., and Berleth, T. (2016). The auxin response factor MONOPTEROS controls meristem function and organogenesis in both the shoot and root through the direct regulation of PIN genes. *New Phytol.* 212, 42–50.
25. Hardtke, C.S., and Berleth, T. (1998). The *Arabidopsis* gene *MONOPTEROS* encodes a transcription factor mediating embryo axis formation and vascular development. *EMBO J.* 17, 1405–1411. Available at:
26. Berleth, T., and Jürgens, G. (1993). The role of the monopteros gene in organising the basal body region of the *Arabidopsis* embryos. *Trends Genet.* 9, 299.
27. Schlereth, A., Möller, B., Liu, W., Kientz, M., Flipse, J., Rademacher, E.H., Schmid, M., Jürgens, G., and Weijers, D. (2010). MONOPTEROS controls embryonic root initiation by regulating a mobile transcription factor. *Nature* 464, 913–916.
28. Weijers, D., Schlereth, A., Ehrismann, J.S., Schwank, G., Kientz, M., and Jürgens, G. (2006). Auxin triggers transient local signaling for cell specification in *Arabidopsis* embryogenesis. *Dev. Cell* 10, 265–270.
29. Odat, O., Gardiner, J., Sawchuk, M.G., Verna, C., Donner, T.J., and Scarpella, E. (2014). Characterization of an allelic series in the MONOPTEROS gene of *Arabidopsis*. *Genesis* 52, 127–133.
30. Hasson, S. (2000). Reporter Gene Assays for Algal-derived Available at: <http://www.springernature.com/series/7651>.
31. Benfey, P.N. (2012). Control of Root Development. *Annu. Rev. Plant Biol.*, 1–17.
32. De Smet, I., Lau, S., Voß, U., Vanneste, S., Benjamins, R., Rademacher, E.H., Schlereth, A., De Rybel, B., Vassileva, V., Grunewald, W., *et al.* (2010). Bimodular auxin response controls organogenesis in *Arabidopsis*. *Proc. Natl. Acad. Sci. U. S. A.* 107, 2705–2710.
33. Péret, B., De Rybel, B., Casimiro, I., Benková, E., Swarup, R., Laplaze, L., Beeckman, T., and Bennett, M.J. (2009). *Arabidopsis* lateral root development: an emerging story. *Trends Plant Sci.* 14, 399–408.

34. Dastidar, M.G., Scarpa, A., Mägele, I., Ruiz-Duarte, P., von Born, P., Bald, L., Jouannet, V., and Maizel, A. (2019). ARF5/MONOPTEROS directly regulates miR390 expression in the *Arabidopsis thaliana* primary root meristem. *Plant Direct* 3.
35. Benková, E., Michniewicz, M., Sauer, M., Teichmann, T., Seifertová, D., Jürgens, G., and Friml, J. (2003). Local, Efflux-Dependent Auxin Gradients as a Common Module for Plant Organ Formation. *Cell* 115, 591–602.

Conclusions and future perspectives

Our results indicate that *MP* activity, during *Arabidopsis* development, is modulated at post-transcriptional and post-translational levels. These events can play specific roles in different plant tissues, integrating auxin signalling out-put. In particular, we described the existence of two different alternative splicing events of *MP* pre-mRNA. In the first one, a portion of *MP* 5'UTR and the initial part of the first exon are recognised as a leader intron. We show that the alternative splicing of this sequence impacts on *MP* translational initiation, leading to the establishment of flexibility in the start codon usage. Thanks to the generation of two CRISPR-based *mp* mutants and by datasets analysis, we found that the fourth AUG on *MP* ORF can be used as translational initiator for the generation of a functional MP protein. Interestingly, leader intron sequence comprises 3 out of 4 uORFs, previously described to negatively affect MP translation. Despite this, we didn't observed differences between canonical and alternative *MP* splicing variants in their association to polysomes, suggesting that the uORFs-mediated translational inhibition doesn't impact on its functionality in inflorescence tissues, at least in the environmental condition tested. Additionally, our results show that *MP* leader intron alternative splicing is positively regulated by high auxin levels. This event is mediated by the action of the alternative splicing regulative module NSRs-*ASCO*, previously described to modulate alternative splicing upon auxin variations. Preliminary results show that MP itself might be involved in the regulation of its own splicing, or in the splicing of downstream targets. This is suggested by the putative interaction of MP with the spliceosome component PRP8, shown also to interact with the long non-coding RNA *ASCO*. In future, we will try to confirm such interaction and describe how *MP* alternative splicing is impaired in absence of PRP8 function. Moreover, it is still unknown whether canonical and leader-intron spliced *MP* variants might be relevant in particular conditions, such as stress responses. We are going to test how this regulative mechanism responds to stress conditions, as well as the behaviour of our CRISPR-generated alleles in such situations. In these cases, translation can occur only from the alternative translational start site, mimicking a constitutive leader intron splicing.

The second alternative splicing event characterised is associated to the retention *MP* eleventh intron. This post-transcriptional regulation leads to the generation of a protein variant, MPint11, which might escape AUX/IAAs binding. MPint11 is largely functional in restoring many *mp*-related aberrant phenotypes and is especially required for correct ovule development process. Interestingly, our results show that during ovules development MP is functional in auxin minima domains acting uncoupled from the classical auxin regulation.

These results suggest that MP c-terminal domain is not strictly required for its function, resulting in a potential ability of MP and MPint11 to work in a vaster number of hormonal contexts respect to what was thought before. Preliminary results indicate that also this alternative splicing event seems to be partially regulated by auxin levels, even if in an opposite way respect to what we observed for *MP* leader intron alternative splicing. Indeed, we found that eleventh intron retention is negatively regulate by high auxin levels. We speculate that auxin might modulate *MP* post-transcriptional regulations in order to provide differential levels of MP activity in diverse environments. The classical auxin signalling model establish that, in auxin minima, class A ARFs should work as transcriptional repressors. Nevertheless, we didn't observe such activity for MP canonical protein during ovule development. Even if, it has been described that MP function is modulated by the interaction with BODENLOS in embryo development, we speculate that this scenario might be different in ovules.

Finally, we observed that MP and MPint11 have a differential functionality in restore *mp* defects at the seedling level. Thanks to reporter lines analyses we found that post-translational regulations are involved in MP modulation in post-embryonic root development. In this case, we observed that auxin is implicated in the regulation of MP protein stability, an aspect of its function on ARFs activity which has never been characterised before. Particularly, high auxin levels stabilise canonical MP protein, which is degraded by the proteasome in domains of low auxin content. MP isoforms show a differential responsiveness to such regulation, resulting in their differential accumulation and potentially differential functions. This kind of control seems to be also present in lateral root development, indicating it as a common feature of MP regulation during root system formation. Our hypothesis is that MP c-terminal domain might be an essential prerogative of this mechanism. Indeed, its absence in MPint11 might explain its differential sensibility to such regulation. The c-terminal domain mediates protein-protein interaction events, which might result in the specific MP degradation in auxin minima. As reported above, low auxin levels stabilise the interaction of MP c-terminal domain with BDL, that might lead to MP degradation. Interestingly, we observed two different *scenarios* in root respect to ovules: while MP canonical protein is absent in domains of auxin minima in root, it seems to be functional for targets activation in the same hormonal environment in ovules primordia. Indeed, our results show that MP degradation is a specific mechanism of root system, while

it doesn't occur in the reproductive tissues. This fact points out the importance of this novel auxin mediated regulation, and how it might impact on MP activity in different tissues.

Taken together our results not only describe completely new levels of MP functions and regulations but might also implement the auxin signalling paradigm. According to our findings, auxin not only regulates ARFs behaviour as transcriptional factors, but also modulates their alternative splicing and protein stability. This makes its signalling a concerted interplay among multiple cellular responses. Additionally, MP can work also partially uncoupled from auxin levels, exponentially integrating its responsiveness in the different hormonal and transcriptomic environments, to drive the developmental processes in which it is involved.

Material and methods

1. Plant material and growth conditions

Arabidopsis thaliana plants were grown in controlled conditions under long-day photoperiod (16 h light, 8 h dark) and 22°C temperature. The mutants *mpS319* [1–3] *arf5-1* (SALK_023812) [4] and reporters DII-VENUS [5] and *DR5:GFP* [6] were previously described.

ASCO-RNAi and *nsr a/b* mutant lines were kindly provided by Martin Crespi. *MP:MP-GFP*, *TMO5::3xGFP*, *TMO3::3xGFP* [7] and *DR5v2::ntdTomato* [8] were provided by Prof. Dolf Weijers.. For *pMP:MPint11-GFP* construct generation, *MP* genomic locus was amplified from -5,033 to +3,379 respect to the start codon and cloned into pGreenII plasmid with gateway technology. *pMP-MP(cDNA)-tMP*, -4,107 bp of *MP* promoter sequence were ligated with 902 bp of *MP*cds and 178 bp of *MP* 3'UTR in pPLV cloning vector. The obtained plasmids were then introgressed into *mpS319* and *arf5-1* backgrounds.

Double purpose reporter lines *MP::MP:VENUS:2aP-mTORQUOISE*, *ARF6::ARF6:VENUS:2aP-mTORQUOISE* and *ARF8::ARF8:VENUS:2aP-mTORQUOISE* were provided by Prof. Anthony Bishopp. *MP:MP-GFP (ct)* was provided by prof. Dolf Weijers. *MP:MP-GFP (mr)* reporter was the same used for ovules development analysis.

MP::MP:VENUS:2aP-mTORQUOISE, *ARF6::ARF6:VENUS:2aP-mTORQUOISE*, *ARF8::ARF8:VENUS:2aP-mTORQUOISE*, *MP:MP-GFP (mr)*, *MP:MP-GFP (ct)*, *mpS319 +/-*, *mpS319 MP::MPint11-GFP* and *mpS319 MP::MP* seeds were sterilised with triton 0.1% and bleach 5% and sown on half strength MS medium. Plates were transferred in growing chambers with a long day photoperiod at 22° C and roots has been analysed 5 days after seeds germination.

2. RNA extraction and cDNA synthesis

RNA was extracted using the NucleoSpin RNA Plant kit (Macherey-Nagel®) and DNase treated and reverse-transcribed with SuperScript™ IV VILO™ Master Mix with ezDNase™ Enzyme (Invitrogen). The synthesised gDNA-less cDNA was used for PCR on *ACTIN8* as a control to ensure gDNA absence and to verify the quality of the cDNA. PCR for AS detection was performed using specific primer pairs, listed un primers table.

3. Droplet digital PCR assay

ddPCR was performed as in [9] using a Bio-rad QX200™ Droplet Digital™ PCR System according to the suppliers instructions and with all required reagents and disposables from Bio-rad. The ddPCR reaction mix contained 2 µL cDNA (150 ng), 10 µL 2× ddPCR™ Supermix for Probes (no dUTP), 1 µL 20× HEX/FAM assay and dH₂O to a volume of 20 µL per sample. Universal DG8™ cartridge, Droplet generation oil for probes and DG8™ gaskets were required for droplet formation into the droplet generator (QX200™). Then, 40 µL droplet emulsion was transferred to a 96-well ddPCR plate (BioRad) and sealed with a PX1™ machine. PCR was performed using the following programme: 95°C for 5 min; 39 cycles of 95°C for 30 s and 60°C for 1 min; 98°C for 10 min then the temperature was held at 12°C. Finally, FAM and HEX fluorescence was read in the droplet reader QX200™ using QuantaSoft™ software. The number of copies/µL of each target locus was determined by setting an identical empirical baseline threshold for all samples.

4. Polysome fraction extraction and RNA extraction

Wild type Col-0 inflorescences were used for polysome isolation, accordingly to the protocol reported in [10]. Briefly, 600 mg of inflorescences were collected, immediately frozen and stirred with liquid nitrogen and plant powder was solubilised into Polysome Buffer (160 mM Tris-HCl pH 8.4, 80 mM KCl and 40 mM MgCl₂, 5.26 mM EGTA, 0.5% (v/v) Octylphenoxy poly(ethyleneoxy)ethanol, branched, 50 µg/ml cycloheximide, 50 µg/ml chloramphenicol). Samples were centrifugated at 16,000g for 15 min at 4 °C to remove pellet debris and the supernatant was transferred on top of a sucrose gradient made of 4 layers of sucrose (50%, 35% and 2 layers of 20%). Gradients added with the cell lysate were centrifuged at 175,000g for 2 h: 45 min at 4 °C, in a SW41Ti Beckman rotor. After that, gradients were analysed by continuous flow absorbance at 254 nm recorded by BioLogic LP software (Bio-Rad). For *MP* canonical and alternative isoforms for the 5' UTR leader intron alternative splicing, fractions collected were: i) not associated, ii) monosome, iii) light polysomes, and iv) heavy polysomes. Concerning the detection of the *MPint11* isoform the fractions considered were: i) monosome, ii) light polysomes, and iii) heavy polysomes. For RNA extraction from the

fractions, samples were incubated with SDS 1% and proteinase K for 1 hour at 37°C and RNA extraction was performed with the phenol/chloroform/isoamyl alcohol method. The same amount of RNA from each fraction was DNase-treated and reverse-transcribed with SuperScript™ IV VILO™ Master Mix with ezDNase™ Enzyme (Invitrogen). The distribution of mRNAs among the fractions was determined by real-time PCR using a CFX96 Detection System with Bio-Rad iTaq SYBR green master mix. primers are listed in primer table. The amount of target mRNA in each fraction was expressed as a percentage of the total amount of mRNA in the translational machinery.

5. Co-IP followed by ms/ms on *MP:MP-GFP (mr)* reporter line

Immunoprecipitation of MP-GFP containing complexes followed by mass spectrometry were performed in collaboration with prof Ueli Grossniklaus lab following the protocol described in [11]. Briefly, wild type col-0 and *MP:MP-GFP* [7] pre-fertilisation inflorescences were collected and immediately frozen in liquid nitrogen. Three biological replicates composed by 3g of grinded frozen material were used for both the Wild type control and for *MP:MP-GFP* line. Plant powder was solubilised into the smallest volume as possible of EB+ buffer. EB+ buffer is obtained from the EB- buffer (100 ml of EB-buffer contains: 5 ml Tris-HCL pH 5.1 1M, 3 ml NaCl 5M, 2 pic tablets, water up to 100 ml) adding 1% of Nonidet P-40. The mixture was sonicated three times for 15s, with resting times of 15s between the sonicating steps. After 30 minutes, NP40 concentration into the solution was reduced to 0.2% adding EB-buffer and then samples were centrifugated for 15 min at 39.000 g at 4°C. The supernatant was added with 100 µL of anti-GFP µBeads from the µMACS kit (Miltenyi) and left in rotation for 2h at 4°C. The cell lysate was applied onto the µMACS columns placed in the magnetic field of the µMACS separator, allowing the immobilisation of the anti-GFP µBeads bound to the MP-GFP containing complexes. After four rinse steps with EB 0.1% NP40 buffer and two rinse steps with ABC buffer (50 µM NH₄HCO₃), columns were removed from the µMACS separator, immediately placed in a tube and added with 50 µL of 95°C ABC buffer, allowing µBeads removal. µBeads conjugated with MP-GFP containing complexes were prepared with proteolytic digestion and analysed with MS/MS. These steps were performed by the protein analysis group of the Functional Genomics Center, Zurich Y 11 H 16 Winterthurerstrasse 190 CH-8057 Zürich.

6. Auxin and Bertezomib treatments

Three to five primary inflorescences for each biological replicate from col-0 wild type, nsra/b or *RNA-i ASCO* plants were treated with 15 μ L of 1 μ M IAA or 10 μ M IAA or water (mock), containing 0.01% Silwet L-77. 3h after treating, inflorescences were collected and immediately frozen in liquid nitrogen. RNA extraction and RT-PCR were performed as described above. *GH3.4* gene (*At1g59500*) were used as positive controls to ensure that auxin treatment was successful. Concerning auxin treatment on *MP::MP:VENUS:2aP-mTORQUOISE* and *DR5::GFP* reporter lines, seedlings were took five days after germination and incubated in liquid half strength MS added with 1 μ M IAA or DMSO mock solution. Bertezomib treatment has been performed similarly with 50 μ M BTZ or DMSO mock on five days old seedlings in liquid half strength MS. In both cases roots have been imaged after 3h of treatments.

7. Real time and data analysis

cDNA checked for gDNA absence was used as template in quantitative Real Time PCR (qRT-PCR) reactions. qRT-PCR was carried out on a CFX96 Real-Time system (Bio-Rad) with Bio-Rad iTaq SYBR. Specific primer pairs are listed in the primers tables. All the data are based on three technical replicates, which were analysed using a Bio-Rad CFX Maestro software (V1.1).

8. Generation, genotyping and phenotyping of CRISPR mutant alleles

The constructs used and the cloning procedure followed to obtain the CRISPR/Cas9 mutants are described in [12]. The CRISPR-P web tool [13] has been used to select the protospacer on the *MP* genomic sequence, calculating a score that allows to minimize the off-target effects. The guideRNA sequence used for genomic editing of *MP* is

CAAGTTGTTTGGTTAATGG, pairing at the beginning of the first exon, 40 base pairs after the canonical ATG of *MP*. Oligonucleotides used for the amplification of genomic region carrying mutations in *mpT56* and *mpA54*, are reported in primer table. *mpT56* and *mpA54* are two independent mutant alleles carrying heterozygous mutation in T₀ generation and the CRISPR cassette T-DNA. Both mutant alleles followed Mendelian segregation of the mutation in *MP* gene and of the T-DNA. Phenotyping has been performed in T₂ and T₃ generation of *mpT56* and *mpA54* which segregated out the CRISPR cassette T-DNA. Observation of *mpT56* and *mpA54* phenotypic traits has been performed with a Leica MZ6 stereomicroscope.

9. Optical and confocal microscopy

Images of inflorescences and pistils were taken with a Zeiss® Axiocam MRc5 camera and a Leica® MZ6 stereomicroscope and were processed using Axiovision (version 4.1) software. For confocal laser scanning microscopy, dissected pistils were mounted in water and observed with an SP2 Leica confocal microscope. eGFP was excited at 488 nm and detected at 498–530 nm, tdTomato was excited at 561 nm and detected at 571–630 nm. Root has been mounted in water with 5% propidium iodide and observed with an SP5 Leica confocal microscope. Propidium iodide was excited at 493 nm and detected at 610–620 nm, VENUS was excited at 515 nm and detected at 530–540 nm. mTORQUOISE was excited at 434 nm and detected at 474–480 nm. We used a 40× water-immersion objective (numerical aperture = 1.25, pinhole), confocal scans were performed with the pinhole at 1 airy unit. Images were collected in multi-channel mode, and overlay images were generated using Leica analysis software LAS AF 2.2.0.

10. RNA deep-sequencing analysis

RNA-seq experiments have been performed in collaboration with prof. Aureliano Bombarely. Briefly, RNA was extracted from wild-type Col-0 pre-fertilization inflorescences using the NucleoSpin RNA Plant kit (Macherey-Nagel®). RNA-Seq libraries were prepared and

sequenced at Novogene (<https://en.novogene.com/>) following the manufacturer's instructions. The library insert size was approximately 300 bp. The DNA was sequenced in an Illumina HiSeq4000 system as 2 × 150-bp pair ends. The data reads were processed using Fastq-mcf from the Ea-utils [14] package. The reads were mapped to the Arabidopsis genome version TAIR10 with STAR [15] using the default parameters. The BAM files were uploaded in IGV with the Arabidopsis genome annotation Araport11. A representation of the coverage was depicted with Keynote.

11. Sequence conservation analysis

The *MONOPTEROS* gene was retrieved from the Phytozome database (accessed on 2019-02-25) using the Locus ID (AT1G19850.1) and then visualised in JBrowser. The VISTA tracks were enabled for all species and each track was manually sorted according to its phylogenetic distance from Arabidopsis. The conservation percentage for the coloured regions were 70% (blue for exons and red for introns) with a box size of 50 bp.

12. Primers table

Alternative splicing detection	
TGGGTAATGTTTTGACTTGG	fw MP11 int
CCACAAACTCTTCCCATGGAT	rv junction 11 12 ex
TGGCACCTTTGGTTTCTCTT	fw can MP leader intron retaining isoform
TTGTCTCTCCCACTCAACAC	rv can Mpleader intron retaining isoform
GTAGTCCCTATTTTACAAGA	fw MP leader intron less isoform
CAAGAACACCGATGTGCATACTA	rv MP leader intron less isoform
CTCAGGTATTGCAGACCGTATGAG	fw actin 8
CTGGACCTGCTTCATCATACTCTG	rv actin 8

Real time PCR on polysomes fractions	
AACTCTTGAGTCTTGCTAAAGCCTA	fw can MP leader intron retaining isoform
CGGCTTTCTTGACCTGACT	rv can Mpleader intron retaining isoform
GTAGTCCCTATTTTACAAGA	fw MP leader intron less isoform
CATAGCTCCGAGTTTATTAC	rv MP leader intron less isoform
CTCAGGTATTGCAGACCGTATGAG	fw actin 8
CTGGACCTGCTTCATCATACTCTG	rv actin 8
CTGGACACAACGAGAGAAG	fw spl3
TGGAGAAACAGACAGAGACA	rv spl3
GTTTCATCAGGGATGAGAAGTCAC	fw MP
CAAGAACACCGATGTGCATACTA	rv MP
CGCGTCCGAACCTACACTAA	fw for MP int11 detection
CAAGAAATTTGTGGAATGAATGAGAGA	rv MP eleventh intron

Expression analyses	
AACTCTTGAGTCTTGCTAAAGCCTA	fw can MP leader intron retaining isoform
CGGCTTTCTTGACCTGACT	rv can MP leader intron retaining isoform
GTAGTCCCTATTTTACAAGA	fw MP leader intron less isoform
CATAGCTCCGAGTTTATTAC	rv MP leader intron less isoform
GTTTCATCAGGGATGAGAAGTCAC	fw MP
CAAGAACACCGATGTGCATACTA	rv MP
CGCGTCCGAACCTACACTAA	fw for MPint11 detection
CAAGAAATTTGTGGAATGAATGAGAGA	rv MP eleventh intron
ATGAATCTCTACGTGCCGGG	fw GH3.4
GACGTCCTGAAGTAGTCGCT	rv GH3.4
TGCATGAGTATCGCCTTGAC	fw CUC1
GGTGACGGCAGAAGAAGAAG	rv CUC1
AAAGGAAGAGCTCCGAAAGG	fw CUC2
TTACGCTCACAGTTGCTCCTC	rv CUC2
CCGAGGAGTGAGACAGCGTCC	fw TMO3
GCTTCTTCCGCCGTGTTGTAAGTACC	rv TMO3
GGCTTTAGCTGCTTCAAAGAGTC	fw TMO5
CTGTTGGGACTTGATACGTGTC	rv TMO5
TCCACTGCCTAGACGAAGAAGC	fw LFY
TCCAGCCATGACGACAAGC	rv LFY
TGGAACTTTTGGAACCCAAG	fw ANT
AGAGTTAGCGCGAAGGAACA	rv ANT
CTCAGGTATTGCAGACCGTATGAG	fw actin 8
CTGGACCTGCTTCATCATACTCTG	rv actin 8
CTGTTACGGAACCCAATTC	fw UBI 10
GGAAAAAGGTCTGACCGACA	rv UBI 10

CRISPR generated InDel check of mpT56 and mpA54	
AACTCTTGAGTCTTGCTAAAGCCTA	fw for fragment amplification for sequencing
TGAGAAAGAAGAAGATGAAAACCTG	rv for fragment amplification for sequencing

Cloning pMP::Mpint1	
GGGACCACTTTGTACAAGAAAGCTGGGTaCTACTCGTTCGTAG TGGTAG	fw on MP promotor with gateway site
GGGACCACTTTGTACAAGAAAGCTGGGTttgtcagattgtgacacaaga aat	rv on MP eleventh intron with gateway site

References

1. Alonso, J.M., Stepanova, A.N., Leisse, T.J., Kim, C.J., Chen, H., Shinn, P., Stevenson, D.K., Zimmerman, J., Barajas, P., Cheuk, R., *et al.* (2003). Genome-wide insertional mutagenesis of *Arabidopsis thaliana*. *Science* 301, 653–7. Available at: <http://www.ncbi.nlm.nih.gov/pubmed/12893945>.
2. Cole, M., Chandler, J., Weijers, D., Jacobs, B., Comelli, P., and Werr, W. (2009). DORNROSCHEN is a direct target of the auxin response factor MONOPTEROS in the *Arabidopsis* embryo. *Development* 136, 1643–1651.
3. Galbiati, F., Sinha Roy, D., Simonini, S., Cucinotta, M., Ceccato, L., Cuesta, C., Simaskova, M., Benkova, E., Kamiuchi, Y., Aida, M., *et al.* (2013). An integrative model of the control of ovule primordia formation. *Plant J.* 76, 446–455.
4. Okushima, Y., Overvoorde, P.J., Arima, K., Alonso, J.M., Chan, A., Chang, C., Ecker, J.R., Hughes, B., Lui, A., Nguyen, D., *et al.* (2005). Functional Genomic Analysis of the AUXIN RESPONSE FACTOR Gene Family Members in *Arabidopsis thaliana*: Unique and Overlapping Functions of ARF7 and ARF19. *Plant Cell* 17, 444–463.
5. Brunoud, G., Wells, D.M., Oliva, M., Larrieu, A., Mirabet, V., Burrow, A.H., Beeckman, T., Kepinski, S., Traas, J., Bennett, M.J., *et al.* (2012). A novel sensor to map auxin response and distribution at high spatio-temporal resolution. *Nature* 482, 103–106.
6. Ottenschläger, I., Wolff, P., Wolverson, C., Bhalerao, R.P., Sandberg, G., Ishikawa, H., Evans, M., and Palme, K. (2003). Gravity-regulated differential auxin transport from columella to lateral root cap cells. *Proc. Natl. Acad. Sci. U. S. A.* 100, 2987–2991.
7. Schlereth, A., Moller, B., Liu, W., Kientz, M., Flipse, J., Rademacher, E.H., Schmid, M., Jurgens, G., and Weijers, D. (2010). MONOPTEROS controls embryonic root initiation by regulating a mobile transcription factor. *Nature* 464, 913–916.
8. Liao, C.-Y., Smet, W., Brunoud, G., Yoshida, S., Vernoux, T., and Weijers, D. (2015). Reporters for sensitive and quantitative measurement of auxin response. *Nat Meth* 12, 207–210.
9. Dibitetto, D., La Monica, M., Ferrari, M., Marini, F., and Pellicoli, A. (2018). Formation and nucleolytic processing of Cas9-induced DNA breaks in human cells quantified by

droplet digital PCR. *DNA Repair (Amst)*. 68, 68–74.

10. Lecampion, C., Floris, M., Fantino, J.R., Robaglia, C., and Laloi, C. (2016). An easy method for plant polysome profiling. *J. Vis. Exp.* 2016, 1–7.
11. Wendrich, R.J., Boeren, S., Moller, K.B., Weijers, D., Rybel De B. (2017) In Vivo identification of Plant Protein Complexes Using IP-MS/MS. *Methods Mol Biol*, vol. 1497.
12. Fauser, F., Schiml, S., and Puchta, H. (2014). Both CRISPR/Cas-based nucleases and nickases can be used efficiently for genome engineering in *Arabidopsis thaliana*. *Plant J.* 79, 348–359.
13. Lei, Y., Lu, L., Liu, H.Y., Li, S., Xing, F., and Chen, L.L. (2014). CRISPR-P: A web tool for synthetic single-guide RNA design of CRISPR-system in plants. *Mol. Plant* 7, 1494–1496.
14. Aronesty, E. (2013). Comparison of Sequencing Utility Programs. *Open Bioinforma. J.* 7, 1–8.
15. Dobin, A., Davis, C.A., Schlesinger, F., Drenkow, J., Zaleski, C., Jha, S., Batut, P., Chaisson, M., and Gingeras, T.R. (2013). STAR: ultrafast universal RNA-seq aligner. *Bioinformatics* 29, 15–21.

Appendices

Auxin and Flower Development: A Blossoming Field

Mara Cucinotta¹, Alex Cavalleri¹, John William Chandler² and Lucia Colombo¹.

Review accepted for publication on “Cold Spring Harbor Perspectives in Biology”

In this review I have actively worked on the writing of the main text, with a specific focus on auxin function during flower meristem initiation, identity acquisition, termination and pistil development. Moreover, I have worked on tables and figures design, realisation and manuscript preparation.

Auxin and Flower Development: A Blossoming Field

Mara Cucinotta,¹ Alex Cavalleri,¹ John William Chandler,² and Lucia Colombo¹

¹Dipartimento di Bioscienze, Università degli Studi di Milano, 20133 Milan, Italy

²Max Planck Institute for Plant Breeding Research, 50829 Cologne, Germany

Correspondence: lucia.colombo@unimi.it



The establishment of the species-specific floral organ body plan involves many coordinated spatiotemporal processes, which include the perception of positional information that specifies floral meristem and floral organ founder cells, coordinated organ outgrowth coupled with the generation and maintenance of inter-organ and inter-whorl boundaries, and the termination of meristem activity. Auxin is integrated within the gene regulatory networks that control these processes and plays instructive roles at the level of tissue-specific biosynthesis and polar transport to generate local maxima, perception, and signaling. Key features of auxin function in several floral contexts include cell nonautonomy, interaction with cytokinin gradients, and the central role of MONOPTEROS and ETTIN to regulate canonical and noncanonical auxin response pathways, respectively. *Arabidopsis* flowers are not representative of the enormous angiosperm floral diversity; therefore, comparative studies are required to understand how auxin underlies these developmental differences. It will be of great interest to compare the conservation of auxin pathways among flowering plants and to discuss the evolutionary role of auxin in floral development.

Angiosperm flowers display extraordinary diversity in their body plan and every aspect of morphology, including organ number and positioning, size, symmetry, color, and organogenesis. The study of select angiosperm species has elaborated the genetic basis of floral identity according to the coordinated expression of transcription factors. However, advances in auxin biology have demonstrated that auxin is a central developmental regulator of floral morphogenesis (Irish 2010; Wellmer et al. 2014).

Auxin is essential for the initiation of floral meristems (FMs) and organs and for terminating meristem growth; however, its role in deter-

mining positional information for floral organ initiation remains less mechanistically well understood than its function in organ outgrowth and development (Chandler 2011). Auxin can also function as a morphogen by generating response gradients, particularly in combination with those of cytokinins, which are instrumental in several aspects of floral organogenesis (Su et al. 2011).

This review summarizes how auxin coordinates diverse and complex regulatory gene networks in FM and organ initiation and development and focuses on the *Arabidopsis* model for which most is known. It also highlights the cen-

Editors: Dolf Weijers, Karin Ljung, Mark Estelle, and Ottoline Leyser
Additional Perspectives on Auxin Signaling available at www.cshperspectives.org

Copyright © 2020 Cold Spring Harbor Laboratory Press; all rights reserved
Advanced Online Article. Cite this article as *Cold Spring Harb Perspect Biol* doi: 10.1101/cshperspect.a039974

M. Cucinotta et al.

tral role of canonical and noncanonical auxin response factors (ARFs) such as MONOPTEROS (MP) and ETTIN (ETT/ARF3), respectively.

AUXIN IS ESSENTIAL FOR FLORAL MERISTEM INITIATION

Floral organ primordia arise from FMs, which initiate as lateral organs at the inflorescence meristem (IM) periphery. The maintenance of the IM required a precise balance between the self-renewal of stem cells and cell differentiation. It has been proposed that the WUSCHEL (WUS) transcription factor achieves this balance by restricting auxin signaling in stem cells and simultaneously allowing low levels of auxin signaling output (Ma et al. 2019), although the precise mechanism of this rheostat function on select auxin signaling components remains to be elucidated.

Precise spatiotemporal local auxin biosynthesis within the IM and its polar transport and accumulation at specific sites from sources elsewhere in the plant are essential for FM initiation (Alvarez-Buylla et al. 2010; Yadav et al. 2019). This is evidenced by classical mutants, for example, in *PIN-FORMED1* (*PIN1*), which encodes a polar auxin efflux carrier (Gälweiler et al. 1998). Occasional flowers on *pin1* inflorescences lack sepals and have a variable number of abnormally shaped petals (Okada et al. 1991) and exogenous auxin application to *pin1-1* inflorescences restores flower formation at the point of application (Reinhardt et al. 2000). Mutation of the gene encoding the PINOID (PID) kinase that regulates PIN activity leads to flowers with supernumerary petals, few sepals and stamens, and mostly *pin*-like carpels (Bennett et al. 1995). Strong mutants of ARF5/MONOPTEROS (MP) produce naked inflorescences (Przemeck et al. 1996), although the hypomorphic *mps319* allele occasionally produces rudimentary flowers (Alonso et al. 2003; Cole et al. 2009). Loss-of-function of *MACCHI-BOU4* (*MAB4*)/*ENHANCER OF PINOID* (*ENP*)/*NAKED PINS IN YUC MUTANTS 1* (*NPY*), hereafter *MAB4*, which encode NONPHOTOTROPIC HYPOCOTYL 3-like proteins that regulate PIN endo-

cytosis, also causes *pin*-like inflorescences (Furutani et al. 2014), due to the abolition of auxin flow from external FM layers inward to create an auxin sink necessary for FM development after initiation.

Auxin response maxima prepattern sites of FM initiation at the IM periphery (Reinhardt et al. 2000), and in addition to the importance of the spatial distribution of auxin within the SAM as an instructive signal, recent high-resolution imaging of auxin response has revealed the importance of a dynamic temporal component to these auxin fluxes (Galvan-Ampudia et al. 2020). In this scenario, high-precision dynamic spatiotemporal auxin gradients within the IM periphery are coordinated with growth, to ensure that cells are exposed to a high level of auxin over time to activate organogenesis. The temporal aspect concerning the timing and duration of exposure of cells to high auxin is relevant because, according to phytomer theory, FMs initiate as lateral organs in the axils of bracts. *Arabidopsis* bracts are cryptic but are histologically and morphologically visible during early floral transition preceding FM initiation (Kwiatkowska 2008). Transcriptional reprogramming associated with bract initiation has been accessed in the *ap1 cal* mutant background by sorting cells that express the bract founder-cell marker *DORNROESCHEN-LIKE* (*DRNL*) (Frerichs et al. 2016). Minor transcriptional changes in genes in the auxin synthesis, transport, and response machinery suggest that its global activation might not be associated with bract initiation, but with FM initiation. This is consistent with spatially distinct domains of *DRNL* and *DR5* expression within the IM (Chandler et al. 2011) and that auxin response minima are required for the formation of axillary vegetative meristems in *Arabidopsis* and tomato (Wang et al. 2014a,b). Interacting concentration gradients of auxin and cytokinin establish the timing of FM outgrowth within the IM, which can be uncoupled from initiation (Besnard et al. 2014).

An early feature of FM initiation is inhibition of the pluripotency of stem cells that form FM primordia, by down-regulation of *SHOOT-MERISTEMLESS* (*STM*). Transcripts of *STM*



overaccumulate in the IM of *mpS319* and more so in an *mp arf3 arf4* triple mutant, resulting in complete loss of flower primordia. ETT directly binds to *STM* and silences its expression for FM fate acquisition. By contrast, MP does not bind *STM*, but directly activates expression of the repressor *FILAMENTOUS FLOWER (FIL)*, which further contributes to *STM* silencing. ETT and FIL also directly bind and repress expression of *BREVIPEDICELLUS (BP)*, which maintains meristematic identity. Although MP, ETTIN, and ARF4 repress *STM* and *BP* expression in parallel pathways, FIL physically interacts with ETTIN and ARF4 to create a complex that recruits chromatin modifiers such as histone deacetylase HDA19, which leads to target-gene silencing (Table 1; Fig. 1; Chung et al. 2019).

THE CENTRAL ROLE OF MP IN FM DEVELOPMENT

MONOPTEROS is the central regulator of FM development and translates a local auxin concentration maximum into a floral primordium by directly transcriptionally activating several transcription factors. These include the master regulator *LEAFY (LFY)*, which, together with its target *APETALA1*, regulates the IM-to-FM identity transition (Weigel et al. 1992). *LFY* expression in incipient flower primordia is enhanced by high auxin levels, via the canonical MP/IAA12 (BODENLOS) module (Yamaguchi et al. 2013). *LFY* expression only partially rescues *mp-S319* flower defects and MP also transcriptionally activates *AINTEGUMENTA (ANT)* and *AINTEGUMENTA-LIKE6 (AIL6)*, which function in parallel and redundantly with *LFY* in FM initiation. Because the *lfy-6 ant-4 ail6-2* triple mutant initiates some flowers, additional auxin-regulated factors probably contribute to FM production. *ANT* and *AIL6* also function upstream of *LFY* and regulate its expression in response to auxin and in parallel to MP. Accordingly, they are expressed earlier than *LFY* (Yamaguchi et al. 2016) and delayed *LFY* expression in *ant ail6* delays FM production. However, expression of *ANT* and *AIL6* in *mp* is reduced but not abolished (Yamaguchi et al. 2013), suggesting that they are also regulated

independently from MP, potentially via other ARFs.

In summary, MP triggers FM initiation and development by transcriptionally up-regulating *LFY*, *ANT*, and *AIL6* via two separate pathways in which *LFY* both targets *ANT/AIL6* and acts in parallel with them. In addition, *LFY* positively feeds back into the auxin pathway, to ensure maintenance of the auxin response network and to lock the auxin response in an “on” state that ensures commitment to flowering (Table 1; Fig. 1). Expression of *DR5er:GFP* positively correlates with *LFY* activity, and feedback regulation on auxin signaling by *LFY* occurs partly by up-regulation of *PID* expression (Li et al. 2013; Yamaguchi et al. 2013).

The reprogramming of MP targets in meristematic cells that develop into floral primordia involves chromatin remodeling via the SWI/SNF ATPases *BRAMA (BRM)* and *SPLAYED (SYD)*, which increase chromatin accessibility in early floral primordia. Initiation of fewer flower primordia and *pin*-like inflorescences in *mpS319 syd* double mutants and *mpS319* plants expressing an artificial microRNA responsible for *BRAHMA* down-regulation demonstrate the functional relevance of *BRM* and *SYD* in FM initiation. Auxin enhances MP binding to *BRM* and *SYD*, which also bind the direct MP targets *FIL*, *LFY*, *ANT*, and *TMO3* (Wu et al. 2015). Therefore, a chromatin switch model explains how binding of *AUX/IAA* proteins to MP at low auxin concentrations prevents the recruitment of SWI/SNF factors by MP, which instead binds to the *TOPLESS (TPL)* corepressor and *HISTONE DEACETYLASE19 (HDA19)*, which promote a repressive chromatin state. Increasing auxin concentrations degrade *AUX/IAA* proteins, enabling MP to recruit SWI/SNF-containing complexes, which promote a permissive chromatin state that up-regulates MP targets (Table 1; Fig. 1; Wu et al. 2015).

FLORAL ORGAN INITIATION

Floral morphogenesis involves the perception of positional information within the FM by floral organ founder cells, to become specified, acquire a particular fate and outgrow. These processes

M. Cucinotta et al.

Table 1. Summary of genes mentioned in the text

Gene	Protein function/relation with auxin	Floral developmental context	References
<i>PIN-FORMED1 (PIN1)</i>	Auxin efflux carrier	Flower initiation (FI), organ initiation (OI)	Okada et al. 1991
<i>PINOID (PID)</i>	Kinase that regulates PIN1 polarization	FI, OI	Bennett et al. 1995
<i>ARF5/MONOPTEROS</i>	Auxin response factor (ARF), transcription factor (TF)	FI, organ boundaries (OBs) OI, organ growth (OG)	Li et al. 2013; Yamaguchi et al. 2013
<i>MACCHI-BOU4 (MAB4) DORNROESCHEN-LIKE (DRNL)</i>	Regulates PIN1 polarization AP2/ETHYLENE RESPONSE FACTOR TF, a floral-organ founder-cell marker whose expression precedes DR5 and genetically interacts with <i>PID</i>	FI FI, petal initiation	Furutani et al. 2014 Chandler et al. 2011
<i>SHOOTMERISTEMLESS (STM)</i>	KNOX TF, <i>STM</i> is repressed by auxin	FI	Chung et al. 2019
<i>ARF3/ETTIN (ETT)</i>	ARF, TF	FI, gynoecium growth, megaspore mother cell (MMC), floral meristem determinacy (FMD)	Sessions et al. 1997; Chung et al. 2019
<i>ARF4</i>	ARF, TF	FI	Chung et al. 2019
<i>FILAMENTOUS FLOWER (FIL)</i>	TF, <i>FIL</i> is activated by auxin	FI	Chung et al. 2019
<i>BREVIPEDICELLUS (BP)</i>	KNOX TF, <i>BP</i> is repressed by auxin	FI	Chung et al. 2019
<i>HISTONE DEACETYLASE19 (HDA19)</i>	Chromatin remodeling factor, interacts with <i>ETT</i> and <i>ARF4</i>	FI	Chung et al. 2019
<i>LEAFY</i>	Transcriptional master regulator connected with auxin maximum maintenance, <i>LFY</i> is activated by MP	FI	Weigel et al. 1992; Li et al. 2013; Yamaguchi et al. 2013
<i>AINTEGUMENTA (ANT)</i>	AP2-domain TF transcriptionally up-regulated by MP	FI, OI	Yamaguchi et al. 2013)
<i>AINTEGUMENTA-LIKE6 (AIL6)</i>	AP2-domain TF transcriptionally up-regulated by MP	FI	Yamaguchi et al. 2013
<i>IAA12/BODENLOS</i>	Aux/IAA protein that interacts with MP	FI	Yamaguchi et al. 2013
<i>TOPLESS (TPL)</i>	Corepressor of MP and <i>ETT</i> targets	FI	Wu et al. 2015
<i>BRAMA (BRM)</i>	SWI/SNF ATPs chromatin remodeling interactor of MP	FI	Wu et al. 2015

Continued

Table 1. *Continued*

Gene	Protein function/relation with auxin	Floral developmental context	References
<i>SPLAYED (SYD)</i>	SWI/SNF ATPs chromatin remodeling interactor of MP	FI	Wu et al. 2015
<i>TARGET OF MONOPTEROS3 (TMO3)</i>	AP2 TF transcriptionally up-regulated by MP	FI, ovules	Wu et al. 2015; Cucinotta et al. 2016
<i>YUCCA (YUC)</i>	Flavin-monoxygenases that catalyse IAA biosynthesis	FI, OI	Cheng et al. 2006
<i>DORNROESCHEN (DRN)</i>	AP2/ETHYLENE RESPONSE FACTOR that genetically interacts with <i>PIN</i>	FI, OI	Chandler and Werr 2014
<i>PUCHI</i>	AP2/ETHYLENE RESPONSE FACTOR that genetically interacts with <i>PID</i>	FI, OI	Chandler and Werr 2014
<i>PERIANTHIA (PAN)</i>	bZIP TF that regulates <i>YUC1</i> and <i>YUC4</i>	OB, petal initiation	Maier et al. 2011
<i>PRESSED FLOWER (PRS)</i>	WUSCHEL-RELATED HOMEODOMAIN, <i>PRS</i> expression is induced by auxin	Petal initiation	Chandler and Werr 2014; Caggiano et al. 2017
<i>ABC1/19</i>	Auxin efflux carrier	FI, anther growth, pollen	Zhao et al. 2013; Cecchetti et al. 2015
<i>CUP-SHAPED COTYLEDON (CUC)</i>	NAC-domain TFs regulated by auxin, <i>CUC</i> function is connected with polar auxin transport (<i>PAT</i>)	OB, ovules	Laufs et al. 2004; Mallory et al. 2005; Galbiati et al. 2013
<i>RABBIT EARS (RBE)</i>	C2H2 zinc finger protein connection with <i>PAT</i>	OB, petal growth	Lampugnani et al. 2013
<i>HANABA TARANU (HAN)</i>	GATA3-type transcriptional repressor with a putative role in <i>PAT</i> regulation	OB	Zhang et al. 2013
<i>PETAL LOSS (PTL)</i>	Trihelix TF connected with <i>PAT</i>	OB, petal growth	Lampugnani et al. 2013
<i>AUX1</i>	Auxin influx carrier	Petal growth	Lampugnani et al. 2013
<i>SUPERMAN (SUP)</i>	C2H2 zinc-finger protein that represses <i>YUC</i> expression, <i>SUP</i> is regulated by <i>LFY</i>	OB	Sakai et al. 1995; Xu et al. 2018
<i>DEVELOPMENT-RELATED MYB-LIKE1 (DRMY1)</i>	MYB-like TF that regulates auxin response	Sepal outgrowth	Zhu et al. 2020
<i>JAGGED (JAG)</i>	Zinc-finger protein that regulates auxin response	Petal growth	Dinnyen et al. 2004; Sauret-Güeto et al. 2013
<i>ARGOS</i>	Auxin-inducible gene that regulates <i>ANT</i>	Petal growth	Hu et al. 2003

Continued

M. Cucinotta et al.

Table 1. *Continued*

Gene	Protein function/relation with auxin	Floral developmental context	References
<i>BIGPETALp</i>	bHLH TF that interacts with ARF8	Petal growth	Varaud et al. 2011
ARF8	ARF, TF	Petal growth, stamen growth	Nagpal et al. 2005; Varaud et al. 2011
ARF8.4	ARF, TF	Stamen growth	Ghelli et al. 2018
ARF6	ARF, TF	Stamen growth	Nagpal et al. 2005
<i>SHORT INTERNODES (SHI)</i>	Zinc-finger TFs that regulate auxin biosynthesis	Anther growth	Estornell et al. 2018
<i>STYLISH1/2 (STY1/2)</i>	Zinc-finger TFs that regulate auxin biosynthesis	Anther growth, gynoecium growth	Trigueros et al. 2009; Estornell et al. 2018
TIR1/AFB	Nuclear auxin receptor	Pollen, female gametophyte (FG)	Cecchetti et al. 2008, 2017
<i>DEFECTIVE IN ANTHER DEHISCENCE1 (DAD1)</i>	Enzyme for JA biosynthesis transcriptionally up-regulated by ARF6/ARF8	Anther dehiscence	Nagpal et al. 2005; Tabata et al. 2010
<i>MYB26</i>	TF, <i>MYB26</i> is induced by ARF6/ARF8	Anther dehiscence	Yang et al. 2017
ARF17	ARF, TF	Anther dehiscence	Xu et al. 2019
<i>MYB108</i>	TF, <i>MYB108</i> is transcriptionally up-regulated by ARF17	Anther dehiscence	Xu et al. 2019
IAA19	Aux/IAA protein	Anther dehiscence	Tashiro et al. 2009; Cecchetti et al. 2017
<i>AGAMOUS (AG)</i>	MADS-box TF, regulates <i>YUC4</i>	FMD	Liu et al. 2011, 2014; Yamaguchi et al. 2018
<i>WUSCHEL (WUS)</i>	Homeobox TF that controls the stem-cell pool, regulated by ETT	FMD	Sun et al. 2009; Liu et al. 2011; Huang et al. 2017
<i>APETALA 2 (AP2)</i>	AP2/EREBP TF, negatively regulates <i>ETT</i>	FMD	Liu et al. 2014
<i>CRABS CLAW (CBR)</i>	YABBY TF that transcriptionally up-regulates <i>TRN</i> and <i>YUC4</i>	FMD	Yamaguchi et al. 2018
<i>TORNADO (TRN2)</i>	Tetraspanin protein that regulates auxin homeostasis	FMD	Yamaguchi et al. 2018
<i>CHROMATIN REMODELING 11/17 (CHR11/17)</i>	Recruited by AG to activate <i>YUC</i>	FMD	Yamaguchi et al. 2018
<i>KANADII/4 (KAN1/4)</i>	GARP TF that interacts with ETT	Gynoecium growth	Pekker et al. 2005
<i>SPATULA (SPT)</i>	bHLH TF that regulates PAT	Gynoecium growth	Moubayidin and Ostergaard 2014

Continued

Table 1. *Continued*

Gene	Protein function/relation with auxin	Floral developmental context	References
<i>INDEHISCENT (IND)</i>	bHLH TF that regulates PAT	Gynoecium growth	Moubayidin and Ostergaard 2014; Kuhn et al. 2019
<i>PIN-FORMED3 (PIN3)</i>	Auxin efflux carrier	Gynoecium growth	Gremski et al. 2007
<i>NGATHA (NGA3)</i>	RAV family TF that regulates YUCs	Gynoecium growth	Trigueros, et al. 2009
<i>TOPLESS-RELATED2 (*TPR2)</i>	Corepressor of ETT targets	Gynoecium growth	Benjamins et al. 2001; Gremski et al. 2007
<i>HECATE (HEC)</i>	bHLH TF that regulates PAT	Gynoecium growth	Gremski et al. 2007

The gene or protein function and relationship to auxin is described in the second column, and the third column shows the specific developmental context within flower development with which these genes are involved. Genes whose proteins have a direct molecular link with auxin are shown in bold.

are associated with the establishment and maintenance of organ boundaries.

Expression of the synthetic auxin response reporters DR5::GFP and DII (van Mourik et al. 2012; Goldental-Cohen et al. 2017) demonstrate that auxin response maxima colocalize with sites of organ initiation. However, it is unclear whether auxin specifies floral organ founder cells, or merely activates outgrowth. Modeling of auxin responses (van Mourik et al. 2012) and the ABCE model of floral organ identity acquisition propose that concentric organ whorls are specified centripetally from outer to inner (Theißen and Saedler 2001). However, *Arabidopsis* floral body plan establishment is more complex and the *DRNL* founder-cell marker reveals biphasic development in which sepals initiate unidirectionally from the center of the IM, petals and lateral stamens arise from adjacent domains, and medial stamens initiate from a ring of *DRNL* prepatterning (Chandler and Werr 2014). Expression of *DRNL* precedes auxin response maxima for some floral organs (Chandler et al. 2011) and the response of *DRNL* to auxin remains enigmatic (Comelli et al. 2020). However, *DRNL* and its close relatives *DRN* and *PUCHI* redundantly determine numbers of all floral organs at the founder-cell level, partly cell-nonautonomously (Table 1; Fig. 1; Chandler and Werr 2017). All three proteins integrate into auxin pathways: *DRN* genetically interacts

with *pin1*, *DRNL* with *pid*, *yuc1* and *yuc4* (Chandler et al. 2011), and *PUCHI* with *pid* (Chandler and Werr 2014). *PERIANTHIA* (*PAN*) regulates the number of *Arabidopsis* perianth organs by targeting YUC-mediated auxin biosynthesis (Maier et al. 2011). The radially symmetrical arrangement of five perianth-whorl organs in *pan* (Running and Meyerowitz 1996) derives from bifurcations of sepal founder-cell populations at abaxial and adaxial positions and is partially dependent on *PRESSED FLOWER* (*PRS*) activity (Chandler and Werr 2014), which promotes cell proliferation in lateral floral primordium domains (Matsumoto 2001). In leaf primordia, auxin up-regulates *PRS* and its paralogue *WOX1* (Caggiano et al. 2017) via MP (Guan et al. 2017). Increased expression of DR5::GFP in the leaf base of *prs wox1* and the increased sensitivity of *prs* leaves to auxin transport inhibitors implies a role for *PRS* in auxin transport (Nakata et al. 2018). By analogy, positive feedback between auxin and *PRS* might exist during sepal initiation. Mutation of *ETT* also leads to one supernumerary petal and sepal (Sessions et al. 1997; Pekker et al. 2005).

FLORAL ORGAN BOUNDARY ESTABLISHMENT

Appropriate spatial positioning of floral organs requires the establishment and maintenance of

M. Cucinotta et al.

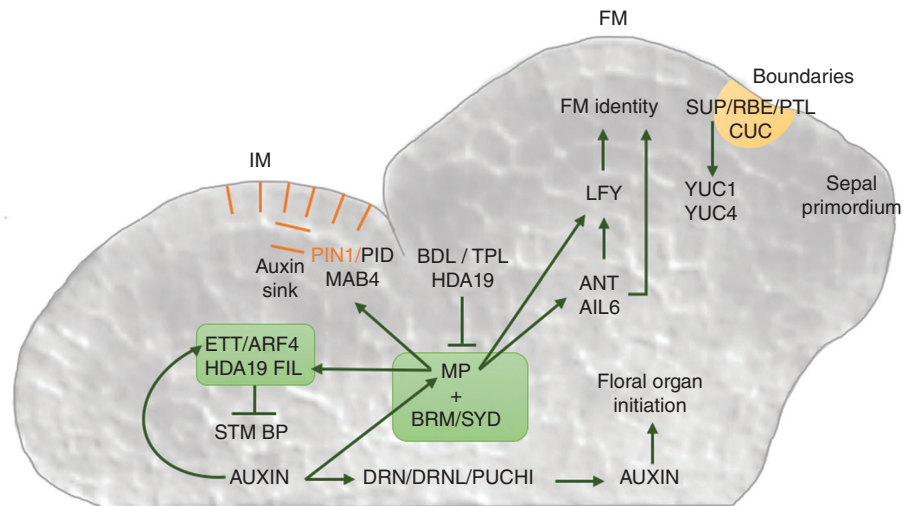


Figure 1. The gene regulatory networks involving auxin that regulate early floral meristem (FM) initiation and development. Schematic diagram of gene regulatory networks superimposed onto an image of an *Arabidopsis* FM emerging from the flank of the inflorescence meristem (IM), to illustrate how auxin coordinates FM initiation and identity and floral organ initiation (see text for details). (ANT) AINTEGUMENTA, (AIL6) AINTEGUMENTA-LIKE6, (ARF4) AUXIN RESPONSE FACTOR4, (BDL) BODENLOS, (BP) BREVIPEDICELLUS, (BRM) BRAHMA, (CUC) CUP-SHAPED COTYLEDON, (DRN) DORNRÖSCHEN, (DRNL) DORNRÖSCHEN-LIKE, (ETT) ETTIN, (FIL) FILAMENTOUS FLOWER, (HDA19) HISTONE DEACETYLASE19, (MAB4) MACCHI-BOU4, (PID) PINOID, (PIN1) PIN-FORMED1, (RBE) RABBIT EARS, (PTL) PETAL LOSS, (PYD) SPLAYED, (STM) SHOOTMERISTEMLESS, (SUP) SUPERMAN, (TPL) TOPLESS, (YUC1) YUCCA1, (YUC4) YUCCA4.

inter-organ boundary zones within floral whorls. In addition to separating organs, boundary domains act as organizing centers to developmentally pattern adjacent tissues. Many transcription factors have boundary functions that relate to auxin signaling (Yu and Huang 2016). A boundary between the IM and FM ensures that the FM buttress separates from the IM. It involves polar auxin transport by ATP-BINDING-CASSETTE B19 (ABCB19) and in *abcb19* mutants, auxin levels increase within the boundary (Zhao et al. 2013). Boundaries are zones of low auxin signaling (Wang et al. 2016), which repress cell division and expansion (Žádníková and Simon 2014; Wang et al. 2016).

The *CUP-SHAPED COTYLEDON* (*CUC*) genes *CUC1*, *CUC2*, and *CUC3* are expressed in different floral organ boundaries (Takada et al. 2001; Hibara et al. 2006; Xu et al. 2008). Their combinatorial mutation leads to fused flo-

ral organs (Laufs et al. 2004; Mallory et al. 2005) and *CUC1* and *CUC2* promote carpel margin meristem (CMM) initiation and positioning (Kamiuchi et al. 2014). Auxin represses *CUC2* expression (Furutani et al. 2004), consistent with boundary domains having low auxin levels, high *CUC* levels, and repressed cell division. Developmental contexts such as cotyledon initiation, leaf serration formation, and ovule primordium initiation have suggested how *CUC2* activate floral organ initiation in adjacent whorls, by up-regulating *PIN1* expression to promote an auxin convergence point, which creates an auxin maximum where organ founder cells are specified (Vernoux et al. 2000; Furutani et al. 2004; Heisler et al. 2005; Bilsborough et al. 2011; Galbiati et al. 2013). The auxin maximum then represses *CUC2* expression and restricts it to the boundary in a negative feedback loop (Vernoux et al. 2000; Bilsborough et al. 2011).



Posttranscriptional regulation of *CUC1* and *CUC2* by three *miRNA164* isoforms and mutation of *MIR164c* (also named *EARLY EXTRA PETALS1 [EEP1]*), leads to supernumerary petals and is associated with additional boundary domains in the second whorl (Baker et al. 2005). After petal primordium formation, *MIR164c/EEP1* expression is repressed in part by RABBIT EARS (*RBE*) (Huang et al. 2012), which also regulates sepal boundaries cell-non-autonomously. *RBE* is also regulated by *PETAL LOSS (PTL)* in the intersepal zone, which establishes sepal boundaries concertedly with *CUC1* and *CUC2* (Lampugnani et al. 2013). *HANABA TARANU (HAN)* is expressed at organ boundaries and *han* mutants display fused sepals and fewer floral organs, which might be caused by impaired polar auxin transport by analogy to embryogenic *HAN* function, which regulates auxin flux to the hypophysis (Nawy et al. 2010; Zhang et al. 2013).

Auxin response within the intersepal boundary zone is controlled by *PTL* (Brewer 2004), which synergistically regulates petal initiation with *RBE* and *PTL*, illustrating that cell-non-autonomy is another important facet of auxin function (Griffith et al. 1999; Brewer 2004; Takeda et al. 2004; Krizek et al. 2006). In *ptl* mutants, petals arise sporadically and are absent in later-arising flowers (Griffith et al. 1999) and sites of petal initiation are restored by directing auxin synthesis within the intersepal zone (Lampugnani et al. 2013). Thus, auxin confers positional information for petal initiation by functioning as a mobile inter-whorl signal. *RBE* and *PTL* both function within the same pathway, with *RBE* downstream of *PTL*. The petal defects of *ptl* and *rbe* mutants are enhanced by mutation of the auxin influx carrier *AUX1* (Lampugnani et al. 2013). Disruption of auxin efflux via *PID* and *PIN1* in the petal initiation zone generally increases petal number, dependent on *PTL* function. *RBE* also defines the second-whorl domain independently of *PTL*, by regulating several boundary genes (Fig. 2).

The SUPERMAN (*SUP*) C2H2 transcription factor, which is closely related to *RBE* (Sakai et al. 1995), limits *APETALA3* expression in

whorl 4, and *sup* mutants produce supernumerary stamens (Bowman et al. 1992). *SUP* expression spans the whorl 3/4 boundary (Prunet et al. 2017) and reduces local auxin biosynthesis by directly binding to *YUC1* and *YUC4* and recruiting Polycomb-repressive complex 2 to repress their expression (Table 1; Fig. 2; Xu et al. 2018). This up-regulation of auxin biosynthesis in *sup* both expands the stem-cell domain between whorls 3 and 4 cell-non-autonomously and prolongs its activity (Xu et al. 2018), leading to supernumerary stamens as the fate of cells in whorl 4 changes from female to male (Prunet et al. 2017). In conclusion, the fine-tuning of auxin synthesis or activity in inter-organ or inter-whorl boundaries is one mechanism for controlling cell divisions and stem-cell availability for organ differentiation.

FLORAL ORGAN OUTGROWTH

The concentration of free auxin, indicated by *DR5::GUS*, is high in the tips of floral organ primordia in all whorls (Aloni et al. 2006), which drives rapid organ outgrowth. After the specification of sepal founder cells in a stereotypic order (Chandler and Werr 2014), sepal outgrowth in *Arabidopsis* is coordinated by DEVELOPMENT-RELATED MYB-LIKE1 (*DRMY1*) (Zhu et al. 2020). Coordinated auxin and cytokinin signaling regulates sepal outgrowth, analogous to the temporal regulation of FM outgrowth (Besnard et al. 2014). *drmy1* mutants display variable sepal sizes due to delayed outgrowth, which results from diffuse auxin and cytokinin response domains in sepal primordia. Wild-type *DRMY1* signaling involves initial auxin responses in the outer primordium cell layer that encroach into the underlying cytokinin signaling domain. These localized and focused auxin and cytokinin signaling domains define regions of competency for outgrowth, in which *DR5::GFP* accumulates at the sepal tips and *TCS* at the base. In tomato, the MADS-box gene *SIMBP21* negatively regulates sepal cell expansion, probably partly via auxin-related pathways.

Auxin contributes to patterning petal shape and size, which depend on cell division during early development and cell expansion during

M. Cucinotta et al.

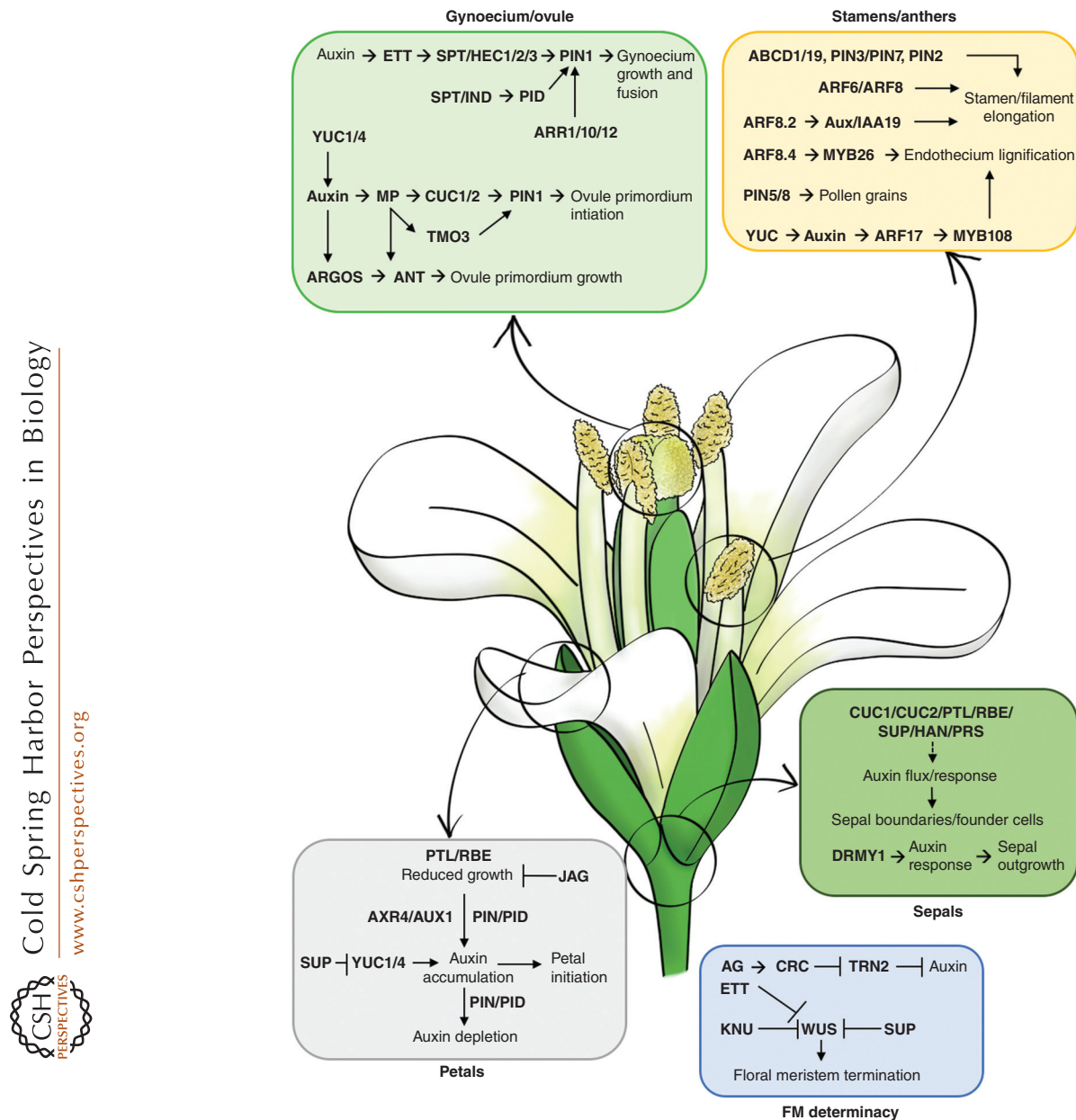


Figure 2. The gene regulatory networks involving auxin that orchestrate development of the different flower organs. A representation of an *Arabidopsis* flower linked to schematic diagrams to show how auxin integrates into the gene regulatory networks that coordinate gynoecium, stamen, petal, and sepal initiation and growth. An additional diagram shows the gene regulatory network involving auxin that relates to floral meristem (FM) determinacy and termination (see text for details). (AG) AGAMOUS, (ARF8/ARF17) AUXIN RESPONSE FACTOR7/17, (AUX1) AUXIN EFFLUX CARRIER1, (Aux/IAA19) AUX/IAA PROTEIN19, (AXR4) AUXIN-RESISTANT4, (CRC) CRABS CLAW, (DRMY1) DEVELOPMENT-RELATED MYB-LIKE1, (HAN) HANABA TARANU, (HEC1/HEC2/HEC3) HECATE1/2/3, (JAG) JAGGED, (KNU) KNUCKLES, (MYB26/MYB108) MYB-DOMAIN PROTEIN26/08, (SPT) SPATULA, (TMO3) TARGET OF MONOPTEROS3, (TRN) TORNADO, (WUS) WUSCHEL (see additional abbreviations in Fig. 1).



late development (Smyth et al. 1990). Many genes directly involved with auxin contribute to petal growth, including *JAGGED* (*JAG*), *ARGOS*, *ANT*, *BIGPETALp* (*BPEp*), and *ARF8*. *JAG* regulates growth by modulating the switch from cell proliferation to cell expansion (Sauret-Güeto et al. 2013). *jag* petals are narrow with a reduced distal region and a jagged or serrated margin (Dinneny et al. 2004). In *jag*, *DR5::GFP* expression is reduced, but is broader when *JAG* is ectopically expressed. Moreover, *JAG* directly represses *PTL* (Sauret-Güeto et al. 2013).

Overexpression of the auxin-inducible gene *ARGOS* increases petal size by increasing the number and size of petal epidermal cells. This can be blocked by loss of *ANT* function, suggesting that *ARGOS* positively regulates *ANT* during petal organogenesis (Hu et al. 2003). Conversely, *BPEp* and *ARF8* together regulate petal size by negatively affecting mitotic growth and restricting cell expansion during early and late petal development, respectively (Varaud et al. 2011), and *arf8* and *bpe* mutants are associated with the up-regulation of early auxin-responsive genes. Notably, interaction between *BPEp* and *ARF8* occurs via the *BPEp* carboxy-terminal domain, which shares sequence similarity with motif III of *ARF* and *AUXIN/INDOLE-3-ACETIC ACID* proteins (Varaud et al. 2011).

The stereotypic conical shape of cells in the *Arabidopsis* adaxial petal epidermis requires auxin signaling and apoplastic pH changes (Dang et al. 2020). Decreased auxin concentration, transport, or signaling abolishes cell-wall acidification and affects the height and shape of conical cells; notably, *arf6-2 arf8-3* displays severe defects in conical cell shape and outgrowth (Tabata et al. 2010).

In *Arabidopsis*, stamens develop asynchronously: primordia of the four long medial stamens arise contemporaneously with petals during stage 5 of flower development, whereas the two short lateral stamens develop slightly later (Bowman et al. 1989). Reduction in auxin biosynthesis, especially by *yuc2* and *yuc6* or polar transport (*pin1* and *pid*), reduces stamen number. The fewer-stamen phenotype of *ett* is enhanced by inhibiting auxin transport, leading to third-whorl organs that often consist of filamen-

tous structures that lack anthers. Moreover, *ABCB/PGP* genes that encode auxin efflux carriers are expressed in young stamen primordia, as well as in tapetum and pollen mother cells (PMCs) entering meiosis, and *abcb1* and *abcb19* show unsynchronized and precocious meiosis (Cecchetti et al. 2015).

The role of auxin during premeiotic phases of stamen development is poorly understood, partly because *DR5* expression is only detected after microspore release (Cheng et al. 2006; Feng et al. 2006; Cecchetti et al. 2008, 2015). The R2D2 auxin reporter revealed that auxin-mediated DII depletion occurs in the locules early in anther development and overlaps with *YUC1* and *YUC4* activity (Cheng et al. 2006; Ståldal et al. 2012). Auxin biosynthesis is positively regulated by *SHI/STY* transcription factors, which are active throughout anther development and affect early anther patterning (Estornell et al. 2018).

Late stamen development involves the coordination of rapid filament elongation with anther dehiscence and pollen maturation and finally terminates with mature pollen-grain release. Anthers of *abcb1 abcb19* overproliferate tapetum cells and show enhanced septum lignification, suggesting that auxin transport regulates cell division and lignification (Cecchetti et al. 2015). Inhibition of auxin efflux (Cecchetti et al. 2017) suggests that auxin flows from the tapetum to the middle layer, where auxin response maxima are important for coordinated pollen maturation and anther dehiscence.

Auxin signaling also represses precocious entry into subsequent developmental steps in several anther cell layers, and anthers of mutants in genes encoding the four TIR/AFB nuclear auxin receptors show premature dehiscence and pollen release compared to wild-type (Cecchetti et al. 2008, 2017). Mutations in *ARF1*, *ARF2* (Ellis et al. 2005), *ETT* (Sessions et al. 1997), *ARF4* (Pekker et al. 2005), *ARF5* (Przemek et al. 1996), *ARF17* (Xu et al. 2019), *ARF6*, and *ARF8* (Nagpal et al. 2005) all cause defects in male reproductive tissues. Stamens of *arf6 arf8* are short with indehiscent anthers due to reduced jasmonic acid (JA) biosynthesis (Nagpal et al. 2005; Tabata et al. 2010). Furthermore, restriction of *ARF6* and *ARF8* domains by

M. Cucinotta et al.

miR167 cleavage is required for anther development and fertility (Wu et al. 2006).

Several flower-specific, intron-retaining splice variants of *ARF8* affect stamen development in *Arabidopsis* (Ghelli et al. 2018). *ARF8.4* transcriptionally activates *MYB26*, which regulates secondary thickening and anther dehiscence (Yang et al. 2007, 2017), and *ARF8.2* regulates JA biosynthesis by activating *DAD1* to promote the final steps of anther dehiscence. The *ARF17*–*MYB108* complex also regulates anther dehiscence in parallel with the *ARF8.4*–*MYB26* pathway (Xu et al. 2019). The stamen-specific *AUX/IAA* gene *IAA19* controls filament elongation (Tashiro et al. 2009) and is regulated by auxin (Cecchetti et al. 2017). *IAA19* is also regulated by *ARF8.4*, but is hardly affected by *ARF8.2* and *ARF8.1*, highlighting the specificity of *ARF8* isoforms during early stamen development (Table 1; Fig. 2; Ghelli et al. 2018).

FLORAL MERISTEM DETERMINACY AND GYNOCIDIUM DEVELOPMENT

The final floral development stage involves termination of FM growth following realization of the species-specific floral body plan. In *Arabidopsis*, the master regulator of FM determinacy, *AGAMOUS* (*AG*), represses the stem-cell marker *WUS* by recruiting Polycomb group (*PcG*) proteins to the *WUS* locus and in parallel, activating the expression of the *WUS* repressor *KNUCKLES* (*KNU*) (Sun et al. 2009; Liu et al. 2011). *APETALA2* (*AP2*) antagonizes *AG* function by activating *WUS* expression (Huang et al. 2017). *AG* directly activates *CRABS CLAW* (*CRC*), which represses *TORNADO* (*TRN2*), a regulator of auxin homeostasis, leading to a shift from meristem maintenance to organ differentiation (Yamaguchi et al. 2017). *AG* and *CRC* both activate the *YUC4* promoter and *AG* recruits *CHROMATIN REMODELING FACTOR11* and *17* (*CHR11/17*), which increases chromatin accessibility (Yamaguchi et al. 2018). Therefore, the regulation of auxin homeostasis by multiple pathways is an important component of FM determinacy (Table 1; Fig. 2).

The *AG*–*AP2* FM determinacy pathway is also mediated by *ETT*. *ETT* and *AG* coordinate-

ly repress *WUS* expression in the FM and combined loss of *ETT* and *AG* strongly enhances defects in FM indeterminacy. Moreover, *ETT* expression is indirectly positively regulated by *AG*. Binding of *ETT* to *WUS* is enhanced by *AG* activity, but independently from the *WUS* repression pathway mediated by *KNU*. In addition, *ETT* function in FM determinacy is negatively regulated by *AP2* (Liu et al. 2014).

The appropriate termination of FM growth relates to gynoecium initiation in the FM center, which depletes the meristematic cell pool. The absence of a gynoecium in *ag* mutants indicates that FM determinacy is essential for female organ differentiation (Marsch-Martinez and de Folter 2016; Yamaguchi et al. 2017).

Gynoecium development involves the establishment of apical–basal and adaxial–abaxial axes. Mutation of *ETT* perturbs gynoecium organogenesis along the apical–basal axis, leading to reduced valve development and the ectopic expansion of transmitting tract and stigma (Sessions and Zambryski 1995; Alvarez and Smyth 1998). A long-standing model for gynoecium development along the apical–basal axis derived from observations that inhibition of auxin transport and auxin biosynthesis or transport mutants all generate a valveless gynoecium topped with stigmatic tissue. This suggests that a high local auxin biosynthesis at the gynoecium tip establishes a basipetally decreasing auxin morphogenetic gradient that specifies style, ovary, and gynophore (Nemhauser et al. 2000). However, *DR5rev::GFP* reports no auxin gradient, only auxin response maxima in carpel founder cells at stage 7, the provasculture at stage 8, apical tissue at stage 9, and the vasculature and stigmatic papillae at stage 12 (Larsson et al. 2013). Additionally, specification of lateral and medial gynoecium domains, including valve outgrowth, depends on *PIN1*-mediated lateral auxin maxima (Larsson et al. 2014). A refined, so-called early action model (Hawkins and Liu 2014) based on early polarity establishment in lateral organs such as leaves, proposes that abaxial–adaxial polarity in early carpel primordia is critical for subsequent development. This is consistent with *YUC1* and *YUC4* activity at the start of organ initiation (Cheng et al. 2006),



which potentially contributes to establishing an adaxial–abaxial boundary. Adaxial–abaxial axis formation also involves protein interactions between KANADI (KAN)1, KAN4, and ETT (Pekker et al. 2005). Therefore, gynoecium patterning involves two distinct phases: the early establishment of abaxial–adaxial identity within the mediolateral axis domains by coordinated auxin synthesis, transport, and signaling. Subsequently, this lateromedial domain is a prerequisite for establishing an apical–basal axis (Hawkins and Liu 2014).

During late gynoecium development, two additional foci of auxin response maxima initiate in the medial domain in addition to two in the lateral domain in the gynoecium apex. Immediately preceding style development, these four foci fuse into a ring due to SPATULA (SPT)/INDEHISCENT (IND)-dependent rearrangement of PIN proteins, which involves the direct repression of *PID* and leads to the acquisition of radial symmetry (Moubayidin and Østergaard 2014). During style and gynoecium development, auxin promotes the function of an ETT–IND complex that also leads to *PID* repression and finely regulates PIN localization and auxin flux (Moubayidin and Østergaard 2017; Kuhn et al. 2019). As well as interaction with IND, SPT associates with HECATE to regulate *PIN1* and *PIN3* expression and block cytokinin signaling (Gremski et al. 2007).

Because auxin biosynthesis mutants still differentiate stigmatic tissue, late gynoecium development is probably independent from the early action model and dependent on local auxin synthesis via *YUC* expression activated by *STYLISH1/2* and *NGA3* transcription factors in the gynoecium tip (Sohlberg et al. 2006; Trigueros et al. 2009; Eklund et al. 2011). *SQUAMOSA PROMOTER-BINDING PROTEIN-LIKE* transcription factors also contribute to style, septum, and transmitting tract development, probably upstream of *YUC4* and by interactions with *CRC*, *ETT*, *SPT*, and *STY1*, which are all involved in auxin homeostasis or responsiveness (Xing et al. 2013).

The direct binding of auxin to the carboxy-terminal domain of *ETT* (Kuhn et al. 2020) reveals an additional layer of auxin regulation that

triggers a rapid and reversible switch of chromatin states during gynoecium development. *ETT* cannot interact with Aux/IAA proteins or mediate canonical auxin signaling because it lacks a PB1 domain. In low-auxin conditions, the *ETT* EAR repressor motif physically interacts with members of the TPL and TPL-RELATED (TPR) family of corepressors, which recruit histone deacetylase HDA19 to maintain chromatin of *ETT* targets in the gynoecium, such as *PID* (Benjamins et al. 2001) and *HECATE1* (*HEC1*) (Gremski et al. 2007) in a repressed state. At higher auxin levels, binding of IAA to *ETT* causes its dissociation from TPL/TPR2, which prevents HDA19 from deacetylating histones at *ETT* target loci and leads to their transcriptional activation.

AUXIN AND OVULE DEVELOPMENT

Auxin maintains the meristematic activity of the placenta and determines the sites of ovule initiation and ovule identity. In most auxin-related mutants, defects in CMM formation cause the reduction or absence of placental tissue and ovules (Cucinotta et al. 2014; Reyes-Olalde and de Folter 2019). In particular, auxin concentration maxima generated by *PIN1* in the placenta determine sites of ovule primordium initiation (Benková et al. 2003; Ceccato et al. 2013; Galbiati et al. 2013). Placental *PIN1* expression is promoted by cytokinins via transcription of the direct MP targets *CYTOKININ RESPONSE FACTOR2/TARGET OF MONOPTEROS3* and *CUC1/CUC2* (Galbiati et al. 2013; Cucinotta et al. 2016, 2020), and a lower *PIN1* level in *crf2* and *cuc2-1 CUC1_RNAi* mutants results in fewer ovule primordia. After ovule initiation, *ANT* promotes primordium cell proliferation and integument growth. Correct *ANT* expression is also controlled by auxin via MP and *AR-GOS* (Hu et al. 2003; Galbiati et al. 2013).

Auxin is critical for the somatic-to-germline fate transition, and for downstream events of megasporogenesis and female gametophyte (FG) development. *PIN1* also drives an auxin maximum in the nucellus at the ovule tip in the L1 surrounding the megaspore mother cell (MMC) (Benková et al. 2003; Ceccato et al.

M. Cucinotta et al.

2013). *ETT* is a negative regulator of MMC identity and is expressed in central ovule regions, where it restricts *WUS* expression, similar to its role in the FM. In the nucellus, *ETT* expression is tightly regulated by *TAS3* tasiRNA, and deregulation of its expression causes supernumerary MMCs (Su et al. 2017).

After MMC enlargement, meiosis generates four haploid megaspores, but only the functional megaspore undergoes three mitoses to form an FG consisting of seven cells of four distinct cell types. During megagametogenesis, auxin response is localized to the chalazal pole in the sporophytic tissues surrounding the FG (Lituiev et al. 2013). This suggested a model in which the auxin cell-non-autonomously indirectly affects cell specification within the gametophyte by functioning in sporophytic tissues (Lituiev et al. 2013). Auxin helps to pattern the micropylar pole of the FG where egg and synergid cells are located (Skinner and Sundaresan 2018), and loss of synergid identity and the occasional acquisition of egg identity results when *TIR1* and ARFs are down-regulated or inactivated in the young FG (Panoli et al. 2015; Liu et al. 2018). Conversely, ectopic *YUC* expression shifts micropylar cell fates toward the chalazal end of the gametophyte, conferring synergid and egg-cell marker expression to the central cell and antipodal cells (Panoli et al. 2015). It remains unknown whether auxin influences mitosis and cell identity within the TM, which could be addressed by live imaging.

CONCLUDING REMARKS

Despite detailed understanding of how auxin integrates into the gene networks that regulate floral development, and major advances in characterizing components of the auxin response machinery, higher-order layers of complexity involved in auxin response continue to emerge. However, understanding how auxin confers positional information for organ initiation requires knowledge concerning spatiotemporal auxin responses at single-cell resolution. Despite the central role of MP in coordinating auxin responses, the complete genome-wide repertoire of direct ARF targets has not been captured and

paradigmatic canonical auxin response signaling might involve as-yet-unknown ARF-binding sequences.

Most importantly, although *Arabidopsis* is the best-studied plant development model, its flowers are hardly representative of angiosperm floral diversity and the molecular-genetic basis of many features of floral development that underlie differences in the floral body plan and morphogenesis in other species have not been considered; some examples include the unidirectional organ initiation, the existence of overlapping temporal organ initiation in different whorl, and common primordia in many legumes (Ferrandiz et al. 1999; Tucker 2003; Benlloch et al. 2015) or flowers that show centripetal, centrifugal (or basipetal), or more chaotic sequences of organ development within a single flower or whorl (Rudall 2010). One recurring theme in floral development is how auxin gradients orchestrate aspects of floral development in concert with those in cytokinin. Despite the characterization of auxin signaling components in comparative species, this needs to be combined with studies on comparative floral morphology at a high spatiotemporal resolution, to identify evolutionarily conserved aspects of the regulation of floral development by auxin to be identified, and to elucidate further levels of complexity not evident in *Arabidopsis*.

ACKNOWLEDGMENTS

A.C. and L.C. were supported by Ministero dell'Istruzione, dell'Università e della Ricerca (MIUR). M.C., A.C., and L.C. were funded by MIUR-PRIN 2012. We thank Sara Comai for drawing the flower in Figure 2.

REFERENCES

- Aloni R, Aloni E, Langhans M, Ullrich CI. 2006. Role of auxin in regulating *Arabidopsis* flower development. *Planta* **223**: 315–328. doi:10.1007/s00425-005-0088-9
- Alonso JM, Stepanova AN, Leisse TJ, Kim CJ, Chen H, Shinn P, Stevenson DK, Zimmerman J, Barajas P, Cheuk R, et al. 2003. Genome-wide insertional mutagenesis of *Arabidopsis thaliana*. *Science* **301**: 653–657. doi:10.1126/science.1086391





- Alvarez J, Smyth DR. 1998. Genetic pathways controlling carpel development in *Arabidopsis thaliana*. *J Plant Res* **111**: 295–298. doi:10.1007/BF02512187
- Alvarez-Buylla ER, Benítez M, Corvera-Poiré A, Cadore C, De Folter S, De Buen AG, Garay-Arroyo A, García-Ponce B, Jaimes-Miranda F, Rigoberto V, et al. 2010. Flower development. *Arabidopsis Book* **8**: e0127. doi:10.1199/tab.0127
- Baker CC, Sieber P, Wellmer F, Meyerowitz EM. 2005. The early extra petals1 mutant uncovers a role for microRNA miR164c in regulating petal number in *Arabidopsis*. *Curr Biol* **15**: 303–315. doi:10.1016/j.cub.2005.02.017
- Benjamins R, Quint A, Weijer D, Hooykaas P, Offringa R. 2001. The PINOID protein kinase regulates organ development in *Arabidopsis* by enhancing polar auxin transport. *Development* **128**: 4057–4067.
- Benková E, Michniewicz M, Sauer M, Teichmann T, Seifertová D, Jürgens G, Friml J. 2003. Local, efflux-dependent auxin gradients as a common module for plant organ formation. *Cell* **115**: 591–602. doi:10.1016/S0092-8674(03)00924-3
- Benlloch R, Berbel A, Ali L, Gohari G, Millán T, Madueño F. 2015. Genetic control of inflorescence architecture in legumes. *Front Plant Sci* **6**: 543. doi:10.3389/fpls.2015.00543
- Bennett SRM, Alvarez J, Bossinger G, Smyth DR. 1995. Morphogenesis in pinoid mutants of *Arabidopsis thaliana*. *Plant J* **8**: 505–520. doi:10.1046/j.1365-3113X.1995.8040505.x
- Besnard F, Refahi Y, Morin V, Marteaux B, Brunoud G, Chambrier P, Rozier F, Mirabet V, Legrand J, Lainé S, et al. 2014. Cytokinin signalling inhibitory fields provide robustness to phyllotaxis. *Nature* **505**: 417–421. doi:10.1038/nature12791
- Bilsborough GD, Runions A, Barkoulas M, Jenkins HW, Hasson A, Galinha C, Laufs P, Hay A, Prusinkiewicz P, Tsiantis M. 2011. Model for the regulation of *Arabidopsis thaliana* leaf margin development. *Proc Natl Acad Sci* **108**: 3424–3429. doi:10.1073/pnas.1015162108
- Bowman JL, Smyth DR, Meyerowitz EM. 1989. Genes directing flower development in *Arabidopsis*. *Plant Cell* **1**: 37–52.
- Bowman JL, Sakai H, Jack T, Weigel D, Mayer U, Meyerowitz EM. 1992. SUPERMAN a regulator of floral homeotic genes in *Arabidopsis*. *Development* **114**: 599–615.
- Brewer PB. 2004. PETAL LOSS, a trihelix transcription factor gene, regulates perianth architecture in the *Arabidopsis* flower. *Development* **131**: 4035–4045. doi:10.1242/dev.01279
- Caggiano MP, Yu X, Bhatia N, Larsson A, Ram H, Ohno CK, Sappl P, Meyerowitz EM, Jönsson H, Heisler MG. 2017. Cell type boundaries organize plant development. *eLife* **6**: e27421. doi:10.7554/eLife.27421
- Ceccato L, Masiero S, Sinha Roy D, Bencivenga S, Roig-Villanova I, Ditengou FA, Palme K, Simon R, Colombo L. 2013. Maternal control of PIN1 is required for female gametophyte development in *Arabidopsis*. *PLoS ONE* **8**: e66148. doi:10.1371/journal.pone.0066148
- Cecchetti V, Altamura MM, Falasca G, Costantino P, Cardarelli M. 2008. Auxin regulates *Arabidopsis* anther dehiscence, pollen maturation, and filament elongation. *Plant Cell* **20**: 1760–1774. doi:10.1105/tpc.107.057570
- Cecchetti V, Brunetti P, Napoli N, Fattorini L, Altamura MM, Costantino P, Cardarelli M. 2015. ABCB1 and ABCB19 auxin transporters have synergistic effects on early and late *Arabidopsis* anther development. *J Integr Plant Biol* **57**: 1089–1098. doi:10.1111/jipb.12332
- Cecchetti V, Celebrin D, Napoli N, Ghelli R, Brunetti P, Costantino P, Cardarelli M. 2017. An auxin maximum in the middle layer controls stamen development and pollen maturation in *Arabidopsis*. *New Phytol* **213**: 1194–1207. doi:10.1111/nph.14207
- Chandler JW. 2011. Founder cell specification. *Trends Plant Sci* **16**: 607–613. doi:10.1016/j.tplants.2011.08.005
- Chandler JW, Werr W. 2014. *Arabidopsis* floral phytomer development: auxin response relative to biphasic modes of organ initiation. *J Exp Bot* **65**: 3097–3110. doi:10.1093/jxb/eru153
- Chandler J, Werr W. 2017. DORNROSCHEN, DORNROSCHEN-LIKE, and PUCHI redundantly control floral meristem identity and organ initiation in *Arabidopsis*. *J Exp Bot* **68**: 3457–3472. doi:10.1093/jxb/erx208
- Chandler JW, Cole M, Jacobs B, Comelli P, Werr W. 2011. Genetic integration of DORNROSCHEN and DORNROSCHEN-LIKE reveals hierarchical interactions in auxin signalling and patterning of the *Arabidopsis* apical embryo. *Plant Mol Biol* **75**: 223–236. doi:10.1007/s11103-010-9721-5
- Cheng Y, Dai X, Zhao Y. 2006. Auxin biosynthesis by the YUCCA flavin monooxygenases controls the formation of floral organs and vascular tissues in *Arabidopsis*. *Genes Dev* **20**: 1790–1799. doi:10.1101/gad.1415106
- Chung Y, Zhu Y, Wu MF, Simonini S, Kuhn A, Armenta-Medina A, Jin R, Østergaard L, Gillmor CS, Wagner D. 2019. Auxin response factors promote organogenesis by chromatin-mediated repression of the pluripotency gene SHOOTMERISTEMLESS. *Nat Commun* **10**: 886.
- Cole M, Chandler J, Weijers D, Jacobs B, Comelli P, Werr W. 2009. DORNROSCHEN is a direct target of the auxin response factor MONOPTEROS in the *Arabidopsis* embryo. *Development* **136**: 1643–1651. doi:10.1242/dev.032177
- Comelli P, Glowa D, Frerichs A, Engelhorn J, Chandler JW, Werr W. 2020. Functional dissection of the DORNROSCHEN-LIKE enhancer 2 during embryonic and phyllo-tactic patterning. *Planta* **251**: 90. doi:10.1007/s00425-020-03381-7
- Cucinotta M, Colombo L, Roig-villanova I. 2014. Ovule development, a new model for lateral organ formation. *Front Plant Sci* **5**: 1–12. doi:10.3389/fpls.2014.00117
- Cucinotta M, Manrique S, Guazzotti A, Quadrelli NE, Mendes MA, Benkova E, Colombo L. 2016. Cytokinin response factors integrate auxin and cytokinin pathways for female reproductive organ development. *Development* **143**: 4419–4424. doi:10.1242/dev.143545
- Cucinotta M, Di Marzo M, Guazzotti A, de Folter S, Kater MM, Colombo L. 2020. Gynoecium size and ovule number are interconnected traits that impact seed yield. *J Exp Bot* **71**: 2479–2489. doi:10.1093/jxb/eraa050
- Dang X, Chen B, Liu F, Ren H, Liu X, Zhou J, Qin J, Lin D. 2020. Auxin signaling-mediated apoplastic pH modification functions in petal conical cell shaping. *Cell Rep* **30**: 3904–3916.e3. doi:10.1016/j.celrep.2020.02.087

M. Cucinotta et al.

- Dinneny JR, Yadegari R, Fischer RL, Yanofsky MF, Weigel D. 2004. The role of JAGGED in shaping lateral organs. *Development* **131**: 1101–1110. doi:10.1242/dev.00949
- Eklund DM, Cierlik I, Ståldal V, Claes AR, Vestman D, Chandler J, Sundberg E. 2011. Expression of *Arabidopsis* SHORT INTERNODES/STYLISH family genes in auxin biosynthesis zones of aerial organs is dependent on a GCC box-like regulatory element. *Plant Physiol* **157**: 2069–2080. doi:10.1104/pp.111.182253
- Ellis CM, Nagpal P, Young JC, Hagen G, Guilfoyle TJ, Reed JW. 2005. AUXIN RESPONSE FACTOR1 and AUXIN RESPONSE FACTOR2 regulate senescence and floral organ abscission in *Arabidopsis thaliana*. *Development* **132**: 4563–4574. doi:10.1242/dev.02012
- Estornell LH, Landberg K, Cierlik I, Sundberg E. 2018. SH1/STY genes affect pre- and post-meiotic anther processes in auxin sensing domains in *Arabidopsis*. *Front Plant Sci* **9**: 150. doi:10.3389/fpls.2018.00150
- Feng XL, Ni WM, Elge S, Mueller-Roeber B, Xu ZH, Xue HW. 2006. Auxin flow in anther filaments is critical for pollen grain development through regulating pollen mitosis. *Plant Mol Biol* **61**: 215–226. doi:10.1007/s11103-006-0005-z
- Ferrandiz C, Navarro C, Gomez MD, Canas LA, Beltran JP. 1999. Flower development in *Pisum sativum*: from the war of the whorls to the battle of the common primordia. *Dev Genet* **25**: 280–290.
- Frerichs A, Thoma R, Abdallah AT, Frommolt P, Werr W, Chandler JW. 2016. The founder-cell transcriptome in the *Arabidopsis apetala1* cauliflower inflorescence meristem. *BMC Genomics* **17**: 855. doi:10.1186/s12864-016-3189-x
- Furutani M, Vernoux T, Traas J, Kato T, Tasaka M, Aida M. 2004. PIN-FORMED1 and PINOID regulate boundary formation and cotyledon development in *Arabidopsis* embryogenesis. *Development* **131**: 5021–5030. doi:10.1242/dev.01388
- Furutani M, Nakano Y, Tasaka M. 2014. MAB4-induced auxin sink generates local auxin gradients in *Arabidopsis* organ formation. *Proc Natl Acad Sci* **111**: 1198–1203. doi:10.1073/pnas.1316109111
- Galbiati F, Sinha Roy D, Simonini S, Cucinotta M, Ceccato L, Cuesta C, Simaskova M, Benková E, Kamiuchi Y, Aida M, et al. 2013. An integrative model of the control of ovule primordia formation. *Plant J* **76**: 446–455. doi:10.1111/tbj.12309
- Galvan-Ampudia CS, Cerutti G, Legrand J, et al. 2020. Temporal integration of auxin information for the regulation of patterning. *eLife* **9**: e55832.
- Gälweiler L, Guan C, Müller A, Wisman E, Mendgen K, Yephremov A, Palme K. 1998. Regulation of polar auxin transport by AtPIN1 in *Arabidopsis* vascular tissue. *Sci* **282**: 2226–2230. doi:10.1126/science.282.5397.2226
- Ghelli R, Brunetti P, Napoli N, De Paolis A, Cecchetti V, Tsuge T, Serino G, Matsui M, Mele G, Rinaldi G, et al. 2018. A newly identified flower-specific splice variant of AUXIN RESPONSE FACTOR8 regulates stamen elongation and endothecium lignification in *Arabidopsis*. *Plant Cell* **30**: 620–637. doi:10.1105/tpc.17.00840
- Goldental-Cohen S, Israeli A, Ori N, Yasuor H. 2017. Auxin response dynamics during wild-type and entire flower development in tomato. *Plant Cell Physiol* **58**: 1661–1672. doi:10.1093/pcp/pcx102
- Gremski K, Ditta G, Yanofsky MF. 2007. The HECATE genes regulate female reproductive tract development in *Arabidopsis thaliana*. *Development* **134**: 3593–3601. doi:10.1242/dev.011510
- Griffith ME, da Silva Conceição A, Smyth DR. 1999. PETAL LOSS gene regulates initiation and orientation of second whorl organs in the *Arabidopsis* flower. *Development* **126**: 5635–5644.
- Guan C, Wu B, Yu T, Wang Q, Krogan NT, Liu X, Jiao Y. 2017. Spatial auxin signaling controls leaf flattening in *Arabidopsis*. *Curr Biol* **27**: 2940–2950.e4. doi:10.1016/j.cub.2017.08.042
- Hawkins C, Liu Z. 2014. A model for an early role of auxin in *Arabidopsis* gynoecium morphogenesis. *Front Plant Sci* **5**: 327.
- Heisler MG, Ohno C, Das P, Sieber P, Reddy GV, Long JA, Meyerowitz EM. 2005. Patterns of auxin transport and gene expression during primordium development revealed by live imaging of the *Arabidopsis* inflorescence meristem. *Curr Biol* **15**: 1899–1911. doi:10.1016/j.cub.2005.09.052
- Hibara K, Karim MR, Takada S, Taoka K, Furutani M, Aida M, Tasaka M. 2006. *Arabidopsis* CUP-SHAPED COTYLEDON3 regulates postembryonic shoot meristem and organ boundary formation. *Plant Cell* **18**: 2946–2957. doi:10.1105/tpc.106.045716
- Hu Y, Xie Q, Chua NH. 2003. The *Arabidopsis* auxin-inducible gene ARGOS controls lateral organ size. *Plant Cell* **15**: 1951–1961. doi:10.1105/tpc.013557
- Huang T, López-Giráldez F, Townsend JP, Irish VF. 2012. RBE controls microRNA164 expression to effect floral organogenesis. *Dev* **139**: 2161–2169. doi:10.1242/dev.075069
- Huang Z, Shi T, Zheng B, Yumul RE, Liu X, You C, Gao Z, Xiao L, Chen X. 2017. APETALA2 antagonizes the transcriptional activity of AGAMOUS in regulating floral stem cells in *Arabidopsis thaliana*. *New Phytol* **215**: 1197–1209. doi:10.1111/nph.14151
- Irish VF. 2010. The flowering of *Arabidopsis* flower development. *Plant J* **61**: 1014–1028. doi:10.1111/j.1365-313X.2009.04065.x
- Kamiuchi Y, Yamamoto K, Furutani M, Tasaka M, Aida M. 2014. The CUC1 and CUC2 genes promote carpel margin meristem formation during *Arabidopsis* gynoecium development. *Front Plant Sci* **5**: 165. doi:10.3389/fpls.2014.00165
- Krizek BA, Lewis MW, Fletcher JC. 2006. RABBIT EARS is a second-whorl repressor of AGAMOUS that maintains spatial boundaries in *Arabidopsis* flowers. *Plant J* **45**: 369–383. doi:10.1111/j.1365-313X.2005.02633.x
- Kuhn A, Runciman B, Tasker-Brown W, Østergaard L. 2019. Two auxin response elements fine-tune PINOID expression during gynoecium development in *Arabidopsis thaliana*. *Biomolecules* **9**: 526. doi:10.3390/biom9100526
- Kuhn A, Ramans Harborough S, McLaughlin HM, Nataraajan B, Verstraeten I, Friml J, Kepinski S, Østergaard L. 2020. Direct ETTIN-auxin interaction controls chromatin states in gynoecium development. *eLife* **9**: e51787. doi:10.7554/eLife.51787



- Kwiatkowska D. 2008. Flowering and apical meristem growth dynamics. *J Exp Bot* **59**: 187–201. doi:10.1093/jxb/erm290
- Lampugnani ER, Kilinc A, Smyth DR. 2013. Auxin controls petal initiation in *Arabidopsis*. *Development* **140**: 185–194. doi:10.1242/dev.084582
- Larsson E, Franks RG, Sundberg E. 2013. Auxin and the *Arabidopsis thaliana* gynoecium. *J Exp Bot* **64**: 2619–2627. doi:10.1093/jxb/ert099
- Larsson E, Roberts CJ, Claes R, Franks RG, Sundberg E. 2014. Polar auxin transport is essential for medial versus lateral tissue specification and vascular-mediated valve outgrowth in *Arabidopsis* gynoecia. *Plant Physiol* **166**: 1998–2012. doi:10.1104/pp.114.245951
- Laufs P, Peaucelle A, Morin H, Traas J. 2004. MicroRNA regulation of the CUC genes is required for boundary size control in *Arabidopsis* meristems. *Development* **131**: 4311–4322. doi:10.1242/dev.01320
- Li W, Zhou Y, Liu X, Yu P, Cohen JD, Meyerowitz EM. 2013. LEAFY controls auxin response pathways in floral primordium formation. *Sci Signal* **6**: ra23.
- Lituiev DS, Krohn NG, Muller B, Jackson D, Hellriegel B, Dresselhaus T, Grossniklaus U. 2013. Theoretical and experimental evidence indicates that there is no detectable auxin gradient in the angiosperm female gametophyte. *Development* **140**: 4544–4553. doi:10.1242/dev.098301
- Liu X, Kim YJ, Müller R, Yumul RE, Liu C, Pan Y, Cao X, Goodrich J, Chen X. 2011. AGAMOUS terminates floral stem cell maintenance in *Arabidopsis* by directly repressing WUSCHEL through recruitment of Polycomb Group proteins. *Plant Cell* **23**: 3654–3670. doi:10.1105/tpc.111.091538
- Liu X, Dinh TT, Li D, Shi B, Li Y, Cao X, Guo L, Pan Y, Jiao Y, Chen X. 2014. AUXIN RESPONSE FACTOR 3 integrates the functions of AGAMOUS and APETALA2 in floral meristem determinacy. *Plant J* **80**: 629–641. doi:10.1111/tpj.12658
- Liu Z, Miao L, Huo R, Song X, Johnson C, Kong L, Sundaresan V, Yu X. 2018. ARF2–ARF4 and ARF5 are essential for female and male gametophyte development in *Arabidopsis*. *Plant Cell Physiol* **59**: 179–189. doi:10.1093/pcp/pcx174
- Ma Y, Miotk A, Štiković Z, Ermakova O, Wenzl C, Medzihradský A, Gaillochot C, Forner J, Utan G, Brackmann K, et al. 2019. WUSCHEL acts as an auxin response rheostat to maintain apical stem cells in *Arabidopsis*. *Nat Commun* **10**: 5093.
- Maier AT, Stehling-Sun S, Offenburger SL, Lohmann JU. 2011. The bZIP transcription factor PERIANTHIA: a multifunctional hub for meristem control. *Front Plant Sci* **2**: 79. doi:10.3389/fpls.2011.00079
- Mallory AC, Bartel DP, Bartel B. 2005. MicroRNA-directed regulation of *Arabidopsis* AUXIN RESPONSE FACTOR17 is essential for proper development and modulates expression of early auxin response genes. *Plant Cell* **17**: 1360–1375. doi:10.1105/tpc.105.031716
- Marsch-Martínez N, de Folter S. 2016. Hormonal control of the development of the gynoecium. *Curr Opin Plant Biol* **29**: 104–114. doi:10.1016/j.pbi.2015.12.006
- Matsumoto N. 2001. A homeobox gene, PRESSED FLOWER, regulates lateral axis-dependent development of *Arabidopsis* flowers. *Genes Dev* **15**: 3355–3364. doi:10.1101/gad.931001
- Moubayidin L, Østergaard L. 2014. Dynamic control of auxin distribution imposes a bilateral-to-radial symmetry switch during gynoecium development. *Curr Biol* **24**: 2743–2748. doi:10.1016/j.cub.2014.09.080
- Moubayidin L, Østergaard L. 2017. Gynoecium formation: an intimate and complicated relationship. *Curr Opin Genet Dev* **45**: 15–21. doi:10.1016/j.gde.2017.02.005
- Nagpal P, Ellis CM, Weber H, Ploense SE, Barkawi LS, Guilfoyle TJ, Hagen G, Alonso JM, Cohen JD, Farmer EE, et al. 2005. Auxin response factors ARF6 and ARF8 promote jasmonic acid production and flower maturation. *Development* **132**: 4107–4118. doi:10.1242/dev.01955
- Nakata MT, Tameshige T, Takahara M, Mitsuda N, Okada K. 2018. The functional balance between the WUSCHEL-RELATED HOMEBOX1 gene and the phytohormone auxin is a key factor for cell proliferation in *Arabidopsis* seedlings. *Plant Biotechnol* **35**: 141–154. doi:10.5511/plantbiotechnology.18.0427a
- Nawy T, Bayer M, Mravec J, Friml J, Birnbaum KD, Lukowitz W. 2010. The GATA factor HANABA TARANU is required to position the proembryo boundary in the early *Arabidopsis* embryo. *Dev Cell* **19**: 103–113. doi:10.1016/j.devcel.2010.06.004
- Nemhauser JL, Feldman LJ, Zambryski PC. 2000. Auxin and ETTIN in *Arabidopsis* gynoecium morphogenesis. *Development* **127**: 3877–3888.
- Okada K, Ueda J, Komaki MK, Bell CJ, Shimura Y. 1991. Requirement of the auxin polar transport system in early stages of *Arabidopsis* floral bud formation. *Plant Cell* **3**: 677–684. doi:10.2307/3869249
- Panoli A, Martin MV, Alandete-Saez M, Simon M, Neff C, Swarup R, Bellido A, Yuan L, Pagnussat GC, Sundaresan V. 2015. Auxin import and local auxin biosynthesis are required for mitotic divisions, cell expansion and cell specification during female gametophyte development in *Arabidopsis thaliana*. *PLoS ONE* **10**: e0126164. doi:10.1371/journal.pone.0126164
- Pekker I, Alvarez JP, Eshed Y. 2005. Auxin response factors mediate *Arabidopsis* organ asymmetry via modulation of KANADI activity. *Plant Cell* **17**: 2899–2910. doi:10.1105/tpc.105.034876
- Prunet N, Yang W, Das P, Meyerowitz EM, Jack TP. 2017. SUPERMAN prevents class B gene expression and promotes stem cell termination in the fourth whorl of *Arabidopsis thaliana* flowers. *Proc Natl Acad Sci* **114**: 7166–7171. doi:10.1073/pnas.1705977114
- Przemeczek GH, Mattsson J, Hardtke C, Sung ZR, Berleth T. 1996. Studies on the role of the *Arabidopsis* gene MONOPTEROS in vascular development and plant cell axialization. *Planta* **200**: 229–237. doi:10.1007/BF00208313
- Reinhardt D, Mandel T, Kuhlemeier C. 2000. Auxin regulates the initiation and radial position of plant lateral organs. *Plant Cell* **12**: 507–518. doi:10.1105/tpc.12.4.507
- Reyes-Olalde JI, de Folter S. 2019. Control of stem cell activity in the carpel margin meristem (CMM) in *Arabidopsis*. *Plant Reprod* **32**: 123–136. doi:10.1007/s00497-018-00359-0
- Rudall PJ. 2010. All in a spin: centrifugal organ formation and floral patterning. *Curr Opin Plant Biol* **13**: 108–114. doi:10.1016/j.pbi.2009.09.019

M. Cucinotta et al.

- Running MP, Meyerowitz EM. 1996. Mutations in the PERIANTHIA gene of *Arabidopsis* specifically alter floral organ number and initiation pattern. *Development* **122**: 1261–1269.
- Sakai H, Medrano LJ, Meyerowitz EM. 1995. Role of SUPERMAN in maintaining *Arabidopsis* floral whorl boundaries. *Nature* **378**: 199–203. doi:10.1038/378199a0
- Sauret-Güeto S, Schiessl K, Bangham A, Sablowski R, Coen E. 2013. JAGGED controls *Arabidopsis* petal growth and shape by interacting with a divergent polarity field. *PLoS Biol* **11**: e1001550. doi:10.1371/journal.pbio.1001550
- Sessions RA, Zambryski PC. 1995. *Arabidopsis* gynoeceum structure in the wild type and in *ettin* mutants. *Development* **121**: 1519–1532.
- Sessions RA, Nemhauser JL, McColl A, Roe JL, Feldmann KA, Zambryski PC. 1997. ETTIN patterns the *Arabidopsis* floral meristem and reproductive organs. *Development* **124**: 4481–4491.
- Skinner DJ, Sundaresan V. 2018. Recent advances in understanding female gametophyte development. *F1000Res* **7**: 804. doi:10.12688/f1000research.14508.1
- Smyth DR, Bowman JL, Meyerowitz EM. 1990. Early flower development in *Arabidopsis*. *Plant Cell* **2**: 755–767.
- Sohlberg JJ, Myrenäs M, Kuusk S, Lagercrantz U, Kowalczyk M, Sandberg G, Sundberg E. 2006. *STY1* regulates auxin homeostasis and affects apical-basal patterning of the *Arabidopsis* gynoeceum. *Plant J* **47**: 112–123. doi:10.1111/j.1365-313X.2006.02775.x
- Ståldal V, Cierlik I, Chen S, Landberg K, Baylis T, Myrenäs M, Sundström JF, Eklund DM, Ljung K, Sundberg E. 2012. The *Arabidopsis thaliana* transcriptional activator *STYLISH1* regulates genes affecting stamen development, cell expansion and timing of flowering. *Plant Mol Biol* **78**: 545–559. doi:10.1007/s11103-012-9888-z
- Su Y-H, Liu Y-B, Zhang X-S. 2011. Auxin–cytokinin interaction regulates meristem development. *Mol Plant* **4**: 616–625. doi:10.1093/mp/ssr007
- Su Z, Zhao L, Zhao Y, Li S, Won S, Cai H, Wang L, Li Z, Chen P, Qin Y, et al. 2017. The THO complex non-cell-autonomously represses female germline specification through the TAS3-ARF3 module. *Curr Biol* **27**: 1597–1609.e2. doi:10.1016/j.cub.2017.05.021
- Sun B, Xu Y, Ng KH, Ito T. 2009. A timing mechanism for stem cell maintenance and differentiation in the *Arabidopsis* floral meristem. *Genes Dev* **23**: 1791–1804. doi:10.1101/gad.1800409
- Tabata R, Ikezaki M, Fujibe T, Aida M, Tian C, Ueno Y, Yamamoto KT, Machida Y, Nakamura K, Ishiguro S. 2010. *Arabidopsis* AUXIN RESPONSE FACTOR6 and 8 regulate jasmonic acid biosynthesis and floral organ development via repression of class 1 KNOX genes. *Plant Cell Physiol* **51**: 164–175. doi:10.1093/pcp/pcp176
- Takada S, Hibara K, Ishida T, Tasaka M. 2001. The CUP-SHAPED COTYLEDON1 gene of *Arabidopsis* regulates shoot apical meristem formation. *Development* **128**: 1127–1135.
- Takeda S, Matsumoto N, Okada K. 2004. RABBIT EARS, encoding a SUPERMAN-like zinc finger protein, regulates petal development in *Arabidopsis thaliana*. *Development* **131**: 425–434. doi:10.1242/dev.00938
- Tashiro S, Tian CE, Watahiki MK, Yamamoto KT. 2009. Changes in growth kinetics of stamen filaments cause inefficient pollination in *massugu2*, an auxin insensitive, dominant mutant of *Arabidopsis thaliana*. *Physiol Plant* **137**: 175–187. doi:10.1111/j.1399-3054.2009.01271.x
- Theißen G, Saedler H. 2001. Floral quartets. *Nature* **409**: 469–471. doi:10.1038/35054172
- Trigueros M, Navarrete-Gómez M, Sato S, Christensen SK, Pelaz S, Weigel D, Yanofsky MF, Ferrándiz C. 2009. The *NGATHA* genes direct style development in the *Arabidopsis* gynoeceum. *Plant Cell* **21**: 1394–1409. doi:10.1105/tpc.109.065508
- Tucker SC. 2003. Floral development in legumes. *Plant Physiol* **131**: 911–926. doi:10.1104/pp.102.017459
- Van Mourik S, Kaufmann K, van Dijk ADJ, Angenent GC, Merks RMH, Molenaar J. 2012. Simulation of organ patterning on the floral meristem using a polar auxin transport model. *PLoS ONE* **7**: e28762. doi:10.1371/journal.pone.0028762
- Varaud E, Brioudes F, Szécsi J, Leroux J, Brown S, Perrot-Rechenmann C, Bendahmane M. 2011. AUXIN RESPONSE FACTOR8 regulates *Arabidopsis* petal growth by interacting with the bHLH transcription factor BIG-PETALp. *Plant Cell* **23**: 973–983. doi:10.1105/tpc.110.081653
- Vernoux T, Kronenberger J, Grandjean O, Laufs P, Traas J. 2000. PIN-FORMED 1 regulates cell fate at the periphery of the shoot apical meristem. *EMBO* **19**: 5157–5165.
- Wang Q, Kohlen W, Rossmann S, Vernoux T, Theres K. 2014a. Auxin depletion from the leaf axil conditions competence for axillary meristem formation in *Arabidopsis* and tomato. *Plant Cell* **26**: 2068–2079. doi:10.1105/tpc.114.123059
- Wang Y, Wang J, Shi B, Yu T, Qi J, Meyerowitz EM, Jiao Y. 2014b. The stem cell niche in leaf axils is established by auxin and cytokinin in *Arabidopsis*. *Plant Cell* **26**: 2055–2067. doi:10.1105/tpc.114.123083
- Wang Q, Hasson A, Rossmann S, Theres K. 2016. *Divide et impera*: boundaries shape the plant body and initiate new meristems. *New Phytol* **209**: 485–498. doi:10.1111/nph.13641
- Weigel D, Alvarez J, Smyth DR, Yanofsky MF, Meyerowitz EM. 1992. *LEAFY* controls floral meristem identity in *Arabidopsis*. *Cell* **69**: 843–859. doi:10.1016/0092-8674(92)90295-N
- Wellmer F, Bowman JL, Davies B, Ferrándiz C, Fletcher JC, Franks RG, Graciet E, Gregis V, Ito T, Jack TP, et al. 2014. Flower development: open questions and future directions. *Methods Mol Biol* **1110**: 103–124. doi:10.1007/978-1-4614-9408-9_5
- Wu M-F, Tian Q, Reed JW. 2006. *Arabidopsis* microRNA167 controls patterns of ARF6 and ARF8 expression, and regulates both female and male reproduction. *Development* **133**: 4211–4218. doi:10.1242/dev.02602
- Wu M, Yamaguchi N, Xiao J, Bargmann B, Estelle M, Sang Y, Wagner D. 2015. Auxin-regulated chromatin switch directs acquisition of flower primordium founder fate. *eLife* **4**: 1–19.
- Xing S, Salinas M, Garcia-Molina A, Höhmann S, Berndtgen R, Huijser P. 2013. *SPL8* and miR156-targeted *SPL* genes redundantly regulate *Arabidopsis* gynoeceum differential patterning. *Plant J* **75**: 566–577. doi:10.1111/tj.12221

- Xu B, Li Z, Zhu Y, Wang H, Ma H, Dong A, Huang H. 2008. *Arabidopsis* genes *AS1*, *AS2*, and *JAG* negatively regulate boundary-specifying genes to promote sepal and petal development. *Plant Physiol* **146**: 566–575. doi:10.1104/pp.107.113787
- Xu Y, Prunet N, Gan E, Wang Y, Stewart D, Wellmer F, Huang J, Yamaguchi N, Tatsumi Y, Kojima M, et al. 2018. SUPERMAN regulates floral whorl boundaries through control of auxin biosynthesis. *EMBO J* **37**: e97499.
- Xu XF, Wang B, Feng YF, Xue JS, Qian XX, Liu SQ, Zhou J, Yu YH, Yang NY, Xu P, et al. 2019. AUXIN RESPONSE FACTOR17 directly regulates *MYB108* for anther dehiscence. *Plant Physiol* **181**: 645–655. doi:10.1104/pp.19.00576
- Yadav S, Kumar H, Yadav RK. 2019. Local auxin biosynthesis promotes stem cell differentiation and organogenesis in *Arabidopsis* shoot apex. bioRxiv doi:10.1101/819342
- Yamaguchi N, Wu MF, Winter CM, Berns MC, Nole-Wilson S, Yamaguchi A, Coupland G, Krizek B, Wagner D. 2013. A molecular framework for auxin-mediated initiation of flower primordia. *Dev Cell* **24**: 271–282. doi:10.1016/j.devcel.2012.12.017
- Yamaguchi N, Jeong CW, Nole-Wilson S, Krizek BA, Wagner D. 2016. AINTEGUMENTA and AINTEGUMENTA-LIKE6/PLETHORA3 induce *LEAFY* expression in response to auxin to promote the onset of flower formation in *Arabidopsis*. *Plant Physiol* **170**: 283–293. doi:10.1104/pp.15.00969
- Yamaguchi N, Huang J, Xu Y, Tanoi K, Ito T. 2017. Fine-tuning of auxin homeostasis governs the transition from floral stem cell maintenance to gynoecium formation. *Nat Commun* **8**: 1125. doi:10.1038/s41467-017-01252-6
- Yamaguchi N, Huang J, Tatsumi Y, Abe M, Sugano SS, Kojima M, Takebayashi Y, Kiba T, Yokoyama R, Nishitani K, et al. 2018. Chromatin-mediated feed-forward auxin biosynthesis in floral meristem determinacy. *Nat Commun* **9**: 5290. doi:10.1038/s41467-018-07763-0
- Yang XY, Li JG, Pei M, Gu H, Chen ZL, Qu LJ. 2007. Overexpression of a flower-specific transcription factor gene *AtMYB24* causes aberrant anther development. *Plant Cell Rep* **26**: 219–228. doi:10.1007/s00299-006-0229-z
- Yang C, Song J, Ferguson AC, Klisch D, Simpson K, Mo R, Taylor B, Mitsuda N, Wilson ZA. 2017. Transcription factor *MYB26* is key to spatial specificity in anther secondary thickening formation. *Plant Physiol* **175**: 333–350. doi:10.1104/pp.17.00719
- Yu H, Huang T. 2016. Molecular mechanisms of floral boundary formation in *Arabidopsis*. *Int J Mol Sci* **17**: 317. doi:10.3390/ijms17030317
- Žádníková P, Simon R. 2014. How boundaries control plant development. *Curr Opin Plant Biol* **17**: 116–125. doi:10.1016/j.pbi.2013.11.013
- Zhang X, Zhou Y, Ding L, Wu Z, Liu R, Meyerowitz EM. 2013. Transcription repressor *HANABA TARANU* controls flower development by integrating the actions of multiple hormones, floral organ specification genes, and *GATA3* family genes in *Arabidopsis*. *Plant Cell* **25**: 83–101. doi:10.1105/tpc.112.107854
- Zhao H, Liu L, Mo H, Qian L, Cao Y, Cui S, Li X, Ma L. 2013. The ATP-binding cassette transporter *ABC19* regulates postembryonic organ separation in *Arabidopsis*. *PLoS ONE* **8**: e60809. doi:10.1371/journal.pone.0060809
- Zhu M, Chen W, Mirabet V, Hong L, Bovio S, Strauss S, Schwarz EM, Tsugawa S, Wang Z, Smith RS, et al. 2020. Robust organ size requires robust timing of initiation orchestrated by focused auxin and cytokinin signalling. *Nat Plants* **6**: 686–698. doi:10.1038/s41477-020-0666-7



Cold Spring Harbor Perspectives in Biology

Auxin and Flower Development: A Blossoming Field

Mara Cucinotta, Alex Cavalleri, John William Chandler and Lucia Colombo

Cold Spring Harb Perspect Biol published online December 22, 2020

Subject Collection [Auxin Signaling](#)

Auxin and Flower Development: A Blossoming Field

Mara Cucinotta, Alex Cavalleri, John William Chandler, et al.

Auxin Control of Root Development

Paul Overvoorde, Hidehiro Fukaki and Tom Beeckman

Approaching Cellular and Molecular Resolution of Auxin Biosynthesis and Metabolism

Jennifer Normanly

Auxin and Plant-Microbe Interactions

Stijn Spaepen and Jos Vanderleyden

Cellular Responses to Auxin: Division versus Expansion

Catherine Perrot-Rechenmann

Auxin Transporters—Why So Many?

Eva Začimalová, Angus S. Murphy, Haibing Yang, et al.

Modeling Auxin-regulated Development

Pawel Krupinski and Henrik Jönsson

Distinct and Dynamic Auxin Activities During Reproductive Development

Eva Sundberg and Lars Østergaard

Context, Specificity, and Self-Organization in Auxin Response

Marta Del Bianco and Stefan Kepinski

Auxin at the Shoot Apical Meristem

Teva Vernoux, Fabrice Besnard and Jan Traas

Control of Leaf and Vein Development by Auxin

Enrico Scarpella, Michalis Barkoulas and Miltos Tsiantis

Auxin Perception—Structural Insights

Luz Irina Calderon-Villalobos, Xu Tan, Ning Zheng, et al.

Odyssey of Auxin

Steffen Abel and Athanasios Theologis

Auxin and Monocot Development

Paula McSteen

Do Trees Grow on Money? Auxin as the Currency of the Cellular Economy

Jodi L. Stewart and Jennifer L. Nemhauser

Integration of Light and Auxin Signaling

Karen J. Halliday, Jaime F. Martínez-García and Eve-Marie Josse

For additional articles in this collection, see <http://cshperspectives.cshlp.org/cgi/collection/>

Alternative splicing generates a MONOPTEOORS isoform required for ovule development

Mara Cucinotta^{1†}, Alex Cavalleri^{1†}, Andrea Guazzotti¹, Chiara Astori¹, Silvia Manrique¹, Aureliano Bombarely¹, Stefania Oliveto^{1,2}, Stefano Biffo^{1,2}, Dolf Weijers³, Martin M. Kater¹ and Lucia Colombo^{1*}

† These authors contributed equally to this work.

* Correspondence to: lucia.colombo@unimi.it

Article accepted for publication on “Current Biology”.

In this manuscript I have actively worked in experiments designs, realisation and results interpretation. I performed experiments for the molecular characterisation of intron eleventh retention, and I have performed the phenotypic and molecular characterisation of MP isoforms functionality in rescue *mp* mutants phenotype. I have worked on the manuscript preparation, including figures and text realisation.

Current Biology

Alternative Splicing Generates a MONOPTEROS Isoform Required for Ovule Development

Highlights

- In ovules, MP localizes and activates its targets in cells with auxin minima
- The MP11ir splicing variant seems to function independently of the AUX/IAAs
- Canonical MP and MP11ir complement *mp* mutants during reproductive development

Authors

Mara Cucinotta, Alex Cavalleri, Andrea Guazzotti, ..., Dolf Weijers, Martin M. Kater, Lucia Colombo

Correspondence

lucia.colombo@unimi.it

In Brief

Cucinotta et al. report that MONOPTEROS in ovules is a transcriptional activator in auxin minima regions. This auxin response factor is functioning independently of auxin regulation during reproductive development as evidenced by the observation that an alternative splicing isoform, uncoupled from auxin regulation, was able to rescue *mp* mutants.

Report

Alternative Splicing Generates a MONOPTEROS Isoform Required for Ovule Development

Mara Cucinotta,^{1,4} Alex Cavalleri,^{1,4} Andrea Guazzotti,¹ Chiara Astori,¹ Silvia Manrique,¹ Aureliano Bombarely,¹ Stefania Oliveto,^{1,2} Stefano Biffo,^{1,2} Dolf Weijers,³ Martin M. Kater,¹ and Lucia Colombo^{1,5,*}

¹Dipartimento di BioScienze, Università degli Studi di Milano, Via Celoria 26, 20133 Milano, Italy

²INGM, National Institute of Molecular Genetics “Romeo ed Enrica Invernizzi,” 20122 Milano, Italy

³Laboratory of Biochemistry, Wageningen University, Dreijenlaan 3, 6703 HA Wageningen, the Netherlands

⁴These authors contributed equally

⁵Lead Contact

*Correspondence: lucia.colombo@unimi.it

<https://doi.org/10.1016/j.cub.2020.11.026>

SUMMARY

The plant hormone auxin is a fundamental regulator of organ patterning and development that regulates gene expression via the canonical AUXIN RESPONSE FACTOR (ARF) and AUXIN/INDOLE-3-ACETIC ACID (Aux/IAA) combinatorial system. ARF and Aux/IAA factors interact, but at high auxin concentrations, the Aux/IAA transcriptional repressor is degraded, allowing ARF-containing complexes to activate gene expression. ARF5/MONOPTEROS (MP) is an important integrator of auxin signaling in *Arabidopsis* development and activates gene transcription in cells with elevated auxin levels. Here, we show that in ovules, MP is expressed in cells with low levels of auxin and can activate the expression of direct target genes. We identified and characterized a splice variant of MP that encodes a biologically functional isoform that lacks the Aux/IAA interaction domain. This *MP11ir* isoform was able to complement inflorescence, floral, and ovule developmental defects in *mp* mutants, suggesting that it was fully functional. Our findings describe a novel scenario in which ARF post-transcriptional regulation controls the formation of an isoform that can function as a transcriptional activator in regions of subthreshold auxin concentration.

INTRODUCTION

Developmental processes in plants require auxin. The auxin signaling pathway is primarily mediated by the interplay between AUXIN RESPONSE FACTOR (ARF) and AUXIN/INDOLE-3-ACETIC ACID (Aux/IAA) proteins.^{1,2} At subthreshold auxin concentrations, Aux/IAA repressor proteins bind to ARF transcription factors, thereby repressing the expression of ARF downstream target genes.^{3,4} Similar to other canonical ARFs, ARF5/MONOPTEROS (MP), contains three domains: a B3 DNA-binding domain (DBD), a middle region (MR), and a carboxy-terminal domain (CTD) that is required for dimerization with Aux/IAA proteins, such as IAA12/BODENLOS (BDL).⁵ It has been proposed that at above threshold auxin levels, MP activates transcription of its targets by recruiting the SWI/SNF chromatin remodelling complex, while at subthreshold auxin concentrations, it is bound by BDL that recruits the TPL/HDA19 co-repressor/histone deacetylase complex to repress transcription.⁶

MONOPTEROS and its many of its identified downstream targets are involved in diverse developmental processes, including embryo development, primary and lateral root formation, vasculature patterning, shoot apical meristem maintenance and floral and ovule initiation.^{7–14} This work focuses on a deeper characterization of the expression pattern of MP and its direct targets during ovule development. The results allowed us to hypothesize the existence of non-canonical MP activity that is capable of

activating target genes in cells with low levels of auxin. Indeed, we show that alternative splicing (AS) can generate a functional MP isoform that lacks the Aux/IAA dimerization domain, which implies that this isoform regulates transcription in an auxin-independent manner. Our findings suggest an alternative scenario to the classical paradigm of how MP, and potentially other activating ARFs, can be controlled for appropriate target gene regulation.

RESULTS AND DISCUSSION

MP and Its Targets Are Expressed in Regions of Auxin Minima in Ovules

In seed plants, the ovule gives rise to and contains the female gametophyte for the purpose of fertilization. Ovule primordia contain three distinct regions: a proximal region from which the funiculus differentiates, a chalaza that will form the integuments, and the nucellus, from which the megaspore mother cell develops. *In situ* hybridization experiments showed that MP was expressed in the proximal region and especially in the chalaza (Figure 1A). At later developmental stages, MP expression was limited to the boundary region between the chalaza and the nucellus (Figures 1B and 1C). The expression profile of a functional MP-GFP fusion, encoded by *pMP:MP-GFP*,¹⁵ displayed the same expression pattern (Figures 1D and 1F).

To investigate auxin response in these tissues, we took advantage of the auxin response reporters *DR5v2::ntdTomato*

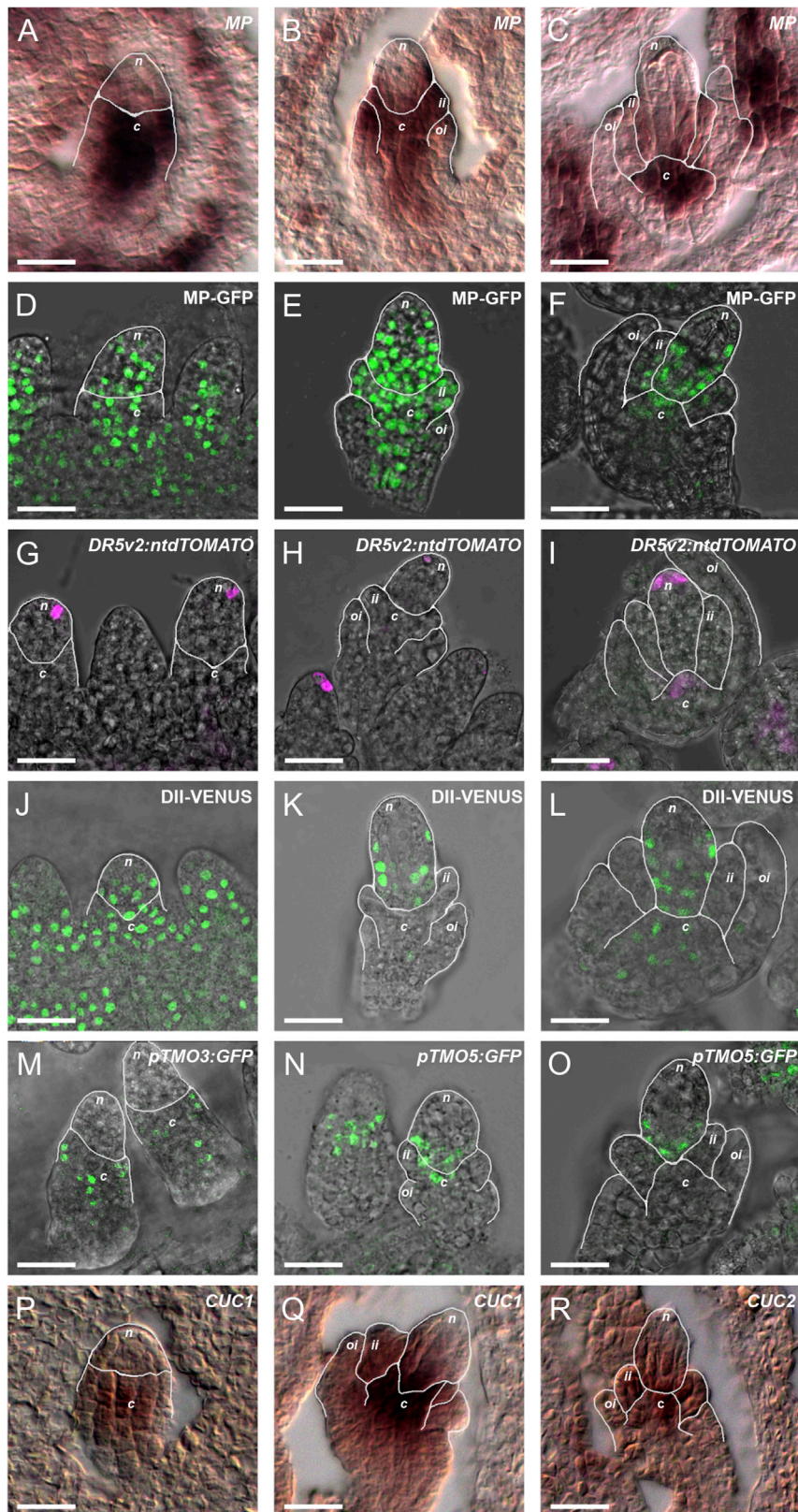


Figure 1. During Ovule Development, MP Transcripts, MP Protein, and Direct MP Targets Are Expressed in Regions Characterized by a Low Auxin Response

(A–C) MP expression detected by *in situ* hybridization, (D–F) expression of *pMP:MP-GFP*, (G–I) *DR5v2::ntdTomato* and (J–L) *DII-VENUS* in three sequential developmental stages from ovule primordium formation to functional megaspore formation.

(M) *pTMO3:GFP*, (N) and (O) *pTMO5:GFP*, and (P–R) *in situ* hybridization of *CUC1* and *CUC2* transcripts in ovules at megasporogenesis stages. The boundaries between the different ovule structures (n: nucellus; c: chalaza; ii: inner-integument; oi: outer-integument) are outlined in white. Scale bar, 20 μ m.

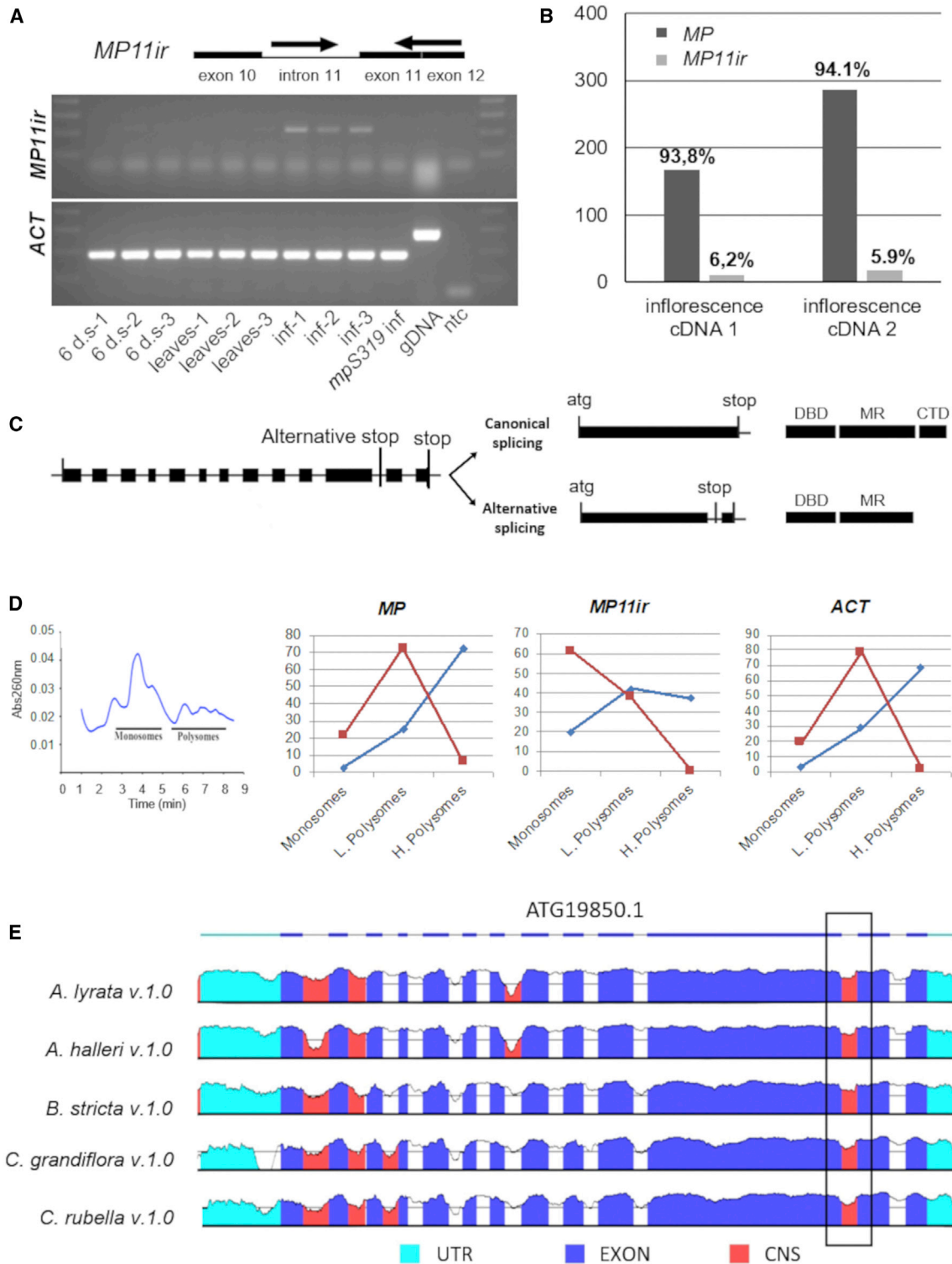


Figure 2. Detection of Alternative Splicing of MP

(A) Schematic structure of the *MP* locus showing the position of primers against the canonical cDNA and *MP11ir* cDNA *MP* genomic sequence used to detect alternative spliced isoforms. The forward primer anneals to intron 11, and the reverse primer to the exon 11–exon 12 junction. Correct annealing of both primers only occurs for *MP11ir*, leading to the amplification of a 239-bp fragment. The cDNA quality was tested with *ACTIN 10*.

(B) Quantitative expression data for canonical *MP* and the *MP11ir* alternative isoform by ddPCR.

(C) Intron 11 introduces a premature stop codon into the *MP* ORF, resulting in the translation of a truncated protein that lacks the CTD domain.

and DII-VENUS.^{16,17} As already described for the classical *DR5* reporter,¹⁰ *DR5v2* showed a peak of auxin response in a few epidermal cells at the tip of the nucellus (Figure 1G–1I). By contrast, DII-VENUS marked cells with low auxin levels, because DII degradation is induced by auxin. Indeed, *DR5v2*-expressing cells showed low DII-VENUS fluorescence (Figure 1J–1L). Strikingly, MP was expressed in ovule cells that showed DII-VENUS activity, confirming its presence in cells with low auxin levels.

To determine whether MP actively regulates transcription in cells of ovule primordia with low auxin levels, we analyzed the expression of the direct MP target genes *TARGET OF MONOPTEROS 3* (*TMO3*), *TMO5*, *CUP-SHAPED COTYLEDON 1* (*CUC1*) and *CUC2*.^{6,10,15} *pTMO3:GFP* was expressed in the proximal region of ovule primordia and in a few cells in the chalaza (Figure 1M). At the same developmental stage, *pTMO5:GFP* expression was also limited to a few cells at the boundary between the chalaza and the nucellus (Figures 1N and 1O). *In situ* hybridization detected *CUC1* and *CUC2* transcripts at the boundaries between ovules,¹⁰ in the chalaza, and in the boundary between the chalaza and the nucellus (Figure 1P–1R). These results show that the expression of *TMO3*, *TMO5*, *CUC1* and *CUC2* spatially overlaps with MP-GFP localization and suggests the existence of a mechanism that allows MP to activate its targets at auxin levels that are insufficient to degrade DII-VENUS or activate *DR5v2*.

Alternative Splicing Generates an MP Protein That Lacks a CTD

The dependence of MP function on auxin, similar to that of other ARF transcription factors, is mediated by Aux/IAA protein interaction with the MP C-terminal PB1 domain.¹⁸ We therefore queried whether naturally occurring MP isoforms that lack the MP C-terminal PB1 domain (CTD) exist. We performed an RNA-seq experiment at high-sequencing depth (100 million reads) using wild-type inflorescences (See STAR Methods). In this dataset, we detected reads that mapped to sequences within, or that entirely spanned, intron 11 of the *MP* gene (Figure S1A). The existence of an alternative *MP* isoform that retains only intron 11 (*MP11ir*) was confirmed using RT-PCR (Figure 2A). Expression of *MP11ir* was high in inflorescences and very low in seedlings, whereas no *MP11ir* was detected in leaves. Using a digital PCR approach, the contribution of *MP11ir* to the amount of total *MP* transcript in inflorescences tissues was determined to be 5.9%–6.2% (Figure 2B). Notably, retention of intron 11 leads to a premature stop codon prior to the CTD domain (Figures 2C and S1B).

Intron retention (IR) is the most prevalent AS event in plants;^{19,20} however, IR generates mostly non-sense mRNAs that harbor premature terminal codons, which are degraded by the nonsense-mediated mRNA decay (NMD) pathway. Consequently, the alternative transcripts might not necessarily represent biologically

functional units. To determine whether *MP11ir* transcripts were translated, their association with ribosomes was investigated by polysome profiling²¹ using pre-fertilization inflorescences (Figure 2D). In inflorescences, approximately 70% of total *MP* mRNA was detected in the heavy polysome fraction, suggesting they were actively translated (Figure 2D). Likewise, *MP11ir* was associated with polysomes, albeit at lower levels (40%; Figure 2D). As reported for many other *Arabidopsis* transcription factors,^{22,23} our data suggest that *MP11ir* transcripts might escape NMD to produce a functional truncated protein.

Furthermore, analysis of the evolutionary conservation of the genomic sequence of *MP* in several species from the *Arabidopsis* genus and in other Brassicaceae taxa revealed that several introns are well conserved (Figure 2E). In particular, introns 1, 2, and 11 are highly conserved among *Arabidopsis thaliana*, *A. lyrata*, *A. halleri*, *Boechera stricta*, *Capsella grandiflora* and *C. rubella*. Among these three introns, intron 11 is the most consistently conserved among the six species, with a degree of conservation comparable to that in the coding sequences (Figure 2E). The sequence conservation of non-coding regions such as introns suggests that these are important for the correct functioning of the gene.

MP11ir Can Restore Pistil and Ovule Formation in *mp* Mutants

Due to the absence of the CTD, *MP11ir* might function as a transcriptional activator irrespective of the auxin level. Indeed, it is well established that the CTD is essential for the heterotypic ARF–Aux/IAA interactions that confer auxin dependency to ARF activity; however, the MP DBD alone is sufficient to bind auxin-responsive promoters and to interact with other ARFs.^{4,24,25}

We hypothesized that *MP11ir* might be functionally relevant during the reproductive phase. To verify this hypothesis, we expressed the shorter *MP11ir* isoform from the *MP* promoter (*pMP:MP11ir-GFP*, hereafter *pMP:MP11ir*) in plants carrying the hypomorphic *mpS319* mutation. The *mpS319* mutant has lateral branching defects and forms only a few flowers with aberrant numbers and morphologies of floral organs (Figures S2 and S3B) and do not develop proper placental tissue or rarely form ovule primordia (Figure 3A). Phenotypic analysis showed that in three independent lines, *pMP:MP11ir* complemented several developmental defects of the *mpS319* mutant. These included a general recovery of plant architecture, lateral branching and inflorescence, and flower morphology (Figure S2). In *mpS319 pMP:MP11ir* plants, the percentage of pistils that contained ovules increased to 67% of the total pistils analyzed (Figure S3), and the mean of number of ovules formed per pistil increased significantly (36 ovules ± SE) (Figure 3A).

(D) Polysome profiling from wild-type inflorescences. In (D), blue curves represent the distribution of *MP*, *MP11ir* and *ACT* mRNAs along the sucrose gradient determined by real-time PCR. The amount of mRNA in each of the three fractions (monosomes, light polysomes and heavy polysomes) is expressed as the percentage of the total amount of the mRNA in the microsomes. Red curves refer to EDTA-treated samples, which disrupts polysomes and shifts target profiles toward lighter fractions.

(E) VISTA plots of the evolutionary conservation of the genomic sequence of *MP* in six species: three from the *Arabidopsis* genus (*Arabidopsis thaliana*, *A. lyrata*, *A. halleri*) and three other Brassicaceae species (*Boechera stricta*, *Capsella grandiflora* and *C. rubella*). The plot represents fragments with more than 70% nucleotide sequence conservation. Colors under the lines highlight the function of the depicted region; conserved non-coding sequences (CNS) representing introns 1, 2 and 11 are depicted in pink. See also Figure S1 and Table S1.

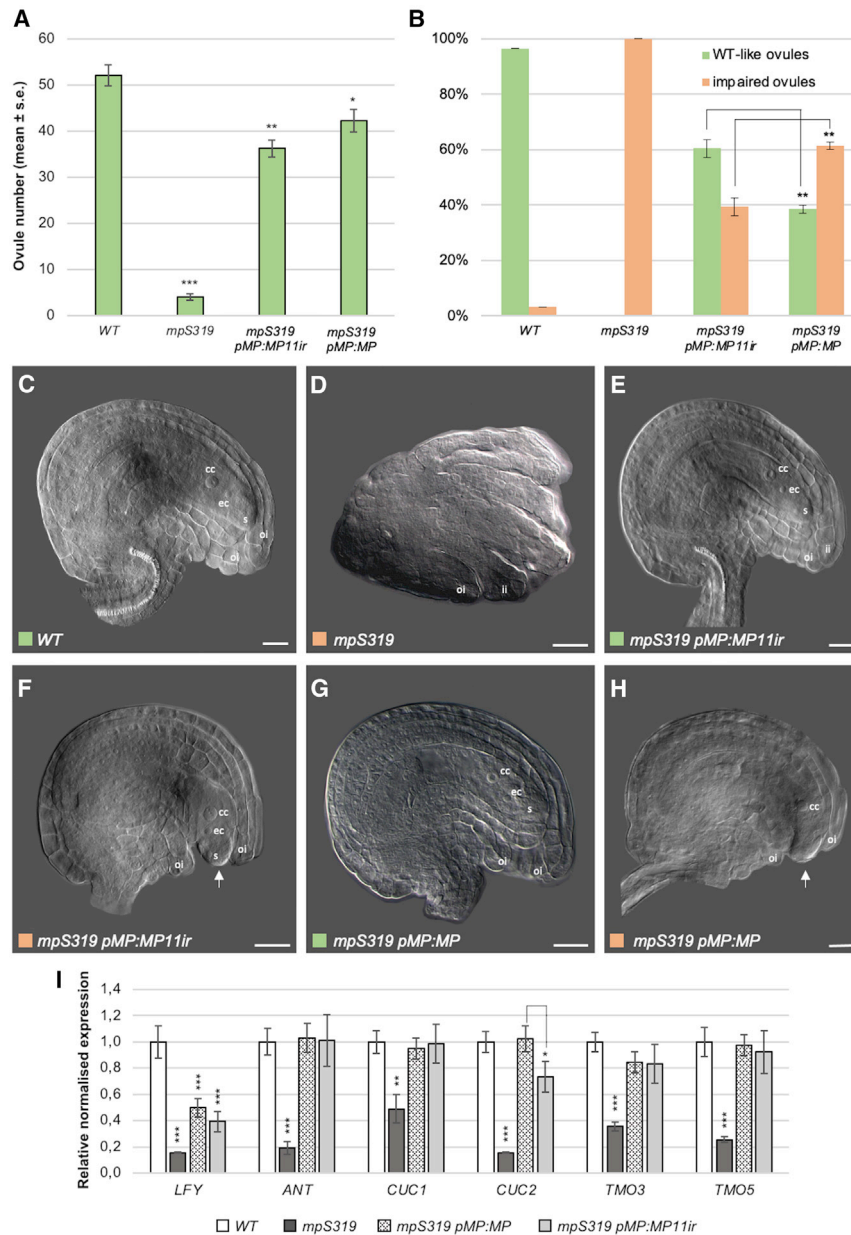


Figure 3. Complementation of Ovule Development in *mpS319 pMP:MP11ir* and *mpS319 pMP:MP*

(A) Ovule number per pistil in wild type, *mpS319*, *mpS319 pMP:MP11ir* and *mpS319 pMP:MP* lines. $p^* < 0.05$; $p^{**} < 0.01$ and $p^{***} < 0.001$ (one-way ANOVA and Tukey's HSD test; $n = 3$ pistils from five plants of three independent lines).

(B) Percentage of phenotypically wild-type and defective ovules out of the total number of ovules analyzed in wild type, *mpS319 pMP:MP11ir* and *mpS319 pMP:MP* compared to *mpS319* $p^{**} < 0.01$ (one-way ANOVA and Tukey's HSD test; $n = 200$ ovules from plants of three independent lines).

(C, E, and G) Wild type, *mpS319 pMP:MP11ir* and *mpS319 pMP:MP* ovules with mature gametophytes.

(D) An aberrant *mpS319* ovule, (F–H) exemplary *mpS319 pMP:MP11ir* and *mpS319 pMP:MP* ovules with unsealed integuments at the micropylar region. White arrows indicate the embryo sac protruding from open integuments. Scale bar, 20 μm . (I) Expression analysis of MP direct targets. *LFY* is a floral meristem identity gene, whereas *ANT*, *CUC1*, *CUC2*, *TMO3* and *TMO5* are involved in ovule development. cc, central cell, ec, egg cell; ii, inner integument; oi, outer integument; s, synergid. Error bars indicate the SE based on three biological replicates. $p^* < 0.05$; $p^{**} < 0.01$ and $p^{***} < 0.001$ (one-way ANOVA and Tukey's HSD test) and data were normalized with respect to *ACT8-2* and *UBI10* mRNA levels. See also Figures S2 and S3.

Collectively, the results show that despite being uncoupled from classical auxin regulation due to the absence of the CTD, MP11ir can still perform several native MP functions during ovule development.

A Lack of MP11ir Impacts Correct Ovule Integument Elongation

To test whether the function of the alternative MP11ir isoform was required during the plant reproductive phase, we expressed the canonical intron-less *MP*

transcript that cannot be differentially spliced, from the *MP* promoter in the *mpS319* mutant background (hereafter *mpS319 pMP:MP*). Before proceeding with this analysis, we showed by qRT-PCR that the expression level of *MP* in three independent transgenic lines was comparable to that of *MP11ir* (Figure S3C). Phenotypic analysis of *mpS319 pMP:MP* plants showed that defects in lateral branching and inflorescence morphogenesis were complemented by the canonical *MP*, similar to the degree of complementation observed by *MP11ir* (Figure S3). Moreover, in the strong *arf5.1* background, *MP* and *MP11ir* complemented defects in plant architecture and inflorescence morphology to similar extents (Figure S2). The complementation of pistil defects by *MP* was more pronounced than that by *MP11ir*; indeed, in *mpS319 pMP:MP* plants, the percentage of pistils that developed ovules (the total of phenotypically wild-type and partially

formed in *mpS319* had an aberrant morphology, impaired integuments, and aborted embryo sacs (Figures 3B and 3D). In *mpS319 pMP:MP11ir*, 60% of the ovules analyzed displayed a normal development of the integuments that correctly covered the mature gametophyte (Figures 3B and 3E). In the remaining 40% of *mpS319 pMP:MP11ir* ovules, the gametophyte was correctly formed, but the integuments did not properly elongate, causing the embryo to protrude from the micropylar side that remained open (Figures 3B and 3F).

Additionally, we tested the ability of *MP11ir* to complement the strong *arf5.1* mutant allele, which carries a T-DNA insertion in the exon that encodes the DBD. Similar to in the *mpS319* background, *pMP:MP11ir* restored fertility, plant and inflorescence morphology in the *arf5.1* background (Figure S2).

At later stages of ovule development, the ovules that rarely formed in *mpS319* had an aberrant morphology, impaired integuments, and aborted embryo sacs (Figures 3B and 3D). In *mpS319 pMP:MP11ir*, 60% of the ovules analyzed displayed a normal development of the integuments that correctly covered the mature gametophyte (Figures 3B and 3E). In the remaining 40% of *mpS319 pMP:MP11ir* ovules, the gametophyte was correctly formed, but the integuments did not properly elongate, causing the embryo to protrude from the micropylar side that remained open (Figures 3B and 3F).

radialised pistils) reached 91% of the total analyzed pistils, whereas for *mpS319 pMP:MP11ir* plants, this percentage was 68% (Figure S3). This suggests that correct apical–basal and abaxial–adaxial patterning of pistils was more efficiently regulated by full-length MP.

The ability to form ovule primordia in *mpS319 pMP:MP* and *mpS319 pMP:MP11ir* plants did not differ significantly, and the number of ovules was approximately 20% less than that observed in wild-type (Figure 3A). At later stages, we detected phenotypically wild-type ovules, and ovules in which the integuments did not correctly surround and seal the mature gametophyte, in *mpS319 pMP:MP* and *mpS319 pMP:MP11ir* plants (Figures 3G and 3H). However, the percentage of impaired ovules was significantly higher in *mpS319 pMP:MP* plants (61%) than in *mpS319 pMP:MP11ir* plants (39%) and accordingly, the percentage of phenotypically wild-type ovules was higher in *mpS319 pMP:MP11ir* plants (Figure 3B), suggesting that *MP11ir* was more efficient than canonical *MP* in complementing the defects in ovule integument morphology in *mpS319*. These results demonstrate that both *MP* and *MP11ir* complemented the *mpS319* and *arf5.1* phenotype, implying that in the majority of developmental contexts that we analyzed, the CTD domain of *MP* is not strictly required. A similar conclusion was proposed, based on the observation that an artificially truncated *MP* protein (*MP Δ*) lacking the CTD, partially restored flower formation and fertility in the severe *mp-G12* mutant.²⁶

The comparison between *mpS319 pMP:MP11ir* and *mpS319 pMP:MP* indicated that the *MP11ir* isoform was not essential for the complementation of lateral branching, flower and pistil morphogenesis, and ovule primordium formation defects, but was also functional in these contexts. On the contrary, the absence of *MP11ir* in *mpS319 pMP:MP* plants resulted in a stronger reduction in integument growth than in *mpS319 pMP:MP11ir* plants, suggesting that *MP11ir* function is tissue- and developmental-specific in ovules.

The inability of either isoforms to fully complement the *mp* mutants suggests that both are required for wild-type development, probably in a spatially and temporally balanced stoichiometry. However, alternatively the constructs we used might miss regulatory elements located in the 5' or 3' regions of the *MP* locus or in the introns, that were not included in the constructs.

Lastly, we quantified the expression of direct *MP* targets involved in ovule development. Consistent with the rescue of pistil and ovule formation in *mpS319 pMP:MP11ir* and *mpS319 pMP:MP* plants, the expression levels of *ANT*, *CUC1*, *TMO3* and *TMO5* were comparable to those in wild-type (Figure 3I). However, the reduction in the expression of *LFY*, which performs a more general function in floral meristem identity, was not fully recovered in *mpS319 pMP:MP11ir* or *mpS319 pMP:MP* plants (Figure 3I). The expression of *CUC2* was slightly lower in *mpS319 pMP:MP11ir* than in wild type and *mpS319 pMP:MP*, but statistically higher than those in *mpS319* (Figure 3I).

These observations again suggest that the activity of *MP* is not strictly regulated via its CTD. The importance of truncated ARFs in several plant species has been highlighted previously. For example, the proportion of truncated ARFs is extremely high in *Medicago truncatula* and *Zea mays*.^{1,2,27,28} The absence of the CTD does not interfere with the DNA binding-domain (DBD) activity of *MP*, because the DBD is sufficient to target

MP to an auxin-responsive reporter gene in protoplast transfection assays.⁴ Furthermore, the absence of the CTD does not impair *MP* homo-dimerization, since protein structure resolution has shown that *MP*–*MP* binding can occur through the DBD.²⁵ An *MP* protein that lacks the CTD should still interact with *BRAHMA* (*BRM*) to activate key regulators of flower primordium initiation.⁶ Moreover, it has been shown that expression of the *MP* DBD domain alone fused to *BUSHY*, which acts as a bridge with *BRM*, could partially complement the *mp* mutant phenotype,⁶ again emphasizing that the transcriptional activation role of *MP* can be uncoupled from auxin regulation. This characteristic of *MP* is clearly fundamental, since several studies^{29,30} have shown that *MP* is responsible for the correct expression and polar localization of the *PIN1* auxin efflux carrier that generates auxin maxima. This means that initially, *PIN1* regulation by *MP* is intrinsically required to anticipate auxin concentration maxima, which provides a logical explanation why *MP* is a functional activator in cells with sub-threshold auxin concentrations. In conclusion, our observations combined with previous studies, suggest that the current model according to which auxin needs to degrade *Aux/IAA* to allow *MP* to activate its target genes during plant development will need revision. Consequently, further efforts will be needed to deeply understand the regulation and activity of *ARF* transcription factors during reproductive development.

STAR★METHODS

Detailed methods are provided in the online version of this paper and include the following:

- KEY RESOURCES TABLE
- RESOURCE AVAILABILITY
 - Lead Contact
 - Materials Availability
 - Data and Code Availability
- EXPERIMENTAL MODEL AND SUBJECT DETAILS
 - Plant material and growth conditions
- METHOD DETAILS
 - Optical and confocal microscopy
 - *In situ* hybridization
 - AS PCR analysis
 - Droplet digital PCR assay
 - Polysome isolation and fractionation
 - RNA-seq analysis
 - Sequence conservation analysis
- QUANTIFICATION AND STATISTICAL ANALYSIS

SUPPLEMENTAL INFORMATION

Supplemental Information can be found online at <https://doi.org/10.1016/j.cub.2020.11.026>.

ACKNOWLEDGMENTS

We would like to thank Dr. John Chandler for editing and discussing the manuscript. The authors thank Dr. Francesca Galbiati and Dr. Luca Tadini for technical support. A.C., A.G., and S.M. were supported by the Ministero dell'Istruzione, dell'Università e della Ricerca (MIUR). M.C. was funded by MIUR-PRIN 2012. A.B. was supported by SEXSEED Project H2020-MSCA-RISE-2015.

AUTHOR CONTRIBUTIONS

M.C. and A.C. contributed equally to this work. Conceived and designed the experiments: M.C., A.C., S.B., M.K., and L.C. Performed the experiments: M.C., A.C., A.G., C.A., and S.O. Analyzed the data: M.C., A.C., M.K., and L.C. Performed bioinformatic analysis: S.M. and A.B. Contributed reagents/materials/analysis tools: S.B., D.W., and L.C. Wrote the paper: M.C., A.C., M.K., and L.C.

DECLARATION OF INTERESTS

The authors declare no competing interests.

Received: June 18, 2019

Revised: November 6, 2020

Accepted: November 11, 2020

Published: December 3, 2020

REFERENCES

- Chandler, J.W. (2016). Auxin response factors. *Plant Cell Environ.* 39, 1014–1028.
- Li, S.B., Xie, Z.Z., Hu, C.G., and Zhang, J.Z. (2016). A Review of Auxin Response Factors (ARFs) in Plants. *Front. Plant Sci.* 7, 47.
- Ulmasov, T., Murfett, J., Hagen, G., and Guilfoyle, T.J. (1997). Aux/IAA proteins repress expression of reporter genes containing natural and highly active synthetic auxin response elements. *Plant Cell* 9, 1963–1971.
- Tiwari, S.B., Hagen, G., and Guilfoyle, T. (2003). The roles of auxin response factor domains in auxin-responsive transcription. *Plant Cell* 15, 533–543.
- Hamann, T., Benkova, E., Bäurle, I., Kientz, M., and Jürgens, G. (2002). The Arabidopsis BODENLOS gene encodes an auxin response protein inhibiting MONOPTEROS-mediated embryo patterning. *Genes Dev.* 16, 1610–1615.
- Wu, M.F., Yamaguchi, N., Xiao, J., Bargmann, B., Estelle, M., Sang, Y., and Wagner, D. (2015). Auxin-regulated chromatin switch directs acquisition of flower primordium founder fate. *eLife* 4, e09269.
- Berleth, T., and Jürgens, G. (1993). The role of the monopteros gene in organising the basal body region of the Arabidopsis embryos. *Trends Genet.* 9, 299.
- De Smet, I., Lau, S., Voss, U., Vanneste, S., Benjamins, R., Rademacher, E.H., Schlereth, A., De Rybel, B., Vassileva, V., Grunewald, W., et al. (2010). Bimodular auxin response controls organogenesis in Arabidopsis. *Proc. Natl. Acad. Sci. USA* 107, 2705–2710.
- Donner, T.J., Sherr, I., and Scarpella, E. (2009). Regulation of preprocambial cell state acquisition by auxin signaling in Arabidopsis leaves. *Development* 136, 3235–3246.
- Galbiati, F., Sinha Roy, D., Simonini, S., Cucinotta, M., Ceccato, L., Cuesta, C., Simaskova, M., Benková, E., Kamiuchi, Y., Aida, M., et al. (2013). An integrative model of the control of ovule primordia formation. *Plant J.* 76, 446–455.
- Hardtke, C.S., and Berleth, T. (1998). The Arabidopsis gene MONOPTEROS encodes a transcription factor mediating embryo axis formation and vascular development. *EMBO J.* 17, 1405–1411.
- Przemeczek, G.K., Mattsson, J., Hardtke, C.S., Sung, Z.R., and Berleth, T. (1996). Studies on the role of the Arabidopsis gene MONOPTEROS in vascular development and plant cell axialization. *Planta* 200, 229–237.
- Weijers, D., Schlereth, A., Ehrismann, J.S., Schwank, G., Kientz, M., and Jürgens, G. (2006). Auxin triggers transient local signaling for cell specification in Arabidopsis embryogenesis. *Dev. Cell* 10, 265–270.
- Yamaguchi, N., Wu, M.-F., Winter, C.M., Berns, M.C., Nole-Wilson, S., Yamaguchi, A., Coupland, G., Krizek, B.A., and Wagner, D. (2013). A molecular framework for auxin-mediated initiation of flower primordia. *Dev. Cell* 24, 271–282.
- Schlereth, A., Möller, B., Liu, W., Kientz, M., Flipse, J., Rademacher, E.H., Schmid, M., Jürgens, G., and Weijers, D. (2010). MONOPTEROS controls embryonic root initiation by regulating a mobile transcription factor. *Nature* 464, 913–916.
- Brunoud, G., Wells, D.M., Oliva, M., Larrieu, A., Mirabet, V., Burrow, A.H., Beeckman, T., Kepinski, S., Traas, J., Bennett, M.J., and Vernoux, T. (2012). A novel sensor to map auxin response and distribution at high spatio-temporal resolution. *Nature* 482, 103–106.
- Liao, C.-Y., Smet, W., Brunoud, G., Yoshida, S., Vernoux, T., and Weijers, D. (2015). Reporters for sensitive and quantitative measurement of auxin response. *Nat. Methods* 12, 207–210, 2, 210.
- Vernoux, T., Brunoud, G., Farcot, E., Morin, V., Van den Daele, H., Legrand, J., Oliva, M., Das, P., Larrieu, A., Wells, D., et al. (2011). The auxin signalling network translates dynamic input into robust patterning at the shoot apex. *Mol. Syst. Biol.* 7, 508.
- Jia, J., Long, Y., Zhang, H., Li, Z., Liu, Z., Zhao, Y., Lu, D., Jin, X., Deng, X., Xia, R., et al. (2020). Post-transcriptional splicing of nascent RNA contributes to widespread intron retention in plants. *Nat. Plants* 6, 780–788.
- Ner-Gaon, H., Halachmi, R., Savaldi-Goldstein, S., Rubin, E., Ophir, R., and Fluhr, R. (2004). Intron retention is a major phenomenon in alternative splicing in Arabidopsis. *Plant J.* 39, 877–885.
- Oliveto, S., Alfieri, R., Miluzio, A., Scagliola, A., Secli, R.S., Gasparini, P., Grosso, S., Cascione, L., Mutti, L., and Biffo, S. (2018). A polysome-based microRNA screen identifies miR-24-3p as a novel promigratory miRNA in mesothelioma. *Cancer Res.* 78, 5741–5753.
- Chaudhary, S., Jabre, I., Reddy, A.S.N., Staiger, D., and Syed, N.H. (2019). Perspective on alternative splicing and proteome complexity in plants. *Trends Plant Sci.* 24, 496–506.
- Kalyna, M., Simpson, C.G., Syed, N.H., Lewandowska, D., Marquez, Y., Kusenda, B., Marshall, J., Fuller, J., Cardle, L., McNicol, J., et al. (2012). Alternative splicing and nonsense-mediated decay modulate expression of important regulatory genes in Arabidopsis. *Nucleic Acids Res.* 40, 2454–2469.
- Krogan, N.T., and Berleth, T. (2012). A dominant mutation reveals asymmetry in MP/ARF5 function along the adaxial-abaxial axis of shoot lateral organs. *Plant Signal. Behav.* 7, 940–943.
- Boer, D.R., Freire-Rios, A., van den Berg, W.A., Saaki, T., Manfield, I.W., Kepinski, S., López-Vidriero, I., Franco-Zorrilla, J.M., de Vries, S.C., Solano, R., et al. (2014). Structural basis for DNA binding specificity by the auxin-dependent ARF transcription factors. *Cell* 156, 577–589.
- Krogan, N.T., Kukurshumova, W., Marcos, D., Caragea, A.E., and Berleth, T. (2012). Deletion of MP/ARF5 domains III and IV reveals a requirement for Aux/IAA regulation in Arabidopsis leaf vascular patterning. *New Phytol.* 194, 391–401.
- Shen, C., Yue, R., Sun, T., Zhang, L., Xu, L., Tie, S., Wang, H., and Yang, Y. (2015). Genome-wide identification and expression analysis of auxin response factor gene family in *Medicago truncatula*. *Front. Plant Sci.* 6, 73.
- Finet, C., Berne-Dedieu, A., Scutt, C.P., and Marlétaz, F. (2013). Evolution of the ARF gene family in land plants: old domains, new tricks. *Mol. Biol. Evol.* 30, 45–56.
- Wenzel, C.L., Schuetz, M., Yu, Q., and Mattsson, J. (2007). Dynamics of MONOPTEROS and PIN-FORMED1 expression during leaf vein pattern formation in Arabidopsis thaliana. *Plant J.* 49, 387–398.
- Bhatia, N., Bozorg, B., Larsson, A., Ohno, C., Jönsson, H., and Heisler, M.G. (2016). Auxin acts through MONOPTEROS to regulate plant cell polarity and pattern phyllotaxis. *Curr. Biol.* 26, 3202–3208.
- Cole, M., Chandler, J., Weijers, D., Jacobs, B., Comelli, P., and Werr, W. (2009). DORNROSCHEN is a direct target of the auxin response factor MONOPTEROS in the Arabidopsis embryo. *Development* 136, 1643–1651.
- Okushima, Y., Overvoorde, P.J., Arima, K., Alonso, J.M., Chan, A., Chang, C., Ecker, J.R., Hughes, B., Lui, A., Nguyen, D., et al. (2005). Functional genomic analysis of the AUXIN RESPONSE FACTOR gene family

- members in *Arabidopsis thaliana*: unique and overlapping functions of ARF7 and ARF19. *Plant Cell* 17, 444–463.
33. Aronesty, E. (2013). Comparison of sequencing utility programs. *Open Bioinforma. J.* 7, 1–8.
 34. Dobin, A., Davis, C.A., Schlesinger, F., Drenkow, J., Zaleski, C., Jha, S., Batut, P., Chaisson, M., and Gingeras, T.R. (2013). STAR: ultrafast universal RNA-seq aligner. *Bioinformatics* 29, 15–21.
 35. Robinson, J.T., Thorvaldsdóttir, H., Winckler, W., Guttman, M., Lander, E.S., Getz, G., and Mesirov, J.P. (2011). Integrative genomics viewer. *Nat. Biotechnol.* 29, 24–26.
 36. Buels, R., Yao, E., Diesh, C.M., Hayes, R.D., Munoz-Torres, M., Helt, G., Goodstein, D.M., Elsik, C.G., Lewis, S.E., Stein, L., and Holmes, I.H. (2016). JBrowse: a dynamic web platform for genome visualization and analysis. *Genome Biol.* 17, 66.
 37. Dibitetto, D., La Monica, M., Ferrari, M., Marini, F., and Pellicoli, A. (2018). Formation and nucleolytic processing of Cas9-induced DNA breaks in human cells quantified by droplet digital PCR. *DNA Repair (Amst.)* 68, 68–74.
 38. Mustroph, A., Juntawong, P., and Bailey-Serres, J. (2009). Isolation of plant polysomal mRNA by differential centrifugation and ribosome immunopurification methods. *Methods Mol. Biol.* 553, 109–126.

STAR★METHODS

KEY RESOURCES TABLE

REAGENT or RESOURCE	SOURCE	IDENTIFIER
Bacterial and Virus Strains		
<i>Escherichia coli</i> DH5 α	N/A	N/A
<i>Agrobacterium tumefaciens</i> GV3101	N/A	N/A
Chemicals, Peptides, and Recombinant Proteins		
Q5 High-Fidelity DNA Polymerase	NEB	Cat#M0491S
Basta Herbicide	BASF	N/A
GoTaq DNA Polymerase	Promega	Cat#M3001
Critical Commercial Assays		
NucleoSpin RNA Plant kit	Macherey-Nagel	Cat#740949.50
TURBO™ DNase	ThermoFisher Scientific	Cat#AM2238
ddPCR™ Supermix for Probes	Bio-Rad	Cat#186-3023
ImProm-II™ Reverse Transcription System	Promega	Cat#A3800
SuperScript™ IV VILO™ Master Mix with ezDNase™	ThermoFisher Scientific	Cat#11766050
iTaq SYBR green master mix	Bio-Rad	Cat#1725121
Cstm ddPCR FAM Assay 200R	Bio-Rad	Cat#10031276
Cstm ddPCR HEX Assay 200R	Bio-Rad	Cat#10031279
DIG RNA Labeling Kit (SP6/T7)	Roche	Cat#11175025910
Deposited Data		
RNA-seq <i>Arabidopsis thaliana</i> Col-0 inflorescences	this study	NCBI Database: SRR12990564, https://www.ncbi.nlm.nih.gov/sra/SRR12990564N
Experimental Models: Organisms/Strains		
<i>Arabidopsis thaliana</i> pTMO3::3xGFP	15	N/A
<i>Arabidopsis thaliana</i> DRv2::ntdTomato	17	N/A
<i>Arabidopsis thaliana</i> mpS319	31	N/A
<i>Arabidopsis thaliana</i> arf5-1	32	N/A
<i>Arabidopsis thaliana</i> DII-VENUS	16	N/A
<i>Arabidopsis thaliana</i> pMP:MP11ir-GFP	this study	N/A
<i>Arabidopsis thaliana</i> pMP:MP	this study	N/A
<i>Arabidopsis thaliana</i> Col-0	The Nottingham <i>Arabidopsis</i> Stock Centre (NASC)	N/A
<i>Arabidopsis thaliana</i> pMP:MP-GFP	15	N/A
<i>Arabidopsis thaliana</i> pTMO5::3xGFP	15	N/A
Oligonucleotides		
Oligonucleotides for cloning and for expression analysis	see Table S1	N/A
Oligonucleotides for detection of alternative splicing	see Table S1	N/A
Recombinant DNA		
Plasmid: pMP:MP11ir-GFP	this study	N/A
Software and Algorithms		
LAS AF 2.2.0	Leica Microsystems Srl	https://www.leica-microsystems.com/
QuantaSoft™	Bio-Rad	https://www.bio-rad.com/en-it/SearchResults?Text=quantasoft

(Continued on next page)

Continued

REAGENT or RESOURCE	SOURCE	IDENTIFIER
BioLogic LP software	Bio-Rad	https://www.bio-rad.com/en-it/product/lp-data-view-software-for-biologic-lp-system
Fastq-mcf (Ea-utils package)	³³	N/A
STAR software	³⁴	https://github.com/alexdobin/STAR
IGV software	³⁵	https://software.broadinstitute.org/software/igv/download
JBrowse	³⁶	https://jbrowse.org/jb2/
Axiovision 4.1	Carl Zeiss AG	https://www.micro-shop.zeiss.com/it/ch/

RESOURCE AVAILABILITY

Lead Contact

Further information and requests for resources should be directed to and will be fulfilled by the Lead Contact, Lucia Colombo (lucia.colombo@unimi.it).

Materials Availability

This study did not generate new unique reagents.

Data and Code Availability

The accession number for the Arabidopsis Col-0 inflorescences RNA-sequencing data AT_COLO_INF1_UNIMI reported in this paper is NCBI Database: SRR12990564, <https://www.ncbi.nlm.nih.gov/sra/SRR12990564>.)

EXPERIMENTAL MODEL AND SUBJECT DETAILS

Plant material and growth conditions

Plants were grown in the greenhouse at 22°C under long-day (16 h light/8 h dark) conditions. *pMP:MP-GFP*, *pTMO5::3 × GFP*, *pTMO3::3 × GFP*¹⁵ and *DR5v2::ntdTomato*¹⁷ were provided by Prof. Dolf Weijers. The mutants *mpS319*,³¹ *arf5.1* (SALK_023812)³² and the *DII-VENUS* reporter¹⁶ have been described previously. To construct *pMP:MP11ir-GFP*, the *MP* genomic locus was amplified from −5,033 to +3,379 with respect to the start codon and cloned into pGreenII to obtain *MP11ir* fused to *GFP*. To construct *pMP:MP(cDNA):tMP*, −4,107 bp of *MP* promoter sequence were ligated with 902 bp of *MPcDs* and 178 bp of *MP* 3′UTR in pPLV cloning vector. The obtained plasmids were then introgressed into *mpS319* and *arf5.1* background.

METHOD DETAILS

Optical and confocal microscopy

Images of inflorescences and pistils were taken with a Zeiss® Axiocam MRC5 camera and a Leica® MZ6 stereomicroscope and were processed using Axiovision (version 4.1) software. For confocal laser scanning microscopy, dissected pistils were mounted in water and observed with an SP2 Leica confocal microscope. eGFP was excited at 488 nm and detected at 498–530 nm, tdTomato was excited at 561 nm and detected at 571–630 nm. We used a 40 × water-immersion objective (numerical aperture = 1.25, pinhole), confocal scans were performed with the pinhole at 1 airy unit. Images were collected in multi-channel mode, and overlay images were generated using Leica analysis software LAS AF 2.2.0.

In situ hybridization

In situ hybridizations were performed as previously described.¹⁰ Digoxigenin-labeled antisense RNA probes were generated by *in vitro* transcription with the DIG RNA Labeling Kit (SP6/T7) by Roche. Developing inflorescences of wild-type *Arabidopsis* plants were fixed and embedded in Paraplast Plus embedding medium; sections were hybridized and then mounted with a coverslip and subsequently observed using a Zeiss Axiophot D1 microscope equipped with differential interface contrast (DIC) optics.

AS PCR analysis

RNA was extracted using the NucleoSpin RNA Plant kit (Macherey-Nagel®), treated with Thermo Fisher Scientific® TURBO DNase and subsequently reverse-transcribed using the Promega® ImProm-II Reverse Transcription System. The synthesized cDNA was used for PCR with *ACTIN* as a control to exclude DNA contamination. PCR for AS detection was performed using primer pairs specific to intron 11 and the exon 11–exon 12 junction. Primers are listed in Table S1.

Droplet digital PCR assay

ddPCR was performed as in³⁷ using a Bio-rad QX200 Droplet Digital PCR System according to the suppliers instructions and with all required reagents and disposables from Bio-rad. The ddPCR reaction mix contained 2 μ L cDNA (150 ng), 10 μ L 2 \times ddPCR Supermix for Probes (no dUTP), 1 μ L 20 \times HEX/FAM assay and dH₂O to a volume of 20 μ L per sample. Universal DG8 cartridge, Droplet generation oil for probes and DG8 gaskets were required for droplet formation into the droplet generator (QX200). Then, 40 μ L droplet emulsion was transferred to a 96-well ddPCR plate (BioRad) and sealed with a PX1 machine. PCR was performed using the following program: 95°C for 5 min; 39 cycles of 95°C for 30 s and 60°C for 1 min; 98°C for 10 min then the temperature was held at 12°C. Finally, FAM and HEX fluorescence was read in the droplet reader QX200 using QuantaSoft software. The number of copies/ μ L of each target locus was determined by setting an identical empirical baseline threshold for all samples. Primers and probes are listed in [Table S1](#).

Polysome isolation and fractionation

The total polysome fraction was prepared as previously described³⁸ with minor modification. Fractionation and RNA extraction were performed as in.²¹ To distinguish miRNAs that sedimented with heavy polysomes but were not physically bound to them, we disrupted polysomes by adding 30 mmol L⁻¹ EDTA after lysate preparation. Equal amounts of RNA were loaded onto a 15%–50% sucrose gradient with or without 10 mmol L⁻¹ EDTA, and centrifuged at 39,000 rpm for 3 h in a SW41Ti Beckman rotor at 4°C. The gradient was then analyzed by continuous flow absorbance at 254 nm, recorded by BioLogic LP software (Bio-Rad), and fractions were collected and kept on ice to avoid RNA degradation. The following fractions were collected: (i) monosome pool, from the top of the gradient to the 80S peak; (ii) light polysomes and (iii) heavy polysomes. Samples were incubated with proteinase K and 1% SDS for 1 h at 37°C. RNA was extracted with phenol/chloroform/isoamyl alcohol and quantified with Nanodrop and Qubit. The same amount of RNA from each fraction was DNase-treated and reverse-transcribed with SuperScript IV VILO Master Mix with ezDNase Enzyme (Invitrogen). The distribution of mRNAs among the three fractions was determined by real-time PCR using a CFX96 Detection System with Bio-Rad iTaq SYBR green master mix. RT-PCR primers are listed in [Table S1](#). The amount of a specific mRNA in each of the three fractions was expressed as a percentage of the total amount of mRNA in the translational machinery.

RNA-seq analysis

RNA was extracted from wild-type Col-0 pre-fertilization inflorescences using the NucleoSpin RNA Plant kit (Macherey-Nagel®). RNA-Seq libraries were prepared and sequenced at Novogene (<https://en.novogene.com/>) following the manufacturer's instructions. The library insert size was approximately 300 bp. The DNA was sequenced in an Illumina HiSeq4000 system as 2 \times 150-bp pair ends. The data reads (100 millions) were processed using Fastq-mcf from the Ea-utils³³ package. The reads were mapped to the *Arabidopsis* genome version TAIR10 with STAR³⁴ using the default parameters. The BAM files were uploaded in IGV³⁵ with the *Arabidopsis* genome annotation Araport11. A representation of the coverage was depicted with Keynote.

Sequence conservation analysis

The *MONOPTEROS* gene was retrieved from the Phytozome database (accessed on 2019-02-25) using the Locus ID (AT1G19850.1) and then visualized in JBrowse.³⁶ The VISTA tracks were enabled for all species and each track was manually sorted according to its phylogenetic distance from *Arabidopsis*. The conservation percentage for the colored regions were 70% (blue for exons and red for introns) with a box size of 50 bp.

QUANTIFICATION AND STATISTICAL ANALYSIS

Statistical analysis was implemented using EXCEL. One-way ANOVAs with post hoc Turkey test was carried out by online tool https://astatsa.com/OneWay_Anova_with_TukeyHSD/. Details of statistical tests are provided in figure legends.

Auxin regulated *MONOPTEROS* leader intron splicing modulates translation initiation in *Arabidopsis thaliana*

Alex Cavalleri, Andrea Guazzotti, Mara Cucinotta, Marco Francesco Bressana, Chiara Mizzotti, Francesca Caselli, Veronica Gregis and Lucia Colombo

Manuscript in preparation

In this work I have participated in experiments designs, realisation and results interpretation. I performed experiments for *MP* isoforms detection and for the evaluation of their translational efficiency. I have worked on the study of auxin function in the regulation of the leader intron splicing and I have worked in the identification of the CRISPR-generated *mp* alleles and in the evaluation of their functionality. I have also contributed in figures and text preparation.

1 ***Auxin regulated MONOPTEROS* leader intron splicing**
2 **modulates translation initiation in *Arabidopsis thaliana***

3

4

5 **RUNNING TITLE**

6 Alternative splicing of *MONOPTEROS* leader intron

7

8 **AUTHORS AND AFFILIATION**

9 *Alex Cavalleri, Andrea Guazzotti, Mara Cucinotta, Marco Francesco Bressana, Chiara Mizzotti, Francesca*
10 *Caselli, Veronica Gregis and Lucia Colombo**

11 *Università degli Studi di Milano, Dipartimento di Bioscienze, Via Celoria 26, Milano, 20133, Italy*

12 ** Corresponding author lucia.colombo@unimi.it*

13

14 **ABSTRACT**

15 *MONOPTEROS (MP)* encodes for an auxin response factor involved in the regulation of
16 several biological processes in *Arabidopsis thaliana*. We investigate a differential splicing
17 event of the leader intron in the 5'UTR of *MP*, which causes the use of an alternative
18 translational start codon resulting into alternative *MP* isoform. Alternative splicing of the
19 leader intron in inflorescences was shown to be controlled by auxin. To study the functional
20 importance of alternative *MP* leader intron splicing and the subsequent usage of
21 downstream translational start sites, we characterize two novel *mp* mutant alleles, generated
22 by CRISPR/Cas9 technology, carrying non-sense mutations downstream the canonical
23 annotated ATG. Unexpectedly, the two mutants show no phenotypic defects in respect to
24 the wild type, suggesting more flexible mechanism of ATG start codon usage for *MP*.

25

26 **KEYWORDS:** Auxin; *MONOPTEROS*; Auxin Response Factors; Alternative Splicing;
27 Leader Intron; Translation Initiation;

28

29

31 INTRODUCTION

32 Alternative splicing (AS) contributes to the formation of protein isoforms with different
33 functions and structures, thereby providing a source of protein diversity and versatility.
34 Precursors of mRNA, known as pre-mRNA, engage a maturation process through which
35 introns are spliced out and exons join together to form the final mature mRNA. Evolutionary
36 conserved mechanisms of differential splicing have been shown to occur in the majority of
37 higher eukaryotes (Pan *et al.*, 2008; Wang *et al.*, 2008; Marquez *et al.*, 2014). In plants, up
38 to 70% of intron-containing genes undergo alternative splicing events (Chamala *et al.*, 2015;
39 Zhang *et al.*, 2017), however, AS is still a largely unexplored field. It has already been shown
40 that AS plays a pivotal role in the regulation of developmental processes such as flowering
41 time and development (Macknight *et al.*, 2002; Nibau *et al.*, 2020) (Dreni *et al.*, 2020),
42 circadian clock (Dantas *et al.*, 2019) and stress responses (Capovilla *et al.*, 2015; Wang *et al.*,
43 2017). Recently, it has been shown that AS events increased upon cold stress in tea
44 plants (Y. Li *et al.*, 2020) and cassava (S. Li *et al.*, 2020). Alternative splicing events include,
45 mostly, exon skipping, alternative 5' and 3' splice sites and intron retention (IR). IR seems
46 to be the most occurring alternative splicing event (Zhang *et al.*, 2017).

47 Introns have been previously described to be potentially able to enhance gene expression
48 in several eukaryote organisms, such as mammals, fungi, insects and plants (Rose *et al.*,
49 2016; Shaul, 2017). Although the mechanisms underneath this process still remain unclear,
50 introns can modulate gene expression through specific DNA motifs by a process known as
51 Intron Mediated Enhancement (IME). It has been demonstrated that IME-related motifs can
52 considerably increase gene expression (Rose *et al.*, 2016; Laxa, 2017; Shaul, 2017;
53 Gallegos and Rose, 2019; Rose, 2019). Furthermore, introns located in the 5' UnTranslated
54 Region (5' UTR), also referred to as leader introns (LI), are known to impact gene expression
55 throughout IME, boost translational efficiency, drive tissue specificity and determine spatial
56 expression in *Arabidopsis* (Curi *et al.*, 2005; Akua *et al.*, 2010; Akua and Shaul, 2013; Liu
57 and Sun, 2013; Laxa *et al.*, 2016; Zhang *et al.*, 2016; Laxa, 2017). In soybean, the leader
58 intron of *Elongation Factor 1A* (*eEF1A*) increases the expression of the gene when present
59 in the 5' regulatory region and decrease gene expression when deleted (Zhang *et al.*, 2016).
60 Recently, the leader intron of a oleate desaturase enzyme encoding-gene (*FAD2-2*) has
61 been shown to have a strong natural variability which associates with oleic and linoleic acid
62 content in olive plant (Salimonti *et al.*, 2020).

63 Plant developmental processes require auxin, whose signalling pathway is primarily
64 mediated by AUXIN RESPONSE FACTORS (ARFs) and AUXIN/INDOLE-3-ACETIC ACID
65 (Aux/IAA) proteins (Chandler, 2016; Li *et al.*, 2016). Under sub-threshold auxin
66 concentrations, Aux/IAA proteins heterodimerize with ARF transcription factors, thereby
67 modulating the expression of ARF downstream targets (Ulmasov *et al.*, 1999a; Ulmasov *et al.*,
68 *et al.*, 1999b; Reed, 2001). ARF proteins are composed by three different domains: a B3 DNA
69 binding domain (DBD), a middle region (MR) and a carboxy-terminal dimerization domain
70 (CTD), required for dimerization with the Aux/IAA (Ulmasov *et al.*, 1997; Ulmasov *et al.*,
71 1999a; Ulmasov *et al.*, 1999b; Tiwari *et al.*, 2003; Guilfoyle and Hagen, 2007). Among the
72 ARF family, *ARF5/MONOPTEROS (MP)* has been extensively studied, unveiling its role in
73 several developmental processes (Berleth and Jürgens, 1993; Przemeck *et al.*, 1996;
74 Hardtke and Berleth, 1998; Weijers *et al.*, 2006; Donner *et al.*, 2009; De Smet *et al.*, 2010;
75 Yamaguchi *et al.*, 2013; Galbiati *et al.*, 2013).

76 We investigate differential splicing of in the intron within the 5' UTR region of the *MP* mRNA
77 and the transcriptional and translational efficiency of the two isoforms. Furthermore, we
78 show that alternative *MP* splicing of the leader intron was increased in inflorescences upon
79 exogenous auxin application. Finally, we demonstrate by introducing a nonsense point
80 mutation in the first exon that the *MP* mRNA is characterized by a flexible use of translational
81 initiation sites that did not impair MP function.

82

83 **RESULTS AND DISCUSSION**

84 **Alternative splicing of *MP* leader intron**

85 The Arabidopsis genome annotation Araport11 (Cheng *et al.*, 2017) predicts a *MP* transcript
86 isoform, due to the possible splicing of an intron located within the 5' UTR and the first exon
87 of the canonical *MP* transcript. In the canonical *MP* mRNA this intron is not spliced (Fig. 1A).

88 To confirm the existence of the predicted additional transcript isoform, we performed a PCR-
89 based assay using as template cDNA retrotranscribed from RNA that was extracted from
90 different tissues. Three pairs of primers were designed for this purpose (Figure S1 and Table
91 S1). As expected (Fig. S1), we were able to distinguish two fragments originating from the
92 two *MP* mRNA isoforms. The most abundant amplified fragment derives from the annotated
93 canonical version of *ARF5/MP* (Fig. 1D). Interestingly, the alternative *MP* transcript, which
94 splices the leader intron, is expressed in inflorescences, seedlings and in lower amounts in
95 young leaf tissue.

96 The leader intron sequence of *MP* is composed by 336 base pairs (bp) of which 84bp
97 encoding the first 28 amino acids of the canonical *MP* protein, including the annotated
98 translation start site and a second ATG within the coding sequence (Fig. 1A). Hence,
99 alternative ATG start codons located either 33bp or 108bp downstream the annotated *MP*
100 translational start site will probably be used for translation of the alternative spliced *MP*
101 isoform (Fig. 1A). Further, downstream ATGs inside the DNA Binding Domain (DBD), are
102 unlikely to be functional translation start sites. The leader intron includes a CGATT motif,
103 previously described as an IME motif (Rose, 2008; Parra *et al.*, 2011). To investigate the
104 putative expression enhancer capacity of this *MP* 5' leader intron we analysed the sequence
105 with the IMEter v2.0 bioinformatic software (Parra *et al.*, 2011). This showed that the IMEter
106 score of this intron is 12.63, a value above 85% of *Arabidopsis thaliana* annotated introns
107 and higher compared to the other internal *MP* introns (mean of 3.54). Thus, we may consider
108 that this intronic region functions as a putative enhancer of expression. Notably, the intron
109 sequence is characterized by a CT-rich region, which has been reported to be present in
110 enhancing introns in spinach and petunia (C. Bolle *et al.*, 1994; Mun *et al.*, 2002; Laxa *et al.*,
111 2016).

112 The sequence features of the *MP* leader intron and the difference in transcript level of the
113 two *MP* isoforms suggest the biological relevance of such regulatory region at the
114 transcriptional level. It still remains unclear whether the severe discrepancy of isoform
115 transcript levels is triggered by splicing efficiency, mRNA stability or post-transcriptional
116 regulation.

117

118 **Canonical and alternative *MP* isoforms show similar translational efficiency**

119 In order to test whether the two transcript isoforms were subjected to a different translation
120 rate, we extracted polysomes from Col-0 wild type inflorescences and collected them in four
121 distinct fractions: i) free (or not associated), ii) monosome, iii) light polysomes, and iv) heavy
122 polysomes. The distribution of mRNAs across the different fractions allowed to discriminate
123 between poorly translated and efficiently translated mRNAs (those with a higher percentage
124 in the heavy polysomes fraction). The cDNA obtained from each fraction was used as
125 template in Real Time qPCR using primer pairs designed to distinguish the canonical and
126 alternative isoforms of *MP*. The results revealed that both isoforms were efficiently translated
127 with most of the mRNA associated to the heavy polysomes (63.39% for the canonical *MP*
128 transcript and 64.58% for the alternative *MP* transcript isoform) (Fig. 1E). The distribution of

129 the two MP isoforms was comparable to well translated Actin control, whereas it had an
130 opposite trend when compared to poorly translated control *SQUAMOSA PROMOTER*
131 *BINDING PROTEIN-LIKE 3 (SPL3)* (Fig. S2).

132 Sequence analysis revealed that three of the four predicted upstream ORFs of *MP* are
133 entirely included in the 5' leader intron, whereas one, uORF4, is only partially included in it
134 (Fig. 1B). It has been previously demonstrated by in vitro assays that these uORFs primarily
135 modulate translation efficiency of *MP* in Arabidopsis seedlings (Nishimura *et al.*, 2005). In
136 the alternative *MP* transcript isoform regulation of translation by these uORFs will not
137 possible, since the region containing the uORFs is not present after splicing of the leader
138 intron. Surprisingly, our results suggest that uORFs present in the 5' UTR of *MP* do not have
139 an effect since the two natural *MP* isoforms did not show changes in translational efficiency
140 in inflorescences. Integrating data coming from TAIR annotation Araport11 and published
141 available datasets (Nishimura *et al.*, 2005; Hayashi *et al.*, 2017; Niu *et al.*, 2020), we found
142 that at least 23 of ARF family member present uORFs in the 5' region. Hence, it would be
143 interesting to verify whether other uORF-containing ARFs expressed are regulated by
144 uORFs..

145

146 **Auxin regulates *MP* leader intron splicing through a long non-coding RNA module**

147 It has been proposed that auxin mediates differential splicing in several genes through a
148 mechanism mediated by long-non-coding RNA Alternative Splicing COmpetitor (ASCO) and
149 Nuclear Speckle RNA-Binding proteins (NSRs) (Bardou *et al.*, 2014).

150 In order to study whether auxin is able to regulate differential splicing of the *MP* leader intron,
151 we have treated wild type Arabidopsis inflorescences with exogenous Indole-3 Acetic Acid
152 (IAA) and collected them after 3 hours. Subsequently, we synthesized cDNA using RNA
153 extracted from the treated and untreated (Mock) material and performed Real Time qPCR.
154 As positive control we have chosen a member of Gretchen Hagen 3 (GH3) gene family,
155 *GH3.4*, which has been demonstrated to be early-responsive to exogenous auxin treatment
156 in seedlings (Sugawara *et al.*, 2015). As expected, *GH3.4* increased its expression with
157 rising concentrations of 1 μ M and 10 μ M IAA (Fig. 2A). Canonical and alternative *MP* isoforms
158 do not change abundance upon treatment with 1 μ M IAA solution whereas a statistically
159 significant change of the alternative *MP* isoform can be identified upon treatment with 10 μ M
160 IAA (Fig. 2A). To further determine the mechanism by which auxin regulates the *MP* leader
161 intron splicing, we repeated the auxin treatment using an ASCO RNA interference (RNAi)

162 line and in *nsr a/b* mutant. We performed the experiment with 10 μ M IAA solution, the same
163 concentration for which we were able to detect a relative increase of the alternative splice
164 variant in wild-type inflorescences. Our analysis showed that no changes in abundance were
165 detected for the canonical *MP* isoform in all genotypes. Conversely, the alternative *MP*
166 isoform showed a statistically significant change in abundance only in the wild type
167 inflorescences but not in ASCO-RNAi and *nsr a/b* lines (Fig. 2B).

168 Our results suggest that auxin is involved in the regulation of the *MP* leader intron splicing,
169 by selectively inducing accumulation of the alternative transcript isoform. Moreover, the
170 induction of the differential splicing of the leader intron of *MP* is lost upon exogenous auxin
171 application in ASCO RNAi and *nsr a/b* lines. These results indicate that auxin is regulating
172 *MP* splicing through the ASCO-NSRs splicing pathway.

173

174 **Generation nonsense codons downstream the canonical translation start codon does** 175 **not compromise MP function**

176 The alternative *MP* mRNA isoform lacking the leader intron does not encode the first two
177 AUG codons to initiate translation. In order to speculate on a flexible usage of translational
178 start codons in the *MP* gene, we have analysed previously published Arabidopsis ribosome
179 profiling studies (Liu *et al.*, 2013; Hsu *et al.*, 2016; Lukoszek *et al.*, 2016). This analysis,
180 performed with the GWIPS-viz software, showed an enrichment of reads mapping *MP*
181 approximately at the 4th Methionine residue (Fig. S3). Based on this observation, we
182 speculated that the actual translational start site of *MP* might be the 4th ATG within the
183 coding sequence.

184 Therefore, we decided to investigate AUG site usage for *MP* translation initiation by
185 introducing non-sense point mutations downstream the canonical ATG start codon.

186 Several *mp* mutants have already been reported in literature (Fig. S4). Mutant alleles with a
187 disrupted DNA Binding Domain (DBD), such as *arf5-1*, *SALK_144183* or *mpB4149*, exhibit
188 high percentage of embryo defects, lacking the primary root or the formation of a single
189 cotyledon (Berleth and Jürgens, 1993; Hardtke and Berleth, 1998; Weijers and Jürgens,
190 2005; Odat *et al.*, 2014; Crawford *et al.*, 2015), and are all considered to be knock-out
191 alleles. Mutant alleles with intact DBD but impaired middle region and C-Terminal Domain
192 (CTD), such as *mpS319*, *mp-g92* or *mp-T730* (Fig. S4), show vascular system defects and
193 inflorescence development is compromised (Przemeck *et al.*, 1996; Cole *et al.*, 2009;
194 Galbiati *et al.*, 2013). Although many *mp* alleles have been described in the last decades,

195 none of them features a mutation close to the annotated translational start codon. In order
196 to obtain such a mutant, we introduced with CRISPR/Cas9 technology a premature stop
197 codon closely downstream the canonical ATG and upstream the 4th ATG. The guide RNA
198 was designed pairing at position +40bp to +60bp after the annotated ATG (Fig. 3B). We
199 generated mutant lines and obtained in the F3 plants without the CRISPR/Cas9 T-DNA.
200 Finally we selected two independent homozygous mutant lines of *mp*, hereafter named
201 *mpT56* and *mpA54*. The *mpT56* contains an insertion of 1 base pair in the first exon at +56
202 position of *MP*, while *mpA54* carries a deletion of 1 base pair at +54 position of *MP* (Fig.
203 3A). Both mutations lead to a frameshift with the subsequent formation of premature stop
204 codons at position +103bp and +71bp, respectively (Fig. 3C).

205 To determine whether *mpT56* and *mpA54* mutant plants may exhibit previously reported
206 defects for other *mp* mutant alleles, we performed a detailed phenotyping. Rosette leaves,
207 inflorescences of young adult plant and flowers of *mpA54* and *mpT56* lines did not show
208 phenotypic defect and the plants were fully fertile (Fig. 3D shows only data for *mpT56*).
209 Since *mpT56* and *mpA54* have identical phenotype, we selected the *mpT56* mutant for
210 further analysis. *MP* has putative multiple translation start codons in frame with the first ATG
211 that might be used without compromising the DBD integrity. Therefore, we crossed *mpT56*
212 with *mpS319* (Cole *et al.*, 2009) to verify whether *mpT56* was able to produce a functional
213 MP protein. The biallelic *mpS319/mpT56* showed a wild type phenotype, meaning that
214 *mpT56* allele could fully complement the *mpS319* phenotype (Fig. 3E).

215 The absence of *mp*-like phenotypes in the *mpT56* and *mpA54* mutant lines strongly
216 suggests that translation initiation of *MP* is characterized by flexible usage of start codons.
217 Eventually, the non-sense point mutations introduced in our mutant clearly demonstrate that
218 aminoacidic residues upstream of the 4th ATG are not essential for *MP* function. Besides,
219 our revision on the translational start site of *MP* is further corroborated by the existence of
220 an auxin-induced alternative *MP* isoform which does not include the annotated ATG in its
221 coding sequence. The alternative *MP* isoform, as demonstrated in this work, retains
222 functionality even though the translation from the annotated first translational start site is
223 prevented.

224

225

226

227

228 **METHODS**

229 **Plant material and growth conditions**

230 *Arabidopsis thaliana* Columbia-0 (Col-0) have been grown under controlled conditions with
231 long-day photoperiod (16 h light, 8 h dark) and 22°C temperature. The *mpS319* mutant allele
232 has been previously characterized (Cole *et al.*, 2009, Galbiati *et al.*, 2013). ASCO-RNAi and
233 *nsr a/b* mutant lines were kindly provided by Martin Crespi.

234

235 **PCR-based Assay**

236 RNA was extracted using Macherey-Nagel® Nucleozol, treated with Thermo Fisher
237 Scientific® TURBO™ DNase and subsequently retro-transcribed using Promega® ImProm-
238 II™ Reverse Transcription System. The synthesized cDNA was used for actin PCR to
239 exclude DNA contamination. Oligos designed and used in this study are shown in Table S6.

240

241 **Polysome fraction extraction and RNA extraction**

242 Polysome were isolated from wild type Col-0 inflorescences following the protocol reported
243 in Lecampion *et al.*, 2016 . Briefly, 600 mg of inflorescences were collected for each sample
244 and lysed in Polysome Buffer (160 mM Tris-HCl pH 8.4, 80 mM KCl and 40 mM MgCl₂, 5.26
245 mM EGTA, 0.5% (v/v) Octylphenoxy poly(ethyleneoxy)ethanol, branched, 50 µg/ml
246 cycloheximide, 50 µg/ml chloramphenicol). To pellet debris a centrifugation at 16,000 x g for
247 15 min at 4 °C was performed and the supernatant was transferred on top of a sucrose
248 gradient made of 4 layers of sucrose (50%, 35% and 2 layers of 20%). The gradients were
249 centrifuged at 175,000 x g for 2 hr 45 min at 4 °C, in a SW41Ti Beckman rotor. After the
250 centrifugation the gradients were analysed by continuous flow absorbance at 254 nm
251 recorded by BioLogic LP software (Bio-Rad), and fractions were collected as following: i) not
252 associated, ii) monosome, iii) light polysomes, and iv) heavy polysomes. Samples were
253 incubated with SDS 1% and proteinase K for 1 hour at 27°C and RNA extraction was
254 performed with the phenol/chloroform/isoamyllic alcohol method. The experiment was
255 performed in triplicate and a representative result from the three independent experiments
256 is shown.

257

258

259 **Auxin treatments**

260 Primary inflorescences from plants carrying the *DR5::GFP/DR5v2::Tomato* marker line (Liao
261 et al., 2015) were treated with 15 μ L of (1 μ M IAA,) 10 μ M IAA or water (mock), containing
262 0.01% Silwet L-77. 3h after treating, inflorescences were collected and immediately frozen
263 in liquid nitrogen. RNA extraction and RT-PCR were performed as described below. The
264 treatments were performed three times, for a total of six biological replicates. *GFP*
265 expression and *GH3.4* gene (*At1g59500*) were used as positive controls to ensure that auxin
266 treatment was successful.

267

268 **Real time and data analysis**

269 The RNA extracted from each polysome fraction and auxin treatments was reverse
270 transcribed using the iScript™ gDNA Clear cDNA Synthesis Kit (Biorad) and the obtained
271 cDNA was used as template in quantitative Real Time PCR (qRT-PCR) reactions. qRT-PCR
272 was carried out on a CFX96 Real-Time system (Bio-Rad) with Bio-Rad iTaq SYBR green
273 master mix using the primer pairs reported in Table S1. The data, from three biological and
274 three technical replicates, were analysed using a Bio-Rad CFX Maestro software (V1.1).

275

276 **Generation, genotyping and phenotyping of CRISPR mutant alleles**

277 The constructs used and the cloning procedure followed to obtain the CRISPR/Cas9
278 mutants are described in Fauser et al. 2014. The CRISPR-P web tool (Lei *et al.*, 2014) has
279 been used to select the protospacer on the *MP* genomic sequence, calculating a score that
280 allows to minimize the off-target effects. The guideRNA sequence used for genomic editing
281 of *MP* is CAAGTTGTTTGGTTAATGG, pairing at the beginning of the first exon, 40 base
282 pairs after the canonical ATG of *MP*. Oligonucleotides used for the amplification of genomic
283 region carrying mutations in *mpT56* and *mpA54*, flanking the gRNA complementary
284 sequence, are reported in Table S1. *mpT56* and *mpA54* are two independent mutant alleles
285 carrying heterozygous mutation in T₀ generation and the CRISPR cassette T-DNA. Both
286 mutant alleles followed Mendelian segregation of the mutation in *MP* gene and of the T-
287 DNA. Phenotyping has been performed in T₂ and T₃ generation of *mpT56* and *mpA54* which
288 segregated out the CRISPR cassette T-DNA. Observation of *mpT56* and *mpA54* phenotypic
289 traits has been performed with a Leica MZ6 stereomicroscope.

290

291 **REFERENCES**

- 292 **Akua, T., Berezin, I. and Shaul, O.** (2010) The leader intron of AtMHX can elicit, in the absence of splicing,
293 low-level intron-mediated enhancement that depends on the internal intron sequence. *BMC Plant Biol.*,
294 **10**.
- 295 **Akua, T. and Shaul, O.** (2013) The arabidopsis thaliana MHX gene includes an intronic element that boosts
296 translation when localized in a 5' UTR intron. *J. Exp. Bot.*, **64**, 4255–4270.
- 297 **Florian Bardou, Federico Ariel, Craig G. Simpson, Natali Romero-Barrios, Philippe Laporte, Sandrine**
298 **Balzerque, John W.S. Brown, Martin Crespi,** Long Noncoding RNA Modulates Alternative Splicing
299 Regulators in Arabidopsis, *Developmental Cell*, Volume 30, Issue 2, 2014, Pages 166-176, ISSN 1534-
300 5807, <https://doi.org/10.1016/j.devcel.2014.06.017>.
- 301 **Berleth, T. and Jürgens, G.** (1993) The role of the monopteros gene in organising the basal body region of
302 the Arabidopsis embryo. , **587**, 575–587.
- 303 **C. Bolle, S. Sopory, Th. Lubberstedt, R.G.H. and R.O.** (1994) bolle 1994.pdf. *Plant J.*, **6(4)**, 513–523.
- 304 **Capovilla, G., Pajoro, A., Immink, R.G. and Schmid, M.** (2015) Role of alternative pre-mRNA splicing in
305 temperature signaling. *Curr. Opin. Plant Biol.*, **27**, 97–103.
- 306 **Chamala, S., Feng, G., Chavarro, C. and Barbazuk, W.B.** (2015) Genome-wide identification of
307 evolutionarily conserved alternative splicing events in flowering plants. *Front. Bioeng. Biotechnol.*, **3**.
- 308 **Chandler, J.W.** (2016) Auxin response factors. *Plant. Cell Environ.*, **39**, 1014–1028.
- 309 **Cheng, C.Y., Krishnakumar, V., Chan, A.P., Thibaud-Nissen, F., Schobel, S. and Town, C.D.** (2017)
310 Araport11: a complete reannotation of the Arabidopsis thaliana reference genome. *Plant J.*, **89**, 789–
311 804.
- 312 **Cole, M., Chandler, J., Weijers, D., Jacobs, B., Comelli, P. and Werr, W.** (2009) DORNROSCHEN is a
313 direct target of the auxin response factor MONOPTEROS in the Arabidopsis embryo. *Development*,
314 **136**, 1643–1651. Available at: <http://dev.biologists.org/cgi/doi/10.1242/dev.032177>.
- 315 **Crawford, B.C.W., Sewell, J., Golembeski, G., Roshan, C., Long, J.A. and Yanofsky, M.F.** (2015)
316 Genetic control of distal stem cell fate within root and embryonic meristems. *Science (80-.)*, **347**, 655–
317 659.
- 318 **Curi, G.C., Chan, R.L. and Gonzalez, D.H.** (2005) The leader intron of Arabidopsis thaliana genes encoding
319 cytochrome c oxidase subunit 5c promotes high-level expression by increasing transcript abundance
320 and translation efficiency. *J. Exp. Bot.*, **56**, 2563–2571.
- 321 **Dantas, L.L.B., Calixto, C.P.G., Dourado, M.M., Carneiro, M.S., Brown, J.W.S. and Hotta, C.T.** (2019)
322 Alternative Splicing of Circadian Clock Genes Correlates With Temperature in Field-Grown Sugarcane.
323 *Front. Plant Sci.*, **10**, 1–15.
- 324 **Donner, T.J., Sherr, I. and Scarpella, E.** (2009) Regulation of preprocambial cell state acquisition by auxin
325 signaling in Arabidopsis leaves. *Development*, **136**, 3235–46.
- 326 **Fausser, F., Schiml, S. and Puchta, H.** (2014) Both CRISPR/Cas-based nucleases and nickases can be

327 used efficiently for genome engineering in *Arabidopsis thaliana*. *Plant J.*, **79**, 348–359.

328 **Galbiati, F., Sinha Roy, D., Simonini, S., et al.** (2013) An integrative model of the control of ovule primordia
329 formation. *Plant J.*, **76**, 446–455.

330 **Gallegos, J.E. and Rose, A.B.** (2019) An intron-derived motif strongly increases gene expression from
331 transcribed sequences through a splicing independent mechanism in *Arabidopsis thaliana*. *Sci. Rep.*, **9**,
332 1–9. Available at: <http://dx.doi.org/10.1038/s41598-019-50389-5>.

333 **Guilfoyle, T.J. and Hagen, G.** (2007) Auxin response factors. *Curr. Opin. Plant Biol.*, **10**, 453–460.

334 **Hardtke, C.S. and Berleth, T.** (1998) The *Arabidopsis* gene *MONOPTEROS* encodes a transcription factor
335 mediating embryo axis formation and vascular development. *EMBO J.*, **17**, 1405–1411. Available at:
336 <http://www.ncbi.nlm.nih.gov/pubmed/9482737>.

337 **Hayashi, N., Sasaki, S., Takahashi, H., Yamashita, Y., Naito, S. and Onouchi, H.** (2017) Identification of
338 *Arabidopsis thaliana* upstream open reading frames encoding peptide sequences that cause ribosomal
339 arrest. *Nucleic Acids Res.*, **45**, 8844–8858.

340 **Hsu, P.Y., Calviello, L., Wu, H.Y.L., Li, F.W., Rothfels, C.J., Ohler, U. and Benfey, P.N.** (2016) Super-
341 resolution ribosome profiling reveals unannotated translation events in *Arabidopsis*. *Proc. Natl. Acad.*
342 *Sci. U. S. A.*, **113**, E7126–E7135.

343 **Laxa, M.** (2017) Intron-mediated enhancement: A tool for heterologous gene expression in plants? *Front.*
344 *Plant Sci.*, **7**, 1–13.

345 **Laxa, M., Müller, K., Lange, N., Doering, L., Pruscha, J.T. and Peterhänsel, C.** (2016) The 5'UTR intron
346 of *Arabidopsis* GGT1 aminotransferase enhances promoter activity by recruiting RNA polymerase II.
347 *Plant Physiol.*, **172**, 313–327.

348 **Lecampion C, Floris M, Fantino JR, Robaglia C, Laloi C.** An Easy Method for Plant Polysome Profiling. *J*
349 *Vis Exp.* 2016;(114):54231. Published 2016 Aug 28. doi:10.3791/54231

350 **Lei, Y., Lu, L., Liu, H.Y., Li, S., Xing, F. and Chen, L.L.** (2014) CRISPR-P: A web tool for synthetic single-
351 guide RNA design of CRISPR-system in plants. *Mol. Plant*, **7**, 1494–1496.

352 **Li, S.-B., Xie, Z.-Z., Hu, C.-G. and Zhang, J.-Z.** (2016) A Review of Auxin Response Factors (ARFs) in
353 Plants. *Front. Plant Sci.*, **7**.

354 **Li, S., Yu, X., Cheng, Z., Zeng, C., Li, W., Zhang, L. and Peng, M.** (2020) Large-scale analysis of the
355 cassava transcriptome reveals the impact of cold stress on alternative splicing. *J. Exp. Bot.*, **71**, 422–
356 434.

357 **Li, Y., Mi, X., Zhao, S., Zhu, J., Guo, R., Xia, X., Liu, L., Liu, S. and Wei, C.** (2020) Comprehensive
358 profiling of alternative splicing landscape during cold acclimation in tea plant. *BMC Genomics*, **21**, 1–
359 16.

360 **Liao, C., Smet, W., Brunoud, G.** Reporters for sensitive and quantitative measurement of auxin response.
361 *Nat Methods* **12**, 207–210 (2015). <https://doi.org/10.1038/nmeth.3279>

362 **Liu, M.J., Wu, S.H., Wu, J.F., Lin, W.D., Wu, Y.C., Tsai, T.Y., Tsai, H.L. and Wu, S.H.** (2013) Translational

363 landscape of photomorphogenic Arabidopsis. *Plant Cell*, **25**, 3699–3710.

364 **Liu, Y.S. and Sun, C.W.** (2013) Characterization of differential expression and leader intron function of
365 Arabidopsis atTOC159 homologous genes by transgenic plants. *Bot. Stud.*, **54**, 1–8.

366 **Lukoszek, R., Feist, P. and Ignatova, Z.** (2016) Insights into the adaptive response of Arabidopsis thaliana
367 to prolonged thermal stress by ribosomal profiling and RNA-Seq. *BMC Plant Biol.*, **16**, 1–13. Available
368 at: <http://dx.doi.org/10.1186/s12870-016-0915-0>.

369 **Macknight, R., Duroux, M., Laurie, R., Dijkwel, P., Simpson, G. and Dean, C.** (2002) Functional
370 Significance of the Alternative Transcript Processing of the Arabidopsis Floral Promoter FCA. *Plant Cell*
371 , **14**, 877–888.

372 **Marquez, Y., Brown, J.W.S., Simpson, C., Barta, A. and Kalyna, M.** (2014) Komplement und Niere : C3
373 Glomerulopathie. , **49**, 2262.

374 **Mun, J.H., Lee, S.Y., Yu, H.J., Jeong, Y.M., Shin, M.Y., Kim, H., Lee, I. and Kim, S.G.** (2002) Petunia
375 actin-depolymerizing factor is mainly accumulated in vascular tissue and its gene expression is
376 enhanced by the first intron. *Gene*, **292**, 233–243.

377 **Nibau, C., Gallemí, M., Dadarou, D., Doonan, J.H. and Cavallari, N.** (2020) Thermo-Sensitive Alternative
378 Splicing of FLOWERING LOCUS M Is Modulated by Cyclin-Dependent Kinase G2. *Front. Plant Sci.*,
379 **10**, 1–14.

380 **Nishimura, T., Wada, T., Yamamoto, K.T. and Okada, K.** (2005) The Arabidopsis STV1 protein,
381 responsible for translation reinitiation, is required for auxin-mediated gynoecium patterning. *Plant Cell*,
382 **17**, 2940–2953.

383 **Niu, R., Zhou, Y., Zhang, Y., et al.** (2020) uORFlight: a vehicle toward uORF-mediated translational
384 regulation mechanisms in eukaryotes. *Database (Oxford)*, **2020**, 1–10.

385 **Odat, O., Gardiner, J., Sawchuk, M.G., Verna, C., Donner, T.J. and Scarpella, E.** (2014) Characterization
386 of an allelic series in the MONOPTEROS gene of arabidopsis. *Genesis*, **52**, 127–133.

387 **Pan, Q., Shai, O., Lee, L.J., Frey, B.J. and Blencowe, B.J.** (2008) Deep surveying of alternative splicing
388 complexity in the human transcriptome by high-throughput sequencing. *Nat. Genet.*, **40**, 1413–1415.

389 **Parra, G., Bradnam, K., Rose, A.B. and Korf, I.** (2011) Comparative and functional analysis of intron-
390 mediated enhancement signals reveals conserved features among plants. *Nucleic Acids Res.*, **39**,
391 5328–5337.

392 **Przemeck, G.H., Mattsson, J., Hardtke, C., Sung, Z.R. and Berleth, T.** (1996) Studies on the role of the
393 Arabidopsis gene MONOPTEROS in vascular development and plant cell axialization. *Planta*, **200**,
394 229–237.

395 **Reed, J.W.** (2001) Roles and activities of Aux/IAA proteins in Arabidopsis. *Trends Plant Sci.*, **6**, 420–425.

396 **Rose, A.B.** (2008) Intron-mediated regulation of gene expression. *Curr. Top. Microbiol. Immunol.*, **326**, 277–
397 290.

398 **Rose, A.B.** (2019) Introns as gene regulators: A brick on the accelerator. *Front. Genet.*, **10**, 1–6.

399 **Rose, A.B., Carter, A., Korf, I. and Kojima, N.** (2016) Intron sequences that stimulate gene expression in
400 *Arabidopsis*. *Plant Mol. Biol.*, **92**, 337–346. Available at: <http://dx.doi.org/10.1007/s11103-016-0516-1>.

401 **Salimonti, A., Carbone, F., Romano, E., et al.** (2020) Association Study of the 5'UTR Intron of the FAD2-2
402 Gene With Oleic and Linoleic Acid Content in *Olea europaea* L. *Front. Plant Sci.*, **11**, 1–17.

403 **Satoko Sugawara, Kiyoshi Mashiguchi, Keita Tanaka, Shojiro Hishiyama, Tatsuya Sakai, Kousuke**
404 **Hanada, Kaori Kinoshita-Tsujimura, Hong Yu, Xinhua Dai, Yumiko Takebayashi, Noriko Takeda-**
405 **Kamiya, Tatsuo Kakimoto, Hiroshi Kawaide, Masahiro Natsume, Mark Estelle, Yunde Zhao, Ken-**
406 **ichiro Hayashi, Yuji Kamiya, Hiroyuki Kasahara,** Distinct Characteristics of Indole-3-Acetic Acid and
407 Phenylacetic Acid, Two Common Auxins in Plants, *Plant and Cell Physiology*, Volume 56, Issue 8,
408 August 2015, Pages 1641–1654, <https://doi.org/10.1093/pcp/pcv088>

409 **Shaul, O.** (2017) How introns enhance gene expression. *Int. J. Biochem. Cell Biol.*, **91**, 145–155. Available
410 at: <http://dx.doi.org/10.1016/j.biocel.2017.06.016>.

411 **Smet, I. De, Lau, S., Voss, U., et al.** (2010) Bimodular auxin response controls organogenesis in
412 *Arabidopsis*. *Proc. Natl. Acad. Sci.*, **107**, 2705–2710. Available at:
413 <http://www.pnas.org/cgi/doi/10.1073/pnas.0915001107>.

414 **Tiwari, S.B., Hagen, G. and Guilfoyle, T.** (2003) The Roles of Auxin Response Factor Domains in Auxin-
415 Responsive Transcription. , **15**, 533–543.

416 **Ulmasov, T., Hagen, G. and Guilfoyle, T.J.** (1999a) Activation and repression of transcription by auxin-
417 response factors. *Proc. Natl. Acad. Sci. U. S. A.*, **96**, 5844–5849.

418 **Ulmasov, T., Hagen, G. and Guilfoyle, T.J.** (1999b) Dimerization and DNA binding of auxin response
419 factors. *Plant J.*, **19**, 309–319.

420 **Ulmasov, T., Murfett, J., Hagen, G. and Guilfoyle, T.J.** (1997) Aux/IAA proteins repress expression of
421 reporter genes containing natural and highly active synthetic auxin response elements. *Plant Cell*
422 *Online* , **9**, 1963–1971.

423 **Wang, E.T., Sandberg, R., Luo, S., Khrebtkova, I., Zhang, L., Mayr, C., Kingsmore, S.F., Schroth, G.P.**
424 **and Burge, C.B.** (2008) Alternative isoform regulation in human tissue transcriptomes. *Nature*, **456**,
425 470–476.

426 **Wang, G., Weng, L., Li, M. and Xiao, H.** (2017) Response of Gene Expression and Alternative Splicing to
427 Distinct Growth Environments in Tomato. *Int. J. Mol. Sci.*, **18**, 475.

428 **Weijers, D. and Jürgens, G.** (2005) Auxin and embryo axis formation: The ends in sight? *Curr. Opin. Plant*
429 *Biol.*, **8**, 32–37.

430 **Weijers, D., Schlereth, A., Ehrismann, J.S., Schwank, G., Kientz, M. and Jürgens, G.** (2006) Auxin
431 triggers transient local signaling for cell specification in *Arabidopsis* embryogenesis. *Dev. Cell*, **10**, 265–
432 270.

433 **Yamaguchi, N., Wu, M.F., Winter, C.M., Berns, M.C., Nole-Wilson, S., Yamaguchi, A., Coupland, G.,**
434 **Krizek, B.A. and Wagner, D.** (2013) A Molecular Framework for Auxin-Mediated Initiation of Flower
435 Primordia. *Dev. Cell*, **24**, 271–282. Available at: <http://dx.doi.org/10.1016/j.devcel.2012.12.017>.

- 436 **Zhang, N., McHale, L.K. and Finer, J.J.** (2016) A leader intron of a soybean elongation factor 1A (eEF1A)
437 gene interacts with proximal promoter elements to regulate gene expression in synthetic promoters.
438 *PLoS One*, **11**, 1–20.
- 439 **Zhang, R., Calixto, C.P.G., Marquez, Y., et al.** (2017) A high quality Arabidopsis transcriptome for accurate
440 transcript-level analysis of alternative splicing. *Nucleic Acids Res.*, **45**, 5061–5073.
- 441 **Zouine, M., Fu, Y., Chateigner-Boutin, A.L., Mila, I., Frasse, P., Wang, H., Audran, C., Roustan, J.P.**
442 **and Bouzayen, M.** (2014) Characterization of the tomato ARF gene family uncovers a multi-levels
443 post-transcriptional regulation including alternative splicing. *PLoS One*, **9**, 1–12.

444

445 **Author contributions statement**

446 A.G., A.C., M.C. and L.C. planned the experiments, A.G., A.C., M.C., F.C., C.M. and V.G.
447 conducted the experiments. A.G., A.C., M.C. and L.C. analysed and discussed the results.

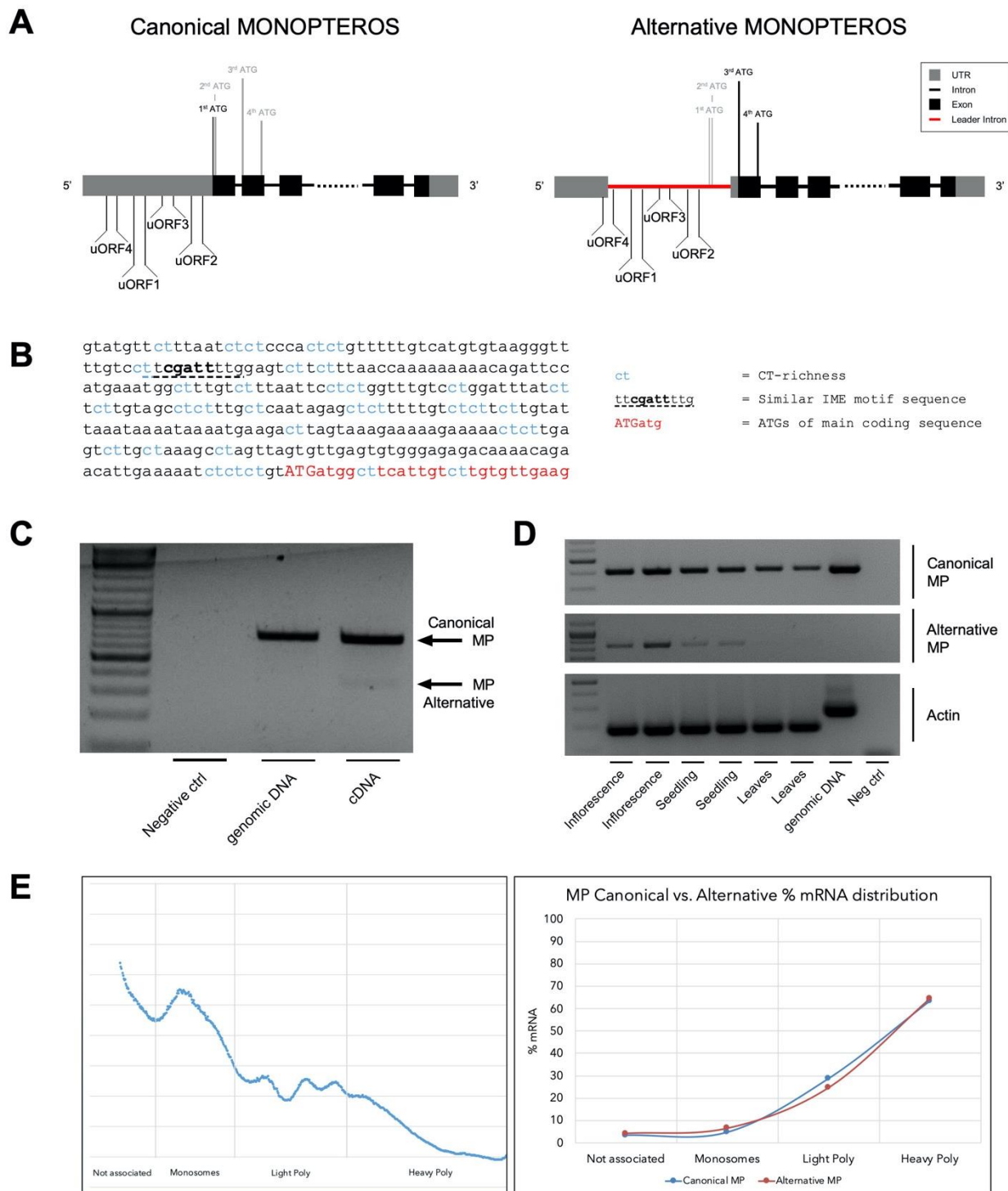
448

449 **Acknowledgements**

450 We thank Chiara Astori for helping in performing some of the experiments.

451

452

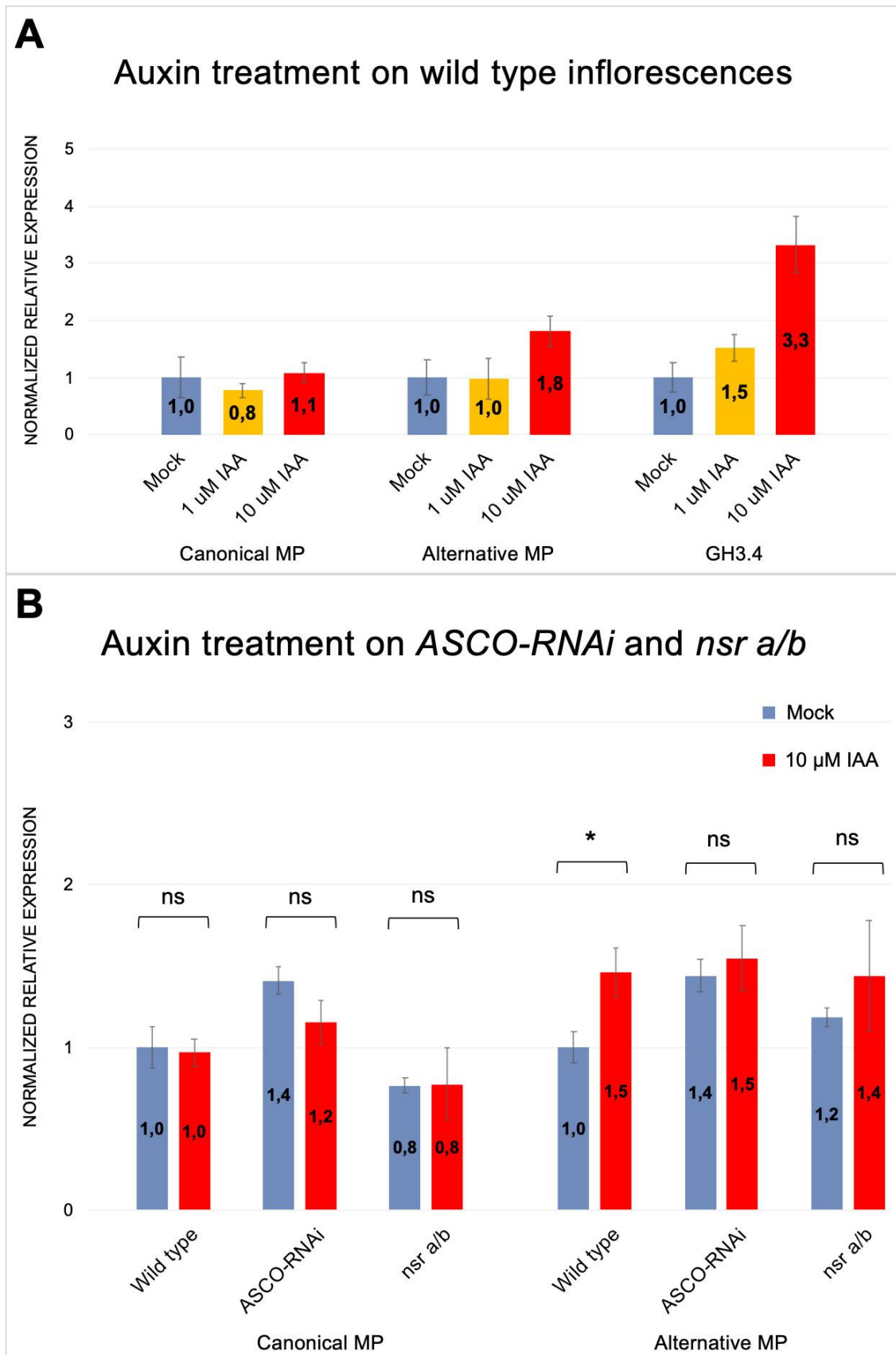


453

454 **Fig. 1 A)** Canonical and alternative *MONOPTEROS* isoforms. The alternative *MP* mRNA
455 isoform lacks the first two translational initiation sites due to the splicing of the leader intron.
456 The ATGs available for initiation of translation downstream the sequences encoding the
457 functional domains are the third and the fourth, located in the first exon. The leader intron
458 includes all the four uORF predicted for *MP* (uORF4 not entirely included) and the canonical
459 annotated ATG. When the leader intron is spliced out, the third ATG in frame with *MP* protein
460 becomes the first available Translational Initiation Site. **B)** Leader Intron sequence analysis.

461 The leader intron of MP is composed by a total of 336 base pairs. The intron sequence
462 contains several CT regions and one Intron Mediated Enhancement motif. The sequence of
463 the leader intron which corresponds to the first part of the Coding Sequence, includes the
464 first ATG annotated as the initiation of translation. **C)** PCR amplifying both isoforms with
465 splicing and non-splicing leader intron on cDNA retro-transcribed from inflorescence-specific
466 RNA. **D)** From the top to bottom: selective PCR amplification of MP canonical isoform,
467 alternative isoform and Actin using cDNA as templates. Tissues used for RNA extraction
468 and subsequent cDNA retrotranscription are indicated below the gel images. Two biological
469 replicates are shown for each tissue sample. Genomic DNA (gDNA) has been used as
470 control template. In the Actin PCR mix, no gDNA is detectable in the cDNA samples. Bands
471 of correct sizes have been detected for cDNA and gDNA template controls. **E)** mRNA
472 distribution across polysomal fractioning. Four fractions have been isolated, from left to right:
473 i) mRNA not associated to Polysomes, ii) Monosomes, iii) Light Polysomes, iv) Heavy
474 Polysomes. In the right box a comparison between mRNA distribution across polysomal
475 fractions of the canonical and alternative isoforms of *MP*. Quantification has been done
476 using Real Time qPCR using CFX96 Detection System with Bio-Rad iTaq SYBR green
477 master mix. mRNA percentage distribution has been calculated based on Ct values dividing
478 each polysomal fraction by the total of the four fractions.

479

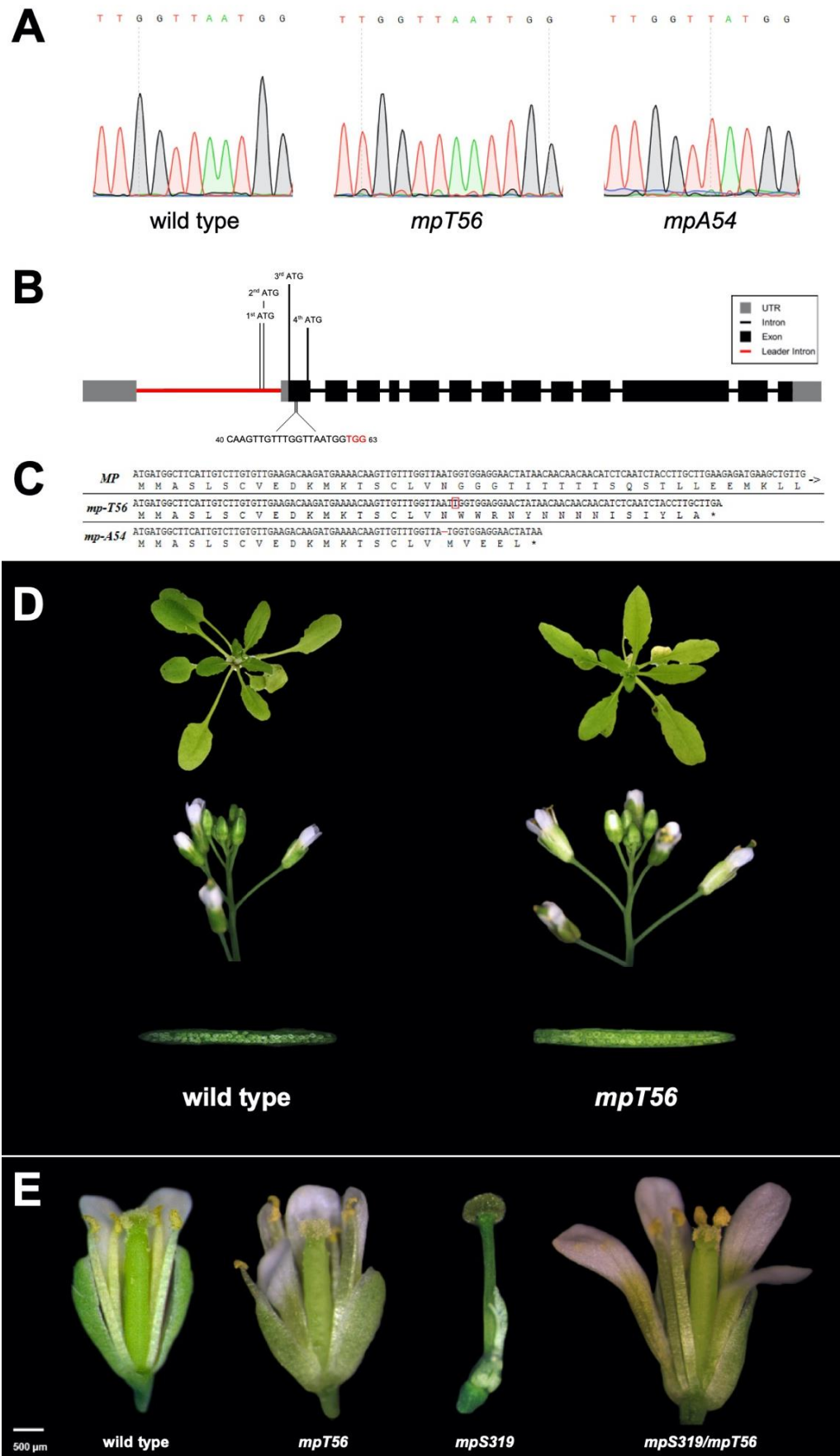


480

481 **Fig. 2** Quantitative Real Time data of inflorescences treated with exogenous IAA. A) Wild
 482 type inflorescences. From left to right, the normalized relative expression of the canonical
 483 isoform of *MP*, the alternative isoform of *MP* and *GH3.4* as positive control. *GH3.4* shows

484 an increasing enrichment of expression along increasing concentration of IAA in the
485 treatment. The alternative *MP* isoform subtly increases its expression in inflorescences upon
486 10 μ M IAA solution application. The results shown in the figure have been generated
487 analysing one single IAA treatment experiment. Four independent experiments with a total
488 of six biological replicates have been performed showing similar results. The Mock value
489 has been set as control and, thus, does not indicate relative expression between canonical
490 MP, alternative MP and GH3.4. Actin has been used as housekeeping gene for
491 normalization. Data have been generated using CFX96 Detection System with Bio-Rad iTaq
492 SYBR green master mix and analysed using Bio-rad CFX Maestro v1.1. B) Exogenous auxin
493 treatment on wild type, ASCO-RNAi and *nsr a/b* inflorescences. The data shows an average
494 of three independent auxin treatment experiments with a total of three biological replicates.
495 Statistical analysis performed with T-test Student, ns= not statistically significant, *=
496 statistically significant, p<0,01.

497



498

499 **Fig. 3 A)** Sanger sequencing of genomic region of *MP* targeted by the guide RNA designed
500 to generate InDels with CRISPR/Cas9. From left to right, electropherograms of wild type,

501 *mpT56* and *mpA54* mutant alleles are shown. **B)** *MP* gene structure with the protospacer
502 designed for CRISPR/Cas-mediated targeting of *MP* 56 nucleotides after the start codon.
503 **C)** A 1bp insertion was detected in genomic DNA of *mpT56* mutant and a 1bp deletion in
504 *mpA54*; both mutations generate an early stop codon. **D and E)** CRISPR/Cas9 *mpT56* and
505 *mpA54* mutant have wild type like phenotypes. D) The *mpT56* and wild type plants display
506 no significant differences at rosette stage, in inflorescences and in siliques showing full seed
507 set in both genotypes. **E)** Phenotypic comparison of the flowers at anthesis stage between
508 wild type Col-0, *mpT56*, *mpS319* and trans-heterozygous *mpS319/mpT56*.

509

510

511

512

513

514

515

516

517

518

519

520

521

522

523

524

525

526

527

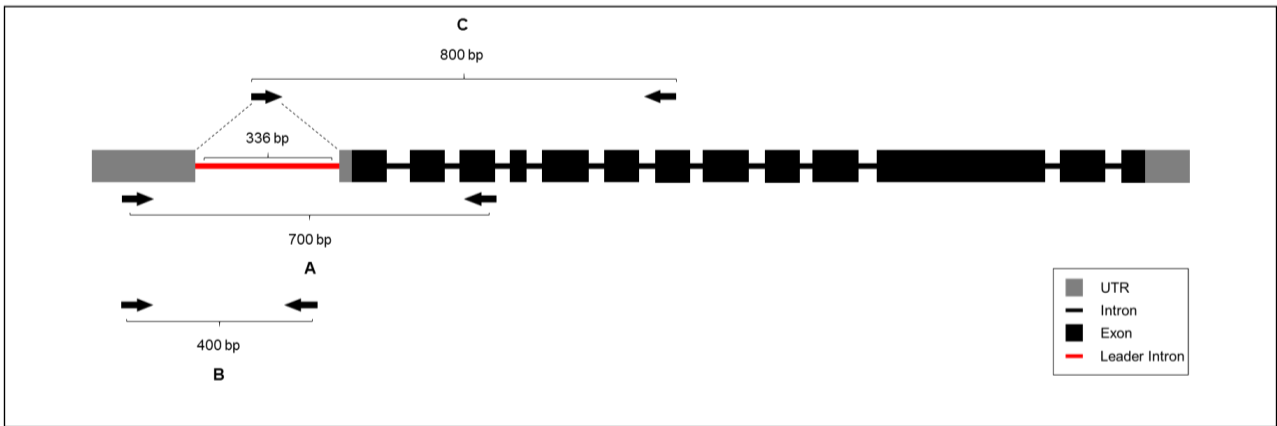
528

529

530

531 **Supplemental information**

532



533

534 **Fig. S1** **A)** Canonical and alternative *MP* amplification mix. **B)** Selective canonical *MP*
535 amplification mix. **C)** Selective alternative *MP* amplification mix. The forward primer has
536 been designed in the junction between the 5'UTR and the first exon of *MP*, in order to be
537 able to discriminate the alternative isoform.

538

539

540

541

542

543

544

545

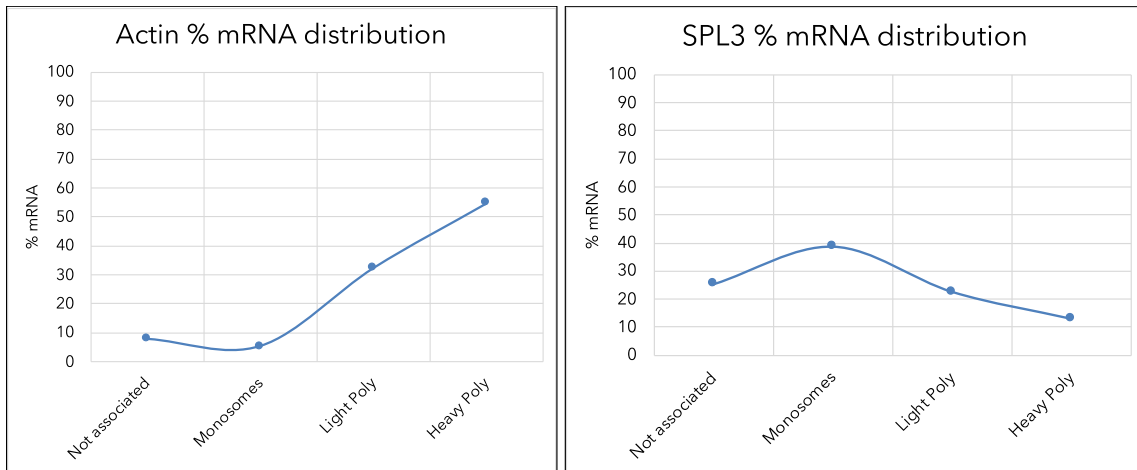
546

547

548

549

550



551

552 **Fig. S2** Positive and negative controls of mRNA distribution through polysome fractions. A)
 553 Positive control, the percentages of distribution of Actin mRNA in the four fractions isolated.
 554 B) Distribution of *SQUAMOSA PROMOTER BINDING PROTEIN-LIKE 3* (SPL3,
 555 *At2g33810*) mRNA isolated in the four fractions are shown, representing a low-rate
 556 translated gene.

557

558

559

560

561

562

563

564

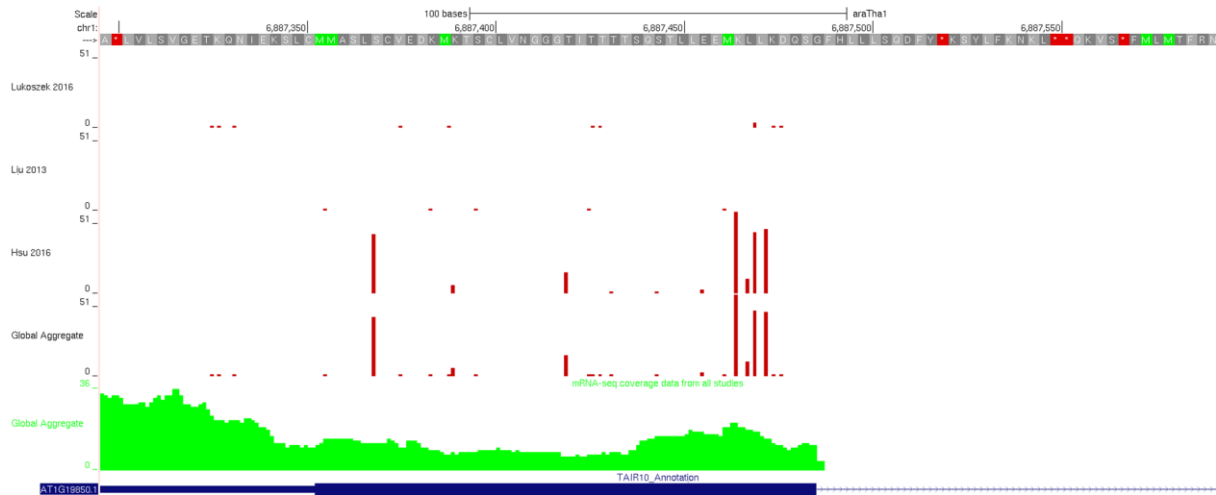
565

566

567

568

569



570

571 **Fig. S3** The image highlights a genomic region which comprehends a portion of the 5'UTR
 572 of *MP*, the whole first exon and the beginning of the first intron of *MP* gene. This region has
 573 been used to map reads coming from the ribosome profiling datasets available online (Hsu
 574 et al., 2016; Lukoszek et al., 2016; Liu et al., 2013). Analysis made with GWIPS-viz. On top,
 575 the corresponding aminoacidic sequence of *MP* protein is indicated. Four rows are shown.
 576 The upper row corresponds to mapped reads datasets from Lukoszek and colleagues
 577 (2016) ribosomal profiling. Second row corresponds to the mapped reads coming from the
 578 ribosome profiling of Liu and colleagues (2013). Third row shows the mapped reads selected
 579 from the ribosome profiling of Hsu and colleagues (2016). Fourth row represents the
 580 combination of reads of all the ribosome profiling analysed in this work and fifth row
 581 corresponds to the global aggregate of mRNA-Seq coverage from the three studies.

582

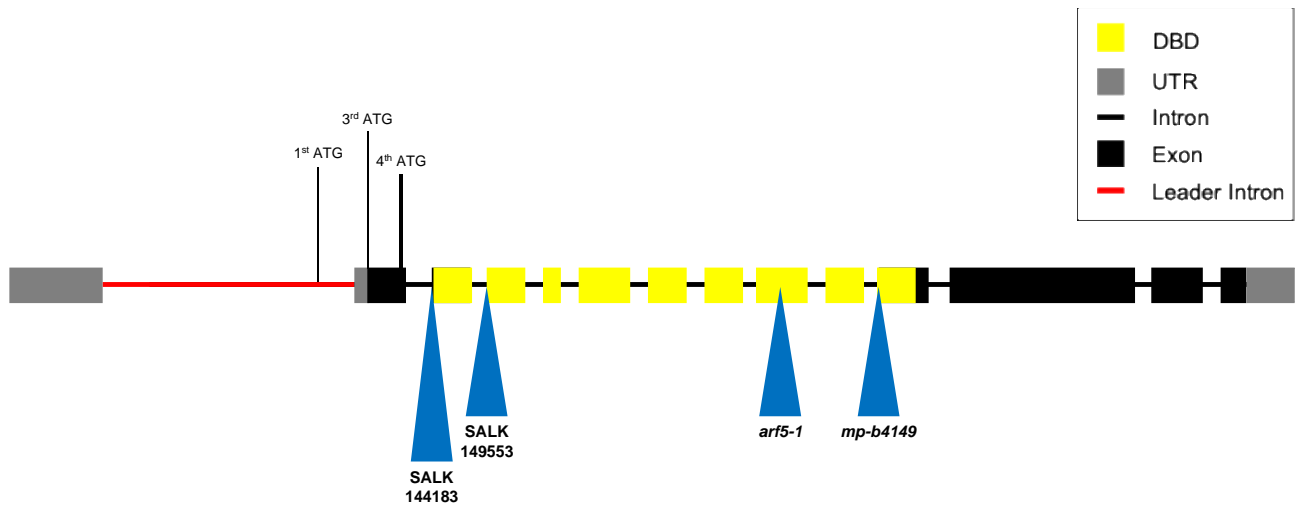
583

584

585

586

587



589 **Fig. S4** Scheme of several *mp* mutant alleles. The blue triangle indicates the position of the
 590 mutation associated with the distinct *mp* mutants. *SALK_144183*, *SALK_149553* and *arf5-*
 591 *1* are T-DNA insertional mutant, whereas *mp-B4149* is a point mutation in the splice acceptor
 592 site of the tenth exon of *MP*.

593
 594
 595
 596
 597
 598
 599
 600
 601
 602
 603
 604
 605
 606
 607
 608
 609

Oligonucleotide sequences for PCR and Real Time qPCR	
Amplification Mix for gDNA contamination check on Actin gene	Forward: CTCAGGTATTGCAGACCGTATGAG Reverse: CTGGACCTGCTTCATCATACTCTG
Canonical and Alternative <i>MP</i> Amplification Mix	Forward: TGGCACCTTTGGTTTCTCTT Reverse: TGTTCAAATCGCATTITTTAGGGGA
Canonical <i>MP</i> PCR Mix	Forward: TGGCACCTTTGGTTTCTCTT Reverse: TTGTCTCTCCCACTCAACAC
Alternative <i>MP</i> PCR Mix	Forward: GTAGTCCCTATTTACAAGA Reverse: CAAGAACACCGATGTGCATACTA
CRISPR generated InDel check of <i>mpT56</i> and <i>mpA54</i>	Forward: AACTCTTGAGTCTTGCTAAAGCCTA Reverse: TGAGAAAGAAGAAGATGAAAACCTG
<i>GH3.4</i> Real Time qPCR Mix	Forward: ATGAATCTCTACGTGCCGGG Reverse: GACGTCTGAAGTAGTCGCT
Canonical <i>MP</i> Real Time qPCR Mix	Forward: AACTCTTGAGTCTTGCTAAAGCCTA Reverse: CGGCTTTCTGTACCTGACT
Alternative <i>MP</i> Real Time qPCR Mix	Forward: GTAGTCCCTATTTACAAGA Reverse: CATAGCTCCGAGTTTATTAC
Actin Housekeeping gene for Normalization of Real Time qPCR	Forward: CTCAGGTATTGCAGACCGTATGAG Reverse: CTGGACCTGCTTCATCATACTCTG
Ubiquitin Housekeeping gene for Normalization of Real Time qPCR	Forward: CTGTTACGGAACCCAATTC Reverse: GGAAAAAGGTCTGACCGACA
<i>SPL3</i> Real Time qPCR	Forward: CTGGACACAACGAGAGAAG Reverse: TGGAGAAACAGACAGAGACA

610

611 **Table S1** List of oligonucleotides used in this work.